DEVELOPING MULTI DEGREE OF FREEDOM CONTROL BRAIN COMPUTER INTERFACE SYSTEM FOR SPINAL CORD INJURY PATIENTS

by

Syahrull Hi-Fi Syam bin Ahmad Jamil

Department of Biomedical Engineering

University of Strathclyde

Glasgow

United Kingdom

Thesis submitted in partial fulfilment of the requirement for the Degree of Doctor of Philosophy

February 2017

You only worry about your head or spinal column. Everything else, some way or another, will repair in time.

Tony McCoy in Brainy Quote

Declaration of Author's Rights

This thesis is the result of the author's original research. It has been composed by the author and has not been previously submitted for examination which has led to the award of a degree.

The copyright of this thesis belongs to the author under the terms of the United Kingdom Copyright Acts as qualified by University of Strathclyde Regulation 3.50. Due acknowledgement must always be made of the use of any material contained in, or derived from, this thesis.

Signed:

Date:

Acknowledgements

Abstract

Brain computer interface (BCI) is a paradigm that offers an alternative communication channel between neural activity generated in the brain and the user's external environment. BCI decodes the brain activity obtained from an electroencephalogram (EEG) signal and convert this information to a sensible output such as commands to control and communicate with the augmentative and assistive devices. Nevertheless, the majority of the existing BCI system associates with healthy subjects operate based on a combination of multiple limbs and bounded by capability of low dimensional control. Besides that, the acquired results also are not an appropriate platform to infer with the neurologically impaired patients (e.g. spinal cord injury patients). This is probably healthy subjects have full control over their limbs and their EEG signatures show a different pattern. On the other hand, neurologically impaired patients have limited access/control over their limbs and the EEG signatures are affected by the side effects of the prescribed medication, deafferentation and cortical reorganization of brain regions as a function of duration, level and type of disease.

This study focuses on the feasibility of developing a multi degree of freedom control BCI system using imagination and intention of movement of a single limb for spinal cord injury (SCI) patients. A pilot study has been conducted on eleven healthy subjects to examine the feasibility of the proposed experimental protocol to record data for implementing the same procedure on SCI patients. In the present study, eighteen SCI patients from Queen Elizabeth National Spinal Injury Unit of the Queen Elizabeth University Hospital voluntarily participated as subjects. The participating subjects have performed and imagined performing right wrist movement towards four centre out directions using a custom made manipulandum triggered by a visual cue whilst EEG, electromyography (EMG) and movement signals are recorded simultaneously through NeuroScan^{TM} Synamp system and CED 1401 (Cambridge Electronic Design). The EEG signal was analysed using signal processing and statistical analysis method. Our findings indicate the detection of Bereitschaft potential 500ms before onset of movement and 500ms after onset of the visual cue. Additionally, there are statistical differences in the relative power within

the EEG signal rhythm components namely, delta, theta, alpha beta and gamma bands during imagination and intention of movement towards the four different directions. The significant changes of the estimated relative power of EEG components were extracted as features associated with direction. The features then were normalised, cross validated and dimensionality reduced before being classified using k nearest neighbour (k-NN), fuzzy k nearest neighbour (FKNN) and quadratic discriminant analysis (QDA) classifier.

The single trial classification results for motor imagery and motor task by k-NN, FKNN and QDA classifier dwell within the range of 52.31%-94.14% and 52.20%-96.51%, respectively. These findings proved that it is possible to develop a functional multi degree of freedom BCI system that employs imagination/intention of movement using a single limb for the SCI population. On top of that the developed BCI system and classification also required no subject training at all.

Contents

List of Figures

List of Tables

List of Abbreviations

AC   Classification accuracy

Ag/AgCl   Silver chloride

AIS grade   ASIA Impairment Scale

Alpha MNs   Alpha motor neurons

ANOVA   Analysis of variance

ASIA   American Spinal Injury Association

B1   Nuclear bag one

B2   Nuclear bag two

BCI   Brain computer interface

Beta MNs   Beta motor neurons

BOLD   Blood oxygenation level dependent

BP   Bereitschaft potential

CAR   Common average reference

CAR+FKNN   Combination of CAR spatial filter with FKNN classifier

CAR+k-NN   Combination of CAR spatial filter with k-NN classifier

CAR+QDA   Combination of CAR spatial filter with QDA classifier

CED   Cambridge Electronic Design system

CH   Nuclear chain

CNS   Central nervous system

cSCI   Complete spinal corf injury

ECG	Electrocardiography
ECoG	Electrocorticography
ECRB	Extensor carpi radialis brevis
ECRL	Extensor carpi radialis longus
ECU	Extensor carpi ulnaris
EEG	Electroencephalogram
EF	Extrafusal fibers
EMG	Electromyography
EOG	Electrooculography
ERD	Event related desynchronization
ERS	Event related synchronisation
ERSP	Event related spectral perturbation
ERF	Event related field
ERP	Event related potential
FCR	Flexor carpi radialis
FES	Functional electrical stimulation
FFT	Fast fourier transform
FKNN	Fuzzy k nearest neighbour
FIM	Functional Independence Measure
fMRI	Functional magnetic resonance imaging
FN	False negative

FP   False positive

FPR   False positive rate

Gamma MNs   Gamma motor neurons

IF   Intrafusal fibers

OC   Outer capsule

iEEG   Intracranial electroencephalogram

IOSS   Intraoperative spinal sonography

iSCI   Incomplete spinal cord injury

ISNCSCI   International Standards for Neurological and Functional Classification
            of Spinal Cord Injury

KS   Kolmogorov-Smirnov

k-NN K-nearest neighbour

LAP   Laplacian

LAP+FKNN   Combination of LAP spatial filter with FKNN classifier

LAP+k-NN   Combination of LAP spatial filter with k-NN classifier

LAP+QDA   Combination of LAP spatial filter with QDA classifier

LCD   Liquid crystal display

LDA   Linear discriminant analysis

LFP   Local field potential

LMNs   Lower motor neurons

LT   Light touch

MEG	Magnetoencephalography
MEP	Motor evoked potential
MI	EEG from motor imagery
MICAR	MI filtered by CAR
MILAP	MI filtered by LAP
MLP	Multilayer perceptron
MRCP	Movement related cortical potential
MRI	Magnetic resonance imaging
MRI-DWI	Magnetic resonance imaging- diffusion weighted
MS	Muscle spindle
MSCT	Multislice computed tomography
MUA	Multi-unit activity
MT	EEG from motor task experiment
MTCAR	MT filtered by CAR
MTLAP	MT filtered by LAP
NASCIS	National Acute Spinal Cord Injury Studies
NHS	National health service
NIRS	Near infrared spectroscopy
NN	Neural network
NS	Negative slope
PCA	Principal component analysis

PET   Positron emission tomography

PP   Pin prick

Pt/Ir   Platinum/Iridium

ROC   Receiver operating characteristic

T   Time

SCI   Spinal cord injury

SCIM   Spinal Cord Independence Measure

SCPs   Slow cortical potentials

SP   Paraplegic subject

ST   Tetraplegic subject

SSEP   Somatosensory evoked potential

SSVEPs   Steady state visual evoked potentials

SUA   Single unit activity

SQUID   Superconducting quantum interferences devices

TN   True negative

TP   True positive

TPR   True positive rate

TMS   Transcranial magnetic stimulation

TTD   Thought-Translation-Device

TVEPs   Transient visual evoked potentials

UIEA   Utah Intracortical Electrode Array

UK	United Kingdom
UMNI	University of Miami Neuro-Spinal Index
UMNs	Upper motor neurons
QDA	Quadratic Discriminant Analysis
QENSIU	Queen Elizabeth National Spinal Cord Injuries Unit
QIF	Quadriplegic Index of Function
VEPs	Visual evoked potentials
WISCI	Walking Index for SCI divorce

List of Symbols

A	Alpha band
β	Beta band
p	*P value*
t_m	Onset of the movement
t_c	Onset of the visual cue
μ	Mu band
γ	Gamma band

Chapter 1. Introduction

1.1 Background

Voluntary movement is the capability that enables a person(s) to have full control over their four limbs and perform action/movement at their own free will. Unfortunately, for some who are unlucky, this capability is taken away from them either through disease or injury such as motor neuron disease, amyotrophic lateral sclerosis disease (ALS) or spinal cord injury (SCI).

SCI has profound and long lasting consequence that confines the patient to a wheelchair and lifetime of medical comorbidity (McDonald and Sadowsky, 2002). SCI also causes loss of sensation, impaired mobility, bladder, bowel and sexual dysfunction (Elliott and Rivera, 2003). In the UK, there are approximately 40,000 individuals who suffer from paralysis due to the SCI (Gall et al., 2008). SCI not only has a continuous negative impact on health condition and lifestyle of the patient but it is also a financial burden to the nation. The cost of caring for SCI patients depends on the nature of the initial injury, timeline of treatment, the length of stay in the hospital and medical cost (Jerome Bickenbach et al., 2013). The common cause of SCI in United Kingdom for 2015 is shown in Figure 1.1 below.

Commonn causes of SCI in the United Kingdom in 2015

Cause	Percentage
Sharp trauma/assault	2.7
Trauma(not specified)	3.3
Knocked over/collision/lifting	4.2
Sport	11.6
Road traffic accidents	36.8
Falls	41.7
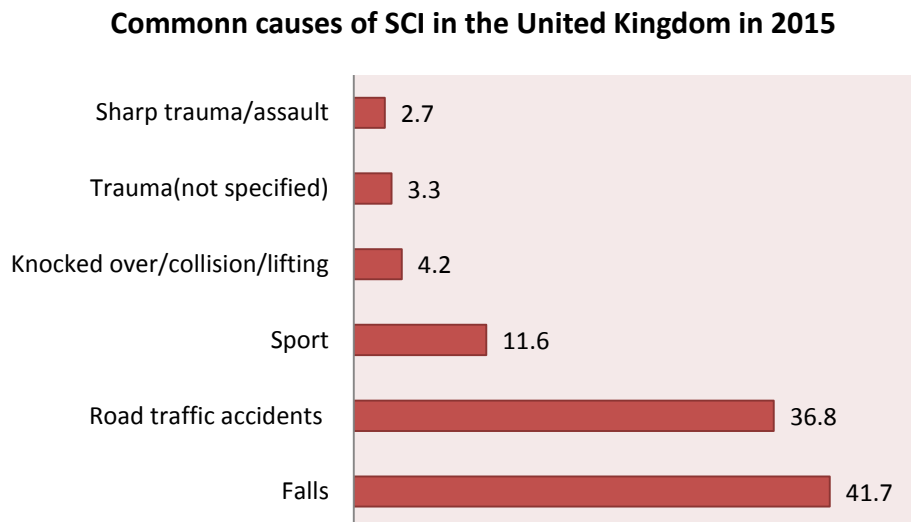
Figure 1.1: Statistic of SCI in the UK in 2015. This figure shows the percentage of common causes of SCI in United Kingdom in 2015. [Adapted from www.statista.com, 16/1/2017].

Despite the negative effect on quality of life due to the limitation of independency, there are two modalities that can offer SCI patients an assistive tool. This can be achieved through invasive and non-invasive modalities namely using stem cells and/or brain computer interface (BCI) approach. Among these two approaches, BCI approach offers new hope due to its relatively lower cost and promising results than the stem cell approach which is restrained by a comparative higher financial burden (Frantz, 2012) and lack of independent validation results of various stem cell treatments (Fehlings and Vawda, 2011).

BCI offers an alternative interaction method that is based on the neural activity generated by the brain which can be detected and measured. BCI applies and decodes the brain activity obtained from an electroencephalogram (EEG) signal and converts this information to a sensible output such as any command to control and/or communicate with the augmentative and assistive devices (Muller-Putz et al., 2011). In the past three decades, the numbers of BCI studies have reported profound and promising results in aiding neurologically impaired/disabled patients, especially in fields of communication, control and motor substitution.

One of the first attempts of providing facilities for communication to neurologically impaired/disabled patients started when the Tubingen BCI group developed the Thought-Translation-Device (TTD) in 1999 by Birbaumer et al., 1999. TTD is a system that could be operated through the modulation of brain signals. The system employs binary decision making for letter selection procedure where the alphabet was iteratively split into two halves with achieved spelling rate of 0.5 char/min.

The results produced by the Tubingen BCI group which developed the TTD triggered a new dimension of communication and control for ALS patients which allow them to operate a standard web browser (Millán et al., 2010). In the first execution which is known as "Descartes" (Karim et al., 2006), the web window was shown for approximately 120s, followed by a navigation screen that presented the links from the current web page as leaves in a tree. Later, a prototype called "Nessi" (Bensch et al., 2007), allowed a more flexible selection of links using an improved user interface. A more advanced prototype was developed employing P300 paradigm (Muglerab et al., 2008). A BCI browser based on P300 can select from as many links

as the elements in the P300 matrix (for a 6×6 matrix, 36), and the selection of a link could be completed in one step, although reliable recognition requires several repetitions of the presentations of row/columns.

On the other hand, work from groups in Heidelberg and Graz reported that combination of BCI system and FES system have shown to be beneficial for the SCI population (Pfurtscheller et al., 2003). In their study, a spinal cord injured patient who suffered from a complete motor paralysis with a missing hand and finger function managed to use a BCI system to restore his lateral grasp. The patient could trigger sequential grasp phases by imagining his foot movements. After many years of training and use of the BCI system, the patient could control the system even during a conversation with other persons.

Later, the same group conducted BCI training on one other tetraplegic patient who was equipped with a freehand system. After completing three days of training, the patient managed to control the grasp sequence of the implanted neuroprosthesis appropriately (Müller-Putz et al., 2005). Furthermore, the same group expanded the BCI application by introducing a new method for controlling the grasp and elbow function (Millán et al., 2010). This study only used one laplacian EEG channel and one motor imagery pattern to control grasp and elbow function.

1.2   Study Statement

BCI is a paradigm that offers an alternative communication channel between the users and their external environment. Nevertheless, the majority of the BCI studies reported in the literature are associated with healthy subjects and are operate based on the movement of a combination of multiple limbs. The acquired results are not an appropriate platform to infer with neurologically impaired patients (e.g. spinal cord injury patients). This is probably healthy subjects having full control over their limbs and their EEG signatures show a different pattern. On the other hand, neurologically impaired patients have limited access/control over their limbs and the EEG signatures are affected by the deafferentation and cortical reorganization of brain regions depending on the duration, level and type of the disease. Therefore, it is

essential to carry a feasibility study which involves the targeted group of patients (in our case i.e. SCI patients) so that the findings can be considered with respect to the SCI patient population. Besides, the participation of actual targeted group of patients would enable researchers to face and solve the important particular and actual issues relevant to SCI subjects rather than dealing with ideal condition presented by healthy abled bodied subjects.

1.3　List of Contributions

This thesis presents our study to investigate the feasibility of developing BCI system for SCI patients. To the best of the author's knowledge, the findings from this study have contributions towards the body of knowledge. The contributions of this study are listed below.

1.　Develop and implemented a multiclass BCI system based on a single limb which required zero subject training.

2.　Demonstrated that the implemented paradigm suits for both healthy and SCI subjects.

3.　Conduct experiment(s) on paraplegic and tetraplegic patients (involvement of big population of SCI patients in term of EEG signal recording).

4.　For the first time, emphasised the prescribed medication will affect the performance of patients in operating the BCI system.

5.　Directional information of imagination/intention of movement using a single limb can be obtained from wide a spectrum of EEG signals using a robust statistical technique, namely ANOVA test.

6.　The successful classification of EEG signals based on a single trial has shown that the implemented BCI system could be possibly developed as online BCI system.

7.　Experimentally verify the importance of using high density montage for surface EEG signal recording to select the best performing electrodes with respect to classification results.

1.4   Thesis Structure

The rest of this thesis is organised as follows. Chapter 2 includes a comprehensive explanation of the terminology, effect and assessment of SCI and involvement of BCI as an alternative communication tool for SCI patients. Chapter 3 describes in detail, the implemented methodology in developing the proposed BCI system for this study. This chapter elicits the employed paradigm, data acquisition, experimental protocol and experimental set up for recording of two physiological signals namely electroencephalogram and electromyography signal. Chapter 4 explains the data processing techniques utilised to extract the important features from the recorded signals. Chapter 4 also describes the classification techniques that were applied to predict imagination/intention and direction of movement by subjects. In chapter 5, the results from the analysis of the recorded signal are presented. Chapter 6 comprises of the discussion regarding the implemented methods and obtained results. Finally, chapter 7 concludes this dissertation highlighting the objectives achieved along with the various research work findings. Chapter 7 further provides the views and suggestions for further research in the BCI area.

1.5   List of publications

1. Ahmad Jamil, S.H.F.S, Lakany, H., Conway, B.A. (2016). Single Trial Classification of EEG in Predicting Intention and Direction of Wrist Movement: Translation Toward Development of Four-Class Brain Computer Interface System Based on a Single Limb. In Proc. COGNITIVE 2016, The Eight International Conference on Advanced Cognitive Technologies and Applications, pages 90-95.

Chapter 2. Literature Review

2.1   Introduction

This chapter will explain the terminology, presentation and assessment techniques of SCI. Literature concerning the control of movement through complex neurophysiological circuits is reviewed. A review of research in the field of BCI systems and their application as an alternative communication tool for neuro-impaired patients, specifically those with SCI is comprehensively presented. Towards the end of this chapter attention will be focussed on addressing the limitations of current BCI technology for SCI users, concluding by highlighting the need for further work.

2.2   Spinal Cord Injury

SCI is a debilitating injury that affects physical and psychological health leading to motor and sensory function impairment (Li et al., 2009), increased risk of depression, drug dependences as well as increased hospital admission and decreased general health (Widerstrom-Noga et al., 2001, Craig et al., 1998). SCI not only inflicts a negative effect towards the patient's life due to limited independency, but also healthcare/welfare involving other parties such as doctors, nurses and physicians for rehabilitation, with an associated economic cost. For instance, paralysis resulting from SCI affects almost 1200 people every year in UK; the estimated annual cost of caring for this growing number of SCI patients is more than £500 million (Apparelyzed 2015).

2.2.1 Description of Spinal Cord Injury

In the human body system, the brain is responsible for coordinating and responding to external stimuli by sending motor signals and receiving sensory signals to/from the rest of the body through the spinal cord. The spinal cord not only plays a crucial role by providing pathways in transmission of signals between the brain and the rest of the body, it is also responsible for spinal reflexes (Martini, 2005a).

The spinal cord is a cylindrical structure of nervous tissue composed of white and grey matter that extends from foramen magnum of the skull to the inferior border of the first lumbar vertebra (L1). It measures approximately 45 cm (adult) in length, comprised of 31 segments that can be classified into four anatomical regions (see Figure 2.1). These four regions are the cervical (8 segments), thoracic (12 segments), lumbar (5 segments), sacral (5 segments) and coccygeal region (1 segment) (Martini, 2005b).
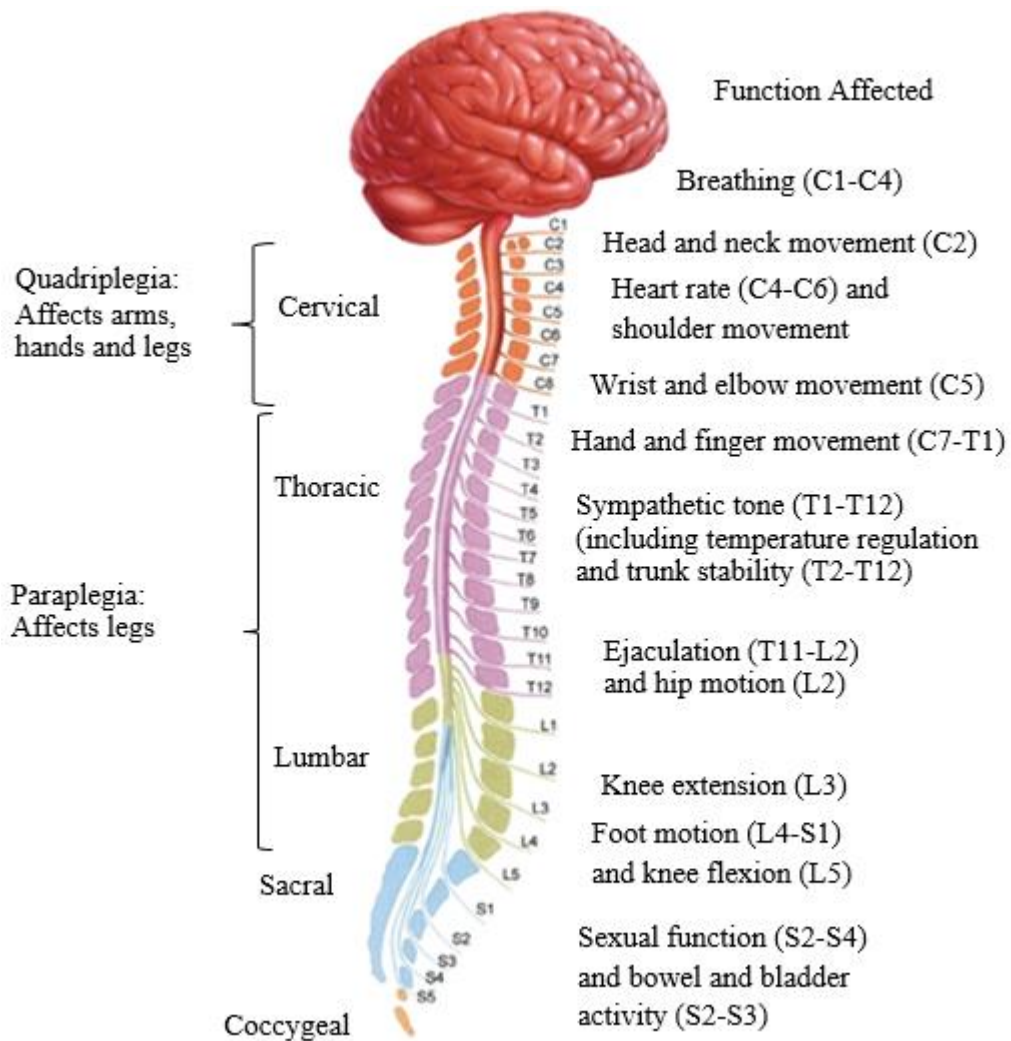
Figure 2.1: Spinal cord segments. This figure shows spinal cord segments with spinal nerves for cervical, thoracic, lumbar, sacral and coccygeal regions. Functions affected by each segment are listed on the right hand side; pathological diagnoses ascribed to SCI at these different segments are listed on the left hand side. Adapted from [www.radiology.wisc.edu/neuroradiology/anatomy/spine].

SCI is diagnosed when the spinal cord is damaged directly by blunt or penetrating trauma. This may be caused by a motor vehicle accident, a fall, gunshot wounds, sports injury, medical/surgical complication or disease (Chen et al., 2013, McDonald and Sadowsky, 2002). The damage/lesion within the spinal cord disrupts the transmission of neural signals, potentially leading to paralysis due to the loss of movement and/or sensation below the lesioned area. The severity of paralysis resulting from SCI depends on the area/location and size of the lesion. Based on the extent of injury, SCI is broadly described as either complete or incomplete, with the latter resulting in relatively better functional outcomes for patients in comparison to the former.

2.2.2 Category and level of Spinal Cord Injury

SCI has huge implications on the transmission of motor and/or sensory signals along the spinal cord below the level of the lesion. It might cause neural signals to become either completely or partially isolated from the brain, resulting in tetraplegia (quadriplegia) or paraplegia.

Complete spinal cord injury (cSCI) can be defined as a situation where no preservation of motor and/or sensory function exists more than 3 segments below the level of lesion (Waters et al., 1991). Thus in cSCI patients, motor and/or sensory signals along the spinal cord below the level of lesion are permanently isolated from the brain, causing a total loss of movement and sensation.

On the other hand, incomplete spinal cord injury (iSCI) refers to the situation where some preservation of motor and/or sensory function exists more than 3 segments below the level of lesion (Waters et al., 1991). In iSCI patients, signals transmitted by the spinal cord below the level of lesion are partially isolated from the brain, resulting in preservation of some motor and/or sensory function below the lesion. There are six types of syndromes caused by iSCI which inflict varying degrees of motor and/or sensory impairment below the level of lesion. These six syndromes are anterior cord syndrome, central cord syndrome, posterior cord syndrome, brown sequard syndrome, cauda equine syndrome and conus medullaris syndrome

(McKinley et al., 2007). The condition and symptoms for each of these syndromes are portrayed in Figure 2.2.
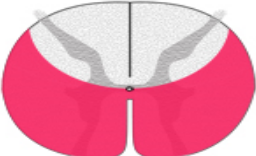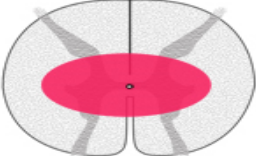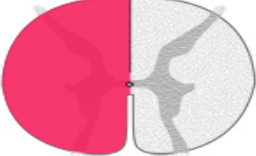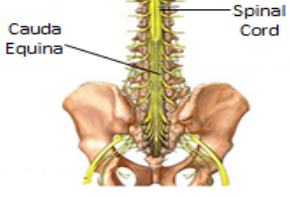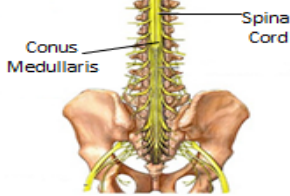
	Anterior Cord Syndrome occurs when injury is towards the front of the spinal cord that caused person to suffer from loss of motor function, impaired ability to sense pain, temperature and touch sensation below the level of injury.
	Central Cord Syndrome occurs when injury is in the centre of the spinal cord. This syndrome will lead to loss of function in the arms, but some of leg function may be preserved. There also may be some control over the bowel and bladder.
	Posterior Cord Syndrome occurs when injury is towards the back of the spinal cord. This type of syndrome may leave the person with good muscle power, pain and temperature sensation. On the other hand they may face difficulty for coordinating the movement of their limbs.
	Brown Sequard Syndrome occur when injury is towards one side of the spinal cord (left/right) resulting in impaired or loss of movement to the injured side, but temperature and pain sensation may be preserved. The opposite side of injury will have normal movement, but temperature and pain sensation will be impaired or loss.
	Cauda Equina Syndrome occurs when injury to the lumbosacral nerve roots within the neural canal. This symptom includes saddle anaesthesia, bladder and bowel dysfunction, variable lower extremities motor and sensory loss and back pain.
	Conus Medullaris Syndrome occurs when injury to the sacral cord (conus) and lumbar nerves roots within the spinal canal. This symptom may cause person to suffer saddle anaesthesia, bladder and bowel dysfunction, variable lower extremities motor and sensory loss and back pain.

Figure 2.2: Incomplete spinal cord injury syndromes. The figure shows the condition of injury for each type of syndrome and also indicates the types of function affected by each syndrome. Adapted from (Richard Snell, 2010).

Tetraplegia (quadriplegia) refers to impairment or loss of motor and/or sensory function due to a lesion in the cervical segments (C1-C8) of the spinal cord. Typically tetraplegia concerns altered function of all four limbs, trunk and pelvic organs without involving brachial plexus or injury to peripheral nerves outside the spinal cord (Bromley, 2006). In addition to paralysis of all four limbs, abdominal and

chest musculature may be affected which can lead to weakened breathing and impair the ability to effectively clear the throat/chest by coughing.

Paraplegia may occur when the spinal cord was lesion below the first thoracic segment (T1-S5). This causes impairment or loss of motor and/or sensory functions encountered due to lesions in the thoracic, lumbar or sacral segments of the spinal cord. In paraplegia, arm and hand function is preserved and the lower body and limbs are effected; however, the overall extent of paralysis depends upon the level of the lesion, and might variably present as impairment of the trunk, legs, and/or pelvic organs (Bromley, 2006). Functional outcomes for patients with cSCI at different levels of the spinal cord, either resulting in tetraplegia or paraplegia, are tabulated in Table 2.1.

Table 2.1: Functional outcomes of patients following SCI. This table lists the possible impairment for each level of injury. Adapted from [www.hopkinsmedicine.org].

Level of injury	Possible impairment
C2-C3	Usually fatal as a result of inability to breathe.
C4	Quadriplegia and breathing difficulty.
C5	Quadriplegia with some shoulder and elbow function.
C6	Quadriplegia with shoulder, elbow, and some wrist function.
C7	Quadriplegia with shoulder, elbow, wrist, and some hand function.
C8	Quadriplegia with normal arm function; hand weakness.
T1-T6	Paraplegia with loss of function below mid-chest; full control of arms.
T6-T12	Paraplegia with loss of function below the waist; good control of torso.
L1-L5	Paraplegia with varying degrees of muscle involvement in the legs.
S1-S6	Paraplegia with various degrees of voluntary bladder, bowel and sexual functions.

2.2.3 The consequence of Spinal Cord Injury on the brain

Paralysis due to the loss of motor and/or sensory function is the most common implication caused by SCI. Unfortunately, in addition to these effects, SCI can also inflict secondary medical complications such as pneumonia, autonomic dysreflexia, deep venous thrombosis, pulmonary embolism, pressure ulcers, fractures and renal calculi (McKinley et al., 1999). Although there is a number of negative implications that stem from SCI, this thesis is concerned with the effect of SCI on the central nervous system, considering the dense interconnectivity between the brain and spinal cord (Nardone et al., 2013). Hence these other symptoms are not discussed any further.

In recent years, there have been a number of published studies investigating motor function associated with SCI. One key advance in this field is the repeated observation that deafferentation of cortical circuits produced by SCI can lead to long term reorganisation of cortical topographic maps (Nardone et al., 2013, Bruehlmeier et al., 1998, Cramer et al., 2005, Shoham et al., 2001, Turner et al., 2003, Kokotilo et al., 2009, Aguilar et al., 2010).

Studies carried out by Cramer et al., 2005 used functional magnetic resonance imaging (fMRI) to compare cerebral motor system function in patients with chronic, complete SCI compared to healthy control subjects. Their results indicated that for SCI patients, occurrences of abnormal activation patterns during attempted movement and abnormal processing in primary sensorimotor cortex during imagination of movement. In addition, they also found reduced volume of activation in primary sensorimotor cortex (4-8% with non SCI subject) and poor modulation of function with change in task demand.

A study carried out by Olsson, 2012 found that after SCI, reorganisation of the motor representation in prefrontal and parietal cortex during complex motor task engagement. In this study, the author implemented fMRI in order to investigate the relationship between specific physical training and preserved motor representations following complete SCI. This study also reported that after complete SCI the motor

cortex representation may not be preserved, and suggested that motor imagery depended strongly on the current ability to perform the task physically.

Furthermore, other neuroimaging and electrophysiological techniques such as transcranial magnetic stimulation (TMS), positron emission tomography (PET) and electroencephalogram (EEG) have also shown that sensorimotor cortex function becomes disorganised after SCI. TMS studies have indicated that there is an enlargement of cortical sensorimotor area dedicated to the preserved muscle above the level of the lesion (Levy Jr et al., 1990), enhanced excitability of motor pathway targeting muscles rostral to the level of spinal transection has also been suggested using TMS (Topka et al., 1991). PET studies suggested that SCI patients have shown wider activation of cortical and subcortical brain regions during hand movements (Bruehlmeier et al., 1998, Curt et al., 2002). Additionally, a study using EEG recordings has reported reorganisation of cortical motor activity towards a more posterior location following SCI (Green et al., 1998).

2.2.4 Assessment of Spinal Cord Injury

It is important to have a standard instrument to measure the severity of functional impairment and neurological deficits caused by SCI. This assessment tool can provide information about the neurological level of SCI, extent of injury to the spinal cord, and the resulting degree of impairment. Moreover, this assessment tool will ideally be capable of helping deliver predicted long-term outcomes for the patient and facilitate communication about their status to caregivers. Currently there are four classes of instrument used for assessing the degree of SCI in clinical and research arenas. These include neurological, functional, neuroimaging and electrophysiological assessments (Steeves et al., 2007, Lammertse et al., 2007).

Neurological examinations are carried out in order to assess the severity and location of lesion(s) in the spinal cord. This assessment uses scales to categorise motor and/or sensory function which depends on the response of the patient and whether he/she is able to cooperate and follow the given instructions. Hitherto, various neurological assessments have been developed for the assessment of SCI; the Frankel scale (van

Middendorp et al., 2011), Yale scale (Daverat et al., 1988), University of Miami Neuro-Spinal Index (UMNI) (Klose et al., 1980), National Acute Spinal Cord Injury Studies scale (NASCIS) (Hadley et al., 2013) and American Spinal Injury Association (ASIA) scale (Maynard et al., 1997). Although there are plenty varieties of neurological assessment to choose from, only a few are widely practised whilst others have not received such widespread acceptance and recognition. The ASIA scale is referred to as the standardised clinical examination of motor and sensory function for use in the case of traumatic SCI (van Middendorp et al., 2011).

Functional assessment is an instrument which implements a scale for measuring the degree of independence by which a neuro-impaired patient can perform specific motor and cognitive tasks. Scales for functional assessment include the Quadriplegic Index of Function (QIF) (Gresham et al., 1986), the Walking Index for SCI (WISCI) (Steeves et al., 2007), the Barthel Index (Tomassen et al., 2000), the Functional Independence Measure (FIM) (da Silva et al., 2012), the Spinal Cord Independence Measure (SCIM) (Glass et al., 2009), and the Spinal Cord Injury Functional Ambulation Inventory (Field-Fote et al., 2001). Among these functional assessments, SCIM III was recommended for classification and evaluation of patients with acute SCI (Furlan et al., 2011).

Sophisticated neuroimaging modalities now enable researchers to visually observe the anatomy of the neural axis and vertebral contents by non-invasive means. A number of these imaging techniques have been implemented for assessing SCI, namely multi-slice computed tomography (MSCT) (Rimkus et al., 2011), magnetic resonance imaging (MRI) (Lammertse et al., 2007), magnetic resonance imaging-diffusion weighted (MRI-DWI) (Shen et al., 2007), functional magnetic resonance imaging (fMRI) (Stroman, 2005), intraoperative spinal sonography (IOSS) (Mirvis and Geisler, 1990) and positron emission tomography (PET) (Roelcke et al., 1997). Although each imaging modality targets different structures within the spinal cord and canal, MRI has been suggested as the preferred imaging modality for evaluating the spinal cord after trauma (Lammertse et al., 2007).

Electrophysiological assessments operate by measuring bioelectric signals (typically EEG) such as somatosensory evoked potential (SSEP) (Curt and Dietz, 1997) and

motor evoked potential (MEP) (Curt et al., 1998). These assessments are particularly helpful when treating patients who cannot participate fully in a reliable physical examination. Electrophysiological assessment also offers additional diagnostic value for the assessment of spinal cord injury. Generally SSEP and MEP are related to the outcome/predictive of ambulatory capacity, hand and bladder function in patients with acute SCI (Curt and Dietz, 1999).

In the present study, the ASIA scale is the only neurological examination applied to assess the level of SCI, henceforth, this method of functional assessment is further discussed below.

2.2.4.1 American Spinal Injury Association (ASIA)

The International Standards for Neurological Classification of SCI were initially developed as the ASIA Standards in 1982 (Waring et al., 2010) and often referred to as "the gold standard" for neurological assessment of SCI (Marino, 2005). In order to improved reliability of assessment and classification, the ASIA scale has been revised in six editions (Marino, 2005) and major revisions were completed in 1992, 1996 and 2000 (Waring et al., 2010). The revision in 1992 comprises the selection of key muscles and the addition of two sensory examinations namely light touch (LT) and pin prick (PP) for the assessment (Marino et al., 2008). Additionally, revisions in 1996 and 2000 included changes related to classification rather than any practical motor and sensory examination procedures (Marino et al., 2008).

The ASIA scale consists of a two-stage protocol of examination and classification. The examinations include sensory (light touch and pin prick) and motor examination. Both of the sensory examinations, light touch and pin prick, are carried out at the key points (C2-C8, T1-T12, L1-L5, S1-S5) in each of the 28 dermatomes on both sides of the body. The light touch test is usually performed using cotton whereas the pin prick test is carried with a disposable safety pin that is stretched apart to allow testing on both ends (pointed and rounded end) (Maynard et al., 1997, Kirshblum et al., 2011).

The motor examination is performed through the testing of key muscles (C5-C8, T1, L2-L5, S1) in the 10 paired myotomes on both sides of the body, according to the rostral-caudal sequence. In myotomes that are not testable by this examination, such as C1-C4, T2-T12, L1, S2-S5, the motor level is presumed to be the same as the sensory level. In order to determine the completeness of the injury, the external anal sphincter is tested for assessing the presence or absence of voluntary anal contraction (Maynard et al., 1997, Kirshblum et al., 2011).

The classification process finalises the outcome of the sensory and motor level, sensory and motor score, the completeness of injury (incomplete or complete), the zone of partial preservation (for incomplete injuries) and the ASIA Impairment Scale (AIS grade). The severities of the injuries are classified either complete or incomplete based on the presence of sensory or motor function in the most caudal sacral segment as determined by the examination. The AIS grade reflecting the degree of impairment is categorised as A, B, C, D or E; details of impairments associated with each grade are provided in Table 2.2.

Table 2.2: ASIA impairment Scale (AIS grade). This table explains the level of impairment for each AIS grade. Adapted from [International Standards for Neurological and Functional Classification of Spinal Cord Injury (ISNCSCI) form].

Grade	Severity	Definition
A	Complete	No sensory or motor function is preserved in the sacral segments S4-S5
B	Sensory incomplete	Sensory but not motor function is preserved below the neurological level and includes the sacral segments S4-S5, AND no motor function is preserved more than three levels below the motor level on either side of the body.
C	Motor incomplete	Motor function is preserved below the neurological level**, and more than half of key muscle functions below the single neurological level of injury have a muscle grade less than 3 (Grades 0–2)
D	Motor incomplete	Motor function is preserved below the neurological level**, and at least half (half or more) of key muscle functions below the neurological level of injury have a muscle grade of 3 or more
E	Normal	Motor and sensory function is normal

2.3 Neural Control of Movement

Movements can be referred to as changes of postures either consciously (voluntarily movements) or automatically (reflex/involuntarily movements) that serve as a platform for interacting and communicating with the physical world (Brooks, 1983). Voluntarily and reflex movements are produced by the synchronised, spatiotemporally coordinated patterns of skeletal muscles contractions and relaxations controlled by neural circuits. Activation and inhibition of these neural circuits is initiated and coordinated by the central nervous system (CNS) (Figure 2.3) (Berkowitz, 2012, Groenewegen, 2003, Purves et al., 2001).
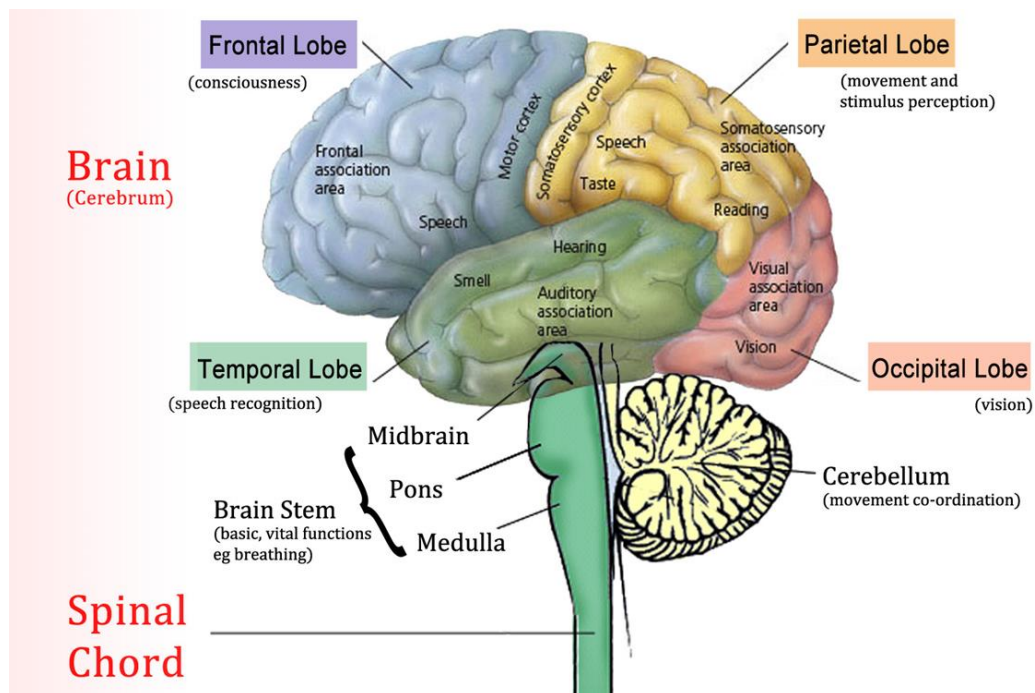
Figure 2.3: Central nervous system. This figure shows components of the central nervous system and indicates the function of various brain regions. Adapted from [www.humananatomydb.com/central-nervous-system-structure/].

CNS consists of two main components; the brain and spinal cord. The brain is responsible for integrating sensory information and synchronising conscious and unconscious bodily functions, whereas the spinal cord acts as conduit for transmitting motor and sensory signals between the brain and the rest of the body. The spinal cord is also responsible for the spinal reflex (Martini, 2005a). Motor and sensory signals within the spinal cord are retrieved and/or conveyed from/to skeletal muscles through mechanisms known as neural circuits (Purves et al., 2001).

Neural circuits are a combination of organised neurons (shown in Figure 2.4) that process specific information to perform a function. Essentially, neural circuits in the spinal cord are formed by 3 main elements: afferent neurons, efferent neurons and interneurons/local circuit neurons. Afferent neurons are nerve cells that transmit sensory information towards the CNS, while efferent neurons are nerve cells that transmit motor information outwards from the CNS. The third element, local circuit neurons, are nerve cells that mediate interactions between the sensory (afferent) and motor (efferent) systems (Purves et al., 2001).
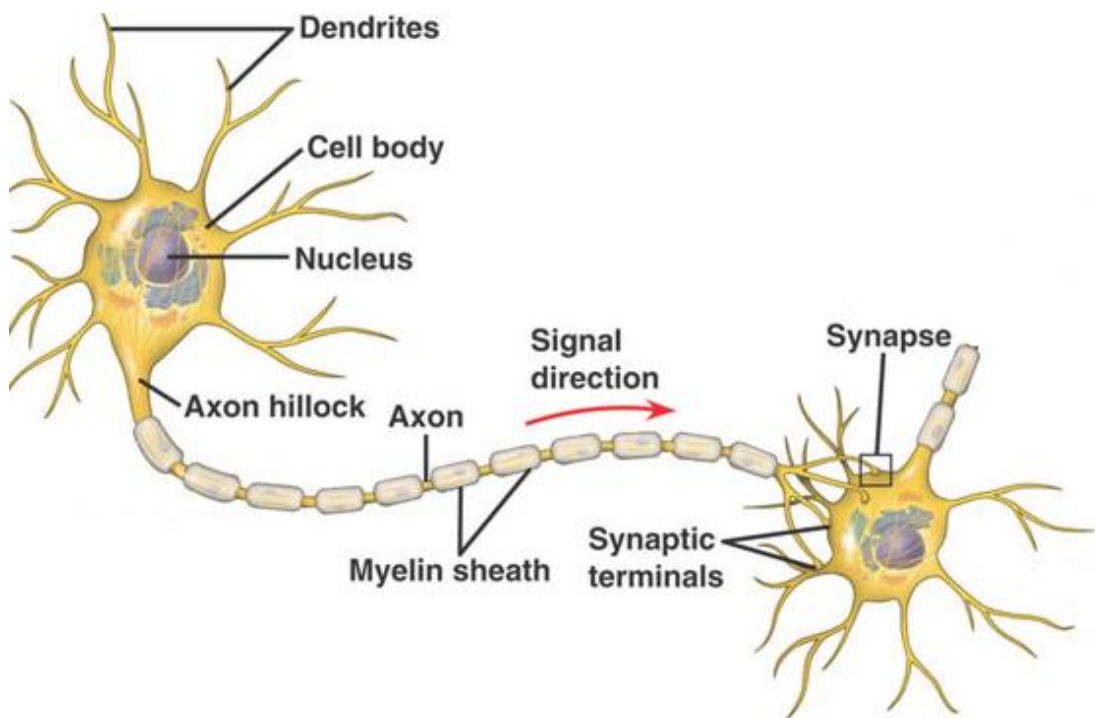
Figure 2.4: Neural circuits. This figure shows the structure of a prototypical neuron. Each neuron is made of a cell body (contain the nucleus), dendrites (that conduct impulses towards the cell body), an axon (carries impulses away from cell body) and synapses (contact points between axon of one neuron and dendrite of another neuron). Adapted from [www.pmgbiology.com/tag/nerve/].

Neural circuits are responsible for performing various functions, one of which is controlling movement. There are four distinct subsystems of neural circuits that are involved in motor control. These are upper motor neurons, lower motor neurons, the cerebellum and basal ganglia (see Figure 2.5). Each of the subsystems plays an important role in the control of movement. For instance, upper motor neurons carry motor information to the lower motor neurons, whereas lower motor neurons

innervate muscle fibres (motor neuron pool), effectively providing a link between upper motor neurons and muscles. The cerebellum modulates activity, acting to reduce the error between intended and actual movements by integrating information from sensory systems. Lastly, the basal ganglia is responsible for preparing upper motor neurons for movement and suppressing unwanted movement (Purves et al., 2001, Monkhouse, 2005).
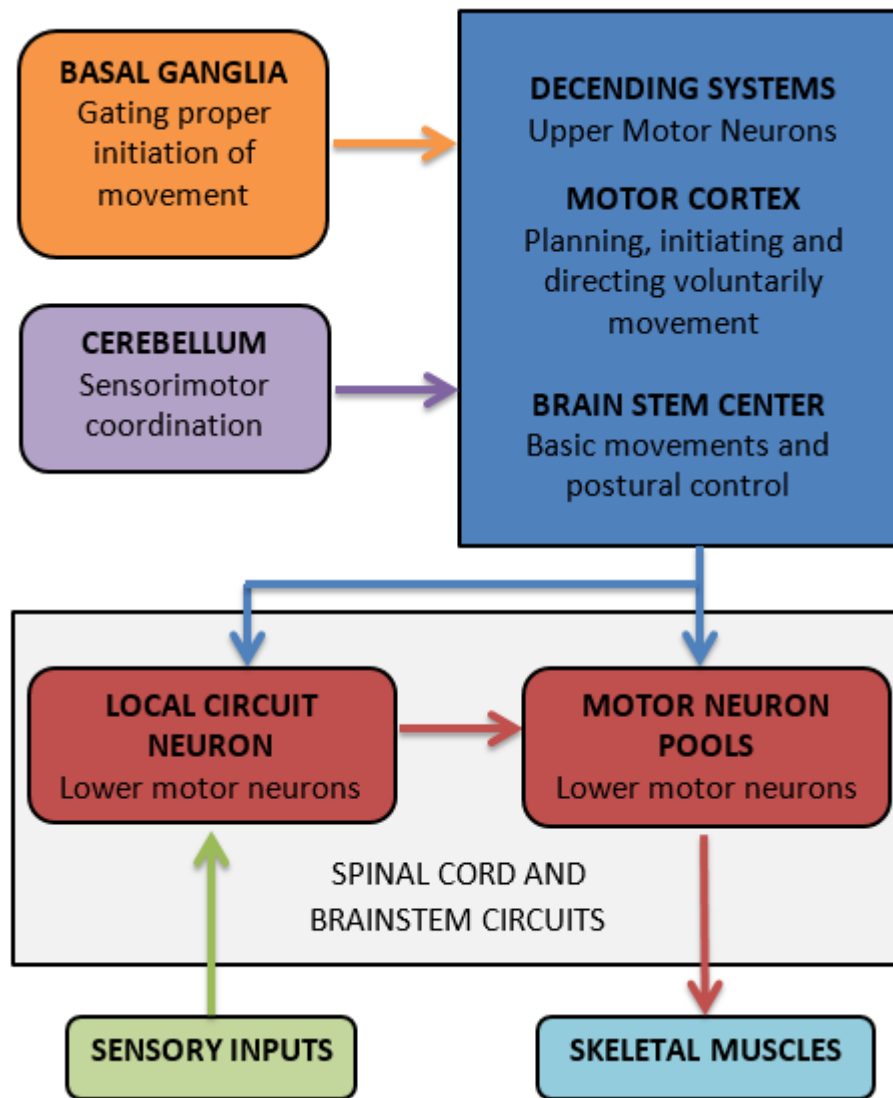
Figure 2.5: Neural structures for control of movement. This figure illustrates the four distinct subsystems involved in control of movement; upper motor neuron, lower motor neuron, the cerebellum and the basal ganglia. Adapted from (Purves et al., 2001).

2.3.1 Voluntary and Reflex Movement

Generally, movement play a major role in enabling the human body to interact and communicate with the outside world. Movement can occur in two different condition and/or situation, which are voluntary and reflex movements, introduced above. Although both of these movements controlled by the CNS, they are inherently different in the sense that voluntary movements are self-generated whereas reflexes are stimulus-bound (Prochazka et al., 2000).

Voluntary movements are initiated from the cerebral cortex to accomplish a specific goal. This may also be categorised as higher order movement because it is initiated by free will and can be performed both automatically and at the level of conscious awareness. Although voluntary movements can be performed automatically as a reflex movement (evoked by sensory stimulus), it is not necessary for an external stimuli to precede the movement. Motor learning processes are also evident in voluntary movements, which improve through experience and learning; i.e. performance improves with practice (Ghez and Krakauer, 1991, Ito, 2012).

On the other hand, reflex movements operate within the spinal cord and brainstem, not necessarily requiring direct involvement from the cerebral cortex. Reflex movements are rapid responses to sensory stimuli which are executed solely by an automatic pattern of activity. In addition, reflexes can be considered as a built-in safety mechanism that protects the human body from harm by reacting to potentially harmful external stimuli (Ito, 2012, Martini, 2005a).

2.3.2 Upper Motor Neurons and control of movement

Upper motor neurons (UMNs) are motor neurons that originate either in the motor region of the cerebral cortex or in the brainstem motor centres. UMNs originating in the cortex are responsible for initiation of voluntary movements and for complex spatiotemporal sequences required for skilled movements. On the other hand, UMNs that originate in the brainstem are essential for ongoing postural control and are highly related to basic navigational movements (Sach et al., 2004, Monkhouse, 2005, Purves et al., 2001, Snell, 2010). UMNs carry motor information down to the lower

motor neurons through descending motor tracts such as pyramidal tracts and extrapyramidal tracts (shown in Figure 2.6) (Snell, 2010).

The pyramidal tracts consist of corticospinal and corticobulbar (Harvey et al., 2008). The corticospinal tract plays a major role in controlling movements that required flexibility and skill (Martin, 2005), whereas the corticobulbar tract is responsible for speech and swallowing functions (Urban et al., 1998).

Aside from these broad functions, the extrapyramidal tract comprises of 5 separate nerve bundles; namely, the reticulospinal, vestibulospinal, rubrospinal, testospinal and olivospinal tracts. The reticulospinal tract is concerned with controlling respiration, blood vessel diameter and muscle tone. The vestibulospinal tract is responsible for adjusting the position of the head and body during angular and linear acceleration. The rubrospinal tract provides communication to influence flexor muscle tone. The testospinal tract is responsible for movement of the head in respond to visual and auditory stimuli. Finally, the olivospinal tract is involved with reflex movements which receives stimuli from within the body (Sembulingam and Sembulingam, 2012, Costanzo, 2010, de Oliveira-Souza, 2012, Snell, 2010).
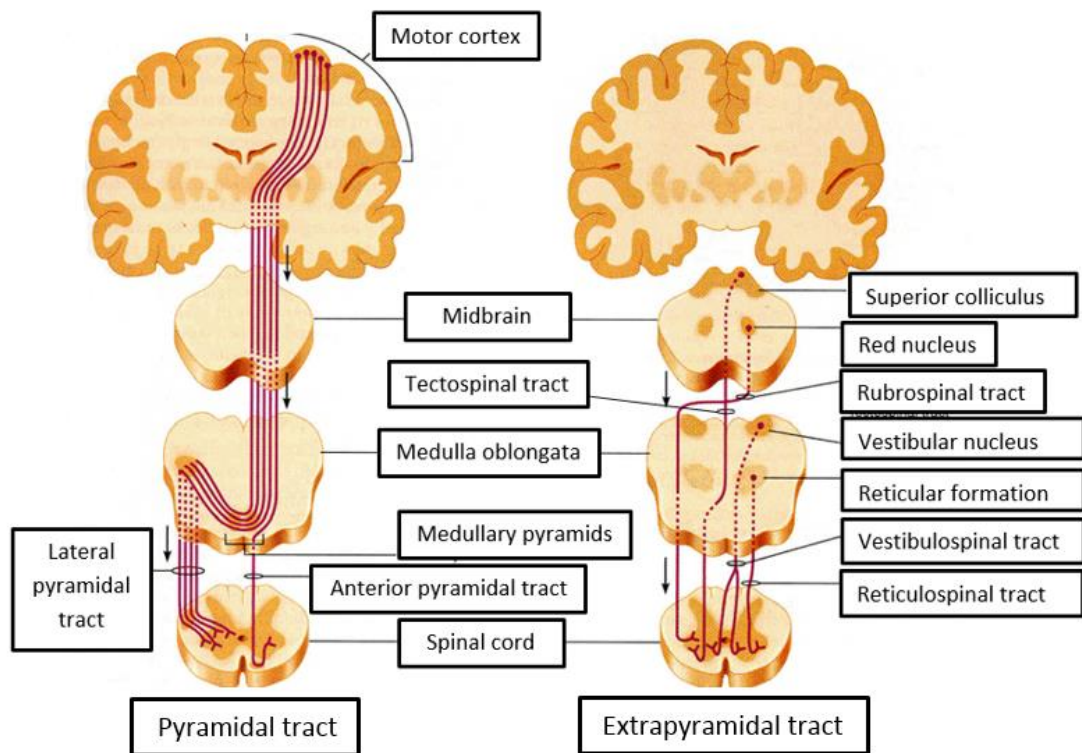
Figure 2.6: Pyramidal and extrapyramidal tracts. This figure shows the pyramidal tract (on the left) and extrapyramidal tract (on the right). The pyramidal tract only displays the lateral pyramidal tract, whereas the extrapyramidal tracts shown are vestibulospinal, rubrospinal, tectospinal and reticulospinal tracts. Adapted from [www.studyblue.com/notes/neural-pathways-the-pyramidal-and-extrapyramidal-systems].

2.3.3 Lower Motor Neurons and control of movement

Lower motor neurons (LMNs) are located in ventral horn grey matter of the spinal cord and in motor nuclei of cranial nerves in the brainstem. LMNs are the only neurons that innervate skeletal muscle fibres and serve as a link between UMNs and muscles (Figure 2.7). LMNs therefore play a crucial role as the final pathway for transmitting the neural information from the central nervous system to skeletal muscles (Purves et al., 2001, Snell, 2010, Sembulingam and Sembulingam, 2012).
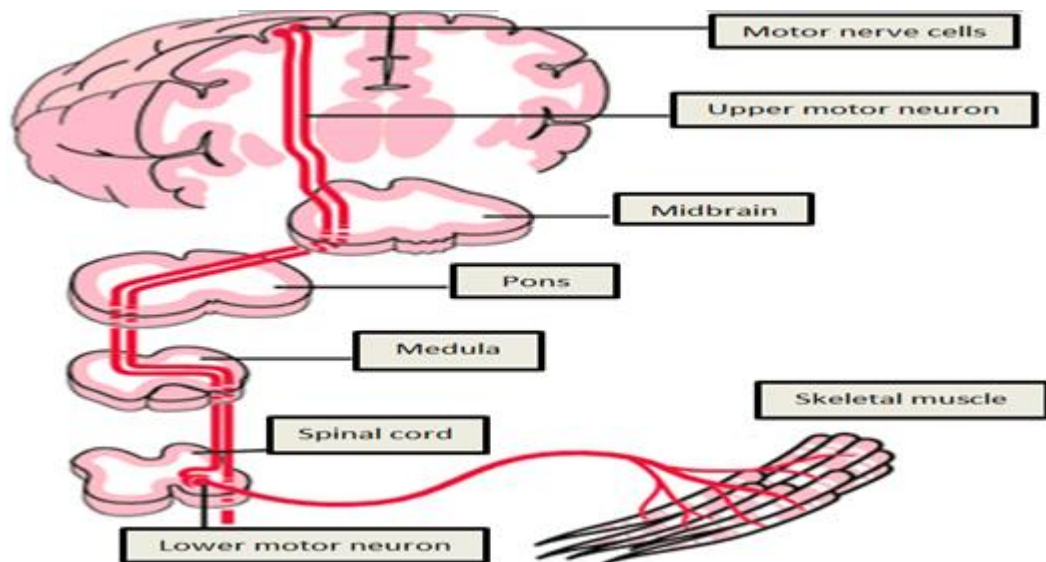
Figure 2.7: Lower motor neurons circuit. This figure illustrates the connections between upper motor neurons, lower motor neurons and skeletal muscle. Adapted from (Damjanov, 2000).

Generally LMNs are comprised of three types of motor neurons; alpha, beta and gamma motor neurons (Figure 2.8). Alpha motor neurons (Alpha MNs) have a large cell body and a well characterised neuromuscular ending. Alpha MNs innervate extrafusal muscle fibres and are responsible for initiating muscle contraction. On the other hand, beta motor neurons (Beta MNs) are smaller and less abundant than Alpha MNs. Beta MNs innervate both intrafusal and extrafusal muscle fibres. Beta MNs are responsible for control of both muscle contraction and responsivity of sensory feedback from the muscle spindle. Beta MNs are comprised of two subtypes; static (innervate nuclear fibres) and dynamic (innervate the nuclear bag fibres of muscle spindles). Gamma motor neurons (Gamma MNs) innervate intrafusal muscle fibres and are responsible for controlling the sensitivity of muscle spindles. There are also two subtypes of gamma MNs; static (connecting to nuclear chain fibres and nuclear bag fibres) and dynamic (connecting only to nuclear bag fibres) (Stifani, 2014, Costanzo, 2010, Manuel and Zytnicki, 2011).
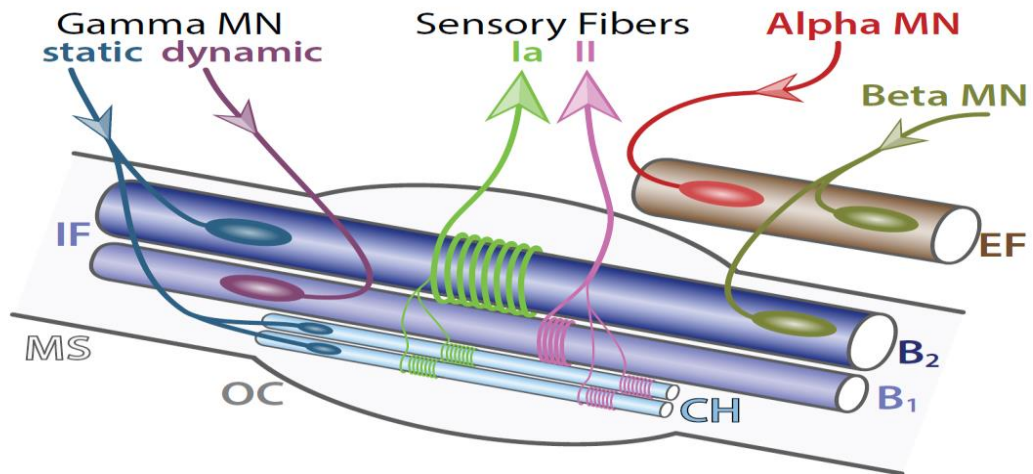
Figure 2.8: Components of lower motor neurons. This figure shows LMNs innervating a muscle spindle (MS). The alpha motor neuron (Alpha MN) innervates extrafusal fibres (EF) only, whereas the beta motor neuron (Beta MN) innervates both EF and intrafusal fibres (IF). The gamma motor neurons (Gamma MN) subtypes shown are static, connecting to nuclear chain (CH) and nuclear bag two (B2), and dynamic, which is connected to nuclear bag one (B1). The outer capsule (OC) is a membrane that isolates the muscle spindle from extrafusal fibres. Sensory afferent axons la and ll convey information to a sensory neuron. Adapted from (Stifani, 2014).

2.3.4 Cerebellum and control of movement

The cerebellum constitutes approximately 10% of the total weight of the brain. Neurons are more densely compacted in the cerebellum compared with other regions of the brain (Figure 2.3) (Glickstein, 2007). Although the cerebellum contributes somewhat to cognitive processing (Baillieux et al., 2008), speech processing (Ackermann and Hertrich, 2000) and emotion control (Schmahmann and Caplan, 2006), it is most frequently associated with movement control (Robinson, 1995).

The cerebellum is highly associated with movement control because of its role in regulating the activity of UMNs (Purves et al., 2001). It is responsible for a various range of movement controls; namely balance, posture and equilibrium, maintenance of muscle tone, locomotion, coordination and timing of movements (Wolf et al., 2009, Morton and Bastian, 2004, Sembulingam and Sembulingam, 2012). In addition to its direct role in motor function, the cerebellum also plays a major part in motor learning (Ito, 2000), integrating skilled voluntary movements (Sembulingam and

Sembulingam, 2012) and detecting the difference between intended and actual movements (Purves et al., 2001).

2.3.5 Basal Ganglia and control of movement

Basal ganglia are scattered masses of grey matter that represent a large and functionally diverse set of nuclei submerged in the subcortical substance of each cerebral hemisphere (Figure 2.9) (Sembulingam and Sembulingam, 2012, Purves et al., 2001). Basal ganglia are comprised of five nuclei; namely caudate, putamen, globus pallidus, substantia nigra and subthalamis nucleus, which are all closely related to motor function (Purves et al., 2001, Berkowitz, 2012). Each of these nuclei also serve as side loops to the cerebral cortex because they receive their input from, and project exclusively back to, the cerebral cortex (Everett and Kell, 2010). Although the basal ganglia is part of the nervous system concerned with movement control, it has no direct connections with the spinal cord (Snell, 2010). Despite having no direct connection with the spinal cord, basal ganglia can influence movement by regulating the activity of UMNs (same as cerebellum) (Purves et al., 2001).
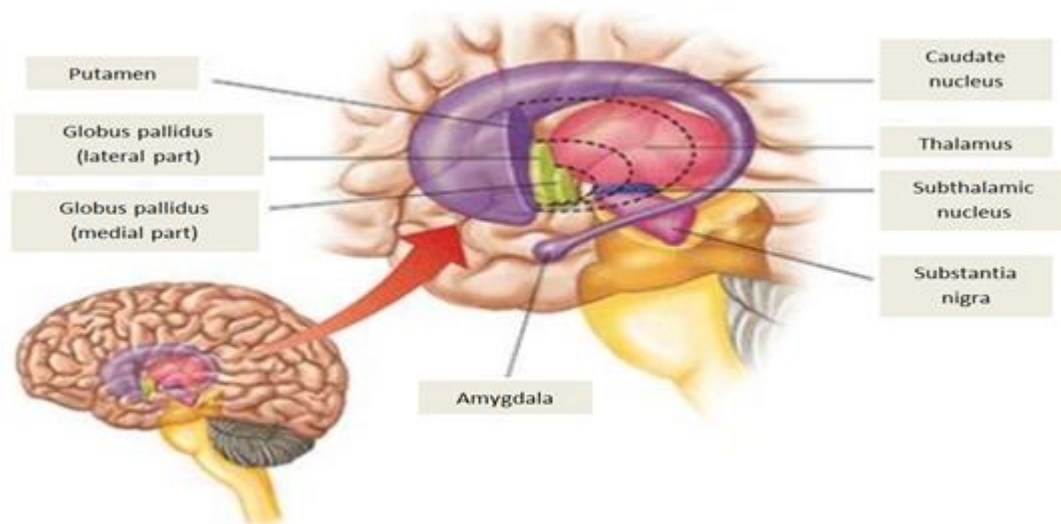
Figure 2.9: Basal ganglia. This figure shows the anatomy of the basal ganglia. Basal ganglia are comprised of the caudate, putamen, globus pallidus, and subthalamic nuclei and the substantia nigra. Adapted from [www.humanphysiology.academy/Neurosciences 2015/Basal Ganglia].

Basal ganglia plays a significant role in movement control where it facilitates desired movements and suppresses unwanted competing movements (Mink, 1996), planning and executing smooth movements (Costanzo, 2010), coordination of skill movements, regulation of automatic associated movements and control of muscle tone (Sembulingam and Sembulingam, 2012).

2.4   Brain Computer Interface

BCI is a communication method based on neural activity generated by the brain, and as such is independent from the normal output pathway of peripheral nerves and muscles. A BCI operates by detecting specific signatures in the user's ongoing brain activity that relates to their intention to initiate control and translates these patterns into control commands. A BCI therefore establishes a direct connection between the brain and an external device, providing an alternative output channel for the brain other than voluntary adaptive control by the user (Vallabhaneni et al., 2005, Wolpaw et al., 2000, Pfurtscheller, 2004, Muller-Putz et al., 2011, Bashashati et al., 2007).

Usually a BCI is categorised either based on the nature of the input signal or the input signal processing modality. Based on the nature of the input signal, BCI systems can be categorised as either endogenous or exogenous. Endogenous BCI systems are based on self-regulation of brain rhythms, potentially through operant conditioning, or in other words, the user's ability to control their electrophysiological activity. For instance, users can learn to modulate the signal power in a frequency band measured from EEG at a specific location to manipulate a target. Endogenous BCI systems also enable the user to have direct interaction with their environment, operate at free will, and independent of any external cues or stimulation (Nicolas-Alonso and Gomez-Gil, 2012, Kleber and Birbaumer, 2005, Roberto Hornero, 2012).

On the other hand, exogenous BCI systems depend on neural activity which is stimulated by an external stimulus. These systems typically use electrophysiological activity evoked by external stimuli, for instance changes in EEG amplitude caused by an infrequent auditory or visual stimulus. Exogenous BCI systems do not required

extensive training; however, the presentation of stimuli is a necessity (Nicolas-Alonso and Gomez-Gil, 2012, Kleber and Birbaumer, 2005, Roberto Hornero, 2012).

Depending on the input signal processing modality BCI systems may be categorised as either synchronous or asynchronous. Synchronous BCI systems operate using a cue. Presentation of the cue triggers a predefined measurement window for analysing brain signals, from which control commands are derived. In this type of synchronous BCI system the user needs to pay attention and respond accordingly to the cue, therefore onset of goal-directed mental activity is detected and associated with the specific cue (Hazrati and Erfanian, 2010, Tsui and Gan, 2007).

Asynchronous BCI systems do not require the use of external cues, rather they operate on a self-pace basis (Nooh et al., 2011). The main advantage of this type of system is that it offers the user a more natural mode of interaction where they control the BCI output according to their needs, at their own pace (Townsend et al., 2004). Due to this mode of operation asynchronous BCI systems have to continuously analyse brain signals, whether or not the user requires a specific action to be taken, making these systems more complex and computationally demanding than synchronous BCIs (Tsui and Gan, 2007).

The fundamental goal of a BCI system is to proficiently detect and distinguish different signatures of brain activity associated with specific intentions or mental tasks (Millán and Carmena, 2010). These brain signatures are later translated into commands that are capable of communicating and/or controlling assistive and augmentative devices. Another consideration in BCI system design, other than the operational category described above, is the functional components which combine to build a working BCI system.

Normally BCI systems are comprised of four main components; a brain signal acquisition, mental effort, feedback and signal translation (Pfurtscheller, 2004, Rajyalakshmi et al., 2013). The first component focuses on the modality of extracting measurements of neural activity generated by the brain. Following the first component, mental effort refers to the technique(s) capable of affecting or modifying the acquired brain signal. Feedback plays a major role in the training phase, user

learning and overall successful implementation of the BCI system. Crucially, the final stage of the BCI system is to translate the brain signature into the correct commands for use by augmentative and/or assistive devices. Further details of each of these BCI components are provided in the following sections.

2.4.1 Brain signal acquisition for BCI

BCI systems use brain signals as the main input in order to identify user intention and translate this into a command. Recording signals from the brain and interpreting them into useful electrical signals is the fundamental principle behind each BCI system. In general two types of brain signal are used to infer and describe user attention; electrophysiological activity and haemodynamic responses (Purkayastha et al., 2014, Castermans et al., 2013).

Electrophysiological activity is produced by the processes of communication throughout neural circuits. Neurons generate ionic currents which are transmitted across neuronal ensembles using the combination of nuclei, axons, synapses and dendrites (Purves et al., 2001). In general, current flow through a neuron can be simplified as a dipole conducting current from source to sink along the dendritic trunk. Conservation of electric charge enforces the current loop to be enclosed by extracellular current flow even through the most distant part of the neuron. Both intracellular (primary) and extracellular (secondary) currents contribute to scalp-recorded electric potentials and magnetic fields measured outside the head (Baillet et al., 2001). Electrophysiological activity is measured in EEG, magnetoencephalography (MEG), single unit activity (SUA), multi-unit activity (MUA), local field potential (LFP), and electrocorticography (ECoG) recording (Purkayastha et al., 2014, Castermans et al., 2013).

In contrast, haemodynamic responses measure the ratio of oxygenated (blood carrying oxygen) to deoxygenated (blood with no oxygen) haemoglobin level changes in blood flow; i.e. a blood oxygenation level dependent (BOLD) signal. Normally increases in blood flow correspond with increases in glucose metabolism in populations of active neurons. Additionally, in an active population of neurons the

BOLD signal changes due to increased flow of oxygenated blood which surpasses deoxygenated blood. The changes of local ratio of oxygenated blood to deoxygenated blood also cause increase in magnetic resonance effects (Laureys and Tononi, 2011). Haemodynamic changes can be quantified using functional magnetic resonance imaging (fMRI), positron emission tomography (PET) and near infrared spectroscopy (NIRS) neuroimaging techniques (Purkayastha et al., 2014, Castermans et al., 2013).

In BCI systems, both electrophysiological and haemodynamic responses are capable of indicating user intentions using invasive (Wang et al., 2013a, Lal et al., 2004, Liang and Bougrain, 2012, Piangerelli et al., 2014) and non-invasive (Millan et al., 2009, Karim et al., 2006, Tavella et al., 2010, Ahmed et al., 2014) approaches.

2.4.1.1 Invasive Brain Computer Interface

Invasive BCI systems require implantation of microelectrode arrays either inside the skull or cortex. This may involve complex, clinically perilous brain surgery in order to record neural activity from and/or stimulate neuronal tissue (Cheung, 2007, Biran et al., 2007). Invasive BCIs should only be utilised when safe for the user and where there is evidence to suggest that it will provide significant improvements in function compared with non-invasive systems. In general there are two types of invasive BCI; intracranial and intracortical (Brumberg and Guenther, 2010).

The intracranial modality uses microelectrode arrays placed on the cortical surface either outside the dura mater, known as epidural electrocorticography (ECoG), or under the dura mater, known as subdural ECoG. Intracranial methods focus on recording neural activity at a mesoscopic level (population of neurons); for instance, recording of the cortical field potential through ECoG (Millán and Carmena, 2010, Nicolas-Alonso and Gomez-Gil, 2012, Brumberg et al., 2010). ECoG may also be referred to as intracranial electroencephalography (iEEG), and requires that a craniotomy be performed in order to implant electrodes on the cortical surface(Ahmed et al., 2014). Usually ECoG applies Platinum/Iridium (Pt/Ir) electrodes and typically records measures from the local field potential (LFP),

including levels of synchronous activity. ECoG can be used as a platform for diagnosing the foci of seizure activity in patients with pre-surgical epilepsy, thus intracranial electrode placement is required to localise pathological tissue for surgical ablation (Morshed and Khan, 2014).

Conversely, intracortical neuronal recordings measure electrical signals from the grey matter of the brain by implanting microelectrode arrays inside of the cortex. This modality is capable of recording neural activity at both the microscopic and mesoscopic levels; for example, recording of single-unit activity (SUA), multi-unit activity (MUA) and LFP. Both SUA and MUA are observed by applying a high pass filter (>300 Hz), whereas LFP is obtained by using a low pass filter (<300 Hz), to intracortical recordings (Waldert et al., 2009). Intracortical recordings can be acquired using single microelectrodes and multi-electrode arrays (Castermans et al., 2013, Nicolas-Alonso and Gomez-Gil, 2012).

Microelectrode techniques are capable of recording neural activity and stimulating neuronal populations simultaneously. Action potentials from a neuron may be recorded by placing the electrode approximately 150μm from the cell (Donoghue, 2008). The recording process can be carried out either from single neuron (SUA) or multiple neurons (MUA) (Lebedev and Nicolelis, 2006).

Multi-electrode arrays share the same functions as microelectrode techniques. These may be comprised of multiple micro wires together in a bundle or a silicon probe platform with etched electrode arrays (Donoghue, 2008). One model of microelectrode array that has been approved by the FDA for use in human studies is the Utah Intracortical Electrode Array (UIEA). The UIEA consists of 100 small diameter silicon micro needles insulated with polyimide and built on a square grid with 400 µm spacing. The UIEA can be inserted 1.5 mm deep into the cerebral cortex (Fernandez et al., 2014, Nordhausen et al., 1996).

2.4.1.2 Non Invasive Brain Computer Interface

In a non-invasive BCI, there is a reduced risk for the user because surgery is not required to record neural activity. Instead brain signals are recorded from outside the head, typically from the scalp. There are five prominent recording non-invasive neuroimaging modalities which may be used in a BCI. These five recording modalities include PET, MEG, fMRI, NIRS and EEG (Morshed and Khan, 2014, Ahmed et al., 2014, Nicolas-Alonso and Gomez-Gil, 2012).

PET is a neuroimaging technique capable of remotely monitoring and recording of brain activity. PET utilises a radionuclide tracer of biologically active molecules which is introduced into the body either by injection or swallowing. The biologically active molecules are administered in micromolar or nanomolar concentrations, labelled with short lived positron-emitting isotopes. An imaging system then constructs a series of three dimensional images of functional bodily processes by detecting gamma rays emitted by the radionuclide tracer (Morshed and Khan, 2014, Quigley et al., 2011, Castermans et al., 2013, Purkayastha et al., 2014).

MEG measures the magnetic field induced by intracellular currents flowing through neurons (Baillet et al., 2001, Waldert et al., 2009). Generally, these magnetic fields are very weak, thus the MEG system requires effective magnetic shielding to minimise interference from external magnetic fields. Furthermore, specially designed magnetic sensors called superconducting quantum interference devices (SQUID) are used for recording magnetic fields in MEG. SQUID comprises of an array of coiled superconducting wires cooled by immersion in liquid helium (Purkayastha et al., 2014, Castermans et al., 2013, Nicolas-Alonso and Gomez-Gil, 2012).

fMRI detects the deviations of magnetic fields influenced by haemoglobin ratio between oxygenated to deoxygenated of blood flow (BOLD). Substances from oxygenated and deoxygenated blood, for example, oxyhemoglobin and deoxyhemoglobin, have huge implications on the magnetic field due to their different magnetic properties. This is because deoxyhemoglobin is pragmatic and causes inhomogeneity of the nearby magnetic field, whereas oxyhemoglobin is diamagnetic and has only a small effect on the nearby magnetic field (Purkayastha et al., 2014).

Due to these magnetic properties, higher concentrations of oxyhemoglobin lead to a better image intensity (Ogawa et al., 1990). This also enables fMRI to provide accurate localisation of active regions within the brain (Castermans et al., 2013).

NIRS is an optical spectroscopy technique capable of assessing brain function haemodynamically by detecting changes of haemoglobin concentration associated with neural activity using infrared light. Infrared light can penetrate the skull to a depth of approximately 1-3 cm below the surface, thus this technique can measure activity from superficial cortical layers only (Castermans et al., 2013, Nicolas-Alonso and Gomez-Gil, 2012). Variation of the haemoglobin concentration provides information regarding blood oxygenation measured based on the optical absorption properties of oxyhemoglobin and deoxyhemoglobin (Purkayastha et al., 2014). The degree of oxygenation in cortical tissue is effectively determined by shining near-infrared light into it and measuring the amount that emerges, unabsorbed (Boas, 2004).

EEG is a non-invasive modality that measures the electric brain activity induced by the secondary current from excitation of cortical neurons (Baillet et al., 2001). The EEG signal is typically considered in terms of five set frequency components, or bands; delta (δ 1-3 Hz), theta (θ 4-7 Hz), alpha (α 8-12 Hz), beta (β 13-30 Hz) and gamma (γ above 30 Hz) (Purkayastha et al., 2014, Roh et al., 2015, Safri and Adnan, 2015). In general, EEG recording systems require placement of electrodes on the surface of the scalp in a specific configuration referred to as a montage. Usually the electrodes are made of silver chloride (AgCl) (Sinclair et al., 2007) and the recording montages used for their positioning may be the standardised 10/20, 10/10 or 10/5 electrode placement systems (Jurcak et al., 2007). Moreover, some montages comprise dense configurations of up to 128 or 256 electrodes (Teplan, 2002). In order to record good quality of EEG, the contact impedance between the electrode and scalp should be below 5 KΩ. To achieve this, conductive paste/jelly/gel is used to provide a conductive path and reduce impedance between the electrode and scalp (Teplan, 2002).

2.4.2 Brain signature in BCI

In the BCI platform, it is essential to extract and translate a brain signature into appropriate commands for controlling augmentative and/or assistive devices. Brain signature refers to unique characteristics produced by changes of mental processes or state (van Gerven et al., 2009). The measured brain signature is typically an event related potential (ERP; based on EEG recording) or event related field (ERF; based on MEG recording) (McFadden and Rojas, 2013). An ERP is the recorded changes of EEG potential that are time-locked to an event/stimulus, whereas an ERF is the corresponding magnetic field changes extracted from MEG (Hillyard and Kutas, 2002).

In general, an ERP is comprised of two type of response; evoked and induced responses (Tallon-Baudry and Bertrand, 1999). Evoked responses are phase- and time-locked to an event/stimulus, thus by averaging the signal over repeated instances of the event/stimulus; unrelated activity is averaged-out leaving the evoked response. Conversely, induced responses are time-locked but not phase-locked to the event. Thus to determine the induced response, spectral power over time during each stimulus presentation may be calculated before averaging, therefore including non-phase-locked oscillatory activity in the quantification (van Gerven et al., 2009, Pfurtscheller and Da Silva, 1999). Although evoked and induced responses have contrasting phase relationships with a timed event, both play a major role in generating that output control signal in BCI systems. For instance, evoked responses such as the slow cortical potential, visual evoked potential and P300, as well as such induced responses as event-related desynchronisation/ synchronisation, have provided brain signatures to drive BCI systems.

Slow cortical potentials (SCPs) are slow event-related direct current shifts of the EEG signal (Strehl et al., 2006), caused by changes in the depolarisation levels of upper cortical dendrites (Vallabhaneni et al., 2005, Birbaumer et al., 2000). Generally, negative SCPs correlate with increased neuronal activity, whereas positive SCPs coincide with decreased activity in individual cells (Birbaumer et al., 1990). SCPs can be self-regulated by both healthy users and neuro-impaired patients through training. In BCI systems, SCPs have been used to derive a control signal for

moving a cursor, target selection and controlling movement of an object on a computer screen (Hinterberger et al., 2004, Birbaumer et al., 2000, Birbaumer et al., 2003).

Visual evoked potentials (VEPs) are another type of evoked response commonly used in BCI systems. Implementation of VEPs as control signals can be seen in applications such as controlling a mobile robot (Kapeller et al., 2013). VEPs refer to modulation of brain activity in the occipital area in response to a visual stimulus that oscillates at a constant frequency, such as flashing light stimulation, check board lattice, gate and random-dot map (Nicolas-Alonso and Gomez-Gil, 2012, Allison et al., 2008). In general, VEPs are distinguished based on the repetition rate of stimulation, i.e., transient visual evoked potentials (TVEPs) and steady state visual evoked potentials (SSVEPs) (Wang et al., 2008). TVEPs occur when the visual frequency stimulation is below 6 Hz whereas SSVEPs occur in reaction to stimuli of higher frequencies (Gao et al., 2003).

The P300 evoked potential is a positive deflection in the EEG signal that occurs approximately 300ms after the onset of an attended oddball stimulus. In an oddball paradigm (Nicolas-Alonso and Gomez-Gil, 2012, Donchin et al., 2000) P300 is associated with the subject's attention being directed towards the infrequent oddball stimulus (van Gerven et al., 2009, Kleber and Birbaumer, 2005). If the user becomes habituated to the infrequent stimulus the P300 amplitude is decreased (Polich et al., 1996), whereas the P300 amplitude increases as oddball stimulus probability is reduced (Donchin et al., 2000). Generally, P300 is most noticeable in parietal and occipital electrodes compared other recording locations over the scalp (Brumberg and Guenther, 2010, Kleber and Birbaumer, 2005). Most notably, P300 is used to provide a control signal for BCI speller systems (De Vos et al., 2014, Chennu et al., 2013, Rivet et al., 2008).

Event related desynchronisation (ERD) and synchronisation (ERS) are components of induced responses that occur because of changes in oscillatory neuronal activity due to sensory stimulation or mental imagery (Pfurtscheller and Neuper, 2001). ERD refers to the decrease in synchronisation of neural firing that causes a decrease of power in a specific frequency band and can be identified by a decrease in the signal

amplitude with respect to a baseline. On the other hand, ERS is characterised by an increase of power in a specific frequency band due to the increased synchronisation of neural firing and can be identified by an increase in the signal amplitude (Vallabhaneni et al., 2005, van Gerven et al., 2009, Nicolas-Alonso and Gomez-Gil, 2012). In general, both ERD and ERS can be measured over the sensorimotor cortex within the mu (μ; 7-13 Hz) and beta (β; above 13 Hz) rhythms (Pfurtscheller and Neuper, 2001). Furthermore, both ERD and ERS have been extensively investigated for motor imagery tasks (Thomas et al., 2012, Yi et al., 2013).

2.4.3 Feedback in BCI

Feedback is one of the most important components of BCI systems as it forms a closed-loop system that consists of two adaptive controllers; namely the brain and the computer (Pfurtscheller, 2004). In BCI systems, feedback may be given in different forms such as visual feedback (Barbero and Grosse-Wentrup, 2010), auditory feedback (Nijboer et al., 2008), vibrotactile feedback (Cincotti et al., 2007) or robot assisted feedback control (Schwartz et al., 2006). All of these types of feedback serve the same purpose; to enable the user to optimally regulate their brain signature through a training phase (Mak and Wolpaw, 2009, Barbero and Grosse-Wentrup, 2010, González-Franco et al., 2011).

Although BCI feedback is capable of inducing cortical plasticity (Nicolas-Alonso and Gomez-Gil, 2012), there is little evidence that it is a critical factor for increasing BCI performance (Barbero and Grosse-Wentrup, 2010, Ramos-Murguialday et al., 2012). The essential point that needs to be considered when designing the feedback is the subject's current skill level (Barbero and Grosse-Wentrup, 2010).

2.4.4 Brain signature translation in BCI

One of the main parameters that affects the success and efficiency of BCI systems is the capability to detect the user's brain signature associated with intention to initiate control and translate it into control commands. The translation of brain signatures

into command signals consists of three stages; pre-processing, features extraction, and features translation (Wolpaw et al., 2002, Vallabhaneni et al., 2005). These three stages are implemented through signal processing algorithms which require a balance between computational demand, time, effort, complexity and performance.

2.4.4.1 Signal Pre-processing methods

In general, the recorded brain signal is always contaminated by artefacts predominantly of non-cerebral origin (Nicolas-Alonso and Gomez-Gil, 2012). These artefacts are caused by multiple factors and are highly capable of reducing the performance of BCI systems and interfere with the neurological phenomenon. The recorded EEG signal is usually contaminated by two sources of artefact; physiological and technical. Physiological artefacts are caused by the users themselves, such as electrocardiography (ECG and minor body movements. On the other hand, technical artefacts that are non-physiological and may be caused by impedance fluctuation, excessive electrode paste and power line noise (Teplan, 2002, Fatourechi et al., 2007) can also contaminate the EEG signal.

Due to the fact that it is practically impossible to record an artefact-free EEG signals, it is essential to pre-process the signal before implementing any further analysis methods. The EEG signal can be pre-processed using referencing, artefact rejection, temporal and spatial filtering.

Fundamentally, EEG signals are recorded based on relative measurements, most often using three types of electrodes; namely: active, reference and ground electrodes. Both active and reference electrodes are responsible for measuring potential changes over time, whereas the ground electrode is responsible for common mode rejection (rejecting common voltages, generally induced by noise, within active and reference electrodes) (Teplan, 2002). Measured EEG, at any instant, is the relative potential difference between the active and the reference electrodes, It is therefore essential to select a reference site with minimum brain activity, which may typically be either the nose, earlobe or mastoid (Dien, 1998, Teplan, 2002).

Artefact rejection is the process of discarding EEG trials/epochs that are contaminated with artefacts and can be performed either manually or automatically. Manual artefact rejection requires visual inspection of each individual EEG trial/ epoch and those which are overtly contaminated are discarded from further analysis. On the other hand, automatic artefact rejection is performed offline based on a predetermined threshold value (Fatourechi et al., 2007, Chadwick et al., 2011), for instance any trial/epoch where the signal voltage exceeds a threshold of $50\mu V/70\mu$ is rejected (Poli et al., 2011).

Independent Component Analysis (ICA) is one of the pre-processing method that has been widely applied to separate eye blink and muscle activity from EEG signal (Hsu et al., 2015). ICA capable of extracting the relevant information within noisy signals and allow the separation of measured signals into their fundamental underlying components (Wang and James, 2007). Wang and James, 2005 reported that, by pre-processed P300 wave using ICA, they manage to get better result with classification accuracy of 96.77% in comparison to simple classifier for classifying the word (only one error out of 31 characters).

Temporal filtering plays a major role in removing or attenuating unwanted frequencies from the raw signal, improving the signal-to-noise ratio (Wolpaw et al., 2002, Al-ani and Trad, 2010). For instance, Müller-Gerking et al., 1999 have proved that the classification accuracy of left hand, right hand, and foot movement can be increased by using a broad range filtering (8-30Hz) in comparison to narrow bands α (8-12 Hz), lower α (8-10 Hz), upper α (10-12 Hz), β (19-26 Hz) and γ (38-42 Hz).

Spatial filtering is also capable of increasing the signal-to-noise ratio and improving classification accuracy (Rivet et al., 2010, Model and Zibulevsky, 2006). Spatial filters isolate the relevant spatial information from the signal by selecting or weighting the coefficient from different electrodes. For instance, McFarland et al., 1997 demonstrated that common average reference (CAR) and Laplacian (LAP) methods are superior to ear-lobe referencing. This is because CAR and LAP enhance the focal activity from local sources (μ rhythm and β activity) and reduce widely distributed activity from distance sources (e.g. EMG and eye movements) (McFarland et al., 1997).

2.4.4.2 Feature extraction methods

Another important step in signal processing of the recorded brain signal is implementing a feature extraction method, where identification or isolation of certain attributes that describe the signal properties is performed. This process has a major impact on the effectiveness of subsequent classification. Additionally, feature extraction can also contribute to reducing computational effort, the amount of stored data and data redundancy (Rak et al., 2012). The three most common types of feature extraction implemented in BCI systems are broadly termed time-domain, frequency-domain and time-frequency.

Time-domain feature extraction focuses on waveform characteristics within a specific measurement window. For example, template matching feature extraction computes similarity or correlation between a pattern of recorded brain activity and a predetermined template filter. Output from the template filter with high correlation indicates that segments highly resemble the template, whereas low correlation suggests segments differ from the template (Krusienki et al., 2011). In addition, template matching approaches are also effective for detecting waveforms with consistent temporal attributes; for instance, this approach has been implemented for event detection (Haw et al., 2006) and P300 speller based BCI systems (Brunner et al., 2010).

Frequency-domain feature extraction methods examine the characteristics of signal frequency/spectral decompositions. For instance, the band-power feature extraction method investigates amplitude modulation over a specific frequency/frequency band by separating frequencies of interest from the signal using a bandpass filter. The filtered signal is then rectified by squaring or computing the absolute value. Adjacent peaks of the rectified signal are then smoothed together either using integration or low pass filtering (Krusienki et al., 2011). The implementation of this method in BCI applications is commonly used for extracting features related to motor imagery (Brodu et al., 2011) and mental tasks (Palaniappan, 2005).

Time-frequency feature extraction methods are capable of studying the recorded brain signal in both the time and frequency domains simultaneously. The most

common approach of this type implemented in BCI systems is the wavelet transform method. Wavelets refer to a simple oscillating amplitude function over time that is relatively localised in both time and frequency (Mohan Kumar and Dharani Kumar, 2014). In general, wavelets can be categorised into two categories; continuous and discrete (Cvetkovic et al., 2008, Al-Fahoum and Al-Fraihat, 2014). This approach builds a feature space from coefficients of wavelet transformations through decomposition of the recorded signal (in both of time and frequency domain at multiple resolution) using a modulated window shifted along of the recorded signal at various scales (Nicolas-Alonso and Gomez-Gil, 2012). Application of this method in the BCI field can be seen in localisation of ERP components (Bostanov, 2004), detection of motor imagery within the delta frequency range (Mason and Birch, 2000) and classification of motor tasks (Tolic and Jovic, 2013).

2.4.4.3 Feature translation methods

Feature translation plays a major role in converting the brain activity which reflects the user's intention into commands that are capable of communicating and controlling augmentative and/or assistive devices. For this purpose, two approaches commonly implemented are the regression method (McFarland and Wolpaw, 2005) or, the more popular approach, the classification method (Penny et al., 2000). Classification employs an algorithm that identifies a pattern of the recorded signal and partitions it into class labelled decision boundaries. Generally, the majority of implemented classification algorithms in BCI systems can be divided into four different categories; nearest neighbour, nonlinear Bayesian, linear and neural network classifiers.

Nearest neighbour is an instance type based classifier which categorises different classes according to their nearest neighbours using distance functions; namely, Euclidean, Mahalanobis, Manhattan (city block) and Minkowski distances (Walters-Williams and Li, 2010). k-nearest neighbour (k-NN) is one version of this classifier used in designing BCI systems (Yazdani et al., 2009, Aydemir and Kayikcioglu, 2013, Nanayakkara and Sakkaff, 2012). k-NN is a discriminative nonlinear classifier (Lotte et al., 2007) that determines a testing sample's class according to the majority

class of the *k* closest training samples (*k*-neighbour) (Aydemir and Kayikcioglu, 2013). Although *k*-NN has not received much attention in the BCI community, it has one advantage compared with other supervised machine learning techniques in that it can easily deal with problems normally associated with categorising multiple classes (Yazdani et al., 2009).

Nonlinear Bayesian classifiers categorise and separate different classes using nonlinear decision boundaries. Although this category of classifier is not widely used for designing BCI systems, it has managed to categorise different types of motor imagery (Solhjoo and Moradi, 2004) and succeeded in mental task classification (Barreto et al., 2004). The Baye's quadratic classifier is another variety of the nonlinear Bayesian classifier that has been used in designing BCI systems (Rezaei et al., 2006). This Baye's quadratic classifier assigns different classes based on probability. This is achieved by computing a *posteriori* probability and implementation of maximum a *posteriori* rule (Lotte et al., 2007)

Linear classifiers are based on discriminant algorithms that employ linear functions in order to distinguish separable different classes. One of the prominent linear classifiers used for designing BCI systems is the linear discriminant analysis (LDA) classifier (Aldea and Fira, 2014, Onishi et al., 2013, Lee et al., 2005). The LDA classifier functions based on the assumption of normally distributed data with an equal covariance matrix for related classes. It employs a separating hyperplane to distinguish different classes. For categorising two classes, the separating hyperplane is obtained through the projection that maximises the distances between the mean of two classes and minimises the interclass variance (Lee et al., 2011). On the other hand, several hyperplanes are used for designing a multiclass BCI system. In multiclass BCIs, the LDA classifier implements a 'one versus the rest' strategy for separating each class from all the others (Lotte et al., 2007).

Artificial neural network (ANN) is another one of the most used classifiers in designing BCI systems. The ANN classifier was motivated based on an elementary principle of the human neural operation system. One type of an ANN classifier is the Multilayer Perceptron (MLP) which comprised of several neuron layers; namely, input, hidden and output layers. In a fully connected architecture, the neurons of each

layer are connected to each neuron of the next layer, and the output layer determine the class of the input feature vector (Reby et al., 1997). Moreover, different combinations of these neuron layers would enable the classifier to determine the nonlinear decision boundaries (Lotte et al., 2007). Although there are a number of different architectures and learning paradigm of ANNs used as a classifier, the MLP architecture and variation of backpropagation learning paradigm is widely used for BCI systems (Haselsteiner and Pfurtscheller, 2000, Barbosa et al., 2009, Sridhar and Rao, 2012).

2.5 BCI and SCI patients

One ultimate purpose of a BCI system is to allow an individual with motor disabilities but cognitively intact, such as SCI patients, to have effective control over devices such as computers, speech synthesisers, assistive appliances or neural prostheses. BCI systems that include acquisition of the brain signals, analysis, translation and classification of the signals would enable SCI patients to drive devices and control applications without producing any overt behaviour (Rajyalakshmi et al., 2013). Besides that, an effective BCI would also increase an individual's independence, leading to an improved quality of life and reduced social burden (Bashashati et al., 2007).

It is undeniable that within past decades, a considerable number of research studies related to BCI applications have been conducted which produced profound and promising outcomes. It should be noted that most of this research has hardly at all involved the target user groups of patients, due to challenges of ethical approval and patient recruitment. Participation and involvement of patients groups such as SCI patients will provide significant impact towards the design of practical BCI systems. This is because healthy control subjects have full control over their limbs and their physiological activity/haemodynamic response behaves normally; whereas SCI patients have limited control over their limbs and their physiological activity/haemodynamic response may be affected by deafferentation and cortical reorganisation depending on the duration and level of injury. The involvement of SCI

patients in BCI research (non-invasive experiment) is summarised in Table 2.3 (Please refer to appendix I).

2.6   Limitations of Current Studies and Future Work

Implementation of real-time BCI applications will surely offer huge advantages to the SCI patient, especially in rehabilitation, communication and increasing their level of independency. This can be seen from the application of controlled functional electrical stimulation (FES) systems (Pfurtscheller et al., 2003), operating spelling devices (Birbaumer et al., 2000) and controlling an orthosis device (Pfurtscheller et al., 2000). Despite these achievements, existing BCI systems are still under the evolution process and constrained by limitation. The majority of these existing BCI systems share common issue with regards to multiple independent control channels due to the low dimensional control (degree of freedom) they currently afford (Mak and Wolpaw, 2009, Maye et al., 2011). This is because BCI systems with low degree of freedom are only capable of recognising a limited number of brain signatures/mental tasks that can be translated to control signals (Yong and Menon, 2015).

In order to overcome this issue, a number of approaches have been considered and investigated; the hybrid BCI system, multi-modal BCI system (Severens et al., 2013) and combination of motor imagery that involves multiple limbs (Pfurtscheller and Neuper, 2001). Although these approaches are capable of increasing the degree of freedom, none are appropriately efficient for neurological-impaired patients. Furthermore, combining two neuroimaging modalities may improve performance, however would inflict excessively high costs rendering it impractical to develop. In addition, neurological -impaired patients would face difficulties in learning how to control several modalities at the same time due to their disability (Severens et al., 2013). Moreover, neurological-impaired patients also have limited access/control over their limbs and their brain signatures are affected by deafferentation and cortical reorganisation of brain regions depending on the duration, level and type of the disease (Kokotilo et al., 2009).

Thus in this study, a non-invasive synchronised BCI approach is proposed capable of producing multi degree of freedom control signals using the same limb. Non-invasive BCI techniques are highlighted because invasive BCI systems require implantation of microelectrode arrays through complex and clinically dangerous brain surgery (Cheung, 2007, Biran et al., 2007). Furthermore, patients may also be potentially exposed to the traumatic operation, tissue damage and infection from the area of implantation to receive experimental, potentially ineffective technologies (Nicolas-Alonso and Gomez-Gil, 2012, Morshed and Khan, 2014). Apart from that, in comparison to other non-invasive techniques, EEG is the best choice due to portability, relative inexpensiveness and simplicity to use (Kaur et al., 2012, Nicolas-Alonso and Gomez-Gil, 2012). Nevertheless, in order to develop a less complex and computationally demanding BCI interface, a synchronous system would favourable compared with an asynchronous system (Tsui and Gan, 2007).

2.7   Objective of Proposed Study

Due to the limitations with the current BCI systems, the present study focuses on investigating the feasibility of developing a BCI system capable to operate with four degrees of freedom which can be controlled by the SCI population. The objectives of the present study are listed as follow:

1. Develop four degree of freedom BCI system based on imagination/intention of movement of single limb for SCI patients.
2. Extract a salient feature vector associated with various (four) directions from the brain signature component of SCI patients that capable of producing a robust and consistent control signal.
3. Examine and implement the proposed BCI system on healthy and SCI subjects.
4. Make comparison of results from healthy to SCI subjects and within the SCI subjects (comparison between paraplegic and tetraplegic subjects).

2.8   Summary

This chapter has elaborated on the fundamental elements related to SCI. In this regard, we have indicated that that spinal cord serves as a pathway in transmitting sensory/motor signals between the brain and the rest of the body. Besides that, the spinal cord is also responsible for spinal reflexes. Any damage/lesion to/at the spinal cord will cause the patient to be either tetraplegia/quadriplegia (injury within cervical segments) or paraplegia (injury within thoracic/lumbar/sacral/coccygeal segments). In general, the severity of functional impairment and neurological deficits caused by SCI are assessed using the ASIA scale and AIS grade.

This chapter has also presented the neurological mechanisms responsible for voluntarily and reflex movements. Reflex movements are based on stimulus-bound response and operate within the spinal cord and brainstem, reflecting a safety mechanism protecting the body from harm. On the other hand, voluntary movements are self-generated and initiated by the CNS through four key subsystems of neural circuits; namely upper motor neurons, lower motor neurons, the cerebellum and basal ganglia.

The current state of the art in BCI system design and involvement of SCI patients has been highlighted in order to emphasise the need to increase dimensional control signals of BCI systems. It has been shown that BCI systems are comprised of four main components, namely brain signal acquisition, mental strategy, feedback and signal analysis process. Apart from that, most BCI systems that involve participation of SCI patients (see Table 2.3) are mainly based on non-invasive techniques. Despite of this large number of BCI studies related to SCI patients, the majority of them share a common issue that is low dimensional control.

Chapter 3. Methods

3.1 Introduction

This study is interested in investigating and developing a BCI system capable of producing multi degree of freedom control using motor imagery and motor execution of a single limb for SCI patients. For this purpose, a non-invasive technique that focuses on extracting surface EEG signals associated with performing and imagining right wrist movements (burst, point-to-point centre out movement) in multiple directions (towards 3, 6, 9 and 12 o'clock) triggered by a visual cue is adopted. Further clarifications regarding the design, choice of parameters, analysis process and set-up for these experiments are detailed in this chapter.

3.2 Experimental Protocols and Procedures

The adopted acquisition protocol in this study is mainly based on motor imagery (kinaesthetic imagery) (Neuper et al., 2005) and motor activation paradigms (Hoffman and Strick, 1999) utilising the right wrist for burst, point-to-point centre out movement. These movements involved flexion, extension and ulnar/radial deviation of the right wrist referring from a neutral position (labelled '0' in Figure 2.3). Movement to the left (towards 9 o'clock direction) was performed by right wrist flexion, and to the right (towards 3 o'clock direction) was done by its extension. On the other hand, ulnar and radial deviations were required to move down (towards 6 o'clock direction) and up (towards 12 o'clock direction), respectively.

For data collection purposes, subjects were seated on a wheelchair facing a liquid crystal display (LCD) monitor at a distance of 1 metre. Subjects held a manipulandum using their right hand. The position of manipulandum was adjusted according to their need so that they were comfortable when performing the movements. Subjects were also attached to NeuroScan™ Synamps2 and Cambridge Electronic Design (CED) systems for EEG, EMG and movement signal recording. The experimental set up arrangement is depicted in Figure 3.1.
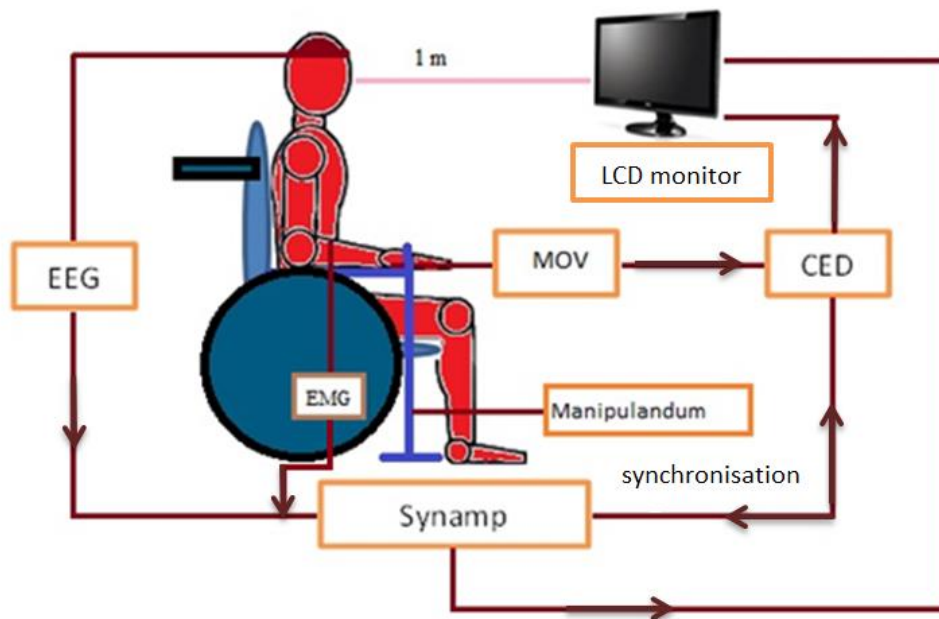
Figure 3.1: Experimental set up for data recording. The figure illustrates a subject sitting on a wheelchair with the manipulandum placed at his/her right side with a distance of 1m from the LCD monitor. The subject is also attached to Synamp and CED systems for EEG, EMG and movement signal recording. Both of the systems are synchronised during recording.

During data recording, subjects were required to hold the manipulandum and perform/imagine performing right wrist movements (burst, point-to-point centre out movement) towards multiple directions (3, 6, 9 and 12) triggered by a visual cue. When subjects see a cue, they have to move/imagine moving the manipulandum as fast as they can to the cue direction. On reaching the cue direction, subjects had to hold/imagine holding the manipulandum at the cue position for as long as the cue remained visible and reposition/imagine repositioning the manipulandum to the neutral position (0) following to the cue. While in the neutral position subjects were instructed to stay calm and relaxed.

The visual cue was displayed through a LCD monitor. It consisted of five small squares with a target initially placed at the centre of the screen whilst subjects were holding the manipulandum in the neutral position (0). The cue then switched to show the target at different directions (3, 6, 9 and 12) randomly with a delay time between consecutive cues of ten seconds (Pfurtscheller and Da Silva, 1999).

In this study, the acquisition protocol comprised of two types of experiment, namely motor task and motor imagery experiments. EEG, EMG and movement signals were recorded simultaneously and synchronised during both of these experiments. For each experiment, subjects participated in ten movements/ten imagination of movements sessions. In every session, there were twenty trials, in which right wrist movements were pseudo randomly directed towards one of four target directions (approximately five repetitions for each direction on average). Each trial consisted of two phases; the movement onset phase (from neutral to one of four different directions) and movement offset phase (from one of four different directions to neutral).

In total, after completing the experiments, subjects had performed and imagined performing four hundred right wrist movements in multiple directions (two hundred repetitions of wrist for each experiment and fifty repetitions for each direction of 3, 6, 9 and 12). Subjects committed one hundred minutes (on average) of their time in order to complete the experiment (approximately eighty minutes for acquisition protocol procedures and twenty minutes for the experiment set up). It is essential to emphasise that subject's participation was voluntarily. Before the experiments commenced, subjects were presented the participant information sheet. If subjects was happy with the explanation and gave consent then the experiment will start. Thus subjects were aware that they could withdraw at any time and it was not compulsory to complete all the sessions.

3.2.1 Motor Task Experiment

In this experiment, subjects were required to hold the manipulandum and performed an actual movement according to the visual cue (as explained in section 3.2). Subjects were presented with two types of visual cue. First visual cue instructed subjects to move the manipulandum from initial position (0) to the targeted direction (3, 6, 9 and 12) and the second visual cue instructed subjects to reposition the manipulandum from the targeted direction back to initial position.The delay time

between two consecutive different directions was ten seconds as shown by the timeline presented in Figure 3.2.
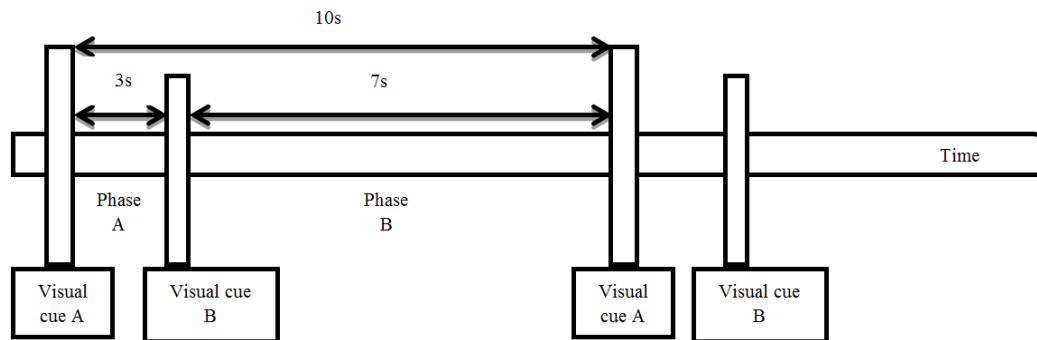
Figure 3.2: Timeline of visual cue presentation. Phase A indicates onset of movement that lasts for three seconds. Phase B indicates offset of movement and lasts for seven seconds. Visual cue A represents the instruction to move the manipulandum towards one of four directions (3, 6, 9 and 12). Visual cue B represents the cue to return to the neutral direction (0).

3.2.2 Motor Imagery Experiment

The motor imagery experiment required subjects to do the same procedure described above, but this time instead of moving the manipulandum physically, subjects had to imagine (kinaesthetic imagery) controlling right wrist to move the manipulandum with burst movement into different directions triggered by the visual cue. The visual cue presentation in this motor imagery experiment was identical with that used in the motor task experiment (Figure 3.2).

3.3   Experimental Data Recording Set Up

The experimental recording set up encompasses the implementation of visual cue presentation, synchronisation, and recording of physiological (EEG and EMG) and movement's signal.

3.3.1 Visual Cue Presentation and Recording Synchronisation

Visual cue presentation was generated using the Psychophysics Toolbox (Brainard, 1997, Pelli, 1997) with code written in Matlab. This program displayed visual cues and at the same time produced sets of digital event markers, essential for synchronisation between visual cue presentation and recorded signals. These digital event markers were sent through the parallel port to the NeuroScan Synamps2 System (Compumedics Neuroscan, Charlotte, NC,USA) and CED 1401 (Cambridge Electronic Design, United Kingdom). Every movement/imagined movement cue generated a unique digital output event that reflected the time and direction of cue appearance, transmitting a time-stamp to the digital ports of the NeuroScan™ Synamps2 System and CED 1401 during data recording. Examples of these digital event markers for both of recordings are tabulated in Table 3.1 and Table 3.2.

It is essential to have this digital event markers especially for time synchronisation between visual cue presentation and signal recording (physiological and movement's signal). Other than for the purpose of synchronisation, digital event markers also provide information regarding the target position of visual cue which is essential for categorising and grouping the trial according to type of direction.

Table 3.1: Digital event markers for EEG and EMG signal recording. This table also indicate the interpretation of the digital codes for NeuroScan™Synamps2 System.

Digital Code	Interpretation
190	Visual cue presented at position neutral (0)
193	Visual cue presented at position 3
196	Visual cue presented at position 6
199	Visual cue presented at position 9
202	Visual cue presented at position 12

Table 3.2: Digital event markers for movement signal recording. This table also indicate the interpretation of the digital codes for CED 1401.

Digital Code	Interpretation
A	Visual cue presented at position neutral (0)
>	Visual cue presented at position 3
;	Visual cue presented at position 6
8	Visual cue presented at position 9
5	Visual cue presented at position 12

3.3.2 EEG Signal Recording Set Up

In this study, EEG signal was recorded by the NeuroScan Synamps2 System using a 128-electrode Easy Cap® (montage number 15) with silver chloride (Ag/AgCl) sintered ring electrodes (Figure 3.3) through Curry Neuroimaging Suite 7.0.8 XSB software. Electrode placement was based on the 10-10 system, referenced to the earlobe with channel AFz used as ground. The 10-10 electrode placement locations system was implemented because it offers higher density electrode coverage over the motor cortex area compared with the 10-20 system (Jurcak et al., 2007).

Before beginning electrophysiological recordings, the contact impedance of each electrode of the montage shown in Figure 3.4 was brought below 5KΩ. The contact impedance was constantly monitored and maintained below 5KΩ throughout the experiment. The EEG signal was recorded using monopolar amplifier configurations with a sampling frequency of 2000 Hz and band-pass filtered between 0.05-500 Hz.
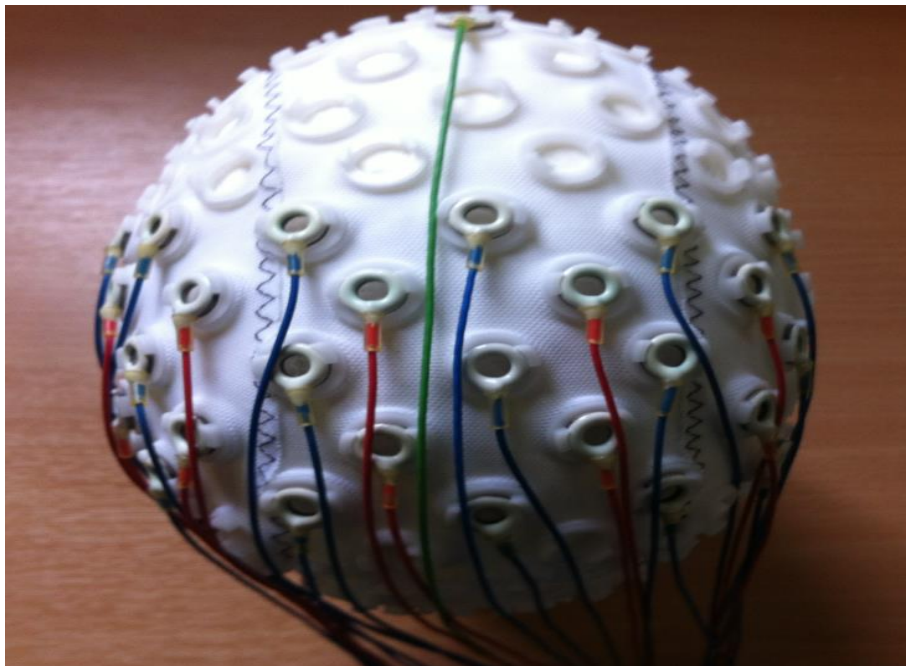
Figure 3.3: EASYCAP®. Green wire is the ground electrode; red and blue represent the active recording electrodes.
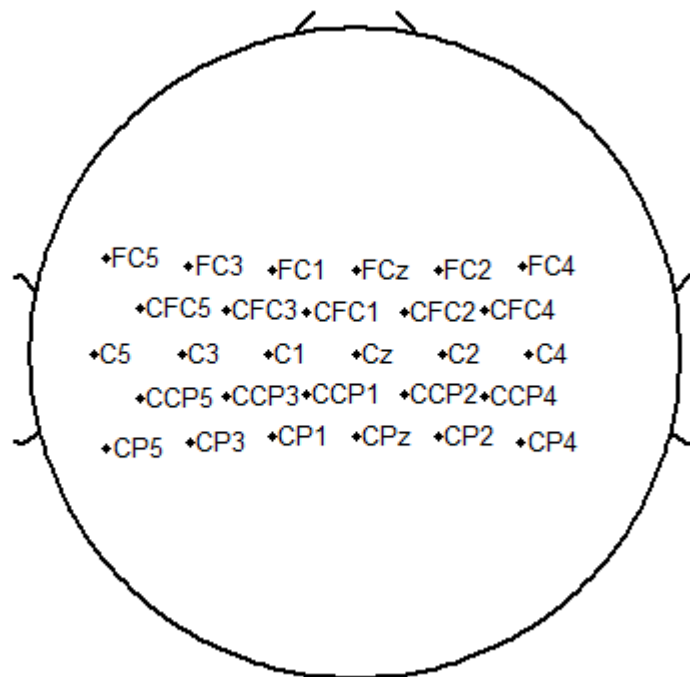
Figure 3.4: EEG recording electrodes placement. 28 electrodes with high density montage are placed focusing on the primary motor cortex area.

To allow online visual inspection of recordings, EEG, EMG and movement signals were displayed to the experimenter on a second monitor. This monitor was placed out of subject's view to avoid any unnecessary distraction during recordings.

3.3.3 EMG Signal Recording Set Up

EMG signals were simultaneously recorded with EEG signals by the NeuroScan Synamps2 System using Ag/AgCl electrocardiograph (ECG) disposable electrodes through Curry Neuroimaging Suite 7.0.8 XSB software. A bipolar configuration was implemented to record EMG signals at a sampling frequency of 2000 Hz and band-pass filtered between 0.05-500 Hz.

EMG was recorded from muscles associated with flexion, extension, and ulnar and radial deviation of the right wrist (Valsan et al., 2006, Hoffman and Strick, 1999); namely, the flexor carpi radialis, extensor carpi ulnaris, extensor carpi radialis brevis and extensor carpi radialis longus muscles (see Figure 3.5) . Recording electrodes were placed on the surface of the corresponding muscles of the right hand, based on

the guide tabulated in Table 3.3. Impedance of EMG recording electrodes was also set below 5KΩ and constantly maintained throughout the experiment; the same criteria which was applied to EEG electrodes. EMG recorded during the motor imagery experiment played an important role in confirming that there was absolutely no movement during the sessions.
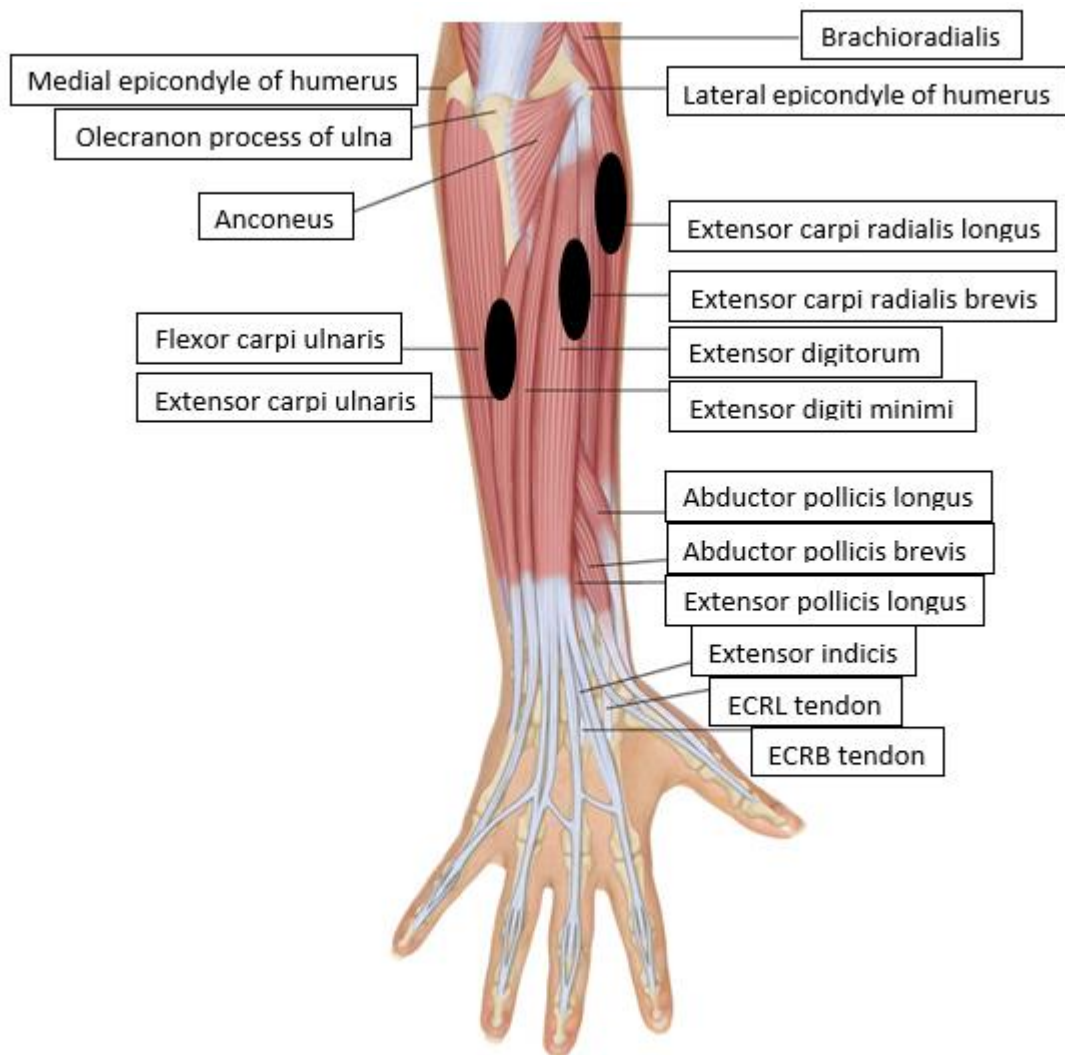
Figure 3.5: EMG recording muscle location. This figure indicates the location of extensor carpi ulnaris, extensor carpi radialis brevis and extensor carpi radialis longus muscles, from which EMG recordings were made. The electrodes placement represented by the black marker. [Adapted from musculoskeletalkey.com, 17/5/2016].

Table 3.3: Guideline for locating EMG recording muscle. These guidelines were obtained from (Chu-Andrews and Johnson, 1986).

Muscle name	Location of muscle
Flexor Carpi Radialis (FCR)	Position the subject's forearm on its medial border in midpronation and ask he/she to bend his/her wrist toward the body. At the same time apply pressure at the midpalm in direction of wrist extension
Extensor Carpi Radialis Longus (ECRL)	Position the subject's forearm in pronation and asked he/she to lift his/her hand towards his/her own face. At the same time apply pressure in direction of wrist flexion on the dorsum of the hand. ECRL located approximately at the elbow level.
Extensor Carpi Radialis Brevis (ECRB)	Position the subject's forearm in pronation and asked he/she to lift his/her hand towards his/her own face. At the same time apply pressure in direction of wrist flexion on the dorsum of the hand. ECRB is adjacent with ECRL.
Extensor Carpi Ulnaris (ECU)	Position the subject's forearm in pronation. Instruct the patient to spread his/her finger and lift his/her hand up as far backwards as he/she. At the same time apply pressure in direction of wrist flexion on the dorsum of the hand. ECU is located on the ulnar side of forearm

3.3.4 Manipulandum and Movement Signal Recording Set Up

During the motor task experiment, subjects used the manipulandum to perform right wrist movements in multiple directions, triggered by the visual cue. The manipulandum (Figure 3.6) is a joystick device made of aluminium, comprised of three main parts; namely the base, adjustable double telescopic stand and manipulandum rings. Design of the base enables the manipulandum to be portable, making it more efficient for use with SCI patients, positioned either beside a wheelchair or next to the patient's bed. Furthermore, the adjustable telescopic stand can be extended horizontally and vertically for multiple purposes such as getting the right height according to the patient's elbow and adjusting the manipulandum ring based on length of the patient's arm.

The manipulandum rings consist of an ergonomic hand grip fitted to a two axis gimbal; one gimbal axis corresponds to wrist flexion-extension (X axis) and the other one corresponds to wrist ulnar-radial deviation (Y axis). In order to detect and measure the changes of movement across the X and Y axes reflecting wrist flexion-

extension and ulnar-radial deviation, each gimbal axis was coupled with a precision servo potentiometer (potentiometer with servo mechanism that use error correction as negative feedback to correct the action of the movement and help control the mechanical position). Both of the precision servo potentiometers were connected with a resistor and use 12V DC power supply for input voltage (see Appendix B). Changes in the voltage across the precision servo potentiometers correspond to manipulandum displacement, providing a measure to monitor whether is the subject or not performing the movement correctly as triggered by the visual cue. Recording the movement signal was also useful in confirming that there was no movement during the motor imagery experiment. Information about voltage changes related to movement direction was tabulated in Table 3.4. This movement signal generated by the manipulandum was recorded using CED 1401 at sampling frequency of 100 Hz.

Table 3.4: Relation between movement and voltage of the potentiometer.

Movement	Axis	Direction	Voltage
Flexion	X	9	$VR_1 > 2.8$ v
Extension	X	3	$VR_1 < 2.2$ v
Ulnar deviation	Y	6	$VR_2 > 2.8$ v
Radial deviation	Y	12	$VR_2 < 2.2$ v
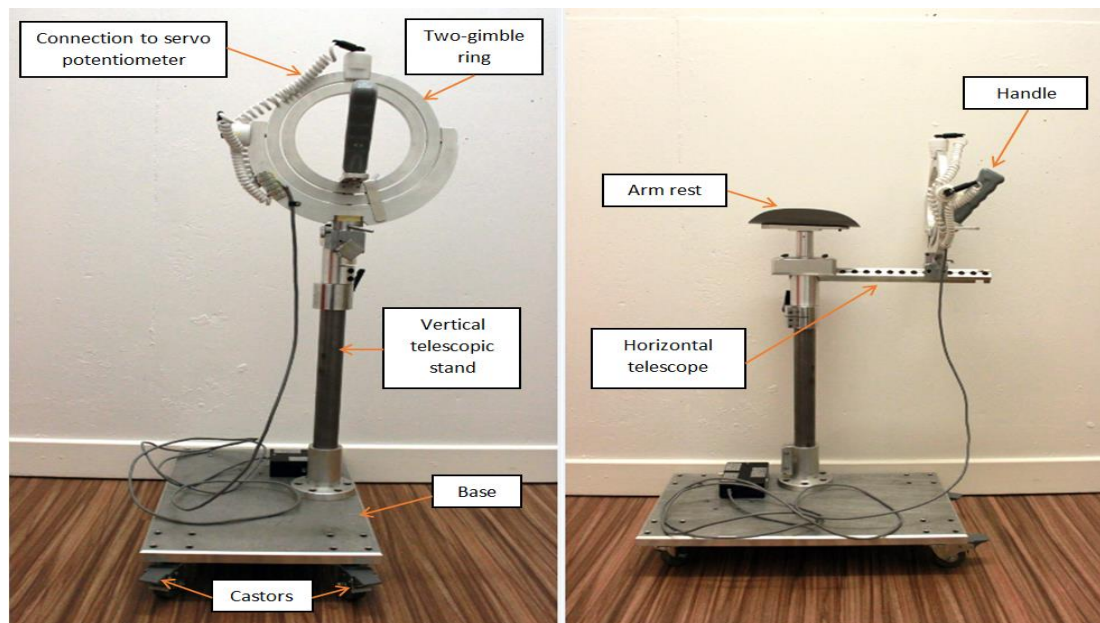
Figure 3.6: The manipulandum. Manipulandum rings coupled with two potentiometers (one at X axis and the other one at Y axis) and connected with a circuit board (covered in black box; schematic diagram in Appendix B).

3.4   Pilot Study

The pilot study played a major role in examining the feasibility of the proposed method for implementation in a larger scale study (Leon et al., 2011). Thus, the experimental protocols and data recording set up in this study were evaluated through a pilot study which is described here.

Eleven subjects (nine male) gave informed consent and participated in the pilot study. All subjects were postgraduate students of the University of Strathclyde with an average age of 28.09 years. All were right hand dominant, had no history of neurological disease and with 20/20 or corrected vision. The participating subjects completed all the trials for both experiments and their feedback was taken into consideration for improving the experimental protocols and the data recording set up. The experimental procedure was approved by the Departmental Ethics Committee of the Biomedical Engineering Department of the University of Strathclyde (Non-invasive electrophysiological studies on the human motor system).

3.5   Subjects and Ethics Approval

This study was granted ethical approval by the National Health Service (NHS) South Glasgow and Clyde Local Research Ethics Committee. The ethical approval was obtained on 27 July 2015 with REC reference number of 15/WS/0116 and IRAS project ID number of 141350 (related documents attached in Appendix C). The targeted group of patients in this study were SCI patients and therefore this study took place at the Queen Elizabeth National Spinal Cord Injuries Unit (QENSIU) of Queen Elizabeth University Hospital. QENSIU of Queen Elizabeth University Hospital is the national centre for SCI patients in Scotland. Potential SCI patients recruited as subjects in this study were screened and identified via consultation with medical staff and their consultants at the QENSIU. Only subjects who satisfied inclusion and exclusion criteria which was included in this study. Potential participants were identified by medical staff with consideration of their level and duration of spinal cord injury. Participating SCI patients in this study were recruited

among inpatients and outpatients (both tetraplegic and paraplegic) receiving treatment at QENSIU of Queen Elizabeth University Hospital.

3.6   Summary

This chapter has described the implemented procedures for developing an endogenous synchronous BCI system through EEG, EMG and movement signal recordings. The developed BCI system requires subjects to perform motor imagery and motor execution of right wrist towards four different directions with zero subjects training.

Although there are three types of signal recorded in this study, EEG signals were designated to play the main role in operating the BCI system. EMG signals were recorded as an instrument to verify movement status during the motor imagery and motor execution experiment. The movement signal was used for detecting movement initiation time and confirming the subject executed the right movement according to the cue direction when performing the motor task experiment.

All hardware, software, procedures and set up involved in developing this BCI system were tested first in a pilot study before being applied in the actual experiment. It was crucial to verify hardware safety and correct parameters for experimental recordings before involving SCI patients to avoid any unnecessary distress from technical faults such as expired conductive gel/ disposable electrodes, software compatible issues, continuity connection of recording electrodes and status of portable appliance testing (PAT test) of the hardware.

Chapter 4. Data Analysis

4.1 Introduction

This chapter describes the data analysis methods applied to EEG, EMG and manipulandum movement signals. The following signal processing technologies were implemented offline in post-hoc analysis. The work-flow of these data analyses was depicted in Figure 4.1.
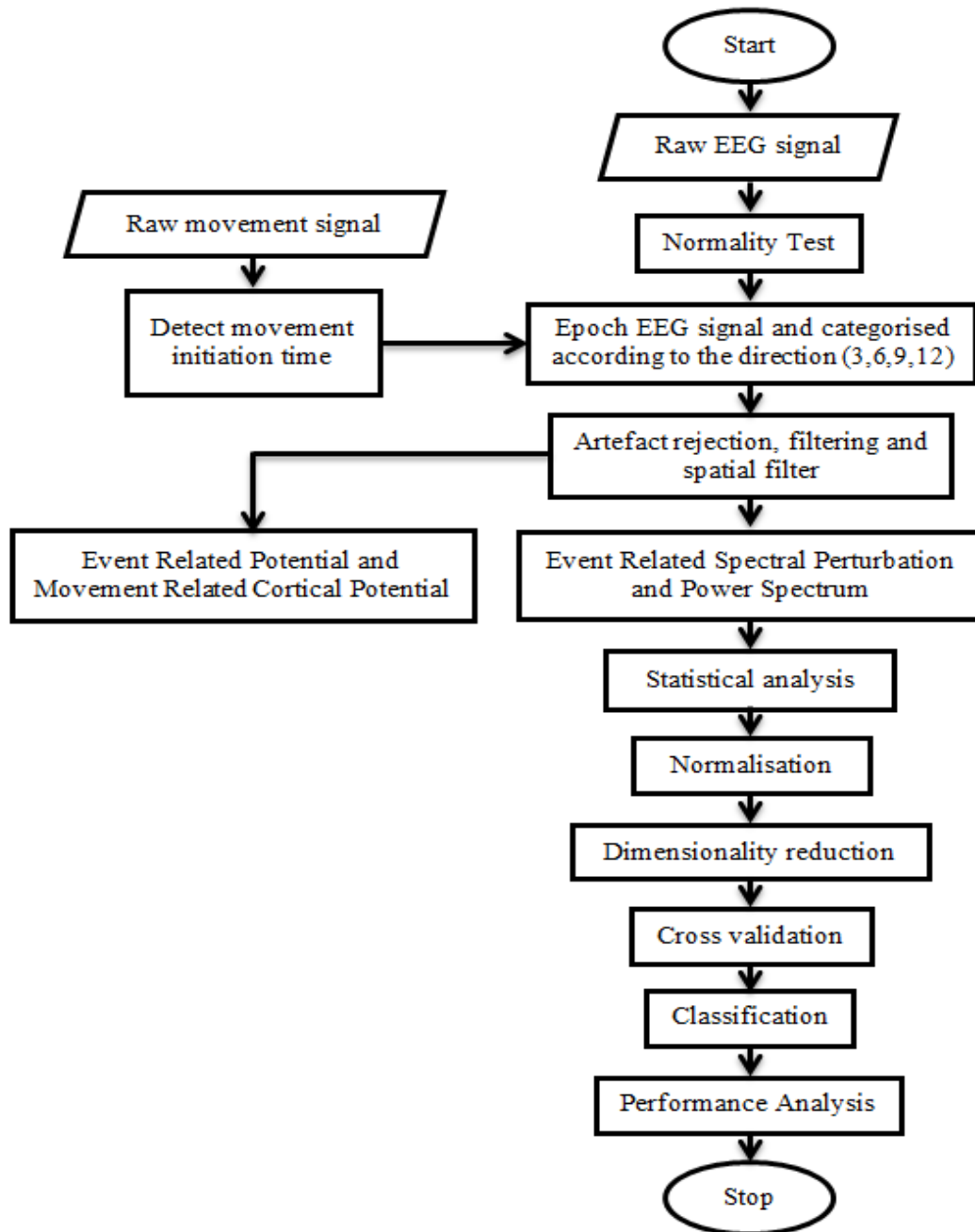
Figure 4.1: Flowchart of implemented signal processing method.

The implemented data analysis techniques include pre-processing, artefact rejection, feature extraction, statistical analysis and pattern recognition. In order to investigate and characterise changes within the EEG signature (before, during and after performing/imagining performing right wrist movement in multiple directions) in both experiments, analysis using time-frequency domain and event related potentials (ERPs) were explored. These signal processing and data analysis methods were detailed in the following sections.

4.2   Demographic Profile

The volunteering subjects included SCI patients, whose identifiable data and personal information were kept confidential. In this study, each subject was assigned with a specific number and data were retrieved using this assigned number. By employing this approach, subjects' anonymity was maintained throughout data recording and analysis. As for presentation of results, only certain parameters were emphasised for further investigation. These parameters comprise gender, age, type of injury, level of injury, AIS scale, duration of injury and medication. It is important to highlight that, none of the disclosed parameters are capable of revealing the identity of subjects.

4.3   Detection of Movement Initiation Time

Movement initiation time refers to the time taken by subject to start moving the manipulandum from the neutral position (0) towards any of the four directions (3, 6, 9 and 12). In order to detect movement initiation time, two parameters were further explored namely, digital event markers and the voltage threshold.

Digital event markers indicate position and direction of the visual cue presentation (tabulated in Table 3.1 and Table 3.2), where each digital code corresponds to a specific direction/location. The voltage threshold for each precision servo potentiometers was set to three categories which are ideal, minimum and maximum. Both of the precision servo potentiometers share the same threshold although they

correspond to different axes (X and Y). The ideal threshold voltage refers to the manipulandum at neutral position (0) and was set within the range of 2.48-2.56 V. The minimum threshold voltage was set below 2.2 V and detects the subject performing wrist extension (X axis) and radial deviation (Y axis). The maximum threshold voltage was set above 2.8 V and detects the subject performing flexion (X axis) and ulnar deviation (Y axis) movements.

Custom Matlab code has been generated for detecting the appearance of digital event markers and changes of the threshold voltage in both axes (X and Y). Based on the value of these two parameters movement initiation time was calculated. Following this, movement initiation time was used for segmenting epochs of EEG signal acquired during the motor task experiment.

4.4   Normality Test

The normality test is a statistical procedure to verify whether or not the collected data follow a normal/Gaussian distribution, assuming that the population from which the samples were taken is normally distributed. Furthermore, the normality test was used to determine the validity and reliability of statistical procedures implemented on the data. For instance, parametric tests were only implemented on data with a Gaussian distribution, whereas non-parametric tests were applied to non-Gaussian distribution data (Ghasemi and Zahediasl, 2012).

Kolmogorov-Smirnov test is a tool to check the normality of data (Öztuna et al., 2006). This test compares the values in the recorded data with the normal distribution. The null hypothesis says that the recorded data has a Gaussian distribution, whereas the alternative hypothesis says that the recorded data distribution is non-Gaussian. The hypothesis result (h) is 0 if the null hypothesis is accepted (h=0), and 1 if the null hypothesis rejected (h=1), with a significance level set at 5 %. In this study the Kolmogorov-Smirnov test was implemented using the Matlab statistics toolbox (version R2013a).

4.5 Event Related Potential (ERP) and Movement Related Cortical Potential (MRCP)

ERP is a change in EEG field potentials in response to a specific event and time-locked to a stimulus (Hillyard and Kutas, 2002, Sur and Sinha, 2009). There are a number of ERP components, namely P50, N1, P2, N2, N300, P300, N400, P600, mismatch negativity, contingent negative variation, post negative variation and the movement related cortical potential (Sur and Sinha, 2009). These components are classified according to their polarity, sensitivity to task manipulation, timing and scalp distribution (Landa et al., 2014).

Among these ERP components, only the movement related cortical potential (MRCP) was further explored due to the implemented experimental protocols involving motor imagery and motor task paradigms (Xu et al., 2014). Generally, MRCP reflects changes of field potentials with a close temporal relationship with either imagery or attempt of movement (Xu et al., 2014). MRCP was computed by averaging the processed epochs of EEG signal across all trials, implemented using the Matlab plug-in EEGLAB (version 12) (Delorme and Makeig, 2004).

4.6 Event Related Spectral Perturbation (ERSP)

Event Related Synchronisation/Desynchronisation (ERS/ERD) elaborates the relative changes in EEG spectral power, induced by a stimulus in relation to a reference signal which comprises of both phase-locked and non-phase-locked activity (Pfurtscheller and Da Silva, 1999). In order to investigate changes in the EEG signature while the subjects were imagining/performing right wrist movements in multiple directions, changes of event related shifts within the frequencies of interest (delta, theta, alpha/mu, beta and gamma) were computed. This was achieved through the Event Related Spectral Perturbation (ERSP) technique. ERSP is a generalization of ERD/ERS which visualizes the entire spectrum in the form of a baseline-normalised spectrogram (Delorme and Makeig, 2004).

ERSP was computed by dividing each epoch into a number of overlapping windows and calculating spectral power for each window. The calculated spectral power was

then normalized (divided with the mean of baseline spectra calculated from the EEG immediately before each event) and averaged over all the trials (Grandchamp and Delorme, 2011). In this study, the ERSP was computed using equation [4.1] (Delorme and Makeig, 2004) shown below :

$$ERSP(f,t) = \frac{1}{n} \sum_{k=1}^{n} \left| F_k(f,t) \right|^2 \qquad [4.1]$$

Where n is the total number of trials and $F_k(f,t)$ is the spectral estimate of trial k at frequency f and time t. A total number of 1024 points of window length multiplied by Hanning window functions were used to calculate the Fast Fourier Transform (FFT) (Ahn et al., 2013). For each time-frequency plot two hundred windows were used. These processes were performed using Matlab (version R2013a) and EEGLAB (version 12) (Delorme and Makeig, 2004).

4.7 EEG Signal Translation

EEG signal translation is a crucial step in developing a reliable and effective BCI system. This is because the signal translation process is responsible for detecting the subject's brain signature associated with intention to initiate control and decode it into a useful command signal. These processes were implemented through signal processing algorithms that encompass pre-processing, feature extraction, statistical analysis, normalisation, dimensionality reduction and pattern recognition. Further clarification regarding each of these steps implemented in signal processing was detailed in following sections/subsections.

4.7.1 Signal Pre-processing

In this study, the artefacts were removed using signal pre-processing method which comprised of signal segmented into epochs, artefact rejection and signal filtering. The implementation of these methods described in the following subsections.

4.7.1.1 Signal segmented into Epochs

EEG signal from both experiments were segmented into epochs using EEGLAB (version 12) and categorised according to direction (3, 6, 9 and 12). In the motor task experiment, the EEG signal was segmented into epochs of three seconds before and three seconds after the onset of movement (movement initiation time, t=0), whereas for the motor imagery experiment the EEG signal was segmented into epochs three seconds before and three seconds after the task initiation time (visual cue presentation).

It is essential that the segmented epochs and categorised EEG signal accurately represent the corresponding task. For instance, in the motor task experiment, subjects move the manipulandum towards the instructed direction in burst movement, and in the motor imagery experiment no movement was performed. Thus before segmented into epochs EEG data from the motor task experiment, movement signal recordings were studied to determine movement initiation time. The movement signal was checked visually to verify that the subject executed the correct movement according to the visual cue in less than 1 second. Any movement trials that did not meet these criteria were discarded from the analysis. On the other hand, for the motor imagery experiment, the movement signal was checked visually in order to confirm no movements were performed. If any movement was detected corresponding imagination trials were excluded from the analysis.

4.7.1.2 Artefact Rejection

Before implementing any further signal processing methods on segmented epochs of EEG signal, it is necessary to make sure that the segmented epochs of EEG signal are free from any unwanted noise and artefacts. This was done using a conventional method, by visually inspecting for, detecting and removing trials containing artefacts caused by eye blinking, jaw clenching, swallowing/coughing or any other irrelevant movements. This artefact rejection procedure was conducted using EEGLAB (version 12).

4.7.1.3 Frequency Signal Filtering and Spatial Filter

After removing any unwanted noise and artefacts, the segmented epochs of EEG signal were frequency filtered through 3 filtering stages. In the first stage, the segmented epochs of EEG signal were frequency filtered by a notch filter for removing noise resulting from the power cables during the recording (Ma et al., 2009). Following this, the segmented epochs of EEG signal were bandpass filtered between 0.5 and 50 Hz (Graimann and Pfurtscheller, 2006) in order to extract 5 frequency bands of the EEG signal, namely the delta (1-3 Hz), theta (4-7 Hz), alpha/mu (8-12 Hz), beta (13-30 Hz) and gamma (31-50 Hz) bands. In the final filtering stage, as to enhance the signal to noise ratio of filtered EEG signal (Lu et al., 2012), the band-pass filtered EEG signal was spatially filtered by common average reference (CAR) and small Laplacian (LAP) methods (McFarland et al., 1997).

CAR is a 'reference-free' technique that is not affected by the problems associated with an actual physical reference such as topographic distortion due to the relative electrical neutral area not employed (Teplan, 2002). In CAR, the potential at each electrode was measured with respect to the average of all electrodes. The CAR was computed using equation [4.2] (McFarland et al., 1997):

$$\ldots\ldots\ldots\ldots\ldots\ldots\ldots\ldots\ldots V_i^{CAR} = V_i^{ER} - \frac{1}{n}\sum_{j=1}^{n} V_j^{ER} \qquad\qquad [4.2]$$

Where V_i^{ER} was the potential between i^{th} electrode and the reference, and n was the number of electrodes in the montage.

LAP serves as a high-pass filter that enhances localised activity while suppressing diffusion activity (Lu et al., 2012). LAP was obtained by subtracting the sum of weighted potential of surrounding electrodes from the current electrode potential, where the weightings applied were dependent on the distance from the current electrode. This was computed using equations [4.3] and [4.4] (McFarland et al., 1997) shown below :

$$\ldots\ldots\ldots\ldots\ldots\ldots\ldots\ldots\ldots V_i^{LAP} = V_i^{ER} - \sum_{j \in Si}^{n} V_j^{ER} g_{ij} \qquad\qquad [4.3]$$

$$\dots\dots\dots\dots\dots\dots g_{ij} = \frac{\dfrac{1}{d_{ij}}}{\displaystyle\sum_{j\in Si}\dfrac{1}{d_{ij}}} \qquad\qquad [4.4]$$

Where S_i was the set of surrounding electrodes of the ith electrode and d_{ij} was the distance between electrodes i and j (where j was a member of S_i).

After completing these filtering stages, the segmented epochs of EEG signal was categorised into the four different directions for subsequent analysis. This categorisation was performed separately for both CAR and LAP methods to compare their relative performance in this BCI system.

4.7.2 Feature Extraction

Feature extraction, where certain salient attributes of the EEG data are identified and isolated, is one of the most computationally demanding processes in this BCI system. In this study, EEG signal recorded from the motor cortex was the focus, logically considering the experimental protocol based upon motor function (motor imagery and motor task paradigms).

Features were extracted from each epoch and divided into two 500ms length windows (Lakany and Conway, 2006, Lakany and Conway, 2005); the first window corresponding with the resting condition where the subject was holding the manipulandum in the neutral position, the second window corresponding with the imagery/movement condition where subject was imagining/performing the wrist movement towards directions 3, 6, 9 and 12. As for the motor task experiment, features were extracted 500ms before onset of the movement (movement initiation time), whereas for the motor imagery experiment features were extracted 500ms after the initiation time (visual cue presentation time). The size of extracted feature vectors for both of motor imagery and motor task experiment tabulated in Table 4.1. The extracted features from each window were then transformed into two datasets. Each of these datasets was then spilt into two groups, namely training and testing datasets,

using a cross validation method for classification process. Features were computed using power spectra and analysis of variance.

Table 4.1: Size of the extracted feature for motor imagery and motor task experiment..

Frequency band	Size of the extracted feature vector for motor imagery and motor task experiment
Delta	8x30
Theta	8x30
Alpha	10x30
Beta	37x30
Gamma	39x30

4.7.2.1 Power Spectrum

Power spectrum denotes EEG signal power in different frequencies (Robeva et al., 2007). In addition to this, power spectrum analysis quantifies EEG signal power in different frequency bands, which may be visualised using different colours (Yeom et al., 2008). With this visualisation tool, it would be easier to investigate the distribution of power within the given frequency range. In this study, power spectrum analysis focuses on the distribution of power within delta, theta, alpha, beta and gamma bands. This was implemented through the ERSP.

4.7.2.2 Statistical analysis

Detecting the intention and discriminating the motor imagery/motor task of different movement within the same limb is a challenging task, due to fact that the motor tasks active region have very close representations on the motor cortex area (Yong and Menon, 2015, Plow et al., 2010). Thus, selection of appropriate statistical tests might offer a feasible solution.

Based on a positive normality test output, repeated measure of analysis of variance (ANOVA) (Ahmad Jamil et al., 2016, Koelstra et al., 2009, Valsan et al., 2006), which is a parametric test, was implemented. Implementation of repeated measure of ANOVA tests play a crucial role in determining whether or not significant difference

occurs in the features extracted from different directions (3, 6, 9 and 12). The repeated measures ANOVA test was implemented across 4 different directions through ERSP at each time and frequency across the measurement window within the range of 0-50 Hz. Output from the repeated measures ANOVA test (p value), was presented as a contour plot mapped in time and frequency. These contour plots of p values indicate the occurrence of regions with statistically significant difference at 5 % across the ERSP in 4 different directions. Power spectrum from each of the ERSP (3, 6, 9 and 12) that fall within the contour plots of p values with statistically significant difference at 5% were concatenated and formed as a feature vector for pattern recognition processes.

4.7.3 Normalisation

Generally, EEG is very complex non-stationary signal, with continuous time-varying dynamics and high variability between subjects (Bogaarts et al., 2016). Due to these factors, it is essential to apply data normalisation as a signal processing step. Normalisation is responsible for scaling data values within a specific range (Al Shalabi et al., 2006). Based on this attribute, normalisation is capable of neutralising the effect of different scales and group data within the same domain (Jain et al., 2005), reduce intra-class variance and increase signal-to-noise ratio (Coyle et al., 2004). The implemented normalisation method in this study was z score normalisation (Wang et al., 2012, Lopez-Larraz et al., 2012), computed using equation [4.5] (Sung et al., 2012) as follow:

$$Z_i = \frac{x - \mu}{\sigma} \qquad [4.5]$$

Where x was the measured EEG signal at time i, μ was the average of EEG signal and σ was the standard deviation of EEG signal.

4.7.4 Dimensionality reduction

Dimensionality reduction involves conversion of high dimensional data into significant representation of reduced dimensionality (Van Der Maaten et al., 2009). Reduction of the dimensions of features space also reduces classification complexity and leads to higher classification accuracy (Bashashati et al., 2007). Principal component analysis (PCA) is one of the most widely used methods of dimensionality reduction in BCI applications.

PCA is a statistical procedure that employs linear transformation for identifying uncorrelated variables called principal components from the analysed data set (Nicolas-Alonso and Gomez-Gil, 2012). Through linear transformation, PCA produces a set of principal components and sorts them according to their corresponding variance. Generally these are sorted in descending order because low order components have high variance and contain the most important aspects of the analysed data set (Bashashati et al., 2007). From this order, PCA will select the smallest number of principle components that represent the maximum variance (Fodor, 2002, Cunningham and Ghahramani, 2015).

In this study, PCA was implemented on features extracted by power spectrum and ANOVA test (p value results) and computed by the steps listed below:

1. Subtract the mean from the data.

2. Compute the covariance matrix.

3. Obtain eigenvalues and eigenvectors of covariance matrix.

4. Sort the eigenvalues in descending order.

5. Choose the eigenvectors that correspond to the largest eigenvalues until the criterion (the percentage of variance of all selected principle components represent 95 % variance of data) was met.

6. Construct the projection matrix from the selected eigenvectors.

7. Transform the original dataset through the projection matrix to obtain new feature vector.

4.7.5 Cross validation

Cross validation is a statistical method that assesses performance of the implemented learning algorithm and its generalisability towards an independent data set (Refaeilzadeh et al., 2009). Cross validation operates by dividing the analysed data set into two sections; one used for training the algorithm and the other used for validating the algorithm. There are various types of cross validation methods such as resubstitution, hold out, leave one out and k fold cross validation.

The implemented cross validation method in this study was k fold cross validation where the k was set to 10 (Lopez-Larraz et al., 2012, Tanaka et al., 2006). This method of cross validation partitioned the data set into k equal subsets. One of these subsets was used for validating and remaining of $k - 1$ subsets were used for training by classifier. The process of training and validating by the classifier was repeated until all of the different k subsets were used for the validation. The recognition rate corresponding to the subset being used for validation is computed by the trained classifier. The performance of the classifier was computed based on the average of the recognition rate of the k subsets (Tanaka et al., 2006).

4.7.6 Pattern Recognition

Pattern classification in this study focuses on recognising the pattern and regularities of EEG signal associated with the direction of imagination/movement, and categorised according to the specific direction. The classification process needs to be trained to recognise particular patterns of feature vector sets; either as a supervised or unsupervised classifier, before it can categorise them into different classes. In the present study, single trial classification was applied, focussing on predicting three major aspects; imagination/intention of movement, target direction, and imagination/intention and direction of movement. Furthermore, the classification

71

process was carried out using three types of classifier; namely *k* Nearest Neighbour classifier (Liu et al., 2013), Fuzzy *k* Nearest Neighbour classifier (Chatterjee et al., 2013) and Quadratic Discriminant Analysis classifier (Bhattacharyya et al., 2010).

Predicting imagination/intention of movement required classifiers to distinguish two different conditions. The first condition refers to when the subject's right wrist remains stationary in the neutral position, and the second condition was when subject starts to imagine/move his/her right wrist toward any direction of 3, 6, 9 and 12. The normalised feature vector of alpha (12 principal components), beta (29 principal components) and gamma (19 principal components) frequency bands from both conditions were cross validated for classification purpose.

This classification process also tries to recognise the direction of imagination/intention of movement. In this instance, the classifier attempts to differentiate whether the subject was stationary in the neutral position or started to imagine/move towards each of the directions 3, 6, 9 and 12 individually. Classification was implemented separately such that for each trial only one direction was considered, for instance, classification between neutral and imagination/intention of movement towards direction 3. For this purpose, the normalised feature vector of alpha (11 principal components), beta (26 principal components) and gamma (24 principal components) frequency bands from each of these directions were cross validated for classification purpose.

It is essential to emphasise that, in predicting imagination/intention of movement and predicting target direction of imagination/intention of movement, only feature vector from alpha, beta and gamma frequency bands considered for the classification process. This is because, majority of the BCI study that investigate sensorimotor activity (employed motor imagery modality and used ERD/ERS feature) concentrate the changes of brain rhythms within alpha, beta and gamma frequency bands (Bashashati et al., 2007, Pfurtscheller and Neuper, 2001, Yi et al., 2013, Nicolas-Alonso and Gomez-Gil, 2012).

Lastly, the classification process attempts to recognise both when the subject starts to imagine/move and also predict the direction of imagination/movement. In this

situation, feature vectors were obtained from the results of the ANOVA (*p* value) test. This feature vector comprises of delta, theta, alpha, beta and gamma frequency bands. Despite the implementation of PCA, the size of feature vectors for each frequency band was not fixed. This is because the significant differences across the ERSP computed for each of the four directions varies across subjects. These feature vectors were also normalised and cross validated for classification purposes.

4.7.6.1 k Nearest Neighbour (*k*-NN) Classifier

The *k*-Nearest Neighbour classifier (k-NN) is an instance-based classifier that operates based on classification of unknown instances by relating the unknown to the known class according to some distance/similarity function. In other words, the k-NN classifier is a method for classifying objects based on majority of closest distance of training examples in the feature space (Aydemir and Kayikcioglu, 2013). In addition, there are two parameters that determine the performance of the classification; namely, type of distance function and number of the *k*-neighbour. Generally, the most common distance functions are Euclidean distance and Manhattan distance. Meanwhile, the number of *k*-neighbour was set at small value and odd number in order to break ties (Palaniappan, 2011).

In this study, in order to calculate the distance between classes in training and testing datasets, Manhattan distance was implemented using equation [4.6] (Palaniappan, 2011) as follow:

$$d = \sum_{i=1}^{n} |x_i - y_i| \qquad [4.6]$$

Where n was the number of variables, x_i and y_i were the values of the ith variables at point x and y, respectively.

The number of *k*-neighbour was determined using equation [4.7] (Palaniappan, 2011) shown below:

$$k = \sqrt{N} \qquad [4.7]$$

Where *N* was number of instances (in the present study N refer to the total number of training data of the feature space). Thus, the number of *k* neighbour was set as follow:

1. *k* neighbour was set at $k = 15$ for predicting imagination/intention of movement.

2. *k* neighbour was set at $k = 7$ for predicting the effect of direction toward imagination/intention of movement.

3. *k* neighbour was set at $k = 9$ for predicting imagination/intention and direction of movement.

4.7.6.2 Fuzzy k Nearest Neighbour (FKNN) Classifier

Fuzzy *k* Nearest Neighbour (FKNN) is a classifier that categorises objects based on majority of the closest *k*-neighbours and those neighbours' membership in the possible classes (Jensen and Cornelis, 2011, Keller et al., 1985). Compared with the k-NN classifier, FKNN considers both the distance of the *k*-neighbour and the neighbours' membership as main factors during the classification process. In this study the neighbours' membership in each possible class was computed using equation [4.8] (Keller et al., 1985) as stated below:

$$\mu_i(x) = \frac{\sum_{j=1}^{K} \mu_{ij} \left(1/\left\| x - x_j \right\|^{2/(m-1)} \right)}{\sum_{j=1}^{K} \left(1/\left\| x - x_j \right\|^{2/(m-1)} \right)} \tag{4.8}$$

Where $\mu_i(x)$ was membership of the training, (x) of the ith class of j samples, k was the number of neighbours, m was a positive real number know as a 'fuzzifier' and $\left\| x - x_j \right\|$ was the distance between x and x_j.

4.7.6.3 Quadratic Discriminant Analysis (QDA) Classifier

Quadratic discriminant analysis (QDA) is a classifier that categories different classes based on the quadratic decision boundary (Pang et al., 2009) . The QDA classifier assumes that collected data from each class is normally distributed and the covariance matric of each class is not identical (Bashashati et al., 2015). In the present study, classification processes using the QDA classifier were computed using equations [4.9], [4.10], [4.11], [4.12], and [4.13] (Omar et al., 2014) as follow:

$$G(x) = \arg\max \delta_k(x) \qquad [4.9]$$

With

$$\delta_k(x) = -\frac{1}{2}\log\left|\sum_k\right| - \frac{1}{2}(x-\mu_k)^T \sum_k^{-1}(x-\mu_k) + \log\pi_k \qquad [4.10]$$

Where

$$\sum_k = \frac{1}{N_k-1}\sum_{i\in k}(x_i-\mu_k)(x_i-\mu_k)^T \qquad [4.11]$$

And

$$\mu_k = \sum_{i\in k}\frac{x_i}{N_k} \qquad [4.12]$$

And #

$$\pi_k = \frac{N_k}{N} \qquad [4.13]$$

The parameters included in these equations were described as follow:

1. x was the set of data.

2. k was the number of classes.

3. $\sum_k$ was the covariance matrix.

4. N was the number of the training instances.

5. N_k was the number of class k observation.

6. π_k was the prior probability of class k.

7. μ_k was the mean of the multivariate distribution for each class.

4.7.7 Performance Analysis

Generally, there are a number of approaches to measure the performance of developed BCI systems; namely classification accuracy, Cohen's kappa, information transfer rate, confusion matrix and receiver operating characteristic graph (Baziyad and Djemal, 2014, Thomas et al., 2013). In this study the performance of k-NN, FKNN and QDA classifiers were evaluated using classification accuracy and receiver operating characteristic graph approaches.

Classification accuracy quantifies the performance of the classifier in categorising individual trials correctly and is principally suitable for evaluating synchronised BCI systems (Thomas et al., 2013). Classification accuracy was computed using equation [4.14] (Bunkhumpornpat et al., 2009) shown below:

$$AC = \frac{TP + TN}{TP + TN + FP + FN} * 100 \qquad [4.14]$$

Where TP is true positive, TN is true negative, FP is false positive and FN is false negative.

On the other hand, receiver operating characteristic (ROC) is a two dimensional graph that plots true positive rate (TPR) on y axis and false positive rate (FPR) rate on x axis, depicting the relative trade-off between benefit (TP) and cost (FP) (Fawcett, 2006). Moreover, the ROC graph can also be considered as a visualising method that quantifies the separability of feature space by the applied classifier (Thomas et al., 2013). TPR and FPR was computed using equations [4.15] and [4.16] (Bunkhumpornpat et al., 2009), respectively, as below:

$$TPR = \frac{TP}{TP + FN} \qquad [4.15]$$

And

$$FPR = \frac{FP}{TN + FP} \qquad [4.16]$$

In the present study, TP refers to the true detection of imagination/intention of movement (there is event of imagination/intention of movement and the classifier correctly identified the event) and TN refers to the true rejection of imagination/intention of movement (there is no event of imagination/intention of movement and classifier correctly identified it as no event detection). FP refers to the false detection of imagination/intention of movement (there is no event of imagination/intention of movement but the classifier wrongly identified detection of the event), whereas FN refers to the false rejection of imagination/intention of movement (there is event of imagination/intention of movement but the classifier wrongly rejects the detection of the event).

4.8 Summary

This chapter has shown that the recorded EEG signal was analysed offline using the signal processing methods which comprised of pre-processing, feature extraction, statistical analysis, classification and performance analysis. All of these processes were implemented using Matlab and EEGLAB. In pre-processing, artefacts and noise were excluded from the epochs signal using visual inspection and filtering processes. The filtering processes comprise of the implementation of notch filter, bandpass filter, and CAR and LAP spatial filters. Features were extracted using power spectrum and ANOVA test (p value). The ANOVA test was implemented to determine whether or not significant differences occur in the epochs of EEG signal across all of the four different directions. The extracted features were normalised using z score and the dimensionality was reduced using PCA. Then the features were classified using k-NN, FKNN and QDA classifiers. The proposed BCI system performance was assed using receiver operating characteristic graph approaches.

Chapter 5. Results on Healthy Subjects

5.1 Introduction

Chapter 5 presents the results from the pilot study which involved the healthy subjects. The results presented in this section cover demographic studies, movement initiation time, normality test, data distribution, movement related cortical potential, event related spectral perturbation, ANOVA, classification results and performance evaluation. Results for each parameter were presented separately based on type of spatial filter and type of classifier.

In this chapter, analyses of the recorded EEG signal in the motor task and motor imagery experiments were both presented. The recorded EEG signal from the motor task experiment was referred to as MT; whereas the recorded EEG signal from motor imagery was referred to as MI. The EEG signal was pre-processed using two spatial filters namely, CAR and LAP. MT filtered by CAR and LAP were further termed as MTCAR and MTLAP. Similarly, MI filtered by CAR and LAP were termed as MICAR and MILAP.

When analysing MT, the analysis was focused on two important instances of time. One of these was the onset of visual cue presentation, which instructs the subjects to perform the movement in one of the four directions. The other important time instance was the onset of movement, which refers to the estimated time when the subjects start to perform the movement (computed from the movement signal) after onset of the visual cue. In the recording, onset of the visual cue is at T=0ms. The onset of the movement normally occurred after a few hundred milliseconds (T $\leq$ 500ms). In order to differentiate with the analysis of motor imagery, the onset of movement was offset corrected at T = 0ms. As a result, the onset of the visual cue preceded onset of movement (T $\geq$ -500 ms). The onset of the movement and onset of the visual cue are denoted as t_m, and t_c, respectively. Similarly, in the motor imagery experiment, subjects only imagined movement in one of four directions without physically moving the manipulandum. Therefore, onset of the visual cue is the focus of analysis in the motor imagery experiment.

5.2 Recorded data

EEG and EMG signals were synchronised and simultaneously recorded whilst subjects imagined/performed wrist movement in four different directions following a visual cue. An example of the recorded EEG and EMG signals were displayed in Figure 5.1.
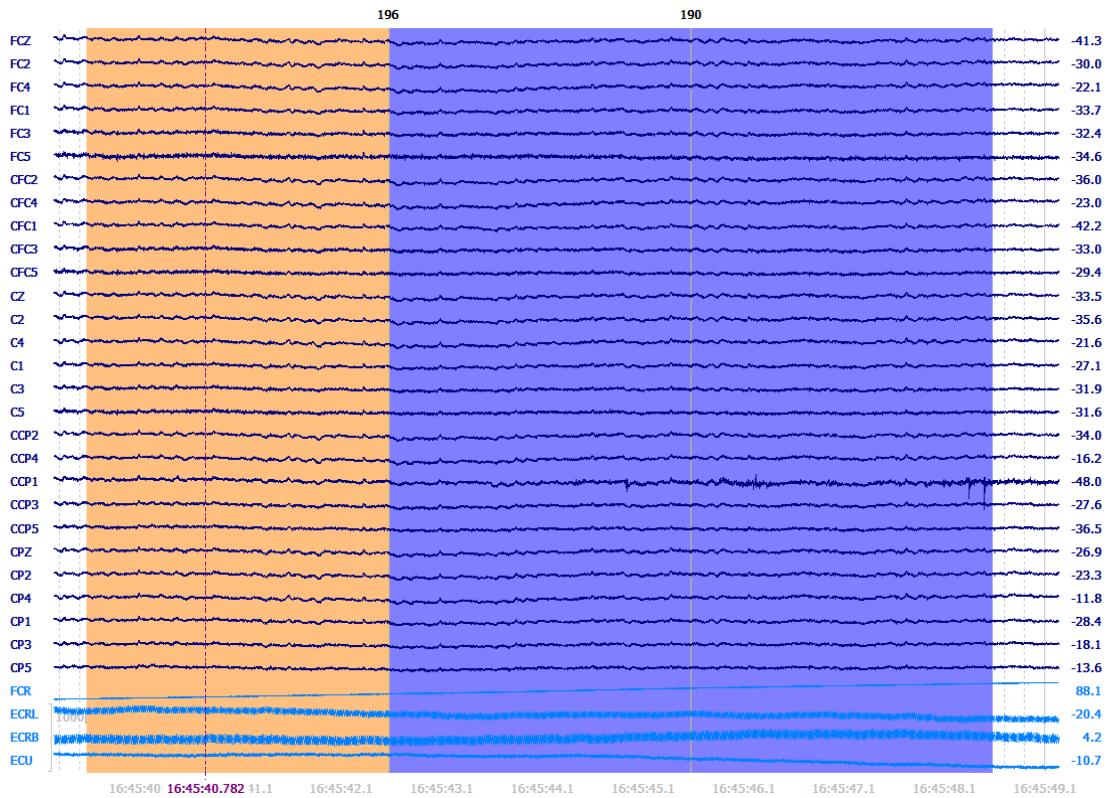
Figure 5.1: Example of recorded EEG and EMG signals. The vertical axis shows thirty two recording electrodes. Top twenty eight represent EEG recording electrodes and the remaining four are EMG recording electrodes. Horizontal axis represents the time of recording. Data recording was synchronised by digital event markers which can be seen on the top of the screen. In this figure, the event markers were '196' and '190' which present the onset of visual cues that instruct the subjects to perform movement in direction 6 and movement back to neutral respectively.

Figure 5.1 illustrates a segment of EEG and EMG signal recordings from subject S11 in one session of the motor task experiment. In Figure 5.1, two digital event markers namely, 196 (in black coloured text) and 190 (in pink coloured text) were shown. Digital event markers 196 and 190 represent the onset of visual cues which instruct the subject to perform movement in direction 6 and movement back to neutral, respectively.

When subjects performed the movement in different directions, several muscles were activated. Table 5.1 lists the muscles involved corresponding to different directions.

Table 5.1: Relation between direction of movement and activation of the muscle.

Direction of the movement	Muscles activated
Direction toward 3	ECRL, ECRB and ECU
Direction toward 6	ECRL, ECRB and FCR
Direction toward 9	FCR
Direction toward 12	ECU and FCR

Figure 5.2 shows a typical EMG recording of subject S11 corresponding to movement in different directions. Figure 5.2 also shows that there was a latency of less than 500ms between the onset of the visual cue and subject performing the movement.
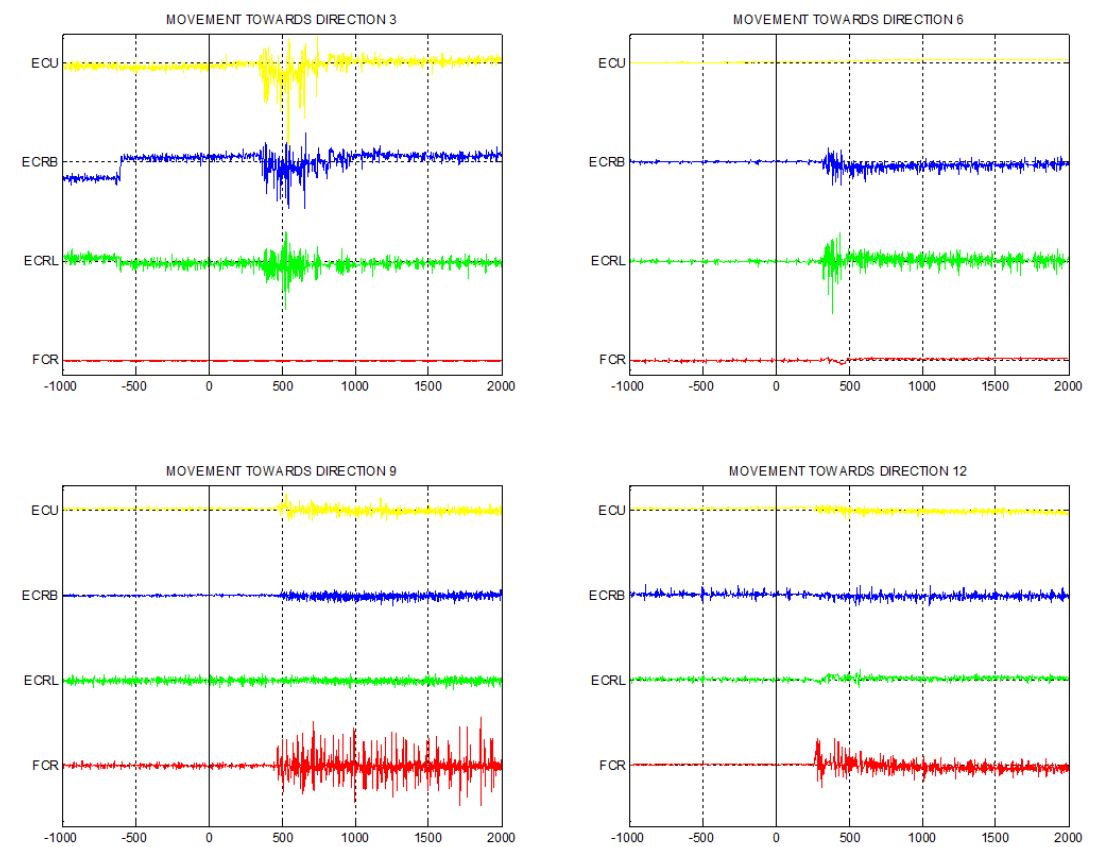
Figure 5.2: EMG recorded signal. Vertical axis shows four recording electrodes. ECU muscle (in yellow colour), ECRB muscle (in blue colour), ECRL muscle (in green colour) and FCR muscle (in red colour) contraction corresponding to four different directions. Horizontal axes represent the time of recording; visual cue onset is at t=0.

81

The movement signal recorded from a potentiometer fitted on the manipulandum was used to validate whether subjects performed the correct movement during the motor task experiment. This was also used to confirm absence of movement in the motor imagery experiment. Figure 5.3 illustrates the movement trajectory of subject S11 in the motor task experiment.
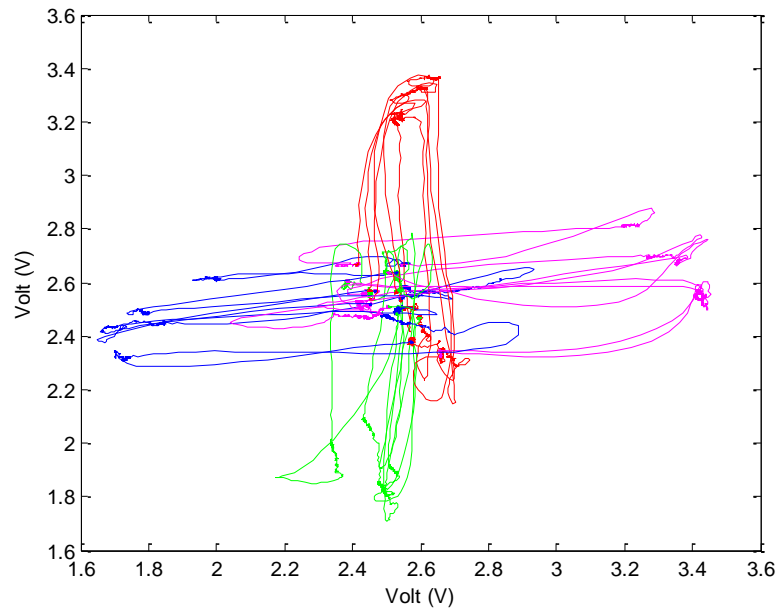
Figure 5.3: Trajectory of movement signal. Y axis shows voltage changes in vertical movement (6 and 12 directions) of the subjects. X axis indicates the voltage changes in horizontal movement (3 and 9 directions) of the subjects.

The trajectory of movement signal in Figure 5.3 was based on 20 trials performed by subject S11 in the motor task experiment. In Figure 5.3, voltage changes caused by movement toward direction 3, 6, 9 and 12 was presented in pink, blue, green, and red respectively.

5.3   Demographic Studies

Eleven postgraduate students (nine male) of the University of Strathclyde with an average age of 28.09 years participated in the pilot study. The details of participated subjects were shown in Table 5.2.

Table 5.2: Details of the healthy subject and their participation with the experiment.

Subject	Gender	Age	Motor imagery experiment	Motor task experiment
S1	Male	44	Participated	Participated
S2	Male	26	Participated	Participated
S3	Male	25	Participated	Participated
S4	Female	26	Participated	Participated
S5	Female	25	Participated	Participated
S6	Male	22	Participated	Participated
S7	Male	24	Participated	Participated
S8	Male	23	Participated	Participated
S9	Male	33	Participated	Participated
S10	Male	27	Participated	Participated
S11	Male	34	Participated	Participated

Table 5.2 shows that, majority of the participated healthy subject aged below 30 years old. All of them managed to participate and completed all the trials in both of experiments.

5.4   Movement Initiation Time

Movement initiation time is the time required by the subject to start moving the manipulandum from the neutral position towards the direction of 3, 6, 9 or 12 after onset of the visual cue. Based on this definition and criteria described in section (4.2), the movement initiation time of motor task experiment for subject S11 was calculated and presented in Figure 5.4.
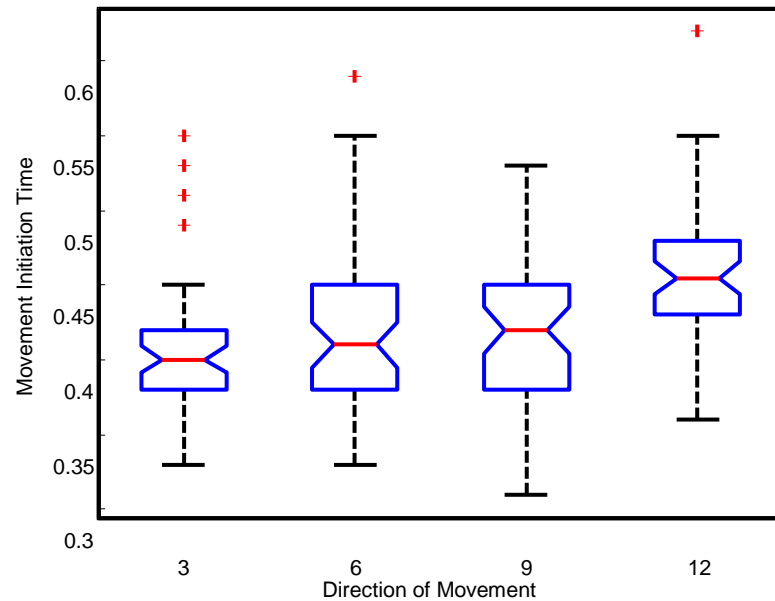
Figure 5.4: Boxplot of Movement Initiation Time for Subject S11.

Figure 5.4 depicts the distribution of movement initiation time towards directions 3, 6, 9 and 12 by subject S11 while performing movements in the motor task experiment. The mean values of initiation time for direction 3, 6, 9 and 12 are 0.36, 0.4, 0.42 and 0.42 second respectively.

ANOVA test has been implemented on the movement initiation time for all healthy subjects while they participated in the motor task experiment (for further clarification of movement initiation time results from other healthy subjects please refers to Appendix D). The ANOVA test was conducted based on significance threshold of 0.05. The results (refer to Table 5.3) indicate that most of the subjects (except for subject S3) display a significant difference between initiation times of movement towards the four different directions.

Table 5.3: P value results of movement initiation time for healthy subjects

Subject	P value results
S1	$p=1.5\times10^{-6}$
S2	$p=0.01$
S3	$p=0.245$
S4	$p=4.8\times10^{-8}$
S5	$p=0.000222$
S6	$p=0.017$
S7	$p=5.56\times10^{-6}$
S8	$p=0.0019$
S9	$p=8.79\times10^{-12}$
S10	$p=5.09\times10^{-12}$
S11	$p=3.7\times10^{-6}$

5.5 Normality Test

The normality test was implemented using the Kolmogorov-Smirnov test (KS) on 28 EEG recording electrodes (Acqualagna et al., 2016) for both of the experiments. Results of these normality tests were be further explained in sections 5.5.1 and 5.5.2.

5.5.1 Data Distribution for Normal Subjects

In the KS test, a result of h=0 indicates that the tested data has a Gaussian distribution, and a result of h=1 indicates that the tested data has a non-Gaussian distribution; with a significance level of 0.05. Table 5.4 and Table 5.5 present the KS test results for both of the motor imagery and motor task experiments, respectively.

Table 5.4: Normality test results of 11 normal subject's data from the motor imagery experiment.

Electrode	S1	S2	S3	S4	S5	S6	S7	S8	S9	S10	S11
FCZ	h=0	h=1	h=0	h=0	h=0	h=0	h=0	h=0	h=0	h=0	h=0
FC2	h=0	h=1	h=0	h=0	h=0	h=0	h=0	h=0	h=0	h=0	h=0
FC4	h=0	h=1	h=0	h=0	h=0	h=0	h=0	h=0	h=0	h=0	h=1
FC1	h=0	h=1	h=0	h=0	h=0	h=0	h=0	h=0	h=0	h=0	h=1
FC3	h=0	h=1	h=0	h=0	h=0	h=0	h=0	h=0	h=0	h=0	h=0
FC5	h=0	h=1	h=0	h=0	h=0	h=0	h=0	h=0	h=0	h=0	h=0
CFC2	h=0	h=0	h=0	h=0	h=0	h=0	h=0	h=0	h=0	h=0	h=0
CFC4	h=0	h=0	h=0	h=0	h=0	h=0	h=0	h=0	h=0	h=0	h=0
CFC1	h=0	h=0	h=0	h=0	h=0	h=0	h=0	h=0	h=0	h=0	h=1
CFC3	h=0	h=0	h=0	h=0	h=0	h=0	h=0	h=0	h=0	h=0	h=0
CFC5	h=0	h=0	h=0	h=0	h=0	h=0	h=0	h=0	h=0	h=0	h=0
CZ	h=0	h=0	h=0	h=0	h=0	h=0	h=0	h=0	h=0	h=0	h=0
C2	h=0	h=0	h=0	h=0	h=0	h=0	h=0	h=0	h=0	h=0	h=0
C4	h=0	h=1	h=0	h=0	h=0	h=0	h=0	h=0	h=0	h=0	h=0
C1	h=0	h=0	h=0	h=0	h=0	h=0	h=0	h=0	h=0	h=0	h=0
C3	h=0	h=0	h=0	h=0	h=0	h=0	h=0	h=0	h=0	h=0	h=0
C5	h=0	h=1	h=0	h=0	h=0	h=0	h=0	h=0	h=0	h=0	h=0
CCP2	h=0	h=0	h=0	h=0	h=0	h=0	h=0	h=0	h=0	h=0	h=0
CCP4	h=0	h=0	h=0	h=0	h=0	h=0	h=0	h=0	h=0	h=0	h=0
CCP1	h=0	h=0	h=0	h=0	h=0	h=0	h=0	h=0	h=0	h=0	h=0
CCP3	h=0	h=0	h=0	h=0	h=0	h=0	h=0	h=0	h=0	h=0	h=0
CCP5	h=0	h=0	h=0	h=0	h=0	h=0	h=0	h=0	h=0	h=0	h=0
CPZ	h=0	h=1	h=0	h=0	h=0	h=0	h=0	h=0	h=0	h=0	h=1
CP2	h=0	h=1	h=0	h=0	h=0	h=0	h=0	h=0	h=0	h=0	h=0
CP4	h=0	h=1	h=0	h=0	h=0	h=0	h=0	h=0	h=0	h=0	h=0
CP1	h=0	h=1	h=0	h=0	h=0	h=0	h=0	h=0	h=0	h=0	h=0
CP3	h=0	h=1	h=0	h=0	h=0	h=0	h=0	h=0	h=0	h=0	h=0
CP5	h=0	h=1	h=0	h=0	h=0	h=0	h=0	h=0	h=0	h=0	h=0

Table 5.4 presents the KS test result of healthy subjects for the motor imagery experiment. From this table it was clearly seen that majority of the healthy subjects have Gaussian distribution in all 28 active recording electrodes, except for subject S2 and subject S11.

Table 5.5: Normality test results of 11 normal subject's data from the motor task experiment. .

Electrode	S1	S2	S3	S4	S5	S6	S7	S8	S9	S10	S11
FCZ	h=0	h=0	h=0	h=0	h=0	h=0	h=0	h=0	h=0	h=0	h=0
FC2	h=0	h=0	h=0	h=0	h=0	h=0	h=0	h=0	h=0	h=0	h=0
FC4	h=1	h=0	h=0	h=0	h=0	h=0	h=0	h=0	h=0	h=0	h=0
FC1	h=1	h=0	h=0	h=0	h=0	h=0	h=0	h=0	h=0	h=0	h=1
FC3	h=0	h=0	h=0	h=0	h=0	h=0	h=0	h=0	h=0	h=0	h=0
FC5	h=1	h=0	h=0	h=0	h=0	h=0	h=0	h=0	h=0	h=0	h=1
CFC2	h=0	h=0	h=0	h=0	h=0	h=0	h=0	h=0	h=0	h=0	h=0
CFC4	h=0	h=0	h=0	h=0	h=0	h=0	h=0	h=0	h=0	h=0	h=0
CFC1	h=1	h=0	h=0	h=0	h=0	h=0	h=0	h=0	h=0	h=0	h=1
CFC3	h=0	h=0	h=0	h=0	h=0	h=0	h=0	h=0	h=0	h=0	h=0
CFC5	h=0	h=0	h=0	h=0	h=0	h=0	h=0	h=0	h=0	h=0	h=0
CZ	h=0	h=0	h=0	h=0	h=0	h=0	h=0	h=0	h=0	h=0	h=0
C2	h=0	h=0	h=0	h=0	h=0	h=0	h=0	h=0	h=0	h=0	h=0
C4	h=0	h=0	h=0	h=0	h=0	h=0	h=0	h=0	h=0	h=0	h=0
C1	h=0	h=0	h=0	h=0	h=0	h=0	h=0	h=0	h=0	h=0	h=0
C3	h=0	h=0	h=0	h=0	h=0	h=0	h=0	h=0	h=0	h=0	h=0
C5	h=0	h=0	h=0	h=0	h=0	h=0	h=0	h=0	h=0	h=0	h=0
CCP2	h=0	h=0	h=0	h=0	h=0	h=0	h=0	h=0	h=0	h=0	h=0
CCP4	h=0	h=0	h=0	h=0	h=0	h=0	h=0	h=0	h=0	h=0	h=0
CCP1	h=0	h=0	h=0	h=0	h=0	h=0	h=0	h=0	h=0	h=0	h=0
CCP3	h=0	h=0	h=0	h=0	h=0	h=0	h=0	h=0	h=0	h=0	h=0
CCP5	h=0	h=0	h=0	h=0	h=0	h=0	h=0	h=0	h=0	h=0	h=0
CPZ	h=0	h=0	h=0	h=0	h=0	h=0	h=0	h=0	h=0	h=0	h=0
CP2	h=1	h=0	h=0	h=0	h=0	h=0	h=0	h=0	h=0	h=0	h=0
CP4	h=0	h=0	h=0	h=0	h=0	h=0	h=0	h=0	h=0	h=0	h=1
CP1	h=1	h=0	h=0	h=0	h=0	h=0	h=0	h=0	h=0	h=0	h=0
CP3	h=0	h=0	h=0	h=0	h=0	h=0	h=0	h=0	h=0	h=0	h=0
CP5	h=0	h=0	h=0	h=0	h=0	h=0	h=0	h=0	h=0	h=0	h=0

Tabulated data in Table 5.5 shows the KS test results of healthy subjects for the motor task experiment. Among these eleven healthy subjects that participated in the motor task experiment, only the EEG signal from subject S1 and S11 have a non-Gaussian distribution.

5.6   Movement Related Cortical Potential (MRCP)

Movement related cortical potential (MRCP) is an electrophysiological response associated with overt and covert movements (Xu et al., 2014). The MRCP results associated with MICAR and MILAP were presented in section 5.6.1. On the other hand, the MRCP results associated with MTCAR and MTLAP were presented in section 5.6.2. All of the MRCP results were computed from electrode C3.

5.6.1 MRCP of Motor Imagery

Figure 5.5 shows the grand average of the MRCP waveforms associated with the MICAR towards directions 3, 6, 9 and 12. T=0 represents onset of the visual cue (t_c). From this figure it can be seen that, after t_c there was increasing negativity of amplitude in all of the MRCP waveforms (T<500ms approximately). All of the MRCP waveforms begin returning to the baseline after T=500ms.
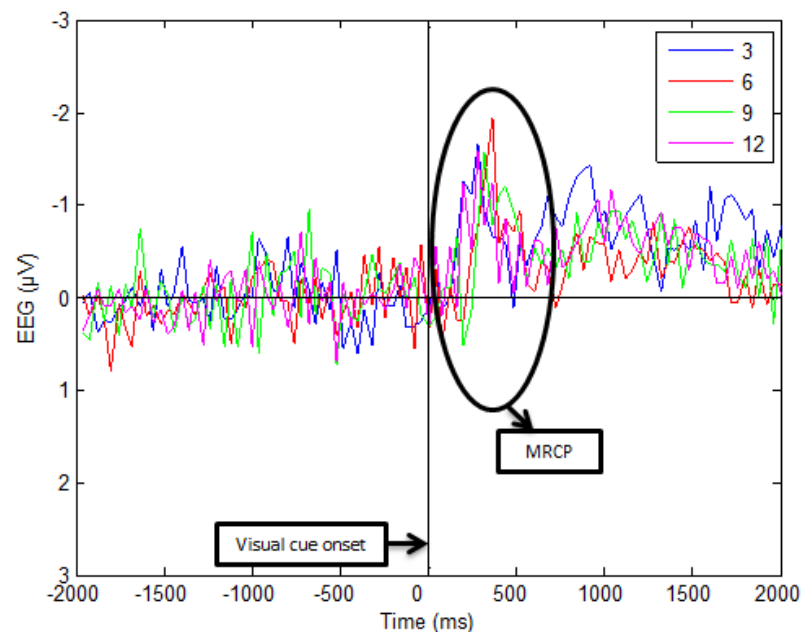
Figure 5.5: MRCP associated with the motor imagery experiment using CAR filter. This figure shows the MRCP recorded from subject S11. X and Y axes represent the recording time and the amplitude of the signal respectively.

The grand average of the MRCP waveforms associated with the MILAP towards direction 3, 6, 9 and 12 were displayed in Figure 5.6. T=0 in this figure represents the visual cue onset (t_c). This figure also shows that there was a small negative increase in amplitude of all the MRCP waveforms 500ms after t_c. These MRCP waveforms then return to baseline approximately after T=500ms.
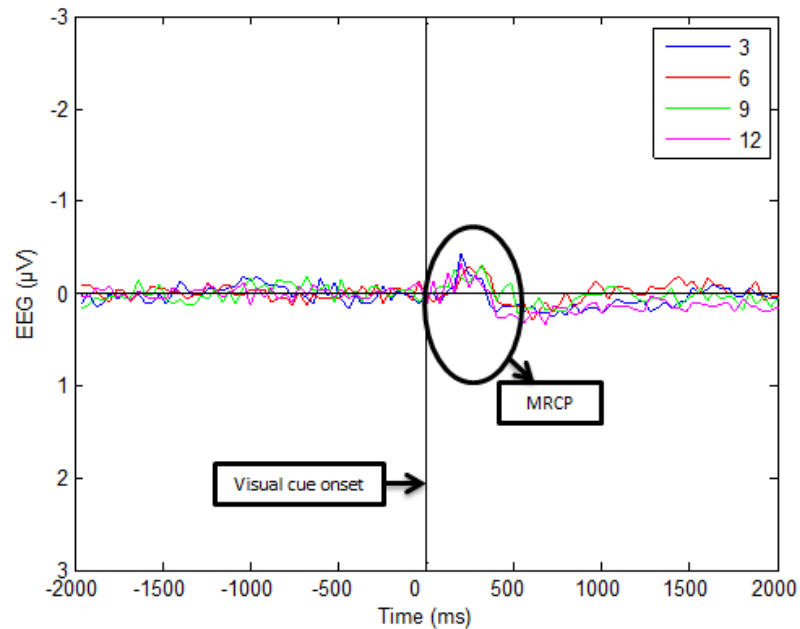
Figure 5.6: MRCP associated with the motor imagery experiment using LAP filter. This figure shows the MRCP recorded from subject S11. X and Y axis represent the recording time and the amplitude of the signal respectively.

5.6.2 MRCP of Motor Task

Electrophysiological changes associated with the MTCAR towards direction 3, 6, 9 and 12 were illustrated by the grand average of the MRCP waveforms in Figure 5.7. In this figure, T=0 indicates the movement initiation time (t_m), and a vertical line in cyan colour (-500ms<T<0) represents the visual cue onset (t_c). This figure also shows that, there was a negativity increase in all of the MRCP waveforms after t_c and decreases when reaching t_m. The entire MRCP waveforms also return towards baseline shortly after t_m (approximately after T>500ms).
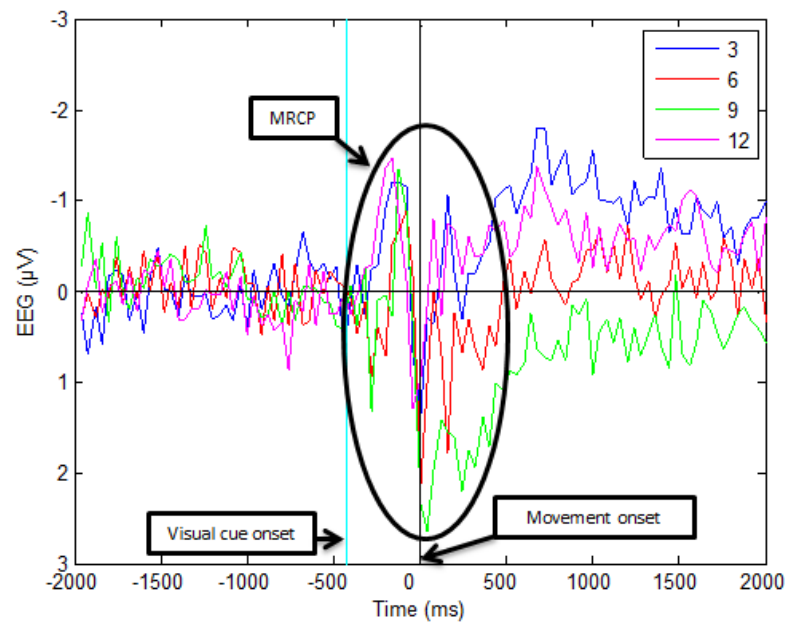
Figure 5.7: MRCP associated with motor task experiment using CAR filter. This figure shows the MRCP recorded from subject S11. X and Y axis represent the recording time and the amplitude of the signal respectively.

The grand average of the MRCP waveforms associated with the MTLAP towards directions 3, 6, 9 and 12 recorded from electrode C3 were portrayed in Figure 5.8. In this figure, T=0 indicates the movement initiation time (t_m), and a vertical line in cyan colour (-500ms<T<0) represents the visual cue onset (t_c). This figure also shows that there is a slightly negativity increase in all of the MRCP waveforms after t_c that decreases when reaching t_m. Although there was a small decline in MRCP negativity after t_c, the entire MRCP waveforms return towards baseline shortly after t_m (approximately after T>500ms).
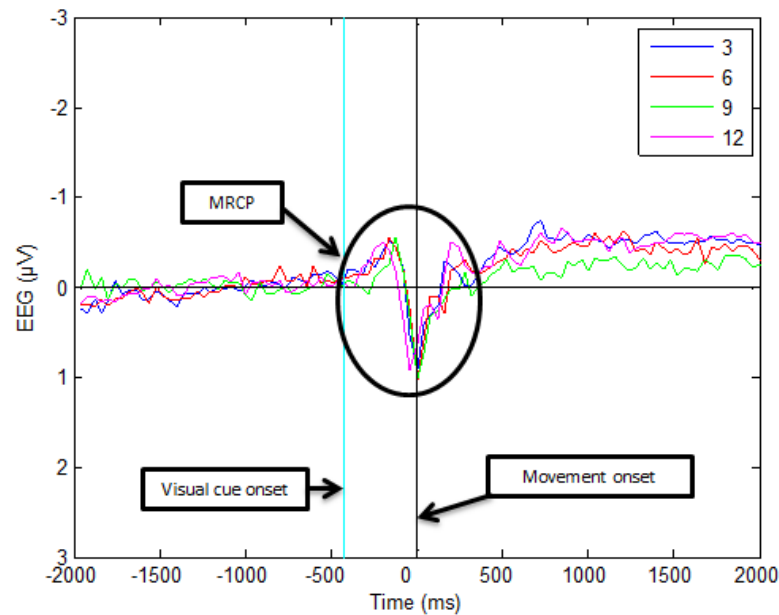
Figure 5.8: MRCP associated with motor task experiment using LAP filter. This figure shows the MRCP recorded from subject S11. X and Y axes represent the recording time and the amplitude of the signal respectively

5.7   ANOVA and ERSP

In this section, results of the ANOVA test were visualised in the same plot of the ERSP. From top to bottom, the first four plots represent the ERSP of movement/imagination of movement towards directions 3, 6, 9 and 12, respectively. The fifth plot illustrates *p* values from the ANOVA test conducted across all ERSPs (top four plots). In the ERSP plots blue and red colouring show the ERD and the ERS, respectively whereas in the ANOVA plot, the blue region represents

significance differences in ERSP across all four directions. All of the ERSP and ANOVA results were computed from electrode C3.

5.7.1 Statistical Difference of Motor Imagery

Figure 5.9 portrays the results from ANOVA test performed on the ERSP associated with MICAR. T=0 represents the onset of the visual cue (t_c). Occurrences of the ERD was seen in frequency bands of beta and gamma for all direction 300ms post t_c., The ERS was detected within delta, theta, alpha, beta and gamma bands before and after t_c. The significant difference exists in ERSP across all four directions after t_c. The significant differences were represented by clustered blue regions which can be seen within delta, theta, alpha and beta frequency bands after t_c. Moreover, there were also significant differences within the delta, theta, alpha, beta and gamma bands before t_c.
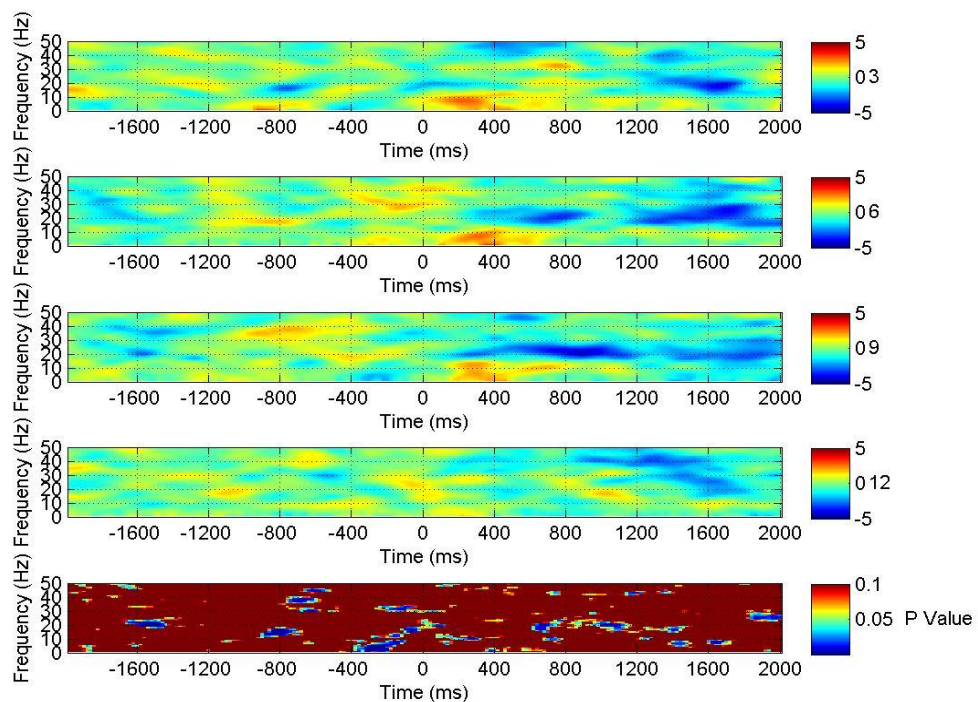
Figure 5.9: ANOVA results associated with motor imagery experiment using CAR filter. Top four plots represent the ERSPs of EEG at electrode C3 recorded from subject S11 when performing imagination of movement towards four different directions; the bottom plot represent ANOVA results of the above ERSPs. Vertical axes represent signal frequency and horizontal axes represent recording time.

Figure 5.10 illustrates the ANOVA results across ERSPs associated with MILAP towards direction 3, 6, 9 and 12; T=0 illustrates the onset of the visual cue (t_c). In this figure, the ERS was detected within delta, theta and alpha bands across all four directions after t_c. Besides that, the ERS also detected in beta and gamma bands before t_c. On the other hand, the ERD was detected within the beta band across of all four directions. Detection of the prolonged ERD (until T>1200ms) within beta bands can be seen in the ERSP associate with direction 6 and 12. From this figure also, it can see that there were significance difference across all four ERSPs, especially after t_c (approximately 500ms before t_m). The significant differences were represented by clustered blue regions within alpha, beta and gamma bands. The significant differences before t_c were detected in delta, theta and alpha frequency bands.
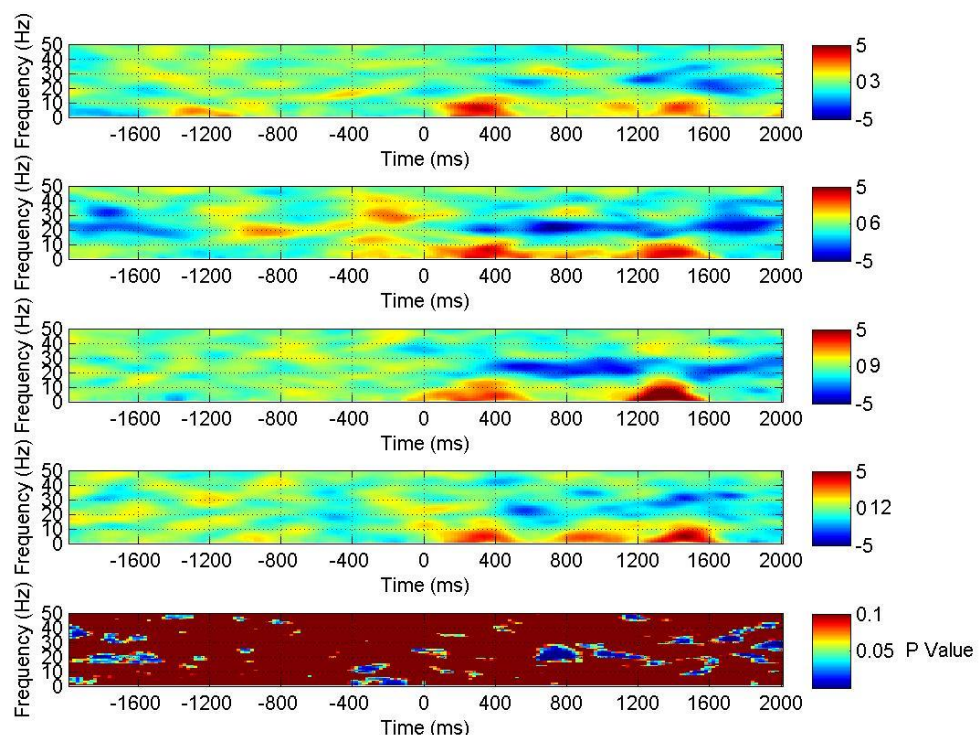
Figure 5.10: ANOVA results associated with motor imagery experiment using LAP filter. Top four plots represent the ERSPs of EEG at electrode C3 recorded from subject S11 when performing imagination of movement towards four different directions; the bottom plot represent ANOVA results of the above ERSPs. Vertical axes represent signal frequency and horizontal axes represent recording time.

5.7.2 *Statistical Difference of Motor Task*

Statistical analysis using the ANOVA test was conducted across ERSPs associated with MTCAR towards direction 3, 6, 9 and 12. Results of this ANOVA test were depicted in Figure 5.11. In this figure, the subject started to perform the movement at T=0 (onset of the movement, t_m). The ERD can be seen in ERSP within beta and gamma bands across all four directions prior to t_m. Apart from that, the ERS was also detected within frequencies of the delta, theta and alpha bands across all four directions. After onset of the movement, when T>0, the appearance of prominent ERD across alpha, beta and gamma bands were also shown in all four directions. It also can be seen that prior to t_m, there were a significant differences across ERSP in all four directions. This significant difference is represented by clustered blue regions within the delta, theta, alpha, beta and gamma bands.
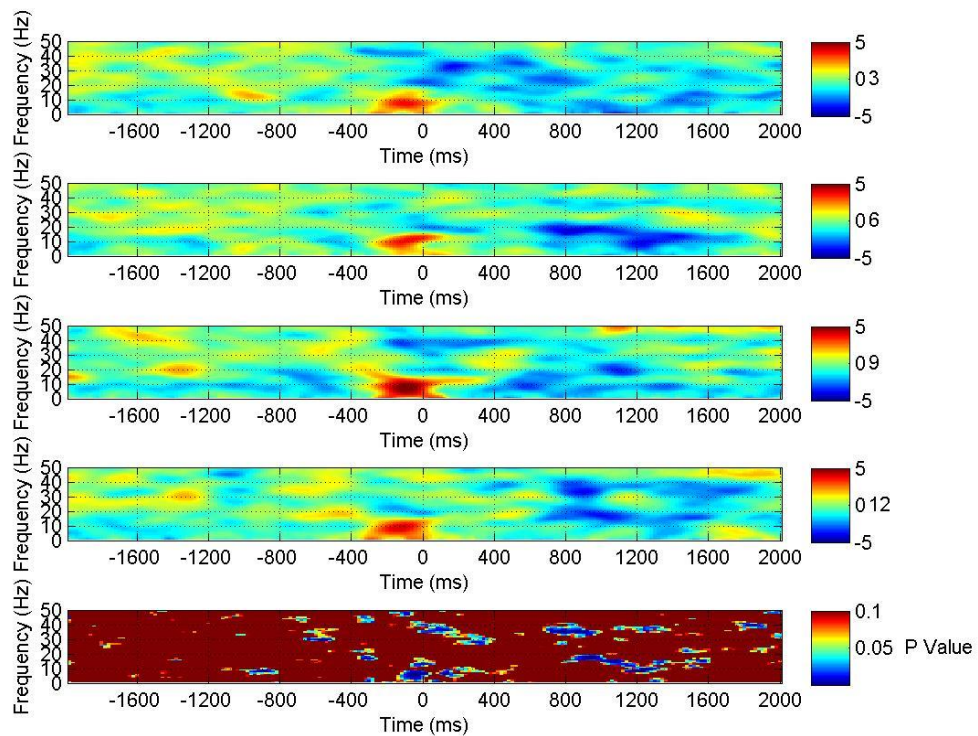
Figure 5.11: ANOVA results associated with motor task experiment using CAR filter. Top four plots represent the ERSPs of EEG at electrode C3 recorded from subject S11 when performing movement towards four different directions; the bottom plot represent ANOVA results of the above ERSPs. Vertical axes represent signal frequency and horizontal axes represent recording time.

The results of ANOVA test across ERSPs associated with MTLAP towards direction 3, 6, 9 and 12 were portrayed in Figure 5.12. Based on this figure, subject started to perform the movement at T=0 (onset of the movement, t_m). The ERD and the ERS were detected before and after t_m. The ERD and the ERS was prominent detected in delta, theta and alpha band 400ms before the t_m. Detection of the prolonged ERD and ERS 400ms before the t_m suggests that during the rest time, subject was cognitively intact. Besides that, the ERD also was detected in beta and gamma bands across the ERSP of all the direction prior to the t_m. After t_m, occurrence of ERD can be seen in delta, theta, alpha, beta and gamma bands in all direction. The significant differences across all ERSPs were detected within delta, theta, alpha and beta bands prior to t_m.
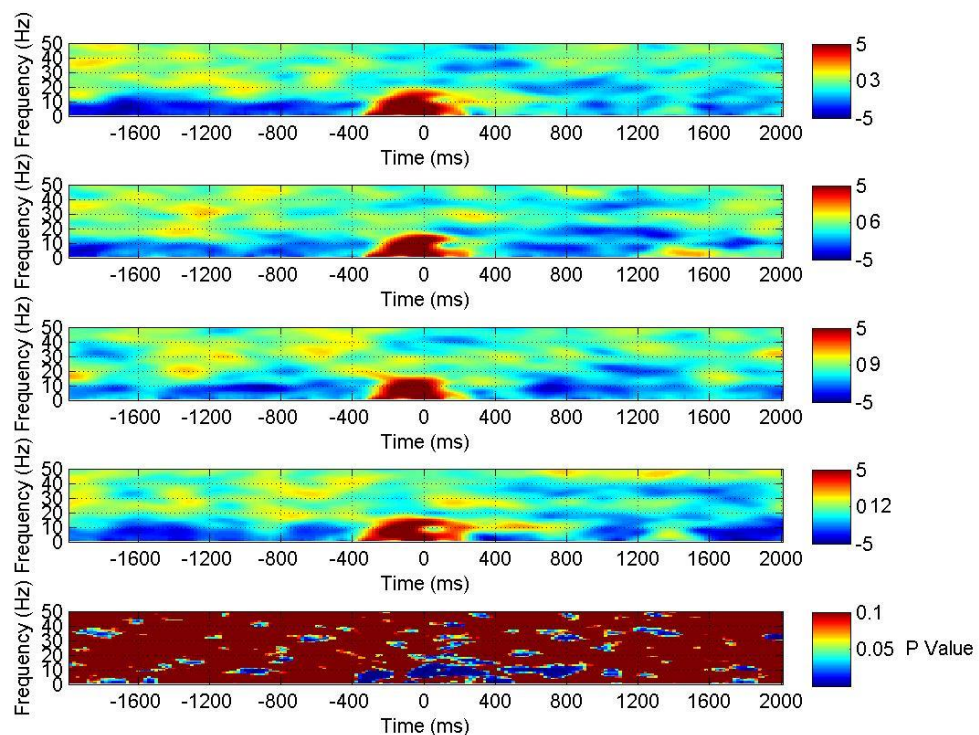
Figure 5.12: ANOVA results associated with motor task experiment using LAP filter. Top four plots represent the ERSPs of EEG at electrode C3 recorded from subject S11 when performing movement towards four different directions; the bottom plot represent ANOVA results of the above ERSPs. Vertical axes represent signal frequency and horizontal axes represent recording time.

95

5.8 Classification Results

Classification is an essential step in translating the EEG brain signature into a command to communicate with the external environment. As discussed in the chapter 4, the classification applied in this study was based on off-line single trials basis. The classification attempts to predict imagination/intention of movement, predict imagination/intention of movement towards direction 3, 6, 9 and 12, and predict imagination/intention combined with direction of movement. Even though the classification was performed on 28 active recording electrodes with multiple EEG signal components (delta, theta, alpha, beta and gamma frequency bands), different spatial filters (CAR and LAP) and classifiers (k-NN, FKNN and QDA), only the combination that achieved highest classification accuracy will be presented for each subject.

5.8.1 Predicting Imagination/ Intention of Movement

In this subsection, predicting the imagination/intention of movement for healthy subjects was further investigated. For this purpose, the classifiers attempted to detect the subject's imagination/intention to move by distinguishing whether the subject's wrist was stationary in the neutral position or when subject start to perform the imagination/movement towards any of the different four directions.

5.8.1.1 Predicting Imagination of Movement from Healthy Subjects

The classification results for healthy subjects in predicting imagination of movement were exhibited in Figure 5.13. In this figure, the classification results for each subject was presented in terms of the spatial filter and classifier combinations applied. The classification accuracies were between 61.00%-94.00% using combination of CAR spatial filter and k-NN classifier (CAR+ k-NN). Combination of CAR spatial filter and FKNN classifier (CAR+FKNN) resulted in accuracies of 63.00%-94.00%, whereas a classification result of 56.00%-95.00% was obtained from the combination of CAR spatial filtering and the QDA classifier (CAR+QDA). On the other hand, the accuracy of the LAP spatial filter combined with k-NN (LAP+ k-NN), FKNN

(LAP+FKNN) and QDA (LAP+QDA) classifiers fall within the ranges of 67.00%-98.00%, 69.00%-99.00% and 60.00%-97.00%, respectively. In comparison among the participated subjects, only subject S10 gave the classification accuracy more than 80.00% in all combinations of spatial filters and classifier applied.
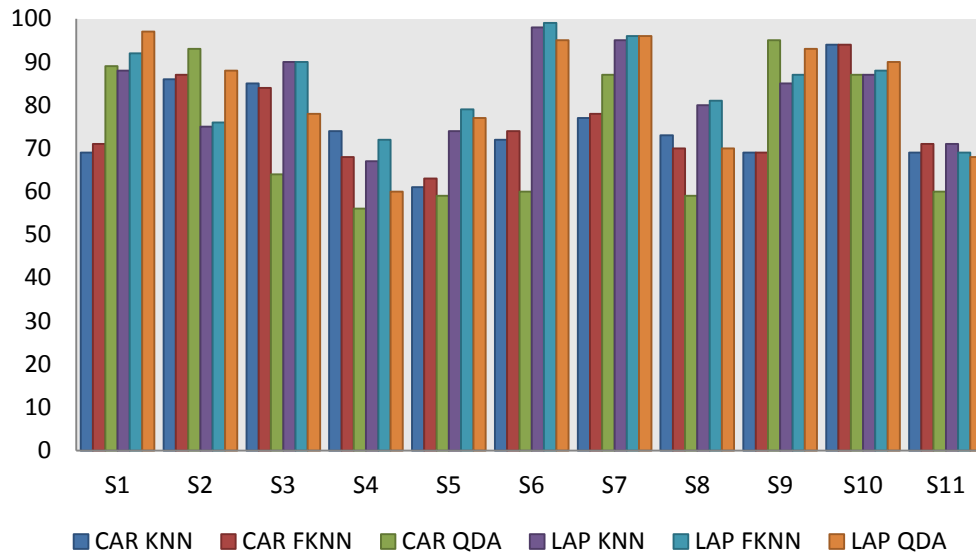
Figure 5.13: Classification results for healthy subjects in predicting imagination of movement. The classification results from each subject were presented based on the combinations of classifiers and spatial filters applied.

The average maximum classification results of predicting imagination of movement by healthy subjects depicted in Figure 5.14. This figure shows that, the average maximum classification results of CAR+ k-NN, CAR+FKNN and CAR+QDA were 75.36%, 75.36% and 73.55% respectively. On the other hand, the average maximum classification results of LAP+ k-NN, LAP+FKNN and LAP+QDA were 82.73%, 84.45% and 82.91% respectively. Besides, this figure also shows that combination of LAP spatial filter with classifier give higher results compared to combination of CAR spatial filter with classifier.
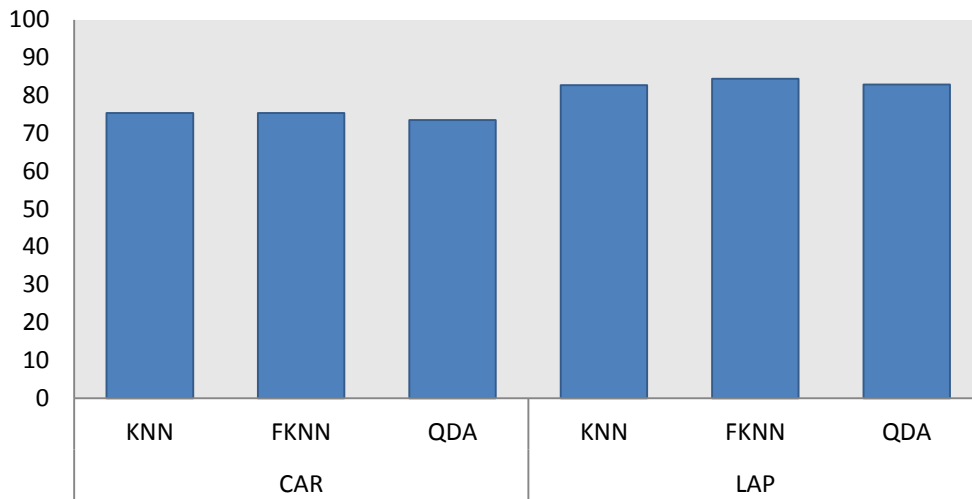
Figure 5.14: The average maximum classification results for healthy subjects in predicting imagination of movement. The classification results were presented based on the combinations of classifiers and spatial filters applied.

The frequency bands associated with the classification results depicted in Figure 5.13 were shown in Table 5.6. Table 5.6 shows that majority of the results was obtained from gamma band. This was supported by, 5 out of 11 (45.45%) of the classification results from CAR+QDA, LAP+FKNN and LAP+QDA were obtained from the gamma band. Besides that, 6 out of 11 (54.55%) of the classification results from CAR+k-NN and 7 out of 11 (63.64%) of the classification results from LAP+k-NN were also obtained from the gamma band. Only 6 out of 11 (54.55%) of the classification results from CAR+FKNN obtained from the alpha band.

Table 5.6: Frequency band associated with the classification results from healthy subjects for predicting imagination of movement.

Subject	Frequency band associated with the maximum classification accuracy					
	CAR			LAP		
	KNN	FKNN	QDA	KNN	FKNN	QDA
S1	ALPHA	ALPHA	BETA	ALPHA	ALPHA	BETA
S2	GAMMA	GAMMA	GAMMA	GAMMA	GAMMA	GAMMA
S3	GAMMA	GAMMA	BETA	GAMMA	GAMMA	BETA
S4	GAMMA	GAMMA	GAMMA	BETA	BETA	GAMMA
S5	ALPHA	ALPHA	ALPHA	ALPHA	ALPHA	ALPHA
S6	ALPHA	ALPHA	ALPHA	ALPHA	ALPHA	GAMMA
S7	GAMMA	GAMMA	GAMMA	GAMMA	GAMMA	GAMMA
S8	GAMMA	ALPHA	ALPHA	GAMMA	BETA	ALPHA
S9	ALPHA	ALPHA	GAMMA	GAMMA	GAMMA	BETA
S10	GAMMA	GAMMA	GAMMA	GAMMA	GAMMA	GAMMA
S11	ALPHA	ALPHA	ALPHA	GAMMA	ALPHA	ALPHA

Table 5.7 presents the list of recording electrodes associated with the classification results portrayed in Figure 5.13. In this table, it shows that the majority of the highest classification accuracy results were obtained from contralateral electrodes. For instance, 8 out of 11 (72.73%) of the classification results from CAR+QDA, LAP+k-NN and LAP+FKNN were obtained from contralateral electrodes. Apart from that, 7 out of 11 (63.64%) of the classification results from CAR+k-NN and 9 out of 11 (81.82%) of the classification results from LAP+QDA were also obtained from the contralateral electrodes. Only 6 out of 11 (54.55%) of the classification results from CAR+FKNN obtained from the ipsilateral electrodes.

Table 5.7: Recording electrode associated with the classification results from healthy subjects for predicting imagination of movement.

Subject	Recording electrode associated with the maximum classification accuracy					
	CAR			LAP		
	KNN	FKNN	QDA	KNN	FKNN	QDA
S1	C5	CFC1	CFC1	CFC1	CFC1	CFC1
S2	C4	C4	FC5	CFC2	CFC2	CFC5
S3	CFC5	FC4	C1	CP4	FC4	FC4
S4	FC3	FC3	CZ	FC3	CFC5	CFC2
S5	C3	CCP4	CP1	CFC1	CFC1	CFC1
S6	FC1	CCP3	CP1	FC2	FC4	FC1
S7	CFC3	CFC3	FC4	CP5	CP5	FC5
S8	C5	FC1	FC1	CCP5	CCP5	CFC1
S9	CCP2	CCP2	FC4	C5	C5	CCP5
S10	FC4	FC4	FC5	C5	C5	CFC5
S11	FC4	FC2	CCP3	CFC5	C3	C3

5.8.1.2   Predicting Intention of Movement from Healthy Subjects

The overall classification results of predicting intention of movement from healthy subjects were presented by Figure 5.15. This figure indicates that, the classification results from CAR+k-NN, CAR+FKNN and CAR+QDA fall within the ranges of 59.00%-91.00%, 63.00%-94.00% and 55.00%-96.00%, respectively. On the other hand, classification results from LAP+k-NN, LAP+FKNN and LAP+QDA lie within the ranges of 69.00%-97.00%, 69.00%-97.00% and 67.00%-99.00% respectively. Among the healthy subjects, only subject S3 has consistent classification accuracy more than 90.00% for all combinations of spatial filter and classifier.
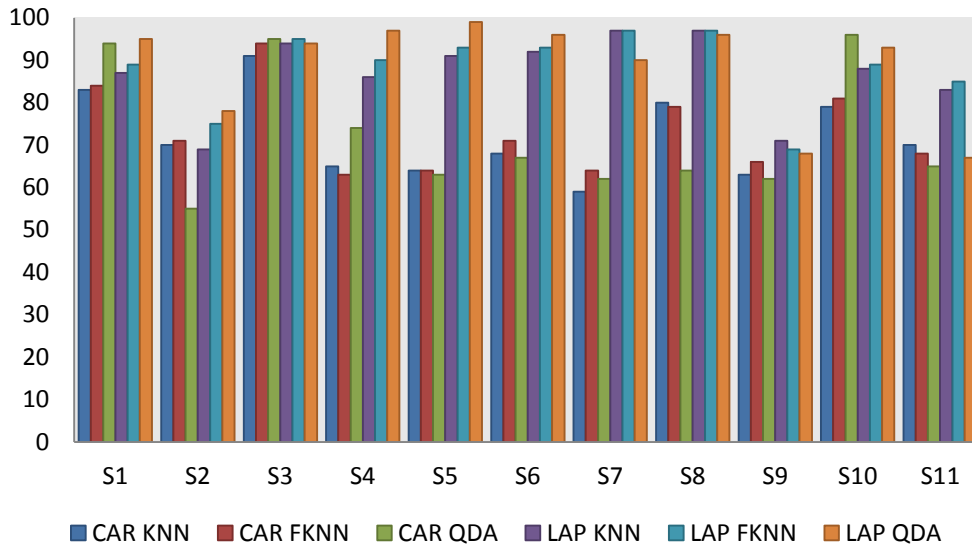
Figure 5.15: Classification results for healthy subjects in predicting intention of movement. The classification results from each subject were presented based on the combinations of classifiers and spatial filters applied.

Table 5.8 shows the frequency band associated with the classification results portrayed in Figure 5.15. This table shows that, 6 out of 11 (54.55%) of the classification results from CAR+FKNN and 5 out of 11 (45.45%) of the classification results from CAR+QDA obtained from alpha bands. Besides that, 6 out of 11 (54.55%) of the classification results from LAP+k-NN and 7 out of 11 (63.64%) of the classification results from LAP+FKNN also obtained from alpha bands. On the other hand, 7 out of 11 (63.64%) of the classification results from CAR+k-NN and 6 out of 11 (54.55%) of the classification results from LAP+QDA were obtained from gamma band.

Table 5.8: Frequency band associated with the classification results from healthy subjects for predicting intention of movement..

| Subject | Frequency band associated with the maximum classification accuracy | | | | | |
| | CAR | | | LAP | | |
	KNN	FKNN	QDA	KNN	FKNN	QDA
S1	ALPHA	ALPHA	GAMMA	ALPHA	ALPHA	GAMMA
S2	GAMMA	GAMMA	ALPHA	ALPHA	ALPHA	GAMMA
S3	GAMMA	GAMMA	GAMMA	GAMMA	GAMMA	GAMMA
S4	GAMMA	ALPHA	BETA	ALPHA	ALPHA	BETA
S5	GAMMA	ALPHA	ALPHA	ALPHA	ALPHA	GAMMA
S6	ALPHA	ALPHA	BETA	GAMMA	ALPHA	BETA
S7	ALPHA	ALPHA	ALPHA	ALPHA	ALPHA	BETA

S8	GAMMA	GAMMA	ALPHA	ALPHA	ALPHA	BETA
S9	ALPHA	ALPHA	ALPHA	GAMMA	GAMMA	BETA
S10	GAMMA	GAMMA	GAMMA	BETA	BETA	GAMMA
S11	GAMMA	GAMMA	GAMMA	GAMMA	GAMMA	GAMMA

The list of recording electrodes associated with the classification results presented in Figure 5.15 was tabulated in Table 5.9. This table shows that most of the classification results were obtained from contralateral electrodes. This is supported by 6 out of 11 (54.55%) of the classification results from CAR+*k*-NN, CAR+FKNN and CAR+QDA were obtained from contralateral electrodes. Besides that, 9 out of 11 (81.82%) of the classification results from LAP+ *k*-NN and LAP+FKNN were also obtained from contralateral electrodes. Furthermore, 8 out of 11 (72.73%) of the classification results from LAP+ QDA also obtained from contralateral electrodes.

Table 5.9: Recording electrode associated with the classification results from healthy subjects for predicting intention of movement..

Subject	Recording electrode associated with the maximum classification accuracy					
	CAR			LAP		
	KNN	FKNN	QDA	KNN	FKNN	QDA
S1	CP5	CP5	CP5	CCP5	CCP5	CCP2
S2	FC5	FC5	CPZ	CCP5	CCP5	CCP3
S3	FC4	FC4	C3	C4	CP1	C1
S4	FC4	C1	CCP1	CCP1	CCP1	CCP1
S5	C3	FC3	FC3	FC4	FC4	C5
S6	CCP5	CFC2	CP5	C5	CCP5	CCP5
S7	CP2	CP4	CP4	FC1	CP1	FC3
S8	FC4	FC4	CCP2	FC1	CP2	FC2
S9	CZ	CCP2	CZ	FC5	FC5	FC5
S10	CP5	CP5	CP5	CP5	CP5	CFC5
S11	CFC5	CFC5	C4	CFC5	CFC5	FC4

5.8.2 *Predicting Imagination/Intention of Movement towards Direction 3, 6, 9 and 12*

Results presented in this section explore the effects of direction on imagination/intention of movement among healthy subjects. For this purpose, the classification result for imagination/intention of movement towards direction 3, 6, 9 and 12 were presented and explained individually along with the frequency band and recoding electrodes that contribute to the maximum accuracy classification results.

5.8.2.1 *Predicting Imagination of Movement towards Direction 3, 6, 9 and 12 from Healthy Subjects*

The overall classification results obtained from the combinations of CAR or LAP spatial filters with k-NN, FKNN and QDA classifiers for predicting imagination of movements towards direction 3 from healthy subjects was depicted in Figure 5.16. This figure demonstrates that the classification results for the combination of CAR+k-NN within the range of 61.00%-86.00%. The combination of CAR+FKNN achieved classification results of 61.00%-86.00%, while 59.00%-94.00% was obtained from the combination of CAR+QDA. Meanwhile the classification results from LAP+k-NN, LAP+FKNN and LAP+QDA lie within the ranges of 70.00%-93.00%, 74.00%-92.00% and 66.00%-94.00%, respectively. The same procedure has been implemented for predicting imagination of movement towards direction 6, 9 and 12 (please refer to Appendix G for further detail).

The maximum classification results for predicting imagination of movement towards direction 6 using CAR+k-NN, CAR+FKNN and CAR+QDA lie within the ranges of 61.00%-74.00%, 59.00%-72.00% and 61.00%-96.00%, respectively. Besides that, classification results of LAP+k-NN, LAP+FKNN and LAP+QDA lie within the ranges of 62.00%-94.00%, 65.00%-95.00% and 63.00%-97.00%, respectively.

The maximum classification results for predicting imagination of movement towards direction 9 using CAR+k-NN, CAR+FKNN and CAR+QDA fall within the ranges of 60.00%-85.00%, 61.00%-91.00% and 59.00%-90.00%, respectively. Furthermore, classification results of LAP+k-NN, LAP+FKNN and LAP+QDA lie within the

ranges of 64.00%-94.00%, 67.00%-94.00% and 69.00%-95.00%, respectively. Between these two types of spatial filter, the LAP method offers higher classification accuracy compared to the CAR spatial filter.

The maximum classification results for predicting imagination of movement towards direction 12 from CAR+k-NN, CAR+FKNN and CAR+QDA dwell within the ranges of 56.00%-73.00%, 59.00%-75.00% and 57.00%-74.00%, respectively. On the other hand, classification results of LAP+k-NN, LAP+FKNN and LAP+QDA lie within the ranges of 62.00%-94.00%, 61.00%-95.00% and 62.00%-96.00%, respectively.

It is essential to emphasise that, most of the classification results for all four directions have a higher classification range when using combination of LAP compared to the CAR spatial filter
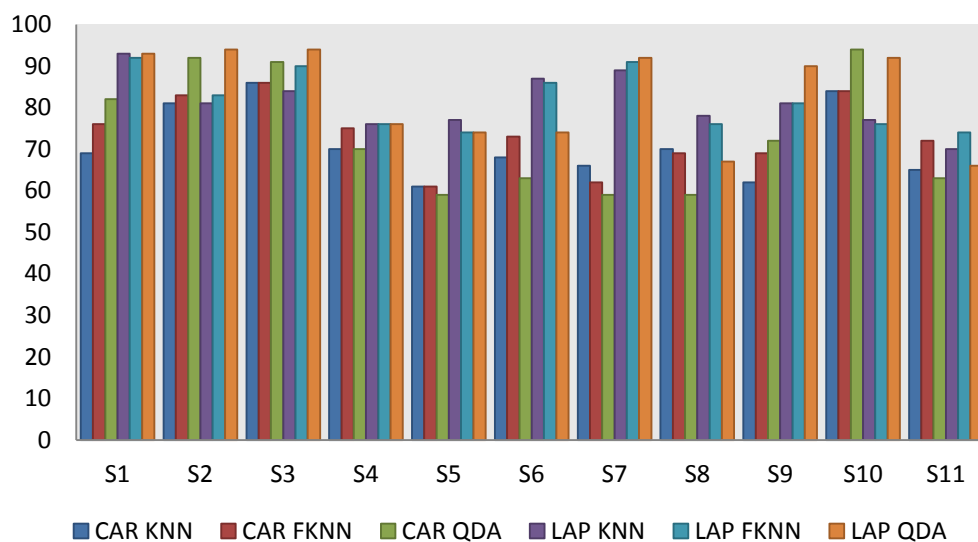
Figure 5.16: Classification results for healthy subjects in predicting imagination of movement towards direction 3. The classification results from each subject were presented based on the combinations of classifiers and spatial filters used.

Tabulated data in Table 5.10 shows the frequency bands associated with the classification results depicted in Figure 5.16. This table demonstrated that, 8 out of 11 (72.73%) of the classification results from CAR+k-NN and CAR+FKNN were obtained from gamma bands. Besides that, 6 out of 11 (75.00%) of the classification results from LAP+FKNN and LAP+QDA were obtained from the alpha band.

Furthermore, 7 out of 11 (63.64%) of the classification results from LAP+ k-NN and 5 out of 11 (45.45%) of the classification results from CAR+QDA were also obtained from gamma band. The same analytical process was carried out to investigate the frequency band associated with highest classification accuracy results from predicting the intention of movement towards direction 6, 9 and 12 (please refer to Appendix G for further detail).

Majority of the highest classification results for predicting imagination of movements towards direction 6 from healthy subjects were obtained from the gamma band. This was supported by 6 out of 11 (54.55%) of the classification results from CAR+k-NN, CAR+FKNN and CAR+QDA were obtained from gamma band. Besides that, 7 out of 11 (63.64%) of the classification results from LAP+k-NN also obtained from gamma band. Only 5 out of 11 (45.45%) of the classification results from LAP+FKNN and LAP+QDA obtained either from alpha or gamma bands.

On the other hand, the alpha band was mostly associated with the highest classification results for predicting imagination of movement towards direction 9. This was supported by 6 out of 11 (54.55%) of the classification results from CAR+k-NN, CAR+FKNN and CAR+QDA obtained from alpha band. Besides that, 5 out of 11 (45.45%) of the classification results from LAP+QDA also obtained from alpha band. Only 6 out of 11 (54.55%) of the classification results from LAP+k-NN and 7 out of 11 (63.64%) of the classification results from LAP+FKNN obtained from gamma band.

Similarly, majority of the highest classification results for predicting imagination of movement towards direction 12 were obtained from the alpha band. This was shown by 9 out of 11 (81.82%) of the classification results from CAR+k-NN and CAR+QDA obtained from alpha band. Besides that, 10 out of 11 (90.91%) of the classification results from CAR+FKNN and 7 out of 11 (63.64%) of the classification results from LAP+k-NN obtained from alpha band. Additionally, 8 out of 11 (72.73%) of the classification results from LAP+FKNN and 6 out of 11 (54.55%) of the classification results from LAP+ QDA were also obtained from alpha band.

It was noticeable that most of the maximum classification results for all four directions were obtained either from alpha or gamma bands.

Table 5.10: Frequency band associate with the classification results from healthy subjects for predicting imagination of movement towards direction 3.

Subject	Frequency band associated with the maximum classification accuracy					
	CAR			LAP		
	KNN	FKNN	QDA	KNN	FKNN	QDA
S1	GAMMA	GAMMA	BETA	GAMMA	GAMMA	GAMMA
S2	GAMMA	GAMMA	GAMMA	GAMMA	GAMMA	GAMMA
S3	GAMMA	GAMMA	GAMMA	GAMMA	GAMMA	GAMMA
S4	GAMMA	GAMMA	GAMMA	BETA	BETA	BETA
S5	GAMMA	GAMMA	ALPHA	GAMMA	GAMMA	ALPHA
S6	ALPHA	ALPHA	ALPHA	ALPHA	ALPHA	ALPHA
S7	GAMMA	GAMMA	ALPHA	GAMMA	GAMMA	GAMMA
S8	GAMMA	GAMMA	ALPHA	GAMMA	GAMMA	ALPHA
S9	ALPHA	ALPHA	GAMMA	ALPHA	ALPHA	BETA
S10	GAMMA	GAMMA	GAMMA	ALPHA	ALPHA	GAMMA
S11	ALPHA	ALPHA	ALPHA	GAMMA	ALPHA	GAMMA

The list of recording electrodes associated with the classification results displayed in Figure 5.16 was tabulated in Table 5.11. This table demonstrates that 7 out of 11 (63.64%) of the classification results from CAR+FKNN and CAR+QDA were obtained from contralateral electrodes. Other than that, 9 out of 11 (81.82%) of the classification results from LAP+k-NN and LAP+FKNN also obtained from contralateral electrodes. In addition, 8 out of 11 (72.73%) of the classification results from LAP+QDA and 5 out of 11 (45.45%) of the classification results from CAR+k-NN also obtained from contralateral electrodes. The same process of analysis has been carried out for examining the recording electrodes associated with classification results used to predict imagination of movement towards direction 6, 9 and 12 (please refer to Appendix G for further detail).

Consistently, majority of the highest classification results for predicting imagination of movement towards direction 6 were obtained by contralateral electrodes. This was proved by, 8 out of 11 (72.73%) of the classification results from CAR+FKNN, LAP+k-NN and LAP+FKNN were obtained from contralateral electrodes. Besides that, 6 out of 11 (54.55%) of the classification results from CAR+QDA and LAP+QDA also obtained from contralateral electrodes. Furthermore all (100.00%) of the classification from CAR+k-NN obtained from contralateral electrodes.

Similarly, majority of the classification results for predicting imagination of movement towards direction 9 were obtained from contralateral electrodes. This was supported by 6 out of 11 (54.55%) of the classification results from CAR+QDA and 10 out of 11 (90.91%) of the classification results from LAP+k-NN obtained from contralateral electrodes. Other than that, 8 out of 11 (72.73%) of the classification results from CAR+FKNN and LAP+FKNN also obtained from contralateral electrodes. Furthermore, 7 out of 11 (63.64%) of the classification results from CAR+ k-NN and LAP+ QDA obtained from contralateral electrodes.

In addition, majority of the classification results for predicting imagination of movement towards direction 12 also obtained from contralateral electrodes. For instance, 7 out of 11 (63.64%) of the classification results from CAR+FKNN and LAP+FKNN were obtained from contralateral electrodes. Besides that, 9 out of 11 (81.82%) of the classification results from CAR+QDA and LAP+k-NN were obtained from contralateral electrodes. Moreover, 6 out of 11 (54.55%) of the classification results from LAP+QDA and 5 out of 11 (45.45%) of the classification results from CAR+k-NN were obtained from contralateral electrodes. From these results, it was clearly shown that most of the maximum classification results for all four directions were obtained from contralateral electrodes.

Table 5.11: Recording electrode associated with the classification results from healthy subjects for predicting imagination of movement towards direction 3.

| Subject | Recording electrode associated with the maximum classification accuracy | | | | | |
| | CAR | | | LAP | | |
	KNN	FKNN	QDA	KNN	FKNN	QDA
S1	CFC5	CFC5	CFC1	CFC5	CFC5	CFC1
S2	C4	C4	C5	CFC2	CFC2	CFC5
S3	CZ	FCZ	CP5	CFC3	CFC3	C1
S4	C3	FC4	C4	FC3	FC3	FC3
S5	C5	FC5	FC1	C3	C3	CFC1
S6	CZ	C3	FC3	C5	FC5	CCP4
S7	C3	C3	FC3	CPZ	CP5	CP2
S8	FC5	C5	CP4	CCP5	CCP5	CFC5
S9	CZ	CP5	FC4	CCP5	C2	C2
S10	FC4	FC4	FC4	FC5	FC5	CFC5
S11	CP2	C3	CCP3	CFC5	CFC1	CFC5

5.8.2.2   Predicting Intention of Movement towards Direction 3, 6, 9 and 12 from Healthy Subjects

Classification results from the healthy subjects for predicting intention of movement towards direction 3 were illustrated in Figure 5.17. In this figure, the classification results from CAR+k-NN lie within the range of 58.00%-90.00%. The combination of CAR+FKNN produced classification results of 57.00%-91.00%, whereas classification results of 56.00%-95.00% were obtained from CAR+QDA. Moreover, the classification results from LAP+k-NN, LAP+FKNN and LAP+QDA dwell within the ranges of 66.00%-91.00%, 70.00%-94.00% and 67.00%-95.00%, respectively. The same procedure of analysis was implemented for predicting intention of movement towards direction 6, 9 and 12 (please refer to Appendix G for further details).

Besides that, the classification results for predicting intention of movement towards direction 6 from CAR+k-NN, CAR+FKNN and CAR+QDA fall within the ranges of 57.00%-85.00%, 58.00%-85.00% and 55.00%-91.00%, respectively. On the other hand, classification results from combination of LAP+k-NN, LAP+FKNN and LAP+QDA lie within the ranges of 62.00%-97.00%, 67.00%-96.00% and 66.00%-93.00%, respectively.

Furthermore the classification results for predicting intention of movement towards direction 9 range from 61.00%-87.00% using the combination of CAR+k-NN. CAR+FKNN produced classification results between 58.00%-89.00%, whereas 61.00%-89.00% was obtained from CAR+QDA. On the other hand, the classification results from LAP+k-NN lie within the range of 63.00%-94.00%. The combination of LAP+FKNN produced classification results of 62.00%-97.00%, and 65.00%-98.00% were obtained from LAP+QDA.

Additionally, the classification results for predicting intention of movement towards direction 12 range from 56.00%-82.00% using the combination of CAR spatial filter with k-NN classifier. The combination of CAR+FKNN produced classification results of 61.00%-83.00%, whereas 57.00%-95.00% were obtained from CAR+QDA. Meanwhile, LAP+k-NN, LAP+FKNN and LAP+QDA combinations

produced classification results within the ranges of 69.00%-92.00%, 69.00%-98.00% and 67.00%-97.00%, respectively.

It is worth to highlight that most of the classification results for all four directions have a higher classification range when using combination of LAP compared to the CAR spatial filter.
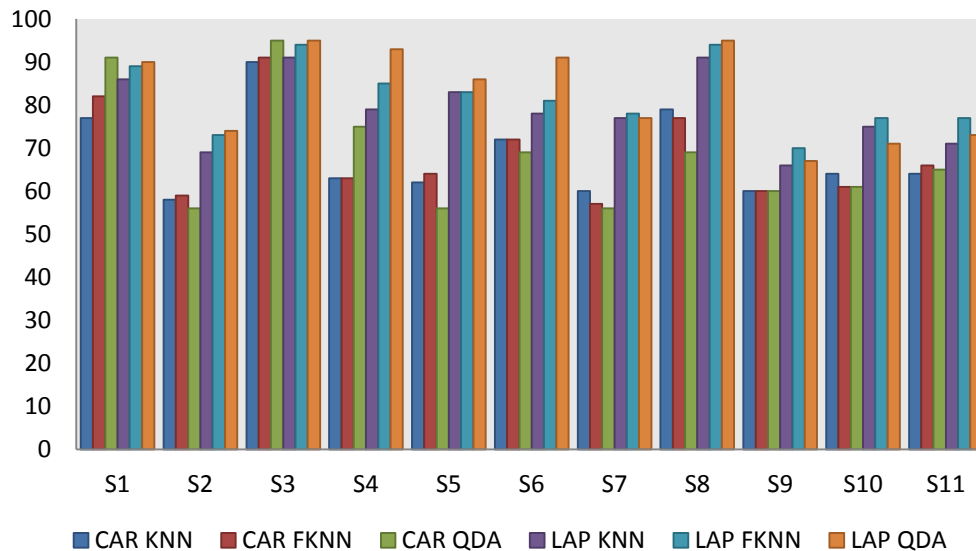
Figure 5.17: Classification results for healthy subjects in predicting intention of movement towards direction 3. The classification results from each subject were presented based on the combinations of classifiers and spatial filters applied.

Table 5.12 presents a list of frequency bands associated with the classification results shown in Figure 5.17. This data demonstrates that 6 out of 11 (54.55%) of the classification results from CAR+k-NN and CAR+FKNN were obtained from gamma bands. Besides that, 8 out of 11 (72.73%) of the classification results from CAR+QDA and LAP+k-NN were obtained from gamma bands. Furthermore, 5 out of 11 (45.45%) of the classification results from LAP+QDA and 7 out of 11 (63.64%) of the classification results from LAP+FKNN were also obtained from alpha band. The same process of analysis has been implemented for investigating the frequency band associated with classification results for predicting intention of movement towards direction 6, 9 and 12 (please refer to Appendix G for further details).

In the meantime, the classification results for predicting intention of movement towards direction 6 were mainly obtained either from alpha or gamma bands. This was evidently shown by 8 out of 11 (72.73%) of the classification results from CAR+k-NN, 7 out of 11 (63.64%) of the classification results from CAR+FKNN and 6 out of 11 (54.55%) of the classification results from CAR+ QDA were obtained from the alpha band. On the other hand, 6 out of 11 (54.55%) of the classification results from LAP+k-NN and LAP+FKNN were obtained from gamma band. Apart from that, 5 out of 11 (45.45%) of the classification results from LAP+ QDA were obtained either from alpha or gamma bands.

Most of the classification results for predicting intention of movement towards direction 9 were obtained from alpha band. This was supported by 8 out of 11 (72.73%) of the classification results from LAP+k-NN and LAP+FKNN were obtained from alpha band. Besides that, 7 out of 11 (63.64%) of the classification results from CAR+k-NN and CAR+FKNN were obtained from alpha band. In addition, 6 out of 11 (54.55%) of the classification results from CAR+QDA were also obtained from alpha band. Only 6 out of 11 (54.55%) of the classification results from LAP+QDA were obtained from gamma band.

The classification results for predicting intention of movement towards direction 12 were obtained mostly from alpha band. This was demonstrated by the fact that 7 out of 11 (63.64%) of the classification results from CAR+k-NN and CAR+FKNN were obtained from the alpha band. Apart from that, 6 out of 11 (54.55%) of the classification results from CAR+QDA, LAP+k-NN and LAP+FKNN also obtained from alpha band. Only 7 out of 11 (63.64%) of the classification results from LAP+QDA were obtained from gamma band.

It is important to highlight that, most of the maximum classification results for all four directions were obtained either from alpha or gamma bands.

Table 5.12: Frequency band associate with the classification results from healthy subjects for predicting intention of movement towards direction 3.

Subject	Frequency band associated with the maximum classification accuracy					
	CAR			LAP		
	KNN	FKNN	QDA	KNN	FKNN	QDA
S1	ALPHA	ALPHA	GAMMA	ALPHA	ALPHA	BETA
S2	GAMMA	GAMMA	ALPHA	GAMMA	GAMMA	GAMMA
S3	GAMMA	GAMMA	GAMMA	GAMMA	GAMMA	GAMMA
S4	ALPHA	ALPHA	BETA	ALPHA	ALPHA	GAMMA
S5	GAMMA	GAMMA	ALPHA	ALPHA	ALPHA	BETA
S6	ALPHA	ALPHA	ALPHA	ALPHA	ALPHA	BETA
S7	ALPHA	GAMMA	ALPHA	GAMMA	GAMMA	ALPHA
S8	GAMMA	GAMMA	ALPHA	ALPHA	ALPHA	ALPHA
S9	ALPHA	ALPHA	ALPHA	ALPHA	ALPHA	ALPHA
S10	BETA	ALPHA	ALPHA	ALPHA	ALPHA	ALPHA
S11	ALPHA	ALPHA	ALPHA	ALPHA	GAMMA	ALPHA

Table 5.13 contains the list of recording electrodes associated with the classification results illustrated in Figure 5.17. This table shows that 9 out of 11 (81.82%) of the classification results from CAR+k-NN and CAR+FKNN were obtained from contralateral electrodes. Besides that, 7 out of 11 (63.64%) of the classification results from LAP+FKNN and LAP+QDA were obtained from contralateral electrodes. Furthermore, 10 out of 11 (90.91%) of the classification results from CAR+QDA and 8 out of 11 (72.73%) of the classification results from LAP+k-NN were also obtained from contralateral electrodes. The same analysis was carried out for examining the recording electrodes associated with classification results for predicting intention of movement towards direction 6, 9 and 12 (please refer to Appendix G for further details).

Apart from that, majority of the classification results for predicting intention of movement towards direction 6 were obtained from contralateral electrodes. This was supported by the finding that 6 out of 11 (54.55%) of the classification results from CAR+k-NN and CAR+FKNN were obtained from contralateral electrodes. Apart from that 7 out of 11 (63.64%) of the classification results from CAR+QDA and LAP+FKNN were obtained from contralateral electrodes. Likewise, 8 out of 11 (72.73%) of the classification results from LAP+QDA and 10 out of 11 (90.91%) of the classification results from LAP+k-NN were also obtained from contralateral electrodes.

Majority of the classification results for predicting intention of movement towards direction 9 were obtained from contralateral electrodes. This was shown by the finding that all (100.00%) of the classification results from LAP+k-NN were obtained from contralateral electrodes. Similarly, 9 out of 11 (81.82%) of the classification results from CAR+k-NN and LAP+FKNN were obtained from contralateral electrodes. Correspondingly, 7 out of 11 (63.64%) of the classification results from CAR+QDA and LAP+QDA were obtained from contralateral electrodes. Furthermore, 8 out of 11 (63.64%) of the classification results from CAR+FKNN were also obtained from contralateral electrodes.

Additionally, majority of the classification results for predicting intention of movement towards direction 12 were obtained from contralateral electrodes. This was demonstrated by 7 out of 11 (63.64%) of the classification results from LAP+k-NN, LAP+FKNN and LAP+QDA were obtained from contralateral electrodes. Besides that, 10 out of 11 (90.91%) of the classification results from CAR+k-NN and CAR+QDA were obtained from contralateral electrodes. Moreover, all (100.00%) of the classification results from CAR+FKNN were also obtained from contralateral electrodes.

Based on these results it is essential to highlight that, the maximum classification results for all four directions were obtained from contralateral electrodes.

Table 5.13: Recording electrode associate with the classification results from healthy subjects for predicting intention of movement towards direction 3.

| Subject | Recording electrode associated with the maximum classification accuracy | | | | | |
| | CAR | | | LAP | | |
	KNN	FKNN	QDA	KNN	FKNN	QDA
S1	CP5	CP5	CP5	CCP5	CCP5	CCP5
S2	FC5	FC5	CCP1	CCP5	CCP5	CFC5
S3	FC5	CFC5	FC3	CP4	CP4	CFC5
S4	CP5	CP5	CCP1	CCP1	CCP1	CCP1
S5	C3	C5	FC2	C5	FC3	FC4
S6	C5	C1	CP5	CCP5	CCP5	CCP5
S7	CZ	CFC5	FC5	FC1	FC1	CP4
S8	CFC5	FC4	CP5	FCZ	FC2	FCZ
S9	CCP4	CP4	FC1	C3	C2	C5
S10	CCP5	C3	CFC3	FC3	FCZ	CPZ
S11	CFC1	CFC1	CFC1	FC4	CFC5	CP5

5.8.3 Predicting Imagination/Intention and Direction of Movement

This section emphasises the importance of directional information towards imagination/intention of movement. As discussed in the chapter 4, the classification processes attempt to predict the direction of the imagination/ intention of the movement. Results in predicting direction of imagination/intention of movement for healthy subjects were presented in the following subsections.

5.8.3.1 Predicting Imagination and Direction of Movement from Healthy Subjects

The classification results for predicting imagination and direction of movement from healthy subjects were illustrated in Figure 5.18. This figure indicates that, classification results from CAR+k-NN, CAR+FKNN and CAR+QDA dwell within the ranges of 35.00%-95.00%, 35.00%-95.00% and 29.00%-84.00%, respectively. On the other hand, the classification results from LAP+k-NN, LAP+FKNN and LAP+QDA lie within the ranges of 37.00%-95.00%, 37.50%-95.00% and 32.00%-83.00%, respectively.
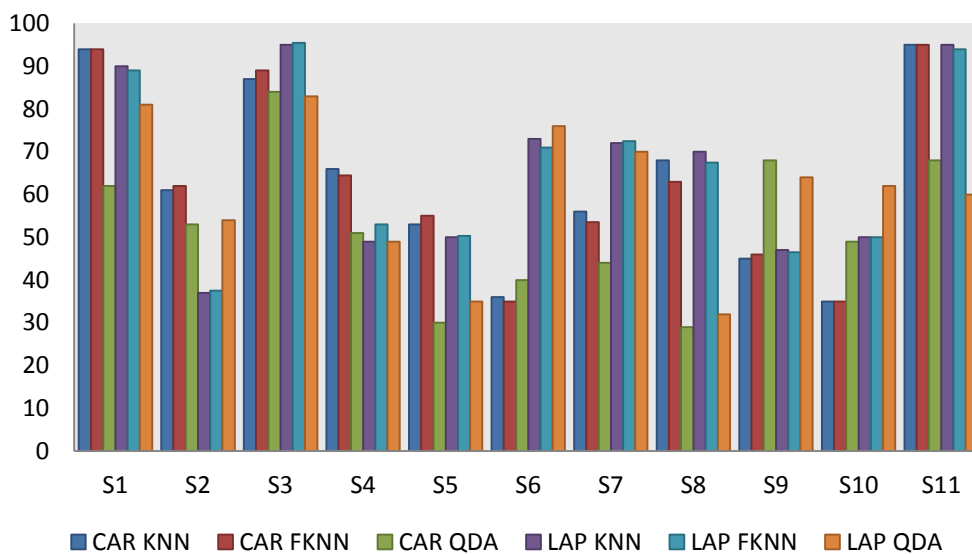
Figure 5.18: Classification results for healthy subjects in predicting imagination and direction of the movement. The classification results from each subject were presented based on the combinations of classifiers and spatial filters applied.

Lists of frequency bands associated with the classification results depicted in Figure 5.18 was provided in Table 5.14. Data in this table indicates that the classification results were obtained from multiple of EEG signal components namely delta, alpha, beta, and gamma bands. Although the classification results were obtained from different frequency bands for each subject, majority of the maximum classification results were obtained from the gamma band. This was supported by 6 out of 11 (54.55%) of the classification results from CAR+k-NN and LAP+FKNN were obtained from gamma band. Besides that, 5 out of 11 (45.45%) of the classification results from CAR+FKNN and LAP+k-NN were obtained from gamma band. Furthermore, 7 out of 11 (63.64%) of the classification results from LAP+QDA were also obtained from gamma band. On the other hand, 3 out of 11 (27.27%) of the classification results from CAR+QDA were obtained from either from theta, alpha or gamma bands.

Table 5.14: Frequency band associate with the classification results from healthy subjects for predicting imagination and direction of the movement..

| Subject | Frequency band associated with the maximum classification accuracy | | | | | |
| | CAR | | | LAP | | |
	KNN	FKNN	QDA	KNN	FKNN	QDA
S1	GAMMA	GAMMA	THETA	GAMMA	GAMMA	BETA
S2	DELTA	THETA	THETA	THETA	GAMMA	GAMMA
S3	GAMMA	GAMMA	GAMMA	GAMMA	GAMMA	GAMMA
S4	GAMMA	GAMMA	DELTA	THETA	THETA	GAMMA
S5	THETA	BETA	THETA	DELTA	DELTA	GAMMA
S6	THETA	THETA	BETA	GAMMA	GAMMA	GAMMA
S7	GAMMA	ALPHA	ALPHA	DELTA	GAMMA	DELTA
S8	BETA	BETA	ALPHA	THETA	DELTA	DELTA
S9	DELTA	DELTA	ALPHA	GAMMA	DELTA	GAMMA
S10	GAMMA	GAMMA	GAMMA	THETA	THETA	GAMMA
S11	GAMMA	GAMMA	GAMMA	GAMMA	GAMMA	BETA

List of recording electrodes associated with the classification results portrayed in Figure 5.18 was tabulated in Table 5.15. Table 5.15 indicates that, majority of the highest classification results were obtained from contralateral electrodes. This was supported by 8 out of 11 (72.73%) of the classification results from CAR+QDA were obtained from contralateral electrodes. Apart from that, 7 out of 11 (63.64%) of the classification results from CAR+k-NN, CAR+ FKNN, LAP+k-NN and LAP+FKNN were also obtained from contralateral electrodes. On the other hand, 5 out of 11

(45.45%) of the classification results from LAP+QDA were obtained from ipsilateral electrodes.

Table 5.15: Recording electrode associate with the classification results from healthy subjects for predicting imagination and direction of the movement..

| Subject | Recording electrode associated with the maximum classification accuracy | | | | | |
| | CAR | | | LAP | | |
	KNN	FKNN	QDA	KNN	FKNN	QDA
S1	CFC5	CFC5	C5	C1	CFC1	C2
S2	C4	C4	CFC3	C4	CP4	CP4
S3	CFC4	CFC4	CZ	CFC1	CFC1	CFC3
S4	FC3	FC3	FC3	FC4	FC4	FC4
S5	C3	C3	CCP5	C5	C5	CP3
S6	FC5	FC5	CCP3	CP2	C5	FC2
S7	CFC3	CFC3	C1	FC1	FC4	CPZ
S8	C5	C5	FC3	CCP5	CCP5	CCP5
S9	C4	CFC4	C4	C5	FC4	C4
S10	CPZ	CPZ	CFC4	C5	C5	FCZ
S11	FC3	FC3	CCP3	CP2	CFC3	C1

5.8.3.2 Predicting Intention and Direction of Movement from Healthy Subjects

Summary of the classification results obtained from combinations of CAR and LAP spatial filters with *k*-NN, FKNN and QDA classifiers for predicting intention and direction of movement from healthy subjects was depicted in Figure 5.19. This figure indicates that, classification results for combination of CAR+*k*-NN lie within the range of 29.00%-83.00%. The combination of CAR+FKNN produced classification results between 28.00%-83.00%, whereas results of 29.00%-67.00% were obtained from CAR+QDA. On the other hand, the classification results of LAP+*k*-NN, LAP+FKNN and LAP+QDA dwell within the ranges of 47.00%-87.00%, 47.50%-85.50% and 34.00%-80.00%, respectively.
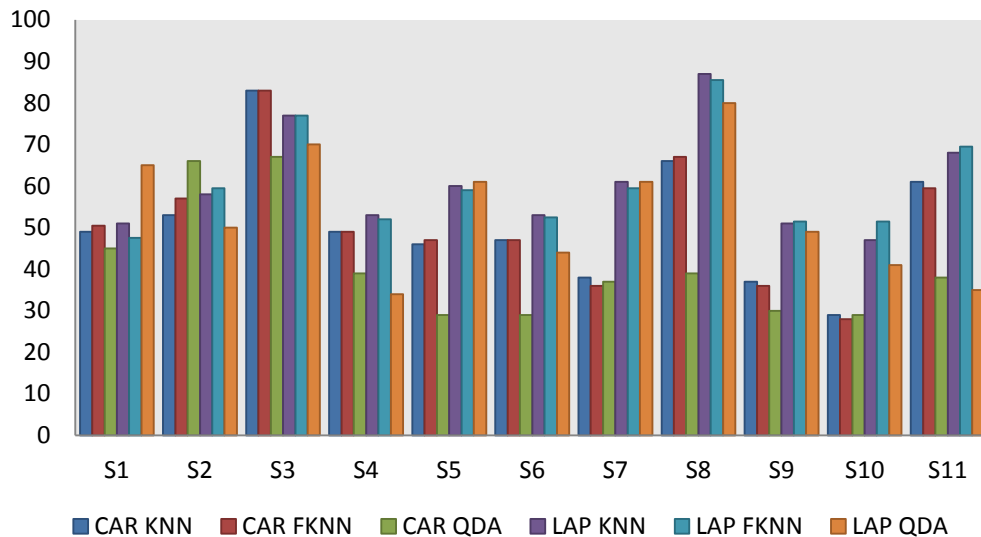
Figure 5.19: Classification results for healthy subjects in predicting intention and direction of the movement. The classification results from each subject were presented based on the combinations of classifiers and spatial filters applied.

Table 5.16 details the frequency bands associated with the classification results depicted in Figure 5.19. This table shows that, classification results were obtained from multiple frequency bands including delta, theta, alpha, beta, and gamma bands. Even though the classification results were obtained from different frequency bands for each subject, majority of the maximum classification results were obtained from the gamma band. This was shown by 7 out of 11 (63.64%) of the classification results from CAR+k-NN and LAP+FKNN were obtained from the gamma band. Besides that, 6 out of 11 (54.55%) of the classification results from CAR+FKNN and LAP+k-NN were obtained from the gamma band. On the other hand, 4 out of 11 (36.36%) of the classification results from CAR+QDA were obtained from the delta band. In addition, 3 out of 11 (27.27%) of the classification results from LAP+QDA were obtained either from delta, beta or gamma bands.

Table 5.16: Frequency band associate with the maximum classification results from healthy subjects for predicting intention and direction of the movement.

Subject	Frequency band associated with the maximum classification accuracy					
	CAR			LAP		
	KNN	FKNN	QDA	KNN	FKNN	QDA
S1	GAMMA	GAMMA	BETA	GAMMA	GAMMA	BETA
S2	GAMMA	GAMMA	DELTA	GAMMA	GAMMA	DELTA
S3	THETA	DELTA	GAMMA	DELTA	GAMMA	GAMMA

S4	GAMMA	GAMMA	ALPHA	ALPHA	GAMMA	ALPHA
S5	GAMMA	GAMMA	BETA	THETA	THETA	THETA
S6	BETA	DELTA	ALPHA	GAMMA	GAMMA	BETA
S7	GAMMA	GAMMA	DELTA	GAMMA	GAMMA	DELTA
S8	GAMMA	THETA	THETA	ALPHA	DELTA	GAMMA
S9	GAMMA	GAMMA	DELTA	GAMMA	THETA	GAMMA
S10	THETA	DELTA	DELTA	GAMMA	GAMMA	BETA
S11	BETA	BETA	ALPHA	THETA	THETA	DELTA

Recording electrodes associated with the classification results depicted in Figure 5.19 were tabulated in Table 5.17. This table shows that majority of the classification results were obtained from contralateral electrodes. This was supported by all (100.00%) of the classification results from LAP+FKNN were obtained from contralateral electrodes. Besides that, 9 out of 11 (81.82%) of the classification results from CAR+k-NN and CAR+FKNN were obtained from contralateral electrodes. Furthermore, 6 out of 11 (54.55%) of the classification results from LAP+QDA, 8 out of 11 (72.73%) of the classification results from CAR+QDA and 10 out of 11 (90.91%) of the classification results from LAP+k-NN were also obtained from contralateral electrodes.

Table 5.17: Recording electrode associate with the maximum classification results from healthy subjects for predicting intention and direction of the movement.

Subject	Recording electrode associated with maximum classification accuracy					
	CAR			LAP		
	KNN	FKNN	QDA	KNN	FKNN	QDA
S1	CFC4	CFC4	CPZ	CCP5	CCP5	CCP2
S2	FC5	CFC5	CFC5	CFC5	CFC5	CFC5
S3	FC5	FC5	CFC4	CFC5	CFC5	FC5
S4	C1	C1	C1	CCP1	C1	CCP1
S5	C3	C3	CP5	C3	CCP5	FC2
S6	FC5	FC5	CP5	CFC5	CFC5	C4
S7	C5	C3	C3	CP3	CP3	CPZ
S8	CFC5	CFC5	FC4	CCP5	CCP5	CP1
S9	C4	C4	CP5	FC5	C5	C5
S10	CP3	FC1	CP5	CPZ	CP3	FC1
S11	CFC5	CFC5	CFC5	CFC5	CFC5	C4

5.9   Receiver Operating Characteristic Graph (ROC)

Receiver operating characteristic graph (ROC) is one of the instruments used to visualise and evaluate classifier performance (Fawcett, 2006). Generally, ROC is a 2D graph representing true positive rate (TPR; plotted on the Y axis) and false positive rate (FPR; plotted on the X axis), with a diagonal line that divides the ROC space into two triangular halves, namely the upper and lower triangles. The upper triangle adjoins to the Y axis, whereas the lower triangle adjoins the X axis. Within the diagonal line the TPR and FPR values are equivalent. In this segment, ROC was produced based on the classification results from each combination of CAR and LAP spatial filters with *k*-NN, FKNN and QDA classifiers. The performance of each combination was evaluated based on the average classification accuracy, represented by a black triangle.

5.9.1 ROC for Predicting Imagination/Intention of Movement

Performance of TPR and FPR from combinations of CAR and LAP spatial filter with *k*-NN, FKNN and QDA classifiers for predicting imagination/intention of movement were evaluated by ROC. Further details regarding the performance of these classifiers are provided in the following subsections.

5.9.1.1   ROC for Predicting Imagination of Movement by Healthy Subjects

Figure 5.20 depicts the ROCs for predicting imagination of movement from healthy subjects. Each ROC was based on one combination of spatial filter and classifier. The first row represents the ROC for CAR+*k*-NN, CAR+FKNN and CAR+QDA, whereas the second row represents the ROC for LAP+*k*-NN, LAP+FKNN and LAP+QDA. Multiple points within the ROC space represented by different symbols refer data from individual subjects (this layout applies to all of the ROC graphs in this section).

Figure 5.20 demonstrates that, all the points within the ROC space for both spatial filters belong to the upper triangle (any point belonging to the lower triangle has high

FPR compared to TPR). Majority of the points within the ROC space for the LAP spatial filter have higher TPR and lower FPR compared to the CAR spatial filter. As for the classifier performance, the combination of LAP+FKNN outperformed other combinations. This is because the combination of LAP+FKNN has high TPR and lowest FPR on average.
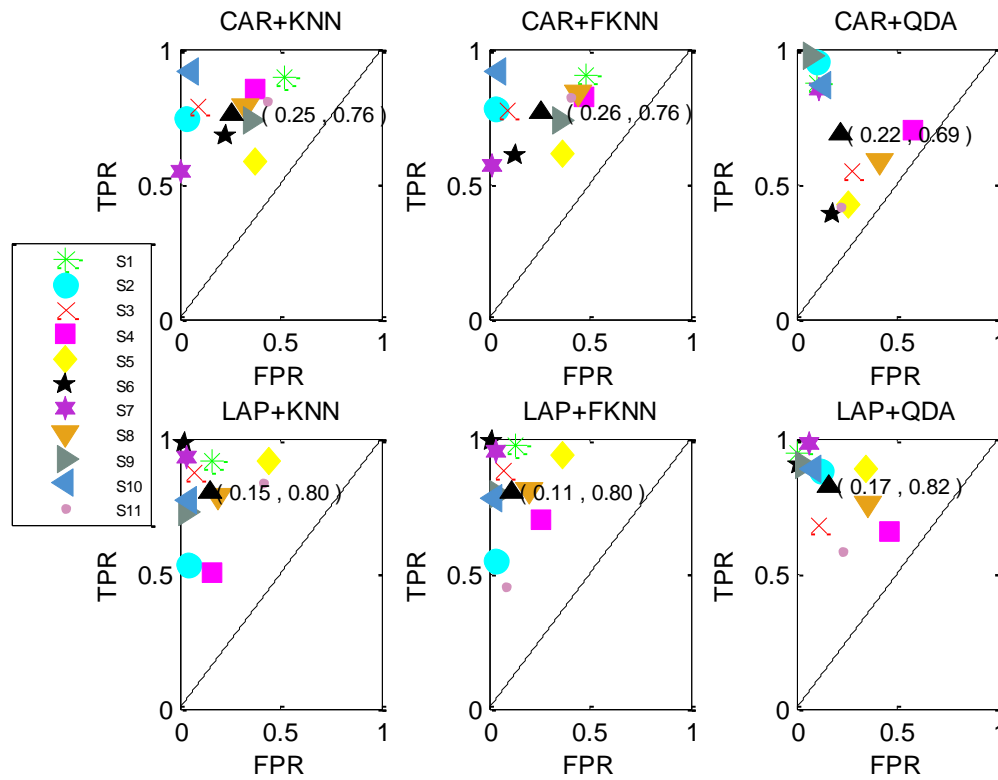
Figure 5.20: ROCs for predicting imagination of movement from healthy subjects. The ROCs were presented based on different combination of spatial filter and classifier. Subjects were represented by different symbols and the average of the classification accuracy was represented by a black triangle.

5.9.1.2 *ROC for Predicting Intention of Movement by Healthy Subjects*

ROC for combinations of CAR and LAP spatial filters with *k*-NN, FKNN and QDA classifiers in predicting intention of movement from healthy subjects were depicted in Figure 5.21. This figure demonstrates that, majority of the points in the ROC space for both spatial filters belong to the upper triangle. Majority of the points within the ROC space of LAP spatial filter have higher TPR and lower FPR compared to points within ROC space of the CAR spatial filter. Among all combinations of the spatial filters and classifiers, LAP+QDA has the highest average of TPR and lowest average of FPR.
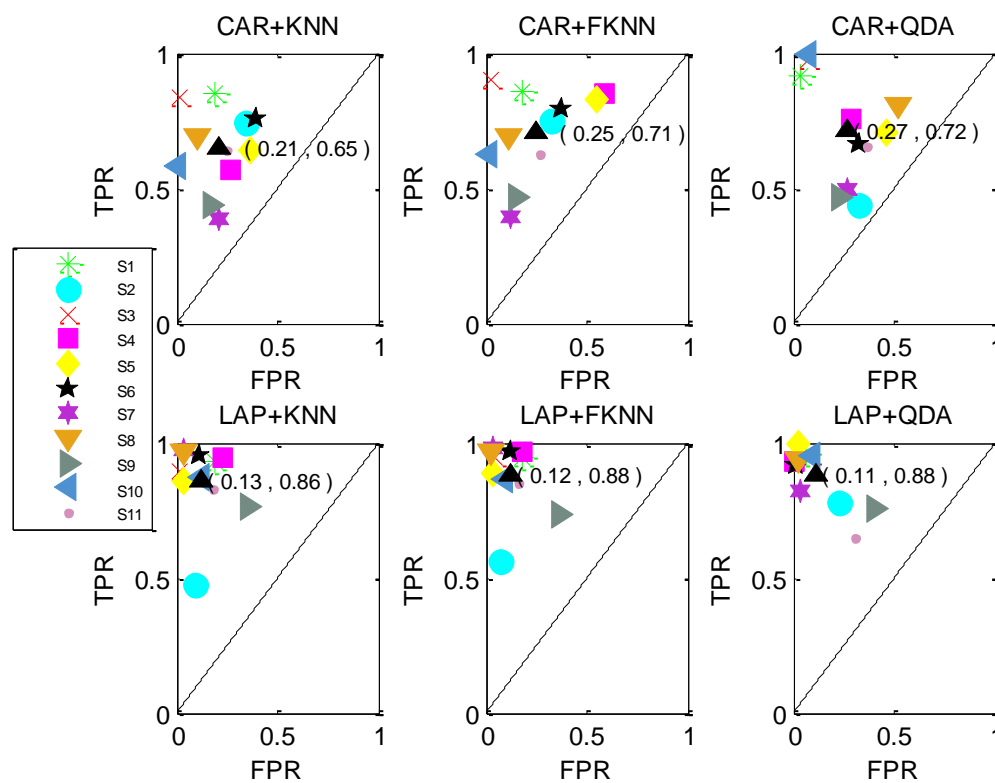
Figure 5.21: ROCs for predicting intention of movement from healthy subjects. The ROCs were presented based on different combination of spatial filter and classifier. Subjects were represented by different symbols and the average of the classification accuracy was represented by a black triangle.

5.9.2 ROC for Predicting Imagination/Intention of Movement towards Direction 3, 6, 9 and 12

In this section, the performance of classification based on different combinations of spatial filters and classifiers for predicting imagination/intention of movement towards direction 3, 6, 9 and 12 from healthy subjects were presented. The performance of these classification methods were presented individually according to the direction of movement.

5.9.2.1 ROC for predicting Imagination of Movement towards Direction 3, 6, 9 and 12 by Healthy Subjects

Figure 5.22 displays the ROC space for combinations of CAR and LAP spatial filters with *k*-NN, FKNN and QDA classifiers in predicting imagination of movement towards direction 3 from healthy subjects. This figure demonstrates that, all of the points within the ROC space for both spatial filters belong to the upper triangle; whereas majority of the points of LAP spatial filter have higher TPR and lower FPR compared to the points of CAR spatial filter. As for the classifiers evaluation, the combination of LAP+QDA outperformed other combinations based on average of highest TPR and low FPR. The same analysis has been implemented for producing ROC graphs for predicting intention of movement towards direction 6, 9 and 12 (please refer to Appendix H for further details).

Besides that, the ROC for predicting imagination of movement towards direction 6 indicates that all the points within ROC space for both spatial filters belong to the upper triangle. Additionally, majority of the points within ROC space of the LAP spatial filter have higher TPR and lower FPR compared to the points within ROC space of the CAR spatial filter. Among all the combinations, LAP+QDA has the best performance with highest TPR and low FPR compared to other combinations.

Apart from that, the ROC for predicting imagination of movement towards direction 9 shows that all the points within the ROC space for both of the spatial filters belong to the upper triangle. The majority of points within ROC space of the LAP spatial filter have higher TPR and lower FPR compared to the points within ROC space of

the CAR spatial filter. Combination of LAP spatial filter with QDA classifier has the best performance because on average it produced highest TPR and low FPR compared to other combinations.

On the other hand, the ROC for predicting imagination of movement towards direction 12 shows that all the points within the ROC space for both of the spatial filters belongs to the upper triangle. The majority of points within ROC space from the LAP spatial filter have higher TPR compared to CAR spatial filter. As for the evaluation of classifiers, the combination of LAP+QDA outperforms other combinations based on having high average of TPR and lowest average of FPR.
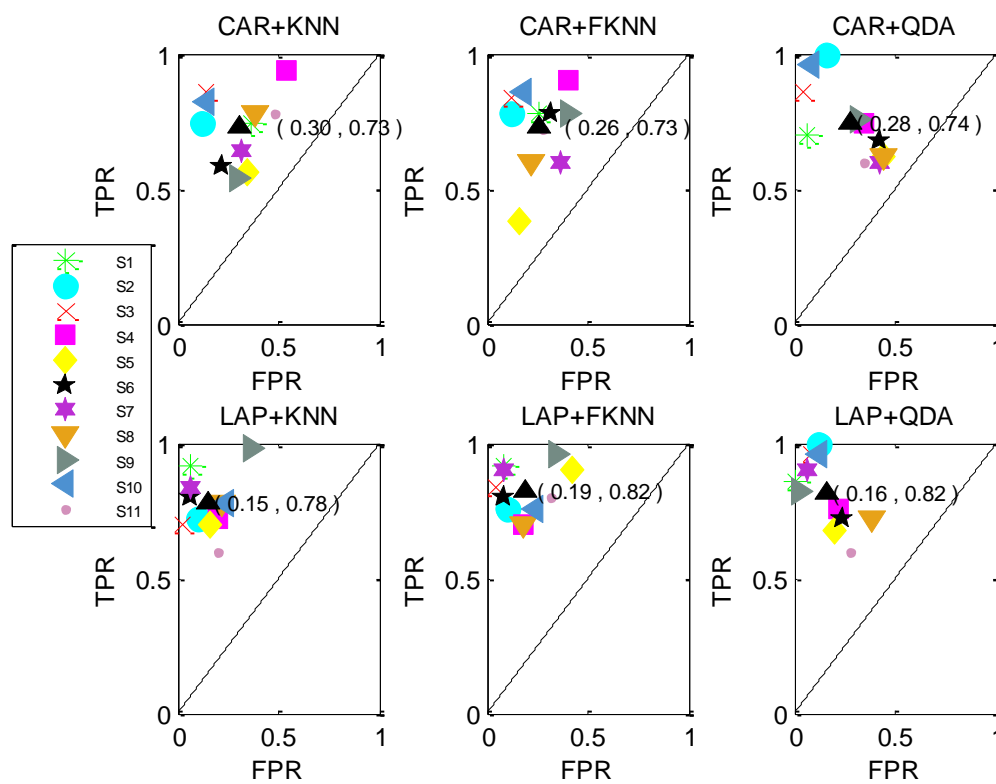
Figure 5.22: ROCs for predicting imagination of movement towards direction 3 from healthy subjects. The ROCs were presented based on combinations of spatial filters and classifiers. Subjects were represented by different symbols and the average of the classification accuracy was represented by a black triangle.

Performance evaluation of the classification results of predicting intention of movement towards direction 3 by healthy subjects was depicted in Figure 5.23. The ROC demonstrates that all of the points within the ROC space for both of the spatial filter belong to the upper triangle. Majority of the points within ROC space of LAP spatial filter have lower FPR compared to the points within ROC space of CAR spatial filter. In term of performance evaluation, combination of LAP+FKNN has average with highest TPR and low FPR which outperformed others combination. Same analysis procedures have been implemented for producing the ROC graphs for predicting imagination of movement towards direction 6, 9 and 12 (please refer Appendix H for further detail).

Addition to that, the ROC for predicting intention of movement towards direction 6 shows that, all the point within ROC space for both of the spatial filter belongs to the upper triangle where majority of points within ROC space of LAP spatial filter have higher TPR and lower FPR compared to the points within ROC space of CAR spatial filter. Besides that, combination of LAP+QDA that has average with highest TPR and lower FPR outperform other classification combination.

Similarly, the ROC for predicting intention of movement towards direction 9 depicted that, all the point within ROC space for both of the spatial filter belongs to the upper triangle where majority of points within ROC space of LAP spatial filter have higher TPR and lower FPR compared to the points within ROC space of CAR spatial filter. As for the evaluation of classification performance, combination of LAP+QDA has the average with highest TPR and lower FPR which outperformed other combination.

Likewise, the ROC for predicting intention of movement towards direction 12 portrayed that, all the point within ROC space for both of the spatial filter belongs to the upper triangle where majority of points within ROC space of LAP spatial filter have higher TPR and lower FPR compared to the points within ROC space of CAR spatial filter. Combination of LAP+QDA has the average of highest TPR and lowest FPR which outperformed other classification combination.
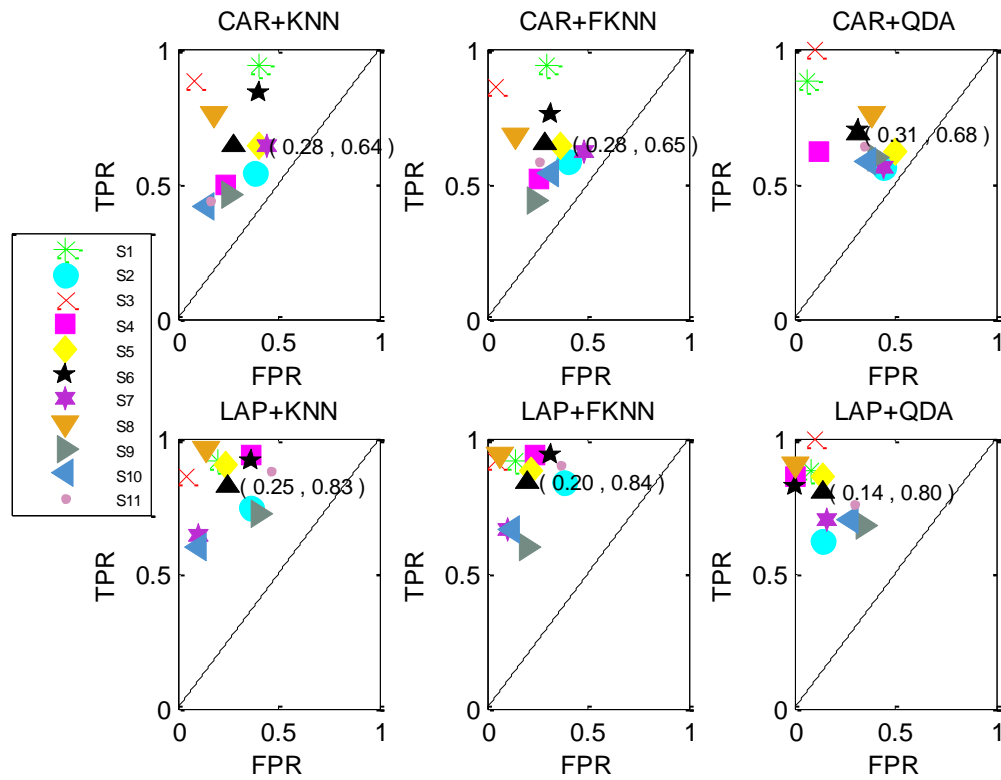
Figure 5.23: ROCs for predicting intention of movement towards direction 3 from healthy subjects. The ROCs were presented based on combinations of spatial filters and classifiers. Subjects were represented by different symbols and the average of the classification accuracy was represented by a black triangle.

5.9.3 ROC for Predicting Imagination/Intention and Direction of Movement

As mentioned in the chapter 4, in predicting imagination/intention and direction of movement, the classifiers attempt to recognise when the subject starts to imagine/move and the direction of the imagination/movement. In this study the direction of movement covers four different directions. In the following subsections classification performance for each direction is further investigated.

ROC that indicates the evaluation of classification performance for predicting imagination and direction of movement for subclass direction towards 3 from healthy subjects was depicted by Figure 5.24. This figure demonstrates that majority of the points within the ROC space for both spatial filters belong to the upper triangle; except for LAP+QDA (S5) and CAR+QDA (S6), which one subject belonged to the lower triangle. In terms of classification performance, the combination of CAR+*k*-NN has low FPR and highest TPR on average, outperforming the other combinations.
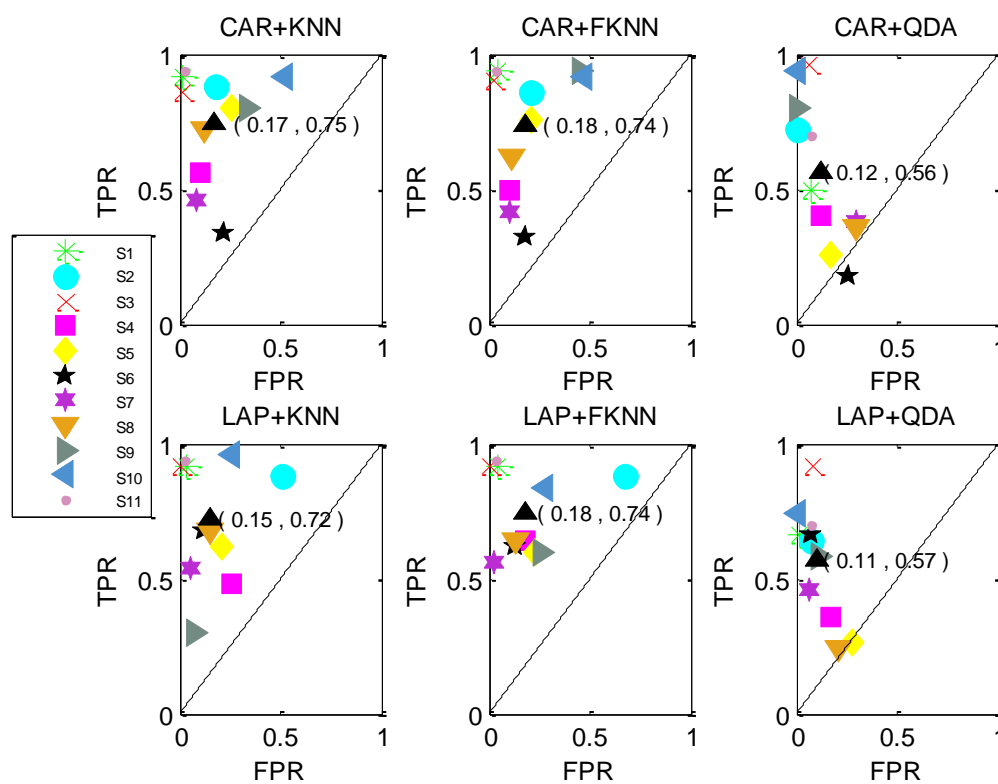
Figure 5.24: ROCs for predicting imagination and direction of movement from healthy subjects (subclass for direction towards 3). The ROCs were presented based on combinations of spatial filters and classifiers. Subjects were represented by different symbols and the average of the classification accuracy was represented by a black triangle.

On the other hand, classification evaluation for predicting imagination and direction of movement for subclass direction towards 6 from healthy subjects was portrayed in Figure 5.25 This figure demonstrates that the majority of points within the ROC space for both spatial filters belong to the upper triangle; except for one, LAP+*k*-NN, where subject S2 belongs to the lower triangle. As for classification performance, the combination of LAP+FKNN outperformed the others based on the average of highest TPR and low FPR.
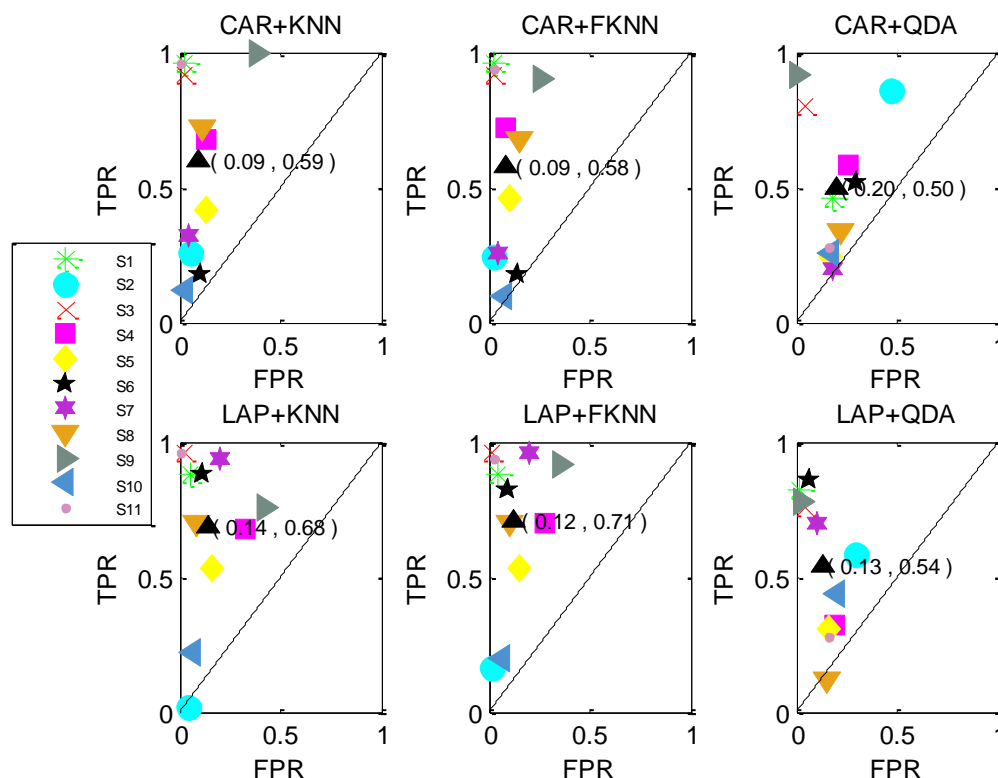
Figure 5.25: ROCs for predicting imagination and direction of movement from healthy subjects (subclass for direction towards 6). The ROCs were presented based on combinations of spatial filters and classifiers. Subjects were represented by different symbols and the average of the classification accuracy was represented by a black triangle.

Furthermore, Figure 5.26 illustrates the ROC from healthy subjects for predicting imagination and direction of movement for subclass direction towards 9. This figure demonstrates that majority of the points within the ROC space for both spatial filters belong to the upper triangle; except for LAP+QDA (S5) and CAR+QDA (S8), which one subject belonged to the lower triangle. Among all the classification combinations, LAP+QDA has the best performance based on average of low FPR and highest TPR.
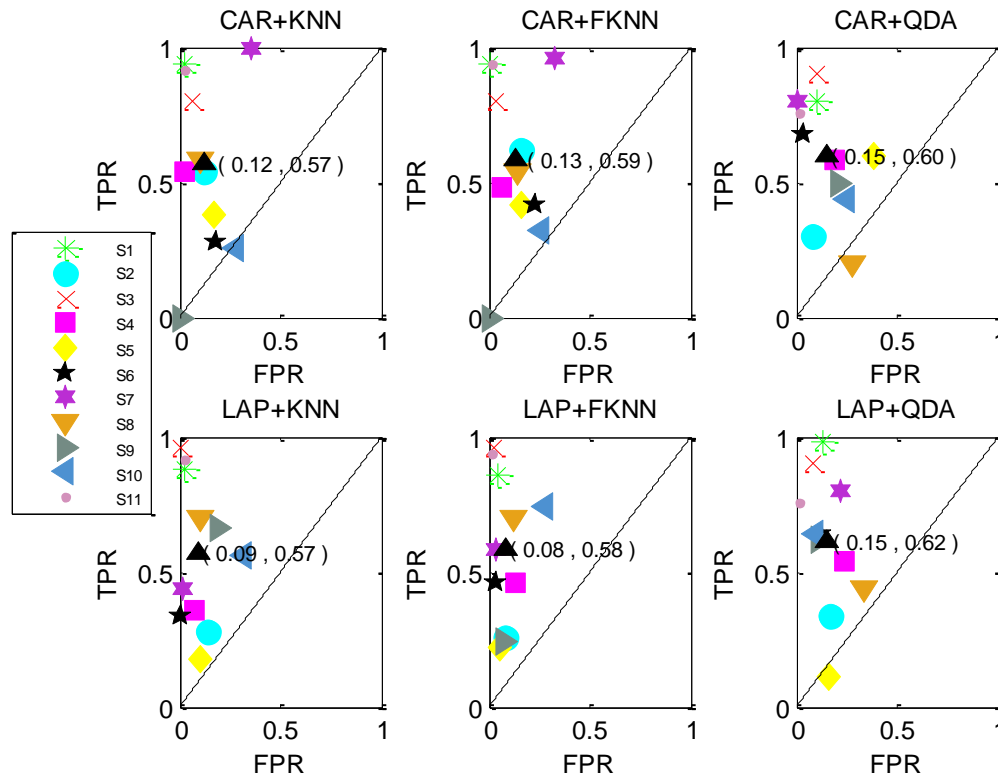
Figure 5.26: ROCs for predicting imagination and direction of movement from paraplegic subjects (subclass for direction towards 9). The ROCs were presented based on combinations of spatial filters and classifiers. Subjects were represented by different symbols and the average of the classification accuracy was represented by a black triangle.

Moreover, Figure 5.27 portrays the ROC of healthy subjects in predicting imagination and direction of movement for subclass direction towards 12. Based on this figure, all points within ROC space for both spatial filters belong to the upper triangle; except for CAR+QDA (S5), which one subject belonged to the lower triangle. As for classification performance, the combination of LAP+QDA has the average of highest TPR and low FPR, outperforming other classification combinations.
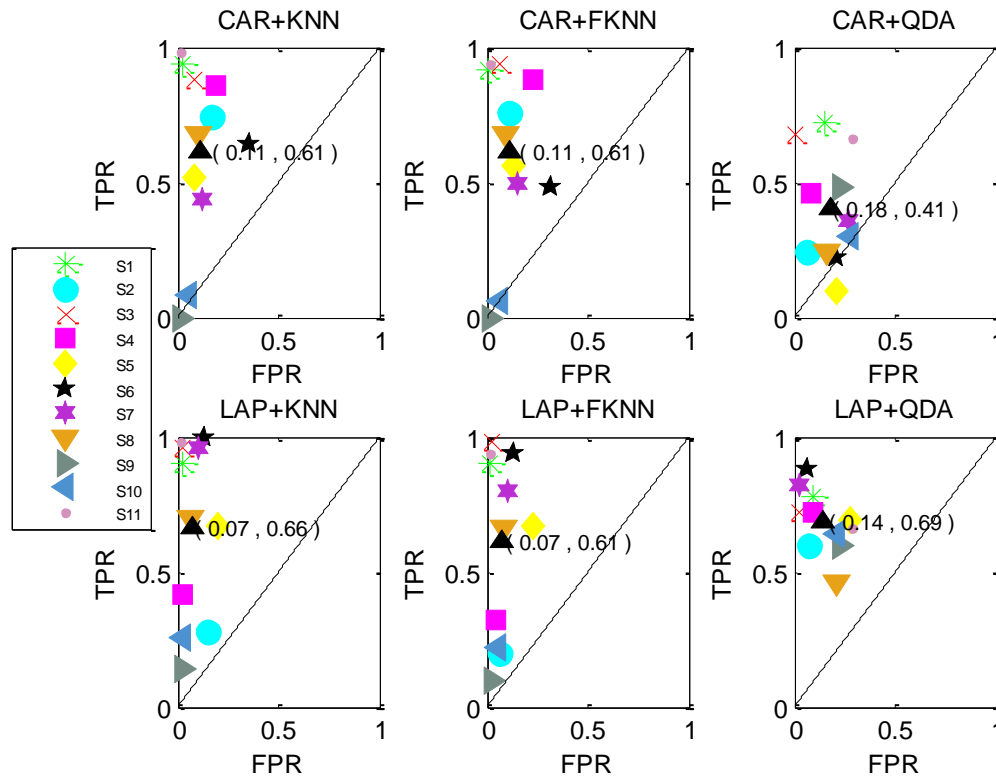
Figure 5.27: ROCs for predicting imagination and direction of movement from healthy subjects (subclass for direction towards 12). The ROCs were presented based on combinations of spatial filters and classifiers. Subjects were represented by different symbols and the average of the classification accuracy was represented by a black triangle.

The performance evaluation of predicting intention and direction of movement for subclass direction towards 3 from healthy subjects was depicted in Figure 5.28. This figure demonstrates that all of the points within the ROC space of LAP spatial filters belong to the upper triangle. On the other hand, CAR+*k*-NN and CAR+FKNN have subject S10 belong to the lower triangle. Besides that, CAR+QDA has two subjects (S9 and S10) that belong to the lower triangle. As for classification performance, the combination LAP+FKNN has an average with highest TPR and low FPR, which outperformed other classification combinations.
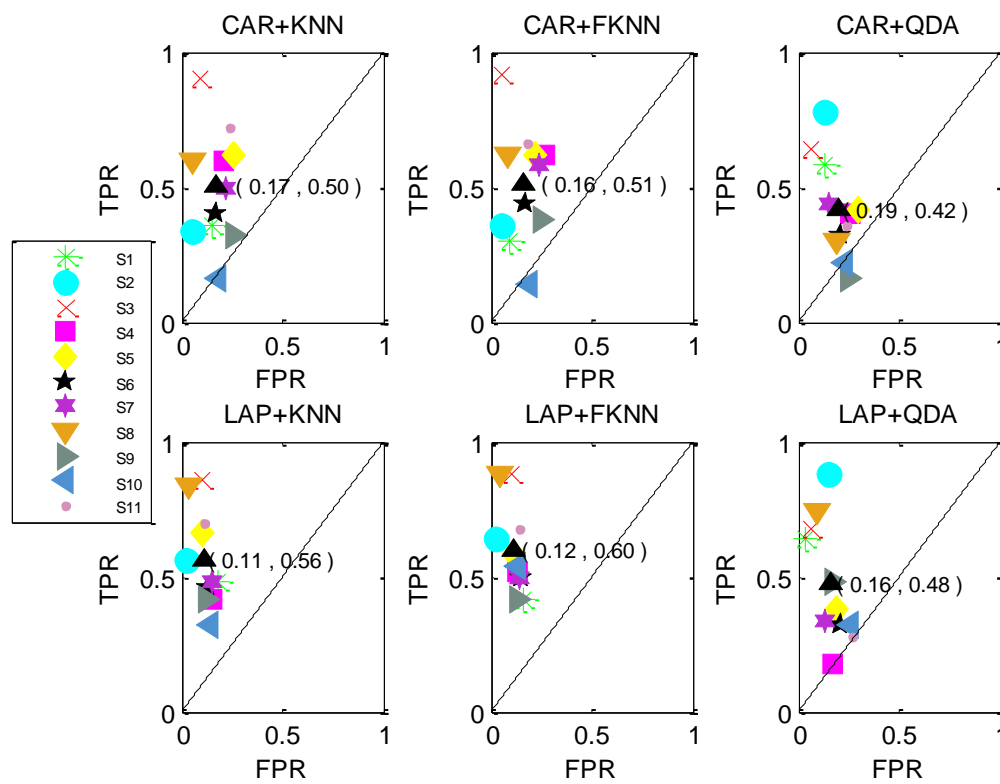
Figure 5.28: ROCs for predicting intention and direction of movement from healthy subjects (subclass for direction towards 3). The ROCs were presented based on combinations of spatial filters and classifiers. Subjects were represented by different symbols and the average of the classification accuracy was represented by a black triangle.

Figure 5.29 illustrates the ROC from healthy subjects for predicting intention and direction of movement for subclass direction towards 6. This figure demonstrates that all of the points within the ROC space for both spatial filters belong to the upper triangle except for CAR+QDA (S6), which one subject belonged to the lower triangle. Among all classification combinations, LAP+*k*-NN has the best performance based on average of highest TPR and low FPR.
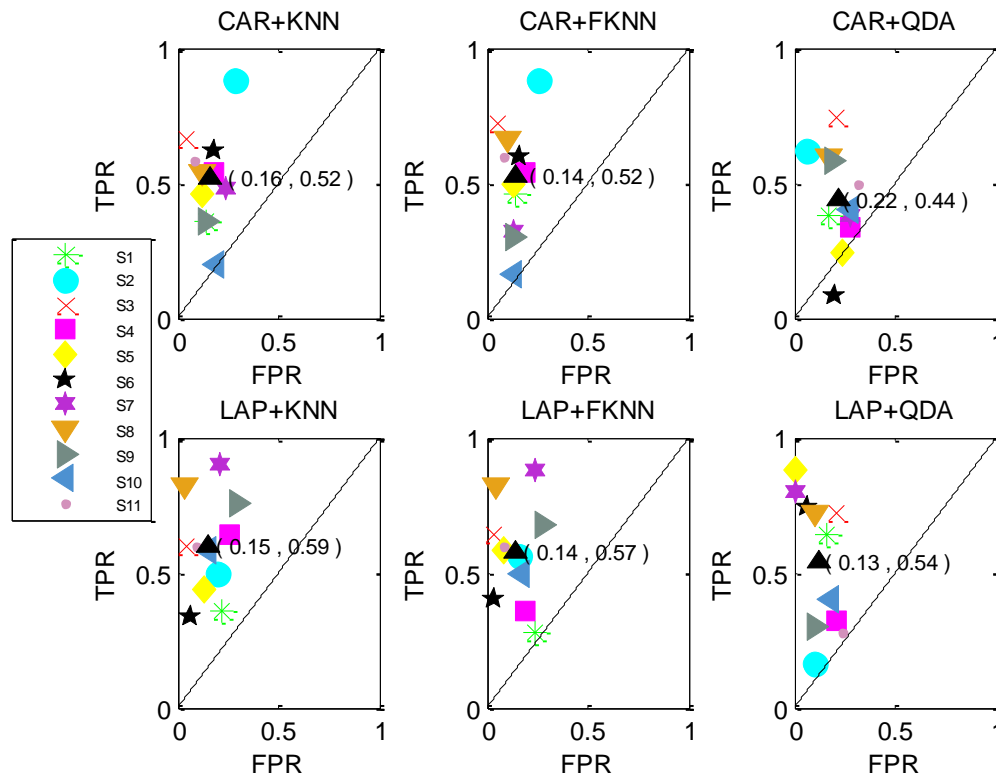
Figure 5.29: ROCs for predicting intention and direction of movement from healthy subjects (subclass for direction towards 6). The ROCs were presented based on combinations of spatial filters and classifiers. Subjects were represented by different symbols and the average of the classification accuracy was represented by a black triangle.

Furthermore, the performance evaluation of classification results from healthy subjects for predicting intention and direction of movement for subclass direction towards 9 were portrayed in Figure 5.30. This figure demonstrates that majority of the points within the ROC space for both spatial filters belong to the upper triangle; except for CAR+FKNN (S7), CAR+QDA (S10) and LAP+QDA (S4), which one subject belonged to the lower triangle. This figure also shows that the combination of LAP+FKNN has average of low FPR and highest TPR, outperforming other classification combinations.
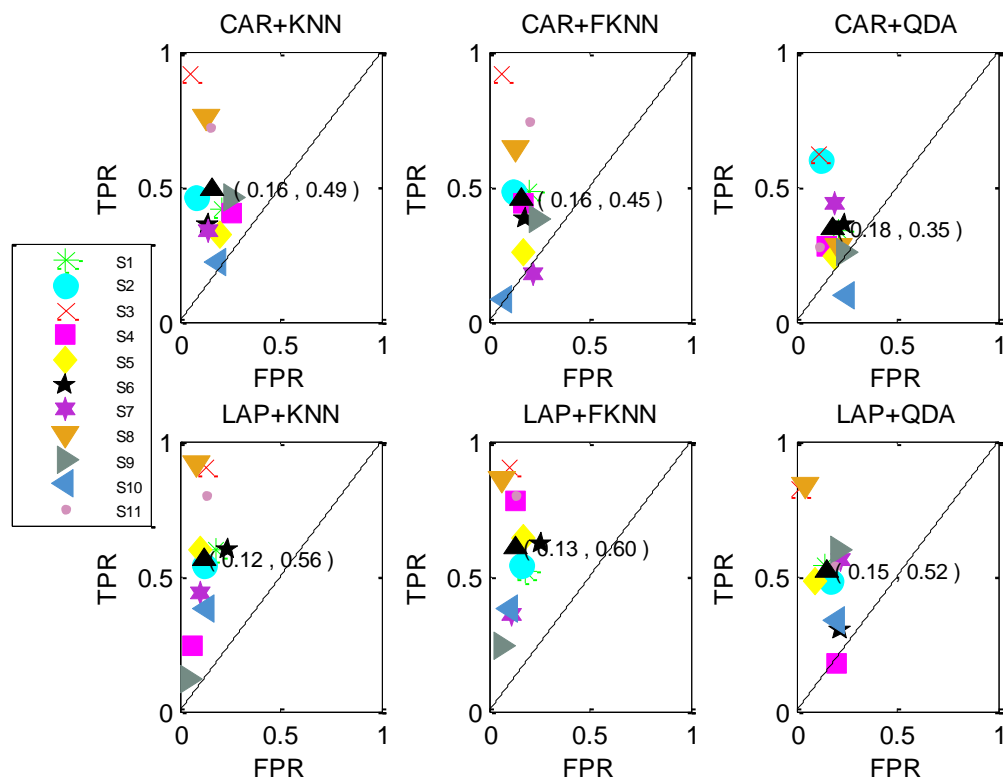
Figure 5.30: ROCs for predicting intention and direction of movement from healthy subjects (subclass for direction towards 9). The ROCs were presented based on combinations of spatial filters and classifiers. Subjects were represented by different symbols and the average of the classification accuracy was represented by a black triangle.

Figure 5.31 depicts the ROC from healthy subjects in predicting intention and direction of movement for subclass direction towards 12. Based from this figure majority of the points within the ROC space for both spatial filters belong to the upper triangle; except for CAR+kNN and CAR+QDA. In CAR+kNN subject S7 belong to the lower triangle whereas in CAR+QDA subject S7 and S10 belong to the lower triangle. As for classification performance, the combination of LAP+k-NN outperformed the others based on average of highest TPR and lowest FPR.
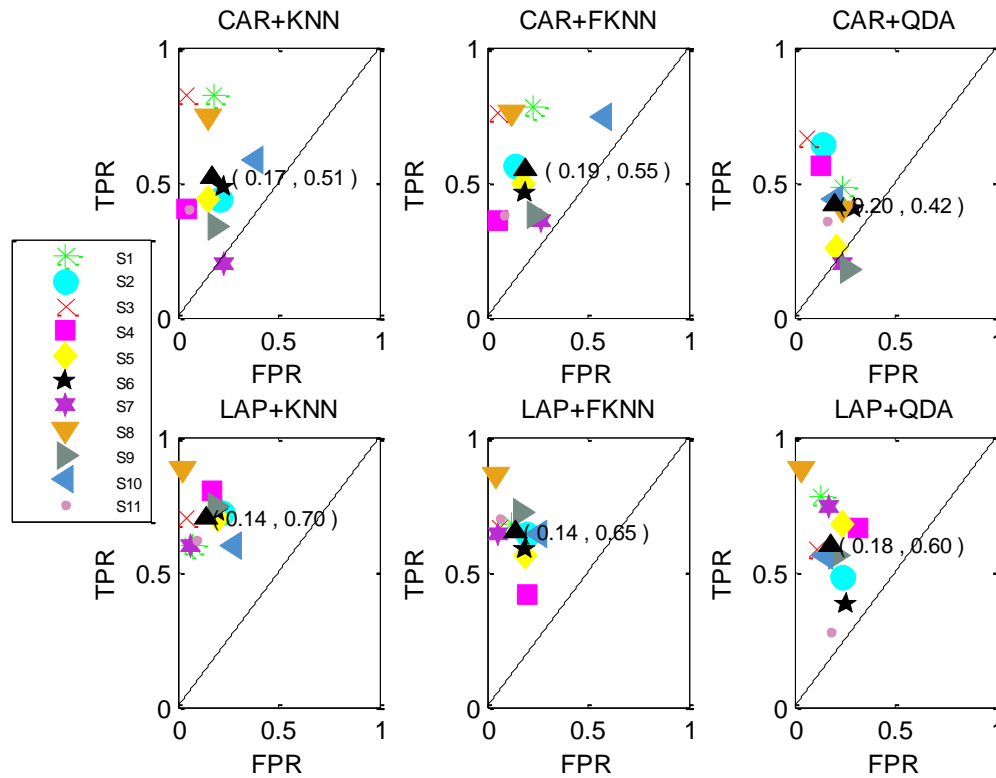
Figure 5.31: ROCs for predicting intention and direction of movement from healthy subjects (subclass for direction towards 12). The ROCs were presented based on combinations of spatial filters and classifiers. Subjects were represented by different symbols and the average of the classification accuracy was represented by a black triangle.

5.10 Summary

This chapter has elicited the pilot test results based on participation of eleven healthy subjects in both of motor imagery and motor task experiments. The conducted ANOVA test with significant level of 0.05 on the movement initiation time shows that, there is significant different (except for subject S3) among initiation times of movement towards the four different directions. This finding suggests that, the times taken by the healthy subjects to perform the movement towards four different directions are different for each of the direction.

The normality test conducted through Kolmogorov-Smirnov test across 28 recording electrodes for both experiments shows that, majority of the recorded EEG signal was having Gaussian distribution. It is undeniable that, there were also non-Gaussian distributions EEG signal was recorded from the healthy subjects. For instance, in motor imagery experiment subject S4 (14 channels show non Gaussian distribution) and subject S11 (4 channels show non-Gaussian distribution) whereas in motor task experiment S1 (6 channels show non-Gaussian distribution) and subject S11 (4 channels show non-Gaussian distribution). Further examination has been implemented on the non-Gaussian recording electrodes. After inspection there was no noise and artefact detected, that can cause the non-Gaussian distribution. On the other hand, there is possibility the accumulation of small changes of the neighbouring recording electrodes could affecting the Gaussian distribution. The recorded EEG signal from healthy subjects was considered having Gaussian distribution due to the fact that most of them show Gaussian distribution in the recorded EEG signal.

Besides that, the MRCP results show the detection of increase amplitude negativity across MRCP of four different directions for MICAR, MILAP, MTCAR and MTLAP. In the MRCP of MICAR and MILAP, the increase of negativity amplitude was detected 500ms after visual cue onset whereas in MTCAR and MTLAP, it was detected from 500ms before movement onset,

Apart from that, the ERSP results show detection of significant power changes across all four directions of MICAR, MILAP, MTCAR and MTLAP. In MICAR and

MILAP, detection of prominent ERD can be seen within beta and gamma bands 500ms after visual cue onset. On the other hand, ERD also was detected within beta and gamma band prior to onset of the movement for MTCAR and MTLAP. Besides that, the p values results (with significance of 0.05) shows that there were significance difference across ERSP of four difference directions. In MICAR and MILAP the significance differences were detected after cue onset whereas in MTCAR and MTLAP it was detected prior to the onset of the movement. Significance of differences was detected within delta, theta, alpha, beta and gamma bands.

Summary of maximum classification results in predicting imagination/intention of movement and predicting the effect of direction towards imagination/intention of movement shows that most of the results were obtained from alpha and gamma bands recorded from contralateral electrodes (most of the recording electrodes locate at parietal lobe of brain region).

Moreover, the classification results in predicting imagination/intention and direction of movement demonstrated that, majority of the results were obtained from gamma band recorded from contralateral electrodes (most of the recording electrodes locate at parietal lobe of brain region).

The results have highlighted the importance of the high density recording electrodes. This is because, high density montage offers selection of more dense recoding electrodes that suit with the SCI patients (affected by reorganisation of cortical topographic).

As for classifier performance, combination of LAP spatial filter with various classifiers outperformed the combination of CAR spatial filter with classifiers.

Chapter 6. Results on SCI Subjects

6.1   Introduction

Chapter 6 reports the analysed results obtained from the SCI subjects. It is essential to mentioned here that, the analysis implemented on the SCI subjects used the same test, code and algorithm employed with the healthy. Thus all the presented results used the same layout. Further results were elicited in the following subchapters.

6.2   Demographic Studies

Eighteen SCI subjects (fourteen tetraplegic patients (ST) and four paraplegic patients (SP)) with average age of 48.35 years from QENSIU voluntarily participated in this study. The condition of each of these subjects was detailed in Table 6.1.

Table 6.1: Details of the subject's condition and their participation with the experiment.

Subject	Gender	Age	Level of injury	AIS scale	Time since injury (months)	Cause of injury	Motor Imagery experiment	Motor Task experiment
ST1	Male	38	C5	A	14	Trauma	Participated	N/A-
ST2	Male	29	C4	A	8	Trauma	Participated	N/A
ST3	Male	27	C6	A	15	Trauma	Participated	N/A
ST4	Male	52	C6	B	88	Trauma	Participated	N/A
ST5	Female	48	C5	A	39	Fall	Participated	N/A
ST6	Male	37	C5	A	93	Fall	Participated	N/A
ST7	Female	58	C5	C	30	Fall	Participated	N/A
ST8	Male	48	C4	C	6	Fall	Participated	N/A
ST9	Male	43	C5	B	240	Stabbing	Participated	N/A
ST10	Male	62	C4	A	7	Disease	Participated	N/A
ST11	Female	69	C6	A	54	Trauma	Participated	Participated
ST12	Male	52	C6	D	66	Fall	Participated	Participated
ST13	Male	69	C6	D	60	Fall	Aborted-	Participated
ST14	Male	22	C6	B	34	Fall	Aborted -	Participated
SP1	Male	47	T12	D	20	Trauma	Participated	Participated
SP2	Male	49	T10	A	10	Disease	Participated	Participated
SP3	Male	57	T3	A	84	Fall	Participated	Participated
SP4	Female	53	L3	A	30	Fall	Participated	Participated

Referring to Table 6.1 there were four main causes of SCI in the participating group. 50.00% (9 out of 18) and 33.33% (6 out of 18) of the injuries were caused by fall and trauma respectively; 11.11% (2 out of 18) were caused by disease and 5.56% (1 out of 18) resulted from crime (stabbing).

All of the tetraplegic subjects (eleven male and three female) suffer SCI injury from level C6 and above. Due to the level of injury, only four tetraplegic subjects (ST11, ST12, ST13 and ST14) were capable of participating in motor task experiment, whereas in the motor imagery experiment 10 of 12 tetraplegic subjects participated. The remaining tetraplegic subjects (ST13 and ST14) did not participate in the motor imagery experiment due to personal circumstances. On the other hand, the paraplegic subjects (three male and one female) participated in both the motor task and motor imagery experiments.

6.3 Movement Initiation Time

The movement initiation time taken by subject SP4 in performing movement towards four different directions was depicted in Figure 6.1 through boxplot.
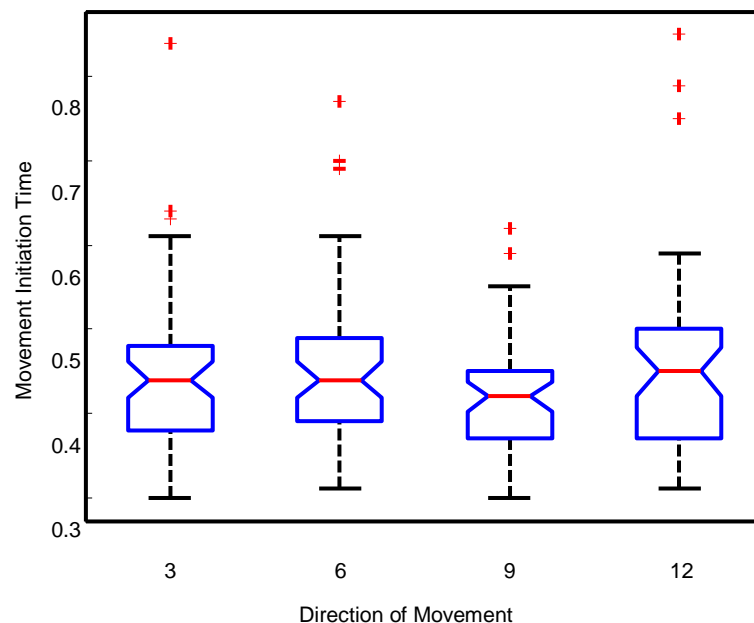
Figure 6.1: Boxplot of Movement Initiation Time for Subject SP4.

Figure 6.1 depicts the distribution of movement initiation time towards directions 3, 6, 9 and 12 by subject SP4 while performing movements in the motor task experiment. The mean values of initiation time for direction 3, 6, 9 and 12 were 0.46, 0.45, 0.42 and 0.45 second respectively.

ANOVA tests have been implemented on the movement initiation time for both paraplegic and tetraplegic subjects while they participated in the motor task experiment (for further clarification of movement initiation time results from other paraplegic subjects please refer to Appendix D). The ANOVA test was conducted based on significance threshold of 0.05. The results indicate that only subjects SP1, SP2 and SP3 display a significant difference between initiation times of movement towards the four different directions. On the other hand, there were no significant differences between the movement initiation time for other paraplegic and tetraplegic subjects (SP4, ST11, ST12, ST13 and ST14), which may suggest that perception of the visual cue and executing movement varies across subjects. Besides that, these results also suggest the initiation time taken by most of the SCI subjects in performing movement towards four different directions were same.

6.4   Normality Test

Data distribution of the recorded EEG signal from the SCI subjects were assed using the Kolmogorov-Smirnov test (KS). The KS test was conducted on the 28 EEG recording electrodes for both of the experiments namely motor imagery and motor task experiments. Results of the tests were further clarified in subsections of 6.4.1 and 6.4.2.

6.4.1 Data Distribution for Tetraplegic Subjects

Results of the normality test for tetraplegic subjects were presented in Table 6.2 (motor imagery experiment) and Table 6.3 (motor task experiment). Results from the test shows that h=0 indicates the tested data has a Gaussian distribution, and a result of h=1 indicates the tested data has a non-Gaussian distribution; with a significance level of 0.05.

Table 6.2: Normality test results of 12 tetraplegic subject's data from the motor imagery experiment.

Electrode	ST1	ST2	ST3	ST4	ST5	ST6	ST7	ST8	ST9	ST10	ST11	ST12
FCZ	h=0	h=0	h=0	h=0	h=0	h=0	h=0	h=0	h=0	h=0	h=0	h=0
FC2	h=0	h=0	h=0	h=0	h=0	h=0	h=0	h=0	h=1	h=0	h=0	h=0
FC4	h=0	h=0	h=0	h=0	h=0	h=0	h=0	h=0	h=0	h=0	h=0	h=0
FC1	h=0	h=0	h=0	h=0	h=0	h=0	h=0	h=0	h=1	h=0	h=0	h=0
FC3	h=0	h=0	h=0	h=0	h=0	h=0	h=0	h=0	h=0	h=0	h=0	h=0
FC5	h=0	h=0	h=0	h=0	h=0	h=0	h=0	h=0	h=0	h=0	h=0	h=0
CFC2	h=0	h=0	h=0	h=0	h=0	h=0	h=0	h=0	h=0	h=0	h=0	h=0
CFC4	h=0	h=0	h=0	h=0	h=0	h=0	h=0	h=0	h=0	h=0	h=0	h=0
CFC1	h=0	h=0	h=0	h=0	h=0	h=0	h=0	h=0	h=1	h=0	h=0	h=0
CFC3	h=0	h=0	h=0	h=0	h=0	h=0	h=0	h=0	h=0	h=0	h=0	h=0
CFC5	h=0	h=0	h=0	h=0	h=0	h=0	h=0	h=0	h=0	h=0	h=0	h=0
CZ	h=0	h=0	h=0	h=0	h=0	h=0	h=0	h=0	h=1	h=0	h=0	h=0
C2	h=0	h=0	h=0	h=0	h=0	h=0	h=0	h=0	h=0	h=0	h=0	h=0
C4	h=0	h=0	h=0	h=0	h=0	h=0	h=0	h=0	h=0	h=0	h=0	h=0
C1	h=0	h=0	h=0	h=0	h=0	h=0	h=0	h=0	h=0	h=0	h=0	h=0
C3	h=0	h=0	h=0	h=0	h=0	h=0	h=0	h=0	h=0	h=0	h=0	h=0
C5	h=0	h=0	h=0	h=0	h=0	h=0	h=0	h=0	h=0	h=0	h=0	h=0
CCP2	h=0	h=0	h=0	h=0	h=0	h=0	h=0	h=0	h=0	h=0	h=0	h=0
CCP4	h=0	h=0	h=0	h=0	h=0	h=0	h=0	h=0	h=0	h=0	h=0	h=0
CCP1	h=0	h=0	h=0	h=0	h=0	h=0	h=0	h=0	h=1	h=0	h=0	h=0
CCP3	h=0	h=0	h=0	h=0	h=0	h=0	h=0	h=0	h=1	h=0	h=0	h=0
CCP5	h=0	h=0	h=0	h=0	h=0	h=0	h=0	h=0	h=0	h=0	h=0	h=0
CPZ	h=0	h=0	h=0	h=0	h=0	h=0	h=0	h=0	h=0	h=0	h=0	h=0
CP2	h=0	h=0	h=0	h=0	h=0	h=0	h=0	h=0	h=1	h=0	h=0	h=0
CP4	h=0	h=0	h=0	h=0	h=0	h=0	h=0	h=0	h=0	h=0	h=0	h=0
CP1	h=0	h=0	h=0	h=0	h=0	h=0	h=0	h=0	h=1	h=0	h=0	h=0
CP3	h=0	h=0	h=0	h=0	h=0	h=0	h=0	h=0	h=1	h=0	h=0	h=0
CP5	h=0	h=0	h=0	h=0	h=0	h=0	h=0	h=0	h=0	h=0	h=0	h=0

Table 6.2 presents the KS test results of tetraplegic subjects for the motor imagery experiment. From this table it is clearly seen that majority of the tetraplegic subjects

have Gaussian distribution in all 28 active recording electrodes, except subject ST9 (nine recording electrodes that have non-Gaussian distribution).

Table 6.3: Normality test results of 4 tetraplegic subject's data from the motor task experiment. .

Electrode	ST11	ST12	ST13	ST14
FCZ	h=0	h=0	h=1	h=0
FC2	h=0	h=0	h=0	h=0
FC4	h=0	h=0	h=0	h=0
FC1	h=0	h=0	h=0	h=0
FC3	h=0	h=0	h=0	h=0
FC5	h=0	h=0	h=1	h=0
CFC2	h=0	h=0	h=0	h=0
CFC4	h=0	h=0	h=0	h=0
CFC1	h=0	h=0	h=0	h=0
CFC3	h=0	h=0	h=0	h=0
CFC5	h=0	h=0	h=1	h=0
CZ	h=0	h=0	h=0	h=0
C2	h=0	h=0	h=0	h=0
C4	h=0	h=0	h=0	h=0
C1	h=0	h=0	h=0	h=0
C3	h=0	h=0	h=0	h=0
C5	h=0	h=0	h=1	h=0
CCP2	h=0	h=0	h=0	h=0
CCP4	h=0	h=0	h=0	h=0
CCP1	h=0	h=0	h=0	h=0
CCP3	h=0	h=0	h=1	h=0
CCP5	h=0	h=0	h=0	h=0
CPZ	h=0	h=0	h=0	h=0
CP2	h=0	h=0	h=0	h=0
CP4	h=0	h=0	h=0	h=0
CP1	h=0	h=0	h=0	h=0
CP3	h=0	h=0	h=0	h=0
CP5	h=0	h=0	h=1	h=0

Tabulated data in Table 6.3 shows the KS test results of tetraplegic subjects for the motor task experiment. Among these four tetraplegic subjects that participated in the motor task experiment, only the EEG signal from subject ST13 had a non-Gaussian distribution in 6 out of 28 recording electrodes.

6.4.2 Data Distribution for Paraplegic Subjects

Table 6.4 shows normality test results of 4 paraplegic subjects based on the recorded EEG signal from the motor imagery experiment. The results from Table 6.4 also show that the majority of recording electrodes have a Gaussian distribution, except subject for subject SP4 (one recording electrodes that have non-Gaussian distribution).

Table 6.4: Normality test results of 4 paraplegic subject's data from motor imagery experiment. .

Electrode	SP1	SP2	SP3	SP4
FCZ	h=0	h=0	h=0	h=0
FC2	h=0	h=0	h=0	h=0
FC4	h=0	h=0	h=0	h=0
FC1	h=0	h=0	h=0	h=0
FC3	h=0	h=0	h=0	h=0
FC5	h=0	h=0	h=0	h=0
CFC2	h=0	h=0	h=0	h=0
CFC4	h=0	h=0	h=0	h=0
CFC1	h=0	h=0	h=0	h=0
CFC3	h=0	h=0	h=0	h=0
CFC5	h=0	h=0	h=0	h=0
CZ	h=0	h=0	h=0	h=0
C2	h=0	h=0	h=0	h=0
C4	h=0	h=0	h=0	h=0
C1	h=0	h=0	h=0	h=0
C3	h=0	h=0	h=0	h=0
C5	h=0	h=0	h=0	h=0
CCP2	h=0	h=0	h=0	h=0
CCP4	h=0	h=0	h=0	h=0
CCP1	h=0	h=0	h=0	h=0
CCP3	h=0	h=0	h=0	h=1
CCP5	h=0	h=0	h=0	h=0
CPZ	h=0	h=0	h=0	h=0
CP2	h=0	h=0	h=0	h=0
CP4	h=0	h=0	h=0	h=0
CP1	h=0	h=0	h=0	h=0
CP3	h=0	h=0	h=0	h=0
CP5	h=0	h=0	h=0	h=0

The normality test results of paraplegic subjects for motor task experiment were shown in Table 6.5 All 4 of the paraplegic patients completed the motor task experiment. Result from Table 6.5 shows that, majority of the subjects have Gaussian distribution in all 28 recording electrodes except subject SP1 (one recording electrodes that have non-Gaussian distribution).

Table 6.5: Normality test results of 4 paraplegic subject's data from motor task experiment. .

Electrode	SP1	SP2	SP3	SP4
FCZ	h=0	h=0	h=0	h=0
FC2	h=0	h=0	h=0	h=0
FC4	h=0	h=0	h=0	h=0
FC1	h=1	h=0	h=0	h=0
FC3	h=0	h=0	h=0	h=0
FC5	h=0	h=0	h=0	h=0
CFC2	h=0	h=0	h=0	h=0
CFC4	h=0	h=0	h=0	h=0
CFC1	h=0	h=0	h=0	h=0
CFC3	h=0	h=0	h=0	h=0
CFC5	h=0	h=0	h=0	h=0
CZ	h=0	h=0	h=0	h=0
C2	h=0	h=0	h=0	h=0
C4	h=0	h=0	h=0	h=0
C1	h=0	h=0	h=0	h=0
C3	h=0	h=0	h=0	h=0
C5	h=0	h=0	h=0	h=0
CCP2	h=0	h=0	h=0	h=0
CCP4	h=0	h=0	h=0	h=0
CCP1	h=0	h=0	h=0	h=0
CCP3	h=0	h=0	h=0	h=0
CCP5	h=0	h=0	h=0	h=0
CPZ	h=0	h=0	h=0	h=0
CP2	h=0	h=0	h=0	h=0
CP4	h=0	h=0	h=0	h=0
CP1	h=0	h=0	h=0	h=0
CP3	h=0	h=0	h=0	h=0
CP5	h=0	h=0	h=0	h=0

6.5 Movement Related Cortical Potential (MRCP)

The grand average of MRCP waveforms of four different directions associated with MICAR and MILAP were presented in Figure 6.2 and Figure 6.3 respectively. Apart from that, the grand average of MRCP waveforms associated with MTCAR and MTLAP were presented in Figure 6.4 and Figure 6.5 respectively. All of the results were computed from electrode C3 by subject SP4.

6.5.1 MRCP of Motor Imagery

The grand average of MRCP waveforms associated with the MICAR towards direction 3, 6, 9 and 12 were illustrated by Figure 6.2. In this figure, T=0 represents the visual cue onset (t_c). From this figure also, it can be seen that increasing amplitude negativity occurs in all of the MRCP waveforms after t_c, at time T<500ms approximately. All of the MRCP waveforms begin returning to the baseline after T=500ms.
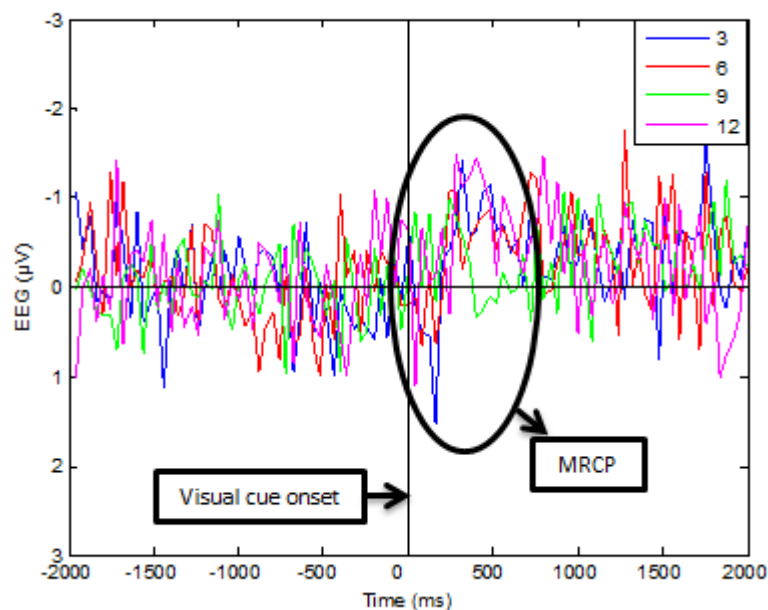
Figure 6.2: MRCP associated with motor imagery experiment using CAR filter. This figure shows the MRCP recorded from electrode C3 of subject SP4. X and Y axis represent the recording time and the amplitude of the signal respectively.

The grand average of the MRCP waveforms associated with the MILAP towards directions 3, 6, 9 and 12 recorded from electrode C3 by subject SP4 were portrayed in Figure 6.3. T=0 in this figure represents the visual cue onset (t_c). This figure also shows that there was a small negative increase in amplitude of all MRCP waveforms 500ms after t_c. These MRCP waveforms then return to baseline approximately after T=1000ms. During the decline of MRCP, there was amplitude difference among the MRCP waveforms; the decline towards 12 is the largest.
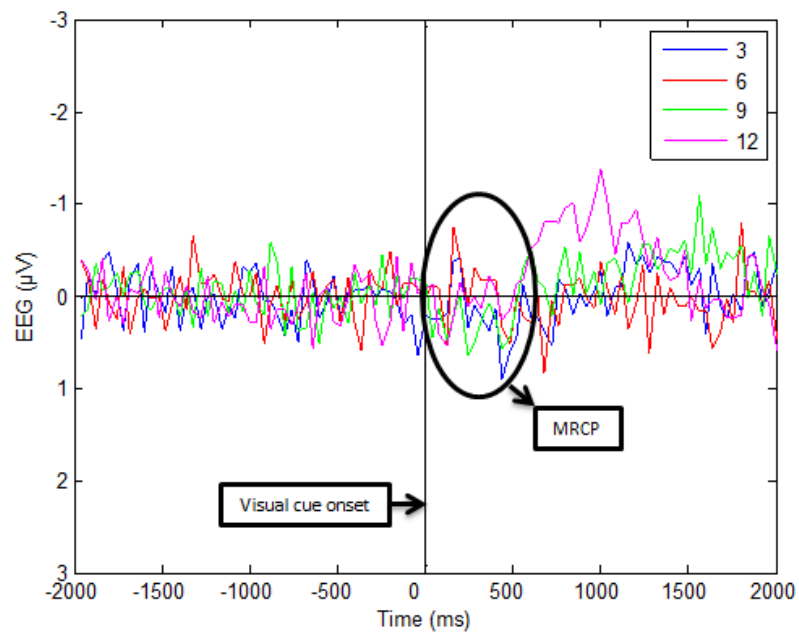
Figure 6.3: MRCP associated with motor imagery experiment using LAP filter.
This figure shows the MRCP recorded from electrode C3 of subject SP4. X and Y axes represent the recording time and the amplitude of the signal respectively

6.5.2 MRCP of Motor Task

Figure 6.4 shows the grand average of the MRCP waveforms associated with the MTCAR towards directions 3, 6, 9 and 12. These waveforms were obtained from electrode C3. In this figure, T=0 represents onset of the movement (t_m), and a vertical line in cyan colour (T >-500ms) represent onset of the visual cue (t_c). On inspection of Figure 6.4, it can be seen that following t_c there was a negative shift in amplitude preceding onset of movement in the MRCP waveforms. After t_m, the MRCP waveforms returned to the baseline approximately after T=500ms.
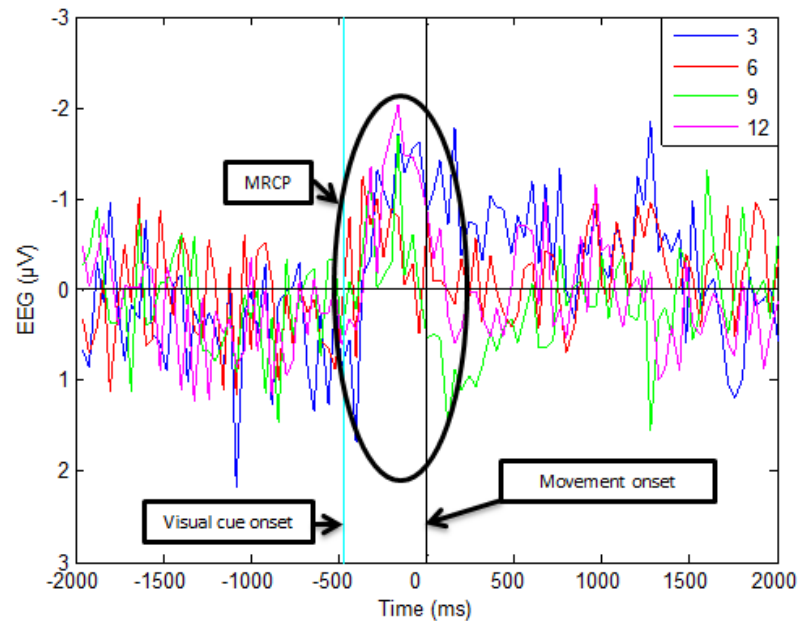
Figure 6.4: MRCP associated with the motor task experiment using CAR filter.
This figure shows the MRCP recorded from electrode C3 by subject SP4. X and Y axes represent the recording time and the amplitude of the signal respectively.

144

The grand average of the MRCP waveforms associated with the MTLAP towards direction 3, 6, 9 and 12 recorded from electrode C3 were displayed in Figure 6.5. In this figure, T=0 indicates the movement initiation time (t_m), and a vertical line in cyan colour (T < -500ms) represents the visual cue onset (t_c). This figure also shows that there was a slightly negativity increase in all of the MRCP waveforms after t_c that decreases when reaching t_m. Although there was a small decline in MRCP negativity after t_c, the entire MRCP waveforms return towards baseline shortly after t_m.
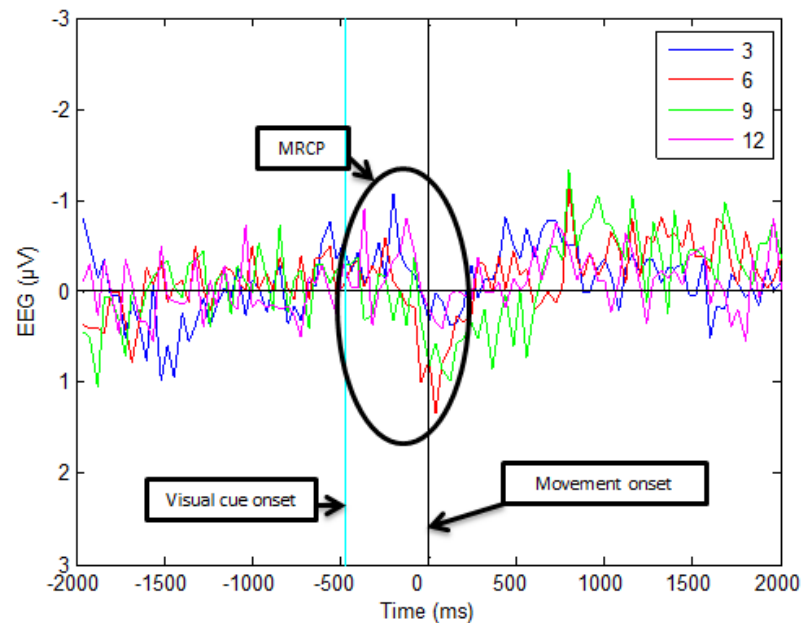
Figure 6.5: MRCP associated with the motor task experiment using LAP filter. This figure shows the MRCP recorded from electrode C3 of subject SP4. X and Y axis represent the recording time and the amplitude of the signal respectively.

6.6 ANOVA and ERSP

The ANOVA test results performed on the ERSP of the four different directions associated with MICAR, MILAP, MTCAR and MTLAP were depicted by Figure 6.6, Figure 6.7, Figure 6.8 and Figure 6.9.respectively. The results were computed from electrode C3 by subject SP4.

6.6.1 Statistical Difference of Motor Imagery

Statistical analysis using the ANOVA test was conducted across ERSP associated with MICAR towards direction 3, 6, 9 and 12. Results of this ANOVA test were depicted in Figure 6.6. In this figure, T=0 represents the visual cue onset. It can be seen that after visual cue onset, there were a significant differences across ERSP in all four directions. The significant differences were represented by clustered blue regions within the delta, theta, alpha, beta and gamma bands.
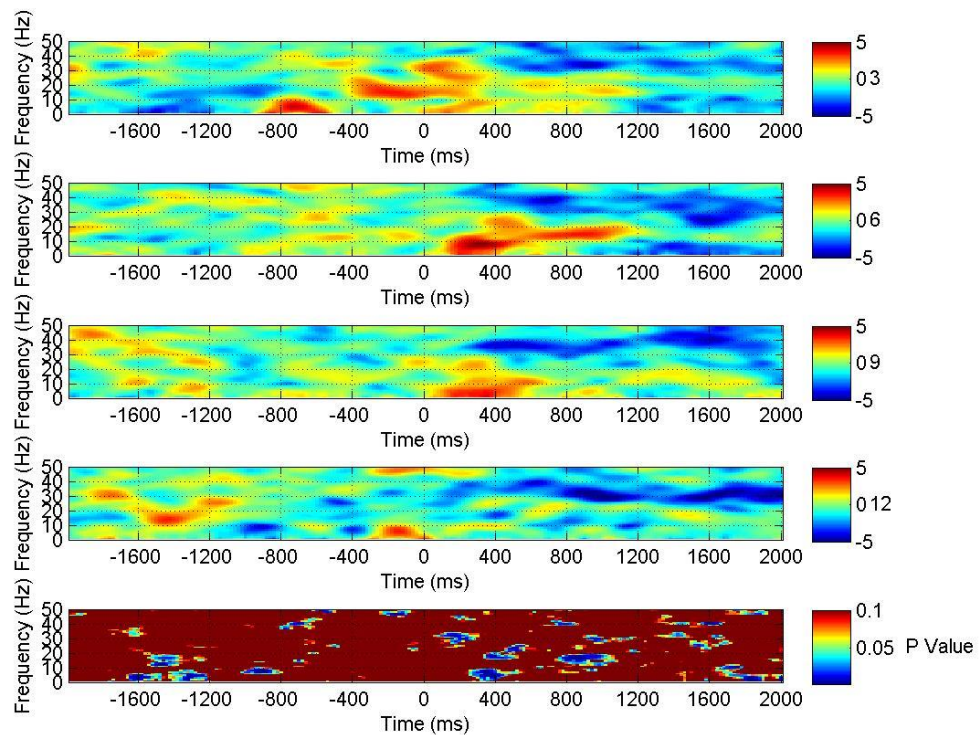
Figure 6.6: ANOVA results associated with motor imagery experiment using CAR filter. Top four plots represent the ERSPs of EEG of electrode C3 recorded from the subject SP4 when performing movement in 4 different directions and the bottom represents the ANOVA results of these 4 ERSPs. Vertical axes represent signal frequency and horizontal axes represent recording time. In ERSP plots blue shows the ERD and red shows the ERS. In the ANOVA plot, blue regions represent that there is statistical difference in ERSPs across all four directions. The significance level of this figure is 0.05.

The ANOVA test results of ERSP associated with MILAP towards direction 3, 6, 9 and 12 were portrayed in Figure 6.7. In this figure, T=0 indicates visual cue onset (t_c). The significant differences across all ERSPs were discovered before and after t_c presented by blue regions within delta, theta, alpha and beta bands. Detection of prominent ERD and ERS before t_c indicates that during the rest period, subject might be engaged with mental task or cognitive activity (try to guess the visual cue direction). Any interference and activity during the resting period will affect the generation of ERD and ERS.
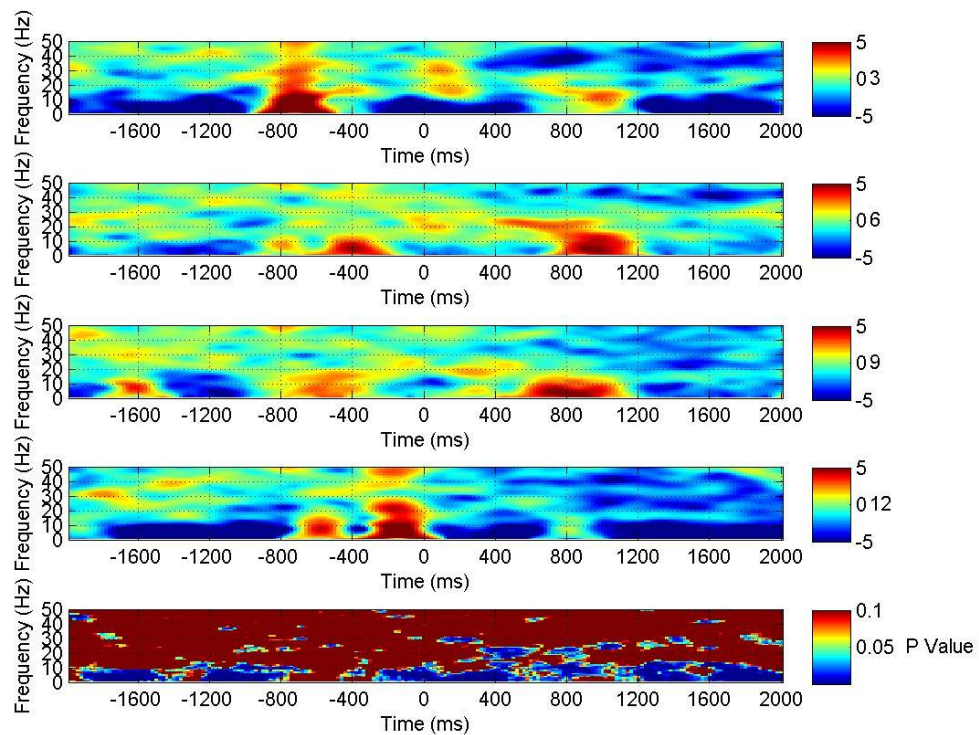
Figure 6.7: ANOVA results associated with motor imagery experiment using LAP filter. Top four plots represent the ERSPs of EEG at electrode C3 recorded from the subject SP4 when performing movement in four different directions and the bottom represents the ANOVA results of these 4 ERSPs. Vertical axes represent signal frequency and horizontal axes represent recording time. In ERSP plots blue shows the ERD and red shows the ERS. In the ANOVA plot, blue regions represent where there is statistical significance from comparing ERSPs across all four directions. The significance level of this figure is 0.05.

147

6.6.2 Statistical Difference of Motor Task

Figure 6.8 portrays the results of ANOVA test performed on the ERSP associated with MTCAR towards direction 3, 6, 9 and 12. In this figure, T=0 represents the onset of movement (t_m). This figure also shows that, there were significant differences exist in the ERSP of all four directions prior to onset of the movement. The significant differences were represented by clustered blue regions which can be seen within delta, theta and alpha frequency bands. Moreover, there is also significant difference within the delta, theta, alpha, beta and gamma bands after the onset of movement, when T>0.
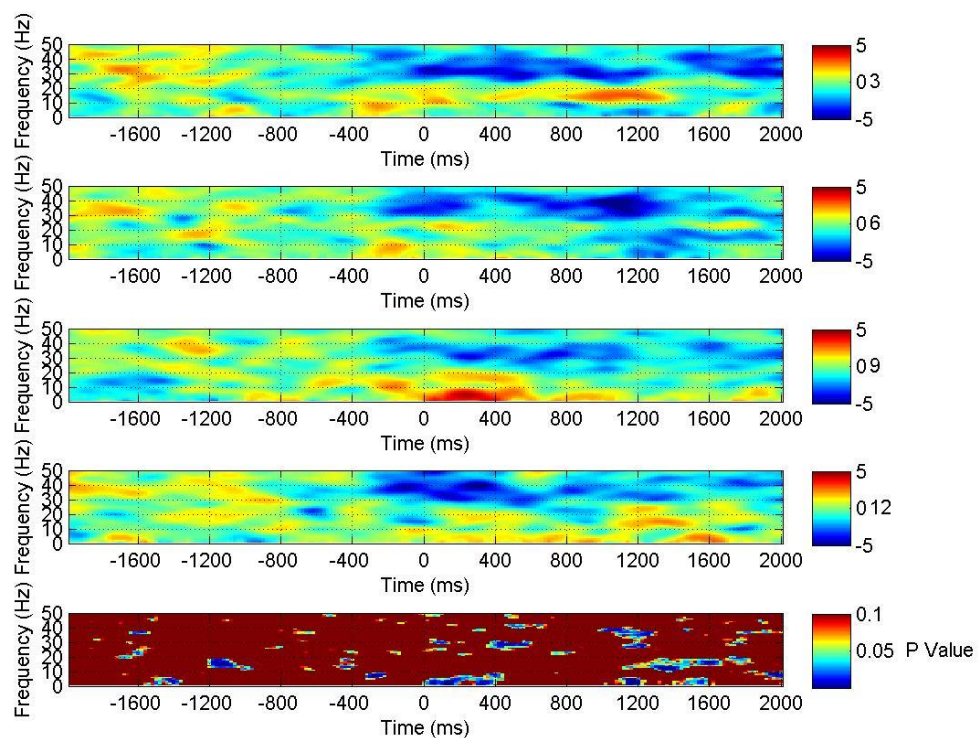
Figure 6.8: ANOVA results associated with motor task experiment using CAR filter. Top four plots represent the ERSPs of EEG at electrode C3 recorded from subject SP4 when performing movement in 4 different directions; the bottom plot represent ANOVA results of the above ERSPs. Vertical axes represent signal frequency and horizontal axes represent recording time. In ERSP plots blue and red colouring shows ERD and ERS, respectively. In the ANOVA plots, the blue region represents statistically significant significance differences in ERSP across all four directions. The significance level of this figure is 0.05.

148

Figure 6.9 illustrates the ANOVA test results implemented across ERSP associated with MTLAP towards direction 3, 6, 9 and 12; T=0 illustrates the onset of movement (t_m). From this figure, it can see that there were significance differences across all four ERSPs, especially after visual cue onset (approximately 500ms before t_m). The significant differences were presented by clustered blue regions within delta, theta, alpha, beta and gamma bands. The significant difference before movement initiation time was detected in delta, theta and alpha frequency bands.
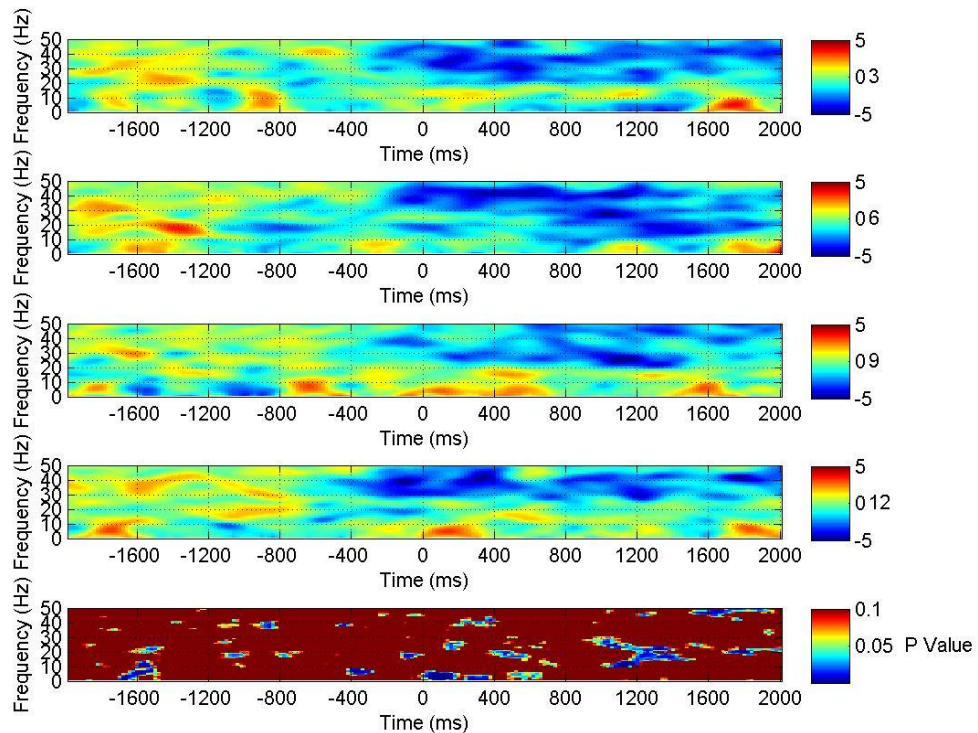
Figure 6.9: ANOVA results associated with motor task experiment using LAP filter. Top four plots represent ERSPs of EEG at electrode C3 recorded from the subject SP4 when performing movement in 4 different directions and the bottom represents the ANOVA results of these 4 ERSPs. Vertical axes represent signal frequency and horizontal axes represent recording time. In ERSP plots blue and red colours show ERD and ERS, respectively. In the ANOVA plot, blue regions represent statistically significant difference in ERSPs across all four directions. The significance level of this figure is 0.05.

6.7   Classification Results

The classification results in predicting imagination/intention of movement, target direction, and imagination/intention and direction of movement from the SCI subjects were further discussed. In this section, the classification results from tetraplegic and paraplegic subjects were presented separately and presented in the following subchapters.

6.7.1 Predicting Imagination/ Intention of Movement

The classification results for predicting imagination of movement from tetraplegic and paraplegic subjects were described in subsection of 6.7.1.1 and 6.7.1.2 respectively. On the other hand, the classification results for predicting intention of movement from tetraplegic subjects were presented in subsection of 6.7.1.3 and the classification results for predicting intention of movement from paraplegic subjects were explained in subchapter of 6.7.1.4.

6.7.1.1   Predicting Imagination of Movement from Tetraplegic Subjects

The maximum classification results in predicting imagination of movement among the tetraplegic subjects were illustrated in Figure 6.10. In this figure, the classification results from CAR+k-NN, CAR+FKNN and CAR+QDA fall within the ranges of 56.67%-86.50%, 60.44%-85.77% and 52.20%-89.42%, respectively. On the other hand, the classification results from LAP+k-NN, LAP+FKNN and LAP+QDA lie within the ranges of 63.33-91.09%, 62.24%-94.14% and 54.07%-96.51%, respectively.

Although the classification results from the combination of spatial filters with multiple classifiers vary among tetraplegic subjects, ST5 has consistently high classification accuracy in all combinations compared with other subjects. In addition, the combination of LAP spatial filter with multiple classifiers achieved higher classification accuracies compared with combinations of the CAR spatial filter with multiple classifiers; except for subject ST6.

Figure 6.10: Summary of classification results for tetraplegic subjects in predicting imagination of movement. The classification results from each subject are presented based on the combinations of classifiers and spatial filters applied.

This is a crude attempt at exploring the effect of duration of injury on subject performance. Figure 6.11 shows classification results of tetraplegic subjects in predicting imagination of movement with respect to the time of injury. This figure shows no particular trend which is expected due to the number of confounding and lurking variables that have not been calibrated. Besides, it is nearly impossible to match and control for level of injury, age, quality of life, prescribed medication, rehabilitation.
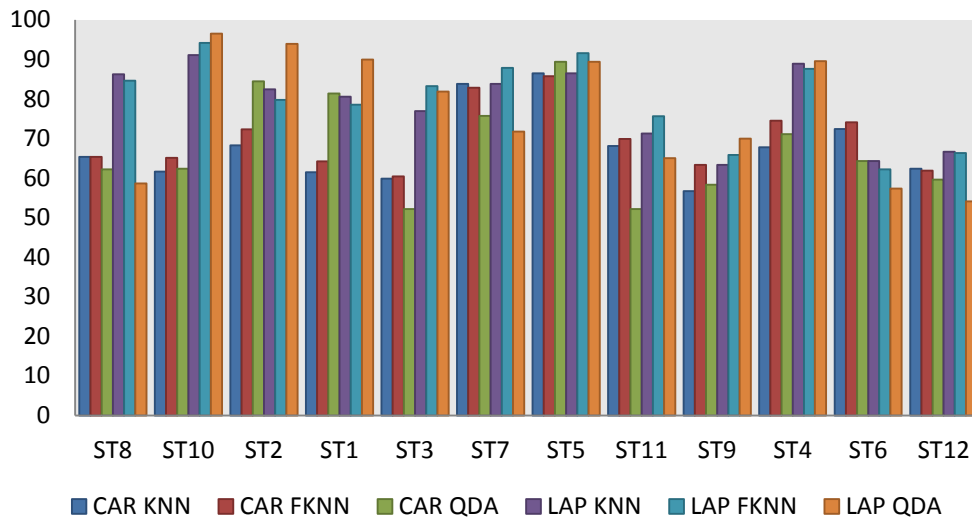
Figure 6.11: Summary of classification results for tetraplegic subjects in predicting imagination of movement with respect to the time of injury. The classification results were presented according to the length of the injury starting with the subject with latest injury. (This figure has been produced at request of the examiners during the viva voce).

The average maximum classification results of predicting imagination of movement by tetraplegic subjects portrayed in Figure 6.12. This figure shows that, the average maximum classification results of CAR+ k-NN, CAR+FKNN and CAR+QDA were 67.86%, 69.99% and 67.79% respectively. On the other hand, the average maximum classification results of LAP+ k-NN, LAP+FKNN and LAP+QDA were 78.51%, 79.79% and 76.51% respectively. Besides, this figure also shows that combination of LAP spatial filter with classifier give higher results compared to combination of CAR spatial filter with classifier.
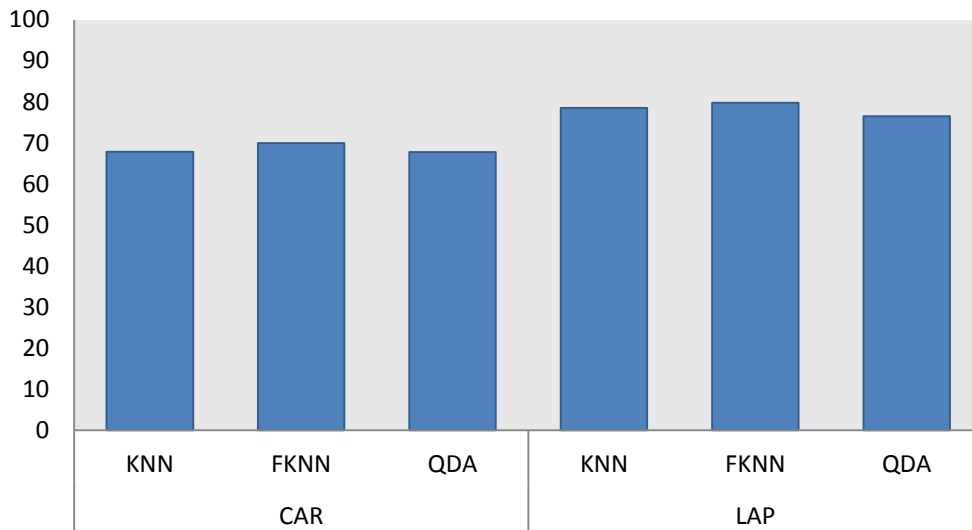
Figure 6.12: Average of maximum classification results for tetraplegic subjects in predicting imagination of movement. The classification results were presented based on the combinations of classifiers and spatial filters applied.

The list of frequency bands associated with the classification results portrayed in Figure 6.10 was tabulated in Table 6.6. Data from this table indicate that, majority of the highest classification results for predicting imagination of movement for tetraplegic patients were obtained from alpha band. This was supported by the finding that 11 out of 12 (91.60%) of the classification results from CAR+k-NN and CAR+FKNN were obtained from the alpha band. Besides that, 8 out of 12 (60.00%) of the classification results from CAR+QDA were also obtained from alpha band. On the other hand, 7 out of 12 (58.30%) of the classification results from LAP+ k-NN and LAP+QDA were obtained from the alpha band. Besides that, 9 out of 12 (75.00%) classification results from LAP+FKNN were also obtained from alpha band.

Table 6.6: Frequency band associated with the classification results from tetraplegic subjects for predicting imagination of movement.

Subject	Frequency band associated with the maximum classification accuracy					
	CAR			LAP		
	KNN	FKNN	QDA	KNN	FKNN	QDA
ST1	Alpha	Alpha	Beta	Alpha	Alpha	Beta
ST2	Alpha	Alpha	Gamma	Beta	Beta	Gamma
ST3	Alpha	Alpha	Alpha	Alpha	Alpha	Beta
ST4	Alpha	Alpha	Alpha	Alpha	Alpha	Alpha
ST5	Alpha	Alpha	Beta	Alpha	Alpha	Beta

153

ST6	Alpha	Alpha	Alpha	Alpha	Alpha	Alpha
ST7	Gamma	Gamma	Beta	Beta	Beta	Beta
ST8	Alpha	Alpha	Alpha	Gamma	Gamma	Alpha
ST9	Alpha	Alpha	Alpha	Gamma	Alpha	Alpha
ST10	Alpha	Alpha	Alpha	Alpha	Alpha	Alpha
ST11	ALPHA	ALPHA	ALPHA	BETA	ALPHA	ALPHA
ST12	ALPHA	ALPHA	ALPHA	ALPHA	ALPHA	ALPHA

Recording electrodes associated with the classification results depicted in Figure 6.10 were tabulated in Table 6.7. Results from Table 6.7 demonstrated that, 6 out of 12 (50.00%) of the classification results from CAR+k-NN and LAP+QDA were obtained either from ipsilateral or contralateral electrodes. Apart from that, 8 out of 12 (60.00%) of the classification results from CAR+FKNN and LAP+FKNN were obtained from contralateral electrodes. Furthermore, 7 out of 12 (58.30%) of the classification results from LAP+k-NN were also obtained from contralateral electrodes. In contrast, 7 out of 12 (58.30%) classification results from CAR+QDA were obtained from ipsilateral electrodes.

Table 6.7: Recording electrode associated with the classification results from tetraplegic subjects for predicting imagination of movement.

Subject	Frequency band associated with the maximum classification accuracy					
	CAR			LAP		
	KNN	FKNN	QDA	KNN	FKNN	QDA
ST1	C5	CFC3	C2	C3	C3	C2
ST2	FC2	CP3	FC3	CZ	CZ	CFC5
ST3	CPZ	FC3	FC4	C3	C3	CCP1
ST4	CP1	CP1	CPZ	CFC3	CFC3	CFC3
ST5	CFC4	CCP2	C2	CFC4	CFC4	C2
ST6	CZ	CZ	CCP1	FC4	FC5	FCZ
ST7	FC3	FC3	CCP5	CCP5	CCP5	CCP5
ST8	CCP5	FCZ	CZ	FC4	FC4	CCP4
ST9	CZ	CZ	CP5	C5	CFC1	CPZ
ST10	FC1	CP3	CFC1	CFC3	CCP4	CCP4
ST11	CP3	CP3	CP2	CCP5	CCP1	CCP1
ST12	CFC2	C3	FCZ	CFC4	C5	CFC3

6.7.1.2   Predicting Imagination of Movement from Paraplegic Subjects

The overall classification results in predicting imagination of movement from paraplegic subjects was depicted in Figure 6.13. This figure indicates that, the classification results from CAR+k-NN, CAR+FKNN and CAR+QDA fall within the ranges of 57.65%-89.34%, 57.38%-89.75% and 52.92%-82.79%, respectively. On the other hand, classification results from LAP+k-NN, LAP+FKNN and LAP+QDA lie within the ranges of 79.87%-89.34%, 72.73%-88.93% and 61.69-95.90%, respectively. Among the paraplegic subjects that participated in the motor imagery experiment, only subject SP4 had consistent classification accuracy across all combinations of spatial filter and classifier.
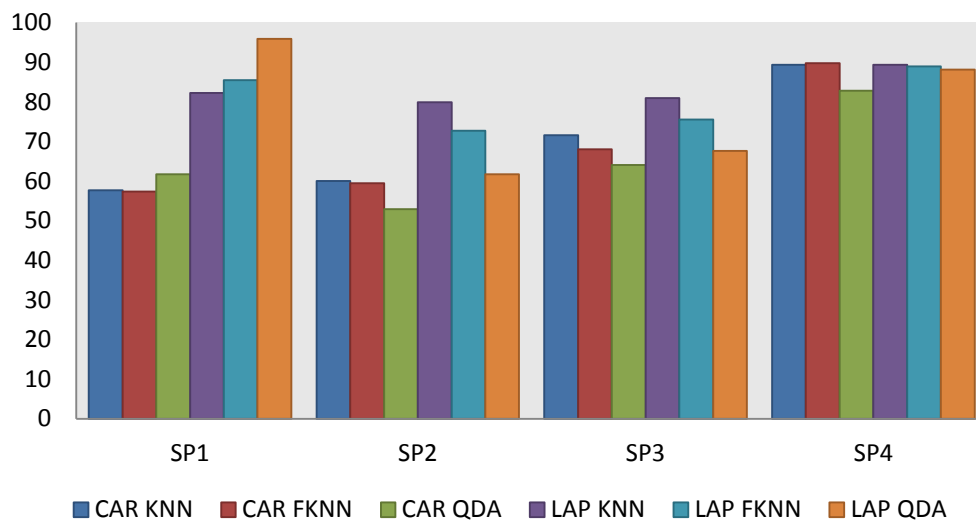
Figure 6.13: Summary of classification results for paraplegic subjects in predicting imagination of movement. The classification results from each subject are presented based on the combinations of classifiers and spatial filters applied.

Table 6.8 shows the frequency band associated with the classification results portrayed in Figure 6.13. This table indicates that 2 out of 4 (50.00%) of the classification results from CAR+k-NN were obtained from either alpha or gamma bands. On the other hand, 3 out of 4 (75.00%) of the classification results from CAR+FKNN were from the alpha band. Meanwhile, 3 out of 4 (75.00%) of the classification results from CAR+QDA were obtained from gamma band.

Apart from that, 3 out of 4 (75.00%) of classification results from LAP+k-NN were obtained from gamma band. Moreover, 2 out of 4 (50.00%) of the classification

results from LAP+FKNN were obtained from the alpha band. Besides that, 3 out of 4 (75.00%) of the classification results from LAP+QDA were obtained from the beta band.

Table 6.8: Frequency band associated with the classification results from paraplegic subjects for predicting imagination of movement..

Subject	Frequency band associated with the maximum classification accuracy					
	CAR			LAP		
	KNN	FKNN	QDA	KNN	FKNN	QDA
SP1	Alpha	Alpha	Gamma	Alpha	Alpha	Beta
SP2	Alpha	Alpha	Alpha	Gamma	Beta	Beta
SP3	Gamma	Alpha	Gamma	Gamma	Alpha	Alpha
SP4	Gamma	Gamma	Gamma	Gamma	Gamma	Beta

The list of recording electrodes associated with the classification results presented in Figure 6.13 was provided in Table 6.9. This table shows that most of the classification results were obtained from contralateral electrodes. This is supported by 3 out of 4 (75.00%) of the classification results from CAR+k-NN, CAR+FKNN and CAR+QDA being obtained from contralateral electrodes. Besides that, all (100.00%) of the results from LAP+ k-NN were obtained from contralateral electrodes. On the other hand, 2 out of 4 (50.00%) of the classification results from LAP+FKNN and LAP+QDA were also obtained from either contralateral electrodes or ipsilateral electrodes.

Table 6.9: Recording electrode associated with the classification results from paraplegic subjects for predicting imagination of movement..

Subject	Recording electrode associated with the maximum classification accuracy					
	CAR			LAP		
	KNN	FKNN	QDA	KNN	FKNN	QDA
SP1	CFC2	CCP1	FC1	CFC5	CCP4	CCP4
SP2	CFC3	CCP1	FCZ	CCP5	CCP5	CCP1
SP3	CFC3	CCP2	CFC3	CFC3	CP2	CFC2
SP4	CCP1	CCP1	CP1	CCP1	C1	CFC3

As for tetraplegic subjects, only 4 out of 14 subjects manage to participate in the motor task experiment. The classification results for predicting intention of movement from the tetraplegic subjects were presented in Figure 6.14. This figure shows that, the classification results from CAR+k-NN, CAR+FKNN and CAR+QDA were within the ranges of 61.96%-69.81%, 62.32%-68.09% and 53.46%-66.98%, respectively. On the other hand, classification results from LAP+k-NN, LAP+FKNN and LAP+QDA fell within the ranges of 57.25%-73.58%, 54.71%-79.25% and 52.31%-65.09%, respectively. Among the four tetraplegic subjects, subject ST13 consistently had the highest classification accuracy in all combinations of spatial filter and classifiers.
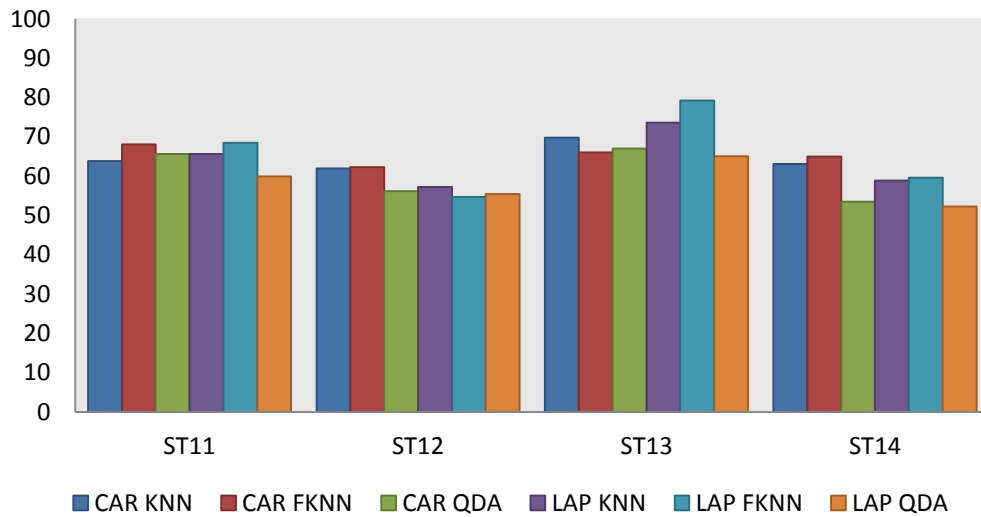
Figure 6.14: Summary of classification results for tetraplegic subjects in predicting intention of movement. The classification results for each subject are presented based on the combinations of spatial filters and classifiers applied.

Frequency bands associated with the classification results depicted in Figure 6.14 were presented in Table 6.10. This table shows that 2 out of 4 (50.00%) of the classification results from CAR+k-NN, CAR+FKNN and CAR+QDA were obtained using either alpha or gamma band. Meanwhile, for the combination of LAP+k-NN and LAP+FKNN, 3 out of 4 (75.00%) of the classification results were obtained from the alpha band. Additionally, 2 out of 4 (50.00%) of the classification results from LAP+QDA were obtained either from alpha or gamma band signals.

Table 6.10: Frequency band associated with the classification results from tetraplegic subjects for predicting intention of movement.

| Subject | Frequency band associated with the maximum classification accuracy | | | | | |
| | CAR | | | LAP | | |
	KNN	FKNN	QDA	KNN	FKNN	QDA
ST11	ALPHA	ALPHA	ALPHA	ALPHA	ALPHA	ALPHA
ST12	ALPHA	ALPHA	ALPHA	ALPHA	ALPHA	ALPHA
ST13	GAMMA	GAMMA	GAMMA	GAMMA	GAMMA	GAMMA
ST14	GAMMA	GAMMA	GAMMA	ALPHA	ALPHA	GAMMA

Tabulated data in Table 6.11 present the list of recording electrodes associated with the classification results portrayed by Figure 6.14. This table indicates that 3 out of 4 (75.00%) of the classification results from CAR+ FKNN and CAR+QDA were obtained from ipsilateral electrodes. Besides that, 2 out of 4 (50.00%) of the classification results from CAR+k-NN were obtained either from ipsilateral electrodes or contralateral electrodes. On the other hand, 3 out of 4 (75.00%) of the classification results from LAP+k-NN and LAP+FKNN were obtained from contralateral electrodes. Furthermore, 2 out of 4 (50.00%) of the classification results from LAP+QDA were obtained either from ipsilateral or contralateral electrodes.

Table 6.11: Recording electrode associated with the classification results from tetraplegic subjects for predicting intention of movement.

| Subject | Recording electrode associated with the maximum classification accuracy | | | | | |
| | CAR | | | LAP | | |
	KNN	FKNN	QDA	KNN	FKNN	QDA
ST11	CP2	CPZ	CPZ	C3	CCP4	CPZ
ST12	CFC3	CFC3	CCP4	CCP3	FC5	FC2
ST13	C5	CCP2	CP4	C5	C5	C3
ST14	FC4	FC4	CP1	C3	CFC5	C5

6.7.1.4 Predicting Intention of Movement from Paraplegic Subjects

The classification results from all paraplegic subjects in predicting intention of movement were exhibited in Figure 6.15. The classification results were between 58.74%-82.42% using combination of CAR spatial filter and *k*-NN classifier (CAR+ *k*-NN). Combination of CAR spatial filter and FKNN (CAR+FKNN) classifier resulted in accuracies of between 59.44%-84.77%, whereas a classification result of 55.76%-87.50% was obtained from the combination of CAR spatial filtering and the QDA classifier (CAR+QDA). On the other hand, the results of the LAP spatial filter combined with classifiers *k*-NN (LAP+ *k*-NN), FKNN (LAP+FKNN) and QDA (LAP+QDA) fall within the ranges of 75.54%-84.38%, 78.38%-88.67% and 62.59%- 94.14%, respectively. In comparison between these subjects, SP4 gave the highest classification accuracy in all combinations of spatial filters and classifier applied.
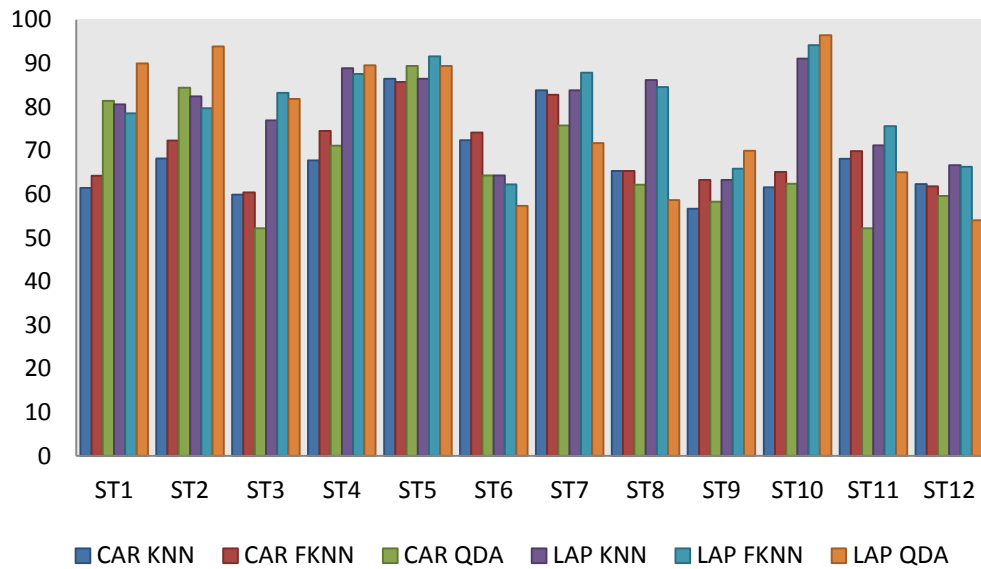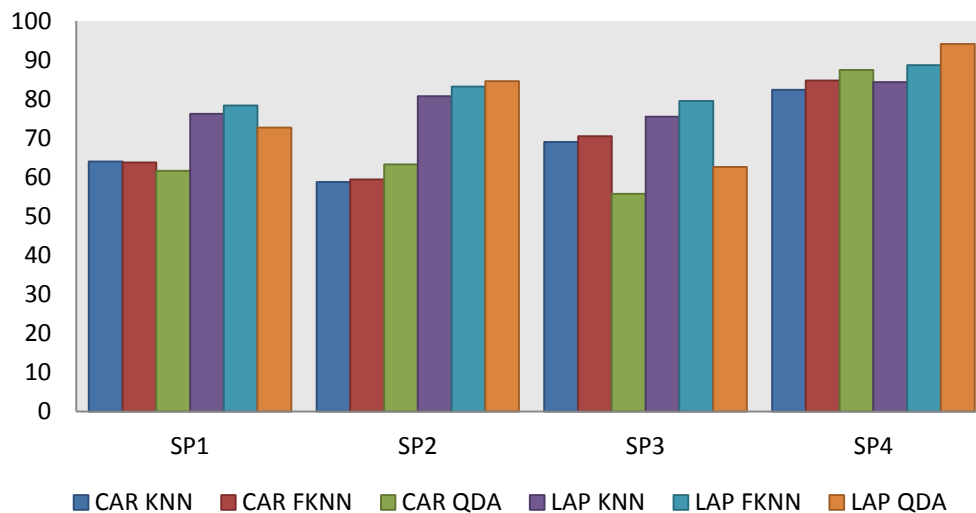

Figure 6.15: Summary of classification results for paraplegic subjects in predicting intention of movement. The classification results from each subject are presented based on the combinations of classifiers and spatial filters applied

Frequency bands associated with the classification results depicted in Figure 6.15 were shown in Table 6.12. This table shows that 3 out of 4 (75.00%) of the classification results from CAR+*k*-NN and CAR+FKNN were obtained from the alpha band. As for combination of CAR+QDA, 2 out of 4 (50.00%) of the classification results were also obtained from alpha band data. On the other hand, all (100%) of the classification results from LAP+*k*-NN and LAP+FKNN were obtained

from the alpha band. In addition, 2 of 4 (50.00%) of the classification results using a combination of LAP+QDA were obtained from the beta band.

Table 6.12: Frequency band associated with the classification results from paraplegic subjects for predicting intention of movement.

| Subject | Frequency band associated with the maximum classification accuracy | | | | | |
| | CAR | | | LAP | | |
	KNN	FKNN	QDA	KNN	FKNN	QDA
SP1	Alpha	Alpha	Alpha	Alpha	Alpha	Beta
SP2	Gamma	Gamma	Beta	Alpha	Alpha	Beta
SP3	Alpha	Alpha	Alpha	Alpha	Alpha	Alpha
SP4	Alpha	Alpha	Gamma	Alpha	Alpha	Gamma

Table 6.13 presents the list of recording electrodes associated with the classification results portrayed in Figure 6.15. In this table, it shows that majority of the highest classification results were obtained from contralateral electrodes. For instance, 3 out of 4 (75.00%) of the classification results using combination of CAR+k-NN, CAR+FKNN and CAR+QDA were obtained from contralateral electrodes. On the other hand, 3 out of 4 (75.00%) of the classification results from LAP+k-NN and LAP+FKNN were also obtained from contralateral electrodes. In addition, 2 out of 4 (50.00%) of the classification results using the combination of LAP+QDA were obtained from contralateral electrodes.

Table 6.13: Recording electrode associated with the classification results from paraplegic subjects for predicting intention of movement.

| Subject | Recording electrode associated with the maximum classification accuracy | | | | | |
| | CAR | | | LAP | | |
	KNN	FKNN	QDA	KNN	FKNN	QDA
SP1	CP4	CZ	CP4	CP2	CP1	CP2
SP2	FC5	FC3	CP5	CCP5	CCP5	CP3
SP3	C1	C1	C1	CPZ	CPZ	CFC2
SP4	CCP1	CCP1	CCP1	CCP1	CCP1	CP1

6.7.2 *Predicting Imagination/Intention of Movement towards Direction 3, 6, 9 and 12*

Results presented in this section explore the effects of direction on imagination/intention of movement among paraplegic and tetraplegic subjects. For this purpose, the classification result for imagination/intention of movement towards direction 3, 6, 9 and 12 are presented and explained individually along with the frequency band and recoding electrodes that contribute to the maximum accuracy classification results.

6.7.2.1 *Predicting Imagination of Movement towards Direction 3, 6, 9 and 12 from Tetraplegic Subjects*

Figure 6.16 depicts the classification accuracies for predicting imagination of movement towards direction 3 from tetraplegic subjects. In this figure, classification results from CAR+k-NN, CAR+FKNN and CAR+QDA are within the ranges of 53.33%-85.19%, 52.78%-90.74% and 53.85%-92.59%, respectively. Apart from that, classification results from LAP+k-NN, LAP+FKNN and LAP+QDA combinations lie within the ranges of 55.71%-87.14%, 62.86%-81.48% and 51.43%-94.29%, respectively. In a comparison of tetraplegic subjects, only ST7 had a classification accuracy of more than 70.00% for every combination of spatial filter and classifier. The same analysis has been implemented for predicting imagination of movement towards direction 6, 9 and 12 from tetraplegic subjects (please refer to Appendix G for further details).

Besides that, classification results for predicting imagination of movement towards direction 6 lie within the range of 53.13%-91.43% using CAR+k-NN. The combination of CAR+FKNN produced classification results of 52.50%-84.29%, whereas classification results of 54.69%-91.43% obtained from CAR+QDA. Apart from that, the classification results from LAP+k-NN, LAP+FKNN and LAP+QDA lie within the ranges of 53.33%-91.43%, 56.67%-90.00% and 55.88%-94.74%, respectively. In comparison to other tetraplegic subjects only data from ST5 had classification results of more than 80.00% in each combination of spatial filter with multiple classifiers.

The classification results for predicting imagination of movement towards direction 9 using the combinations of CAR+k-NN, CAR+FKNN and CAR+QDA dwell within the ranges of 57.50%-81.82%, 56.67%-88.57% and 59.09%-93.18%, respectively. On the other hand, the classification results from LAP+k-NN, LAP+FKNN and LAP+QDA lie within the ranges of 55.26%-81.94%, 61.11%-85.71% and 59.72%-95.45%, respectively. Among twelve tetraplegic subjects that participated in the motor imagery experiment, only ST5 and ST7 have classification results of more than 70.00% for combinations of both spatial filters with multiple classifiers.

Furthermore, the classification results for predicting imagination of movement towards direction 12 from CAR+k-NN, CAR+FKNN and CAR+QDA fall within the ranges of 58.62%-77.03%, 53.33%-68.42% and 56.90%-83.78%, respectively. Apart from that, results of LAP+k-NN, LAP+FKNN and LAP+QDA combinations dwell within the ranges of 53.33%-78.85%, 55.56%-83.78% and 50.00%-84.21%, respectively. Among the tetraplegic subjects, combinations of LAP+k-NN, LAP+FKNN and LAP+QDA for subjects ST4, ST5 and ST7 achieved classification results of more than 70.00%
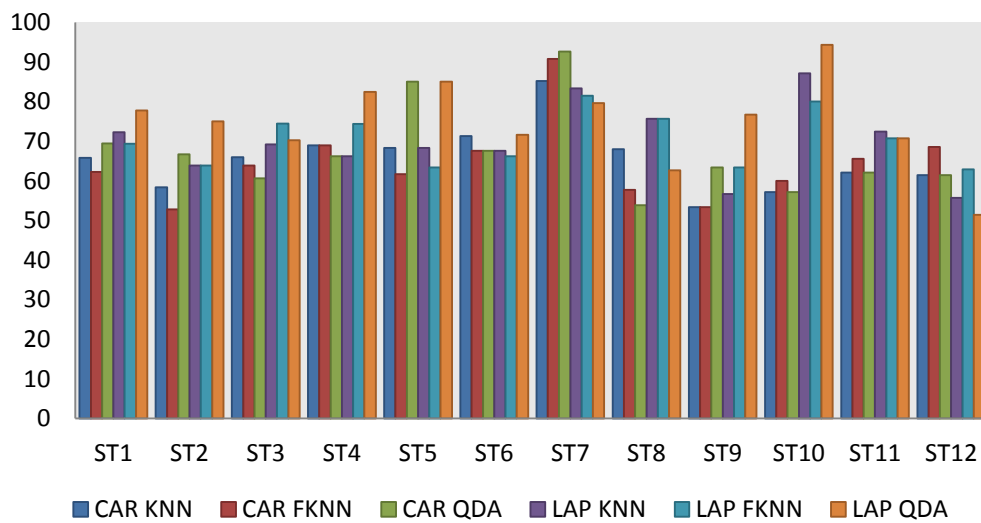
Figure 6.16: Classification results for tetraplegic subjects in predicting imagination of movement towards direction 3. The classification results from each subject are presented based on the combinations of classifiers and spatial filters applied.

Table 6.14 contains the list of frequency bands associated with the classification results presented in Figure 6.16. This data indicates that, majority of the classification results were obtained from the alpha band. This was evidently shown by the finding that 8 out of 12 (60.00%) of the classification results from CAR+k-NN and CAR+FKNN were obtained from alpha band. Additionally, 6 out of 12 (50.00%) of the classification results from CAR+QDA were obtained from the alpha band. Besides that, 9 out of 12 (75.00%) of the classification results from LAP+FKNN and LAP+QDA were also obtained from the alpha band. Apart from that, 5 out of 12 (41.60%) of the classification results from LAP+k-NN were also obtained from the alpha band. The same process of analysis has been implemented for investigating the frequency band associated with the classification results for predicting imagination of movement towards direction 6, 9 and 12 from tetraplegic subjects (please refer to Appendix G for further details).

Majority of the classification results for predicting imagination of movement towards direction 6 were obtained from the alpha band. This was supported by the finding that 10 out of 12 (83.00%) of the classification results from CAR+FKNN and 9 out of 12 (75.00%) of the classification results from CAR+k-NN were obtained from the alpha band. Besides that, 8 out of 12 (60.00%) of the classification results from CAR+QDA were also obtained from the alpha band. Apart from that, 7 out of 12 (58.30%) of the classification results from LAP+FKNN and LAP+QDA were obtained from the alpha band. Meanwhile, 8 out of 12 (60.00%) of the classification results from the combination of LAP+k-NN were also obtained from the alpha band.

Similarly, the classification results for predicting imagination of movement towards direction 9 were mainly obtained from the alpha band. This was supported by the finding that 9 out of 12 (75.00%) of the classification results from CAR+k-NN were obtained from alpha band. Besides that, 8 out of 12 (60.00%) of the classification results from CAR+FKNN were obtained from alpha band. Apart from that, 7 out of 12 (58.30%) of the classification results from CAR+QDA were also obtained from the alpha band. On the other hand, 6 out of 12 (50.00%) of the classification results from LAP+k-NN were obtained from the alpha band. In addition, 9 out of 12 (75.00%) of the classification results from LAP+FKNN were also obtained from the

alpha band. Furthermore, 7 out of 12 (58.30%) of the classification results from LAP+QDA were also obtained from the alpha band.

Moreover, most of the classification results for predicting imagination of movement towards direction 12 were obtained from the alpha band. This was supported by the fact that 11 out of 12 (91.60%) of the classification results from CAR+k-NN and CAR+QDA were obtained from the alpha band. Similarly, 11 out of 12 (91.60%) of the classification results from combinations of LAP+FKNN and LAP+QDA were obtained from the alpha band. Apart from that, 9 out of 12 (75.00%) of the classification results from CAR+QDA and LAP+k-NN were also obtained from the alpha band.

Table 6.14: Frequency band associate with the classification results from tetraplegic subjects for predicting imagination of movement towards direction 3.

Subject	Frequency band associated with the maximum classification accuracy					
	CAR			LAP		
	KNN	FKNN	QDA	KNN	FKNN	QDA
ST1	ALPHA	ALPHA	BETA	ALPHA	ALPHA	ALPHA
ST2	ALPHA	BETA	ALPHA	ALPHA	ALPHA	ALPHA
ST3	ALPHA	ALPHA	GAMMA	BETA	ALPHA	ALPHA
ST4	GAMMA	GAMMA	GAMMA	GAMMA	GAMMA	ALPHA
ST5	ALPHA	ALPHA	ALPHA	ALPHA	ALPHA	ALPHA
ST6	ALPHA	ALPHA	ALPHA	ALPHA	ALPHA	ALPHA
ST7	GAMMA	GAMMA	GAMMA	GAMMA	GAMMA	GAMMA
ST8	GAMMA	GAMMA	GAMMA	GAMMA	GAMMA	GAMMA
ST9	ALPHA	ALPHA	GAMMA	BETA	ALPHA	ALPHA
ST10	ALPHA	ALPHA	ALPHA	ALPHA	ALPHA	ALPHA
ST11	ALPHA	ALPHA	ALPHA	GAMMA	ALPHA	GAMMA
ST12	GAMMA	ALPHA	ALPHA	BETA	ALPHA	ALPHA

The recording electrodes associated with the classification results portrayed in Figure 6.16 were listed in Table 6.15. Data in this table demonstrates that most of the classification results were recorded from both of contralateral and ipsilateral electrodes. For instance, 9 out of 12 (75.00%) of the classification results from CAR+k-NN and 7 out of 12 (58.30%) of the classification results from CAR+FKNN were obtained from contralateral electrodes. On the other hand, 7 out of 12 (58.30%) of the classification results from CAR +QDA were obtained from ipsilateral electrodes. Moreover, 6 out of 12 (50.00%) of the classification results from LAP+k-

NN were obtained either from contralateral or ipsilateral electrodes. Besides that, 8 out of 12 (60.00%) of the classification results from LAP+QDA were obtained from contralateral electrodes. In contrast, 9 out of 12 (75.00%) of the classification results from LAP+FKNN were obtained from ipsilateral electrodes. The same process of analysis has been implemented for investigating the recording electrodes associated with the classification results for predicting imagination of movement towards direction 6, 9 and 12 from tetraplegic subjects (please refer to Appendix G for further details).

Apart from that, most of the classification results for predicting imagination of movement towards direction 6 were recorded from contralateral electrodes. This was evidently proven by the finding that 8 out of 12 (60.00%) of the classification results from both combinations of CAR+k-NN and LAP+k-NN were obtained from contralateral electrodes. Similarly, 7 out of 12 (58.30%) of the classification results from CAR+FKNN and 7 out of 12 (58.30%) of the classification results from LAP+QDA were also obtained from contralateral electrodes. On the other hand, 9 out of 12 (75.00%) of the classification results from the combination of CAR+QDA were obtained from ipsilateral electrodes. Meanwhile, 6 out of 12 (50.00%) of the classification results from LAP+FKNN were obtained either from ipsilateral or contralateral electrodes.

Furthermore, classification results for predicting imagination of movement towards direction 9 were recorded from both contralateral and ipsilateral electrodes. This was shown by the finding that 6 out of 12 (50.00%) of the classification results from CAR+QDA and 6 out of 12 (50.00%) of the classification results from LAP+k-NN and LAP+FKNN were obtained either from contralateral or ipsilateral electrodes. On the other hand, 7 out of 12 (58.30%) of the classification results from CAR+k-NN and 8 out of 12 (60.00%) of the classification results from CAR+FKNN were obtained from ipsilateral electrodes. Meanwhile, 7 out of 12 (58.30%) of the classification results from the combination of LAP+QDA were obtained from contralateral electrodes.

Additionally, the classification results for predicting imagination of movement towards direction 12 were mostly obtained from either contralateral or ipsilateral

electrodes. This was evidently supported by the finding that 7 out of 12 (58.30%) of the classification results from CAR+k-NN and CAR+QDA were recorded from contralateral electrodes. Following this, 7 out of 12 (58.30%) of the classifications results from LAP+QDA were also obtained from contralateral electrodes. In contrast, 7 out of 12 (58.30%) of the classification results from CAR+FKNN and 8 out of 12 (60.00%) of the classification results from LAP+k-NN were obtained from ipsilateral electrodes. Meanwhile, 6 out of 12 (50.00%) of the classification results from the combination of LAP+FKNN were obtained either from contralateral or ipsilateral electrodes.

Table 6.15: Recording electrode associate with the classification results from tetraplegic subjects for predicting imagination of movement towards direction 3.

| Subject | Frequency band associated with the maximum classification accuracy | | | | | |
| | CAR | | | LAP | | |
	KNN	FKNN	QDA	KNN	FKNN	QDA
ST1	CFC5	CFC5	CP2	CCP2	CCP2	C1
ST2	CCP2	C1	CCP2	CZ	CCP4	C3
ST3	CP1	CP1	C1	C5	C3	CCP2
ST4	FC4	FC2	FC4	FC4	FC4	CFC3
ST5	CFC4	FC2	C2	CFC4	CFC4	C2
ST6	CFC5	C1	CPZ	FC5	C4	C3
ST7	FC3	FC3	FC3	FC3	FC3	C3
ST8	FC5	FC5	FC3	FC4	FC4	FC4
ST9	CFC3	CP2	CP5	CCP1	FC3	FC3
ST10	FC3	FCZ	FC5	CCP4	CCP4	CCP4
ST11	CP3	CP5	CP4	CCP5	C4	CCP5
ST12	FC5	FC4	CZ	CCP5	FCZ	CFC5

6.7.2.2 Predicting Imagination of Movement towards Direction 3, 6, 9 and 12 from Paraplegic Subjects

Classification results from the paraplegic subjects for predicting imagination of movement towards direction 3 were illustrated in Figure 6.17. In this figure, the classification results from CAR+k-NN lie within the range of 62.82%-73.68%. The combination of CAR+FKNN produced classification resaults between 60.26%-73.68%, whereas classification results of 64.13%-80.26% were obtained from CAR+QDA. Moreover, the classification results from LAP+k-NN, LAP+FKNN and LAP+QDA dwell within the ranges of 64.13%-80.00%, 66.30%-78.95% and 69.23%-88.33%, respectively. The same procedure of analysis was implemented for predicting imagination of movement towards direction 6, 9 and 12 (please refer to Appendix G for further details).

Besides that, the classification results for predicting imagination of movement towards direction 6 from CAR+k-NN, CAR+FKNN and CAR+QDA fall within the ranges of 63.16%-83.33%, 65.56%-81.67% and 60.00%-81.67%, respectively. On the other hand, the classification results from LAP+k-NN, LAP+FKNN and LAP+QDA combinations lie within the ranges of 72.37%-83.33%, 78.95%-87.50% and 60.53%-88.33%, respectively. In comparison of the paraplegic subjects that participated in the motor imagery experiment, SP4 consistently had classification results of more than 80.00% in combinations of both of spatial filters with multiple classifiers.

Furthermore the classification results for predicting imagination of movement towards direction 9 ranged from 56.67%-75.00% using the combination of CAR+k-NN. CAR+FKNN produced classification accuracy between 60.00%-73.33%, whereas 57.78%-73.33% was obtained from CAR+QDA. On the other hand, the classification results from LAP+k-NN lie within the range of 70.51%-78.79%. The combination of LAP+FKNN produced classification results of 69.23%-83.33%, and 61.54%-86.67% was obtained from LAP+QDA.

Additionally, the classification results for predicting imagination of movement towards direction 12 range from 56.25%-84.38% using the combination of CAR spatial filter with k-NN classifier. The combination of CAR+FKNN produced

classification results of 59.37%-85.94%, whereas 59.21%-75.00% was obtained from CAR+QDA. Meanwhile, LAP+k-NN, LAP+FKNN and LAP+QDA combinations produced classification results within the ranges of 65.63%-85.11%, 67.19%-92.19% and 72.37%-91.49% respectively. In comparison between the paraplegic subjects, SP4 had the classification accuracy of more than 75.00% for combinations of both spatial filters with multiple classifiers.
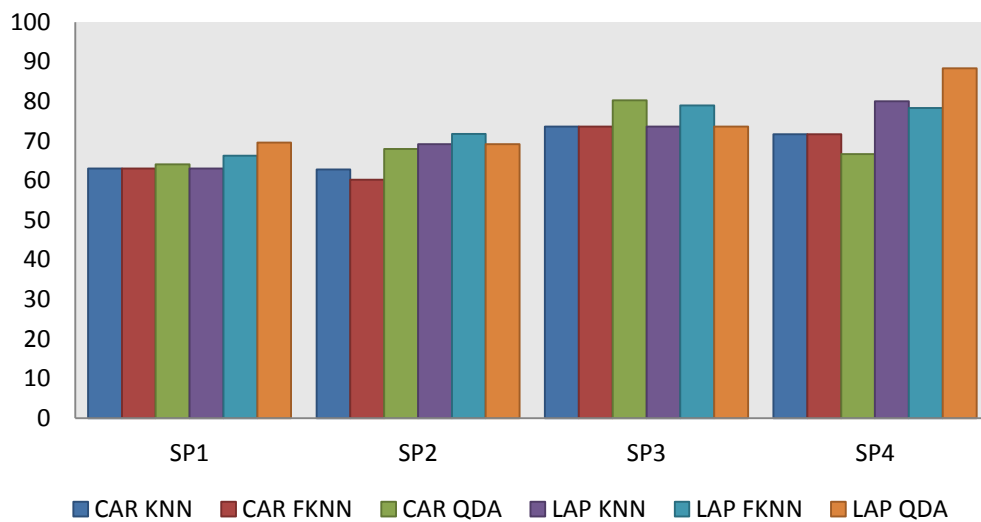
Figure 6.17: Classification results for paraplegic subjects in predicting imagination of movement towards direction 3. The classification results from each subject are presented based on the combinations of classifiers and spatial filters applied.

Table 5.12 presents the list of frequency bands associated with the classification results shown in Figure 6.17. This data demonstrates that 2 out of 4 (50.00%) of the classification results from CAR+k-NN and CAR+FKNN were obtained either from alpha or gamma bands. As for the combination of CAR+QDA, 3 out of 4 (75.00%) of the classification results were obtained from the alpha band. On the other hand, 3 out of 4 (75.00%) of the classification results from LAP+FKNN and LAP+QDA were obtained from the alpha band. Similarly, 2 out of 4 (50.00%) of the classification results from LAP+k-NN were also obtained from the alpha band. The same process of analysis has been implemented for investigating the frequency band associated with the classification results for predicting imagination of movement towards direction 6, 9 and 12 (please refer to Appendix G for further details).

In the meantime, the classification results for predicting imagination of movement towards direction 6 were obtained from alpha or gamma bands. This was evidently shown by 2 out of 4 (50.00%) of the classification results from CAR+k-NN and CAR+FKNN obtained from either the alpha or gamma band. Similarly, 2 out of 4 (50.00%) of the classification results from LAP+k-NN and LAP+FKNN were also obtained either from alpha or gamma bands. On the other hand, 3 out of 4 (75.00%) of the classification results from CAR+QDA were obtained from the gamma band. On the contrary, 3 out of 4 (75.00%) of the classification results from the combination of LAP+QDA were obtained from the alpha band.

Most of the classification results for predicting imagination of movement towards direction 9 were also obtained from alpha or gamma bands. This was supported by the finding that all (100.00%) of the classification results from CAR+QDA were obtained from the gamma band. Besides that, 3 out of 4 (75.00%) of the classification results from CAR+k-NN were obtained from the alpha band. Apart from that, 2 out of 4 (50.00%) of the classification results from CAR+FKNN were obtained from the alpha band. Additionally, 3 out of 4 (75.00%) of the classification results from LAP+k-NN and LAP+QDA were obtained from the alpha band. Furthermore, 2 out of 4 (50.00%) of the classification results from LAP+FKNN were obtained either from the alpha or gamma band.

The classification results for predicting imagination of movement towards direction 12 were obtained from both alpha and beta bands. This was demonstrated by the fact that 3 out of 4 (75.00%) of the classification results from CAR+FKNN and CAR+QDA were obtained from the alpha band. On the other hand, 2 out of 4 (50.00%) of the classification results from CAR+k-NN were obtained either from the alpha or beta band. Similarly, 2 out of 4 (50.00%) of the classification results from LAP+FKNN and LAP+QDA were obtained either from alpha or beta bands. Furthermore, 3 out of 4 (75.00%) of the classification results from the combination of LAP+k-NN were obtained from beta bands.

169

Table 6.16: Frequency band associate with the classification results from paraplegic subjects for predicting imagination of movement towards direction 3.

Subject	Frequency band associated with the maximum classification accuracy					
	CAR			LAP		
	KNN	FKNN	QDA	KNN	FKNN	QDA
SP1	GAMMA	GAMMA	GAMMA	ALPHA	ALPHA	ALPHA
SP2	GAMMA	ALPHA	ALPHA	BETA	GAMMA	GAMMA
SP3	ALPHA	ALPHA	ALPHA	GAMMA	ALPHA	ALPHA
SP4	ALPHA	GAMMA	ALPHA	ALPHA	ALPHA	ALPHA

Based on these results it is essential to highlight that, the maximum classification results for all four directions were obtained from contralateral electrodes.

Table 5.13 contains the list of recording electrodes associated with the classification results illustrated in Figure 6.17. This table shows that all (100%) of the classification results from LAP+k-NN and LAP+QDA classifier were obtained from contralateral electrodes. Besides that, 3 out of 4 (75.00%) of the classification results from LAP+FKNN were also obtained from contralateral electrodes. Contralateral electrodes also accounted for 3 out of 4 (75.00%) classification results from CAR+FKNN. On the other hand, 2 out of 4 (50.00%) classification results from CAR+k-NN and CAR+QDA were obtained either from contralateral or ipsilateral electrodes. The same analysis was carried out for examining the recording electrodes associated with classification results for predicting imagination of movement towards direction 6, 9 and 12 (please refer to Appendix G for further details).

Apart from that, majority of the classification results for predicting imagination of movement towards direction 6 were obtained from either contralateral or ipsilateral electrodes. This was supported by the finding that 2 out of 4 (50.00%) of the classification results from CAR+k-NN and CAR+FKNN were obtained either from of contralateral or ipsilateral electrodes. On the other hand, all (100%) of the classification results from CAR+QDA were obtained from contralateral electrodes. Similarly, 3 out of 4 (75.00%) of the classification results from LAP+k-NN and LAP+FKNN were obtained from contralateral electrodes. Moreover, 3 out of 4 (75.00%) of the classification results from LAP+QDA were obtained from ipsilateral electrodes.

However, majority of the classification results for predicting imagination of movement towards direction 9 were obtained from contralateral electrodes. This was shown by the finding that all (100.00%) of the classification results from CAR+QDA were obtained from contralateral electrodes. Similarly, 3 out of 4 (75.00%) of the classification results from CAR+*k*-NN were also obtained from contralateral electrodes. On the other hand, 3 out of 4 (75.00%) of the classification results from CAR+FKNN were obtained from ipsilateral electrodes. Apart from that, 3 out of 4 (75.00%) classification results from CAR+*k*-NN and CAR+FKNN were obtained from contralateral electrodes. Besides that, 2 out of 4 (50.00%) of the classification results from LAP+QDA were obtained either from ipsilateral or contralateral electrodes.

Additionally, majority of the classification results for predicting imagination of movement towards direction 12 were obtained from contralateral electrodes. This was demonstrated by the fact that 3 out of 4 (75.00%) of the classification results from CAR+*k*-NN, CAR+FKNN and CAR+QDA were obtained from contralateral electrodes. Similarly, 3 out of 4 (75.00%) of the classification results from LAP+*k*-NN and LAP+FKNN were also obtained from contralateral electrodes. Only 2 out of 4 (50.00%) of the classification results from the combination of LAP+QDA were obtained from ipsilateral electrodes.

Table 6.17: Recording electrode associate with the classification results from paraplegic subjects for predicting imagination of movement towards direction 3.

Subject	Recording electrode associated with the maximum classification accuracy					
	CAR			LAP		
	KNN	FKNN	QDA	KNN	FKNN	QDA
SP1	CP4	C4	CP4	C1	CCP4	C1
SP2	C5	CFC4	C2	CCP5	CCP5	CFC5
SP3	CFC2	CFC2	CCP1	CFC3	CFC3	CFC1
SP4	CCP1	CCP1	C1	CFC1	CFC1	CFC1

6.7.2.3 Predicting Intention of Movement towards Direction 3, 6, 9 and 12 from Tetraplegic Subjects

The classification results for predicting intention of movement towards direction 3 from tetraplegic subjects using combinations of CAR and LAP spatial filters with k-NN, FKNN and QDA classifiers was depicted in Figure 6.18. This figure exhibits the classification results from CAR+k-NN lie within the range of 57.35%-62.50%. CAR+FKNN produced classification accuracy between 57.35%-65.28%, while 56.06%-72.06% was obtained from CAR+QDA. On the other hand, classification results from LAP+k-NN, LAP+FKNN and LAP+QDA lie within the ranges of 50.00%-70.83%, 51.52%-66.67% and 57.58%-70.83%, respectively. In comparison between these two types of spatial filter, LAP appears to offer higher classification accuracy compared with the CAR spatial filter. The same procedure of analysis has been implemented for predicting intention of movement towards direction 6, 9 and 12 (please refer to Appendix G for further detail).

Besides that, the classification results for predicting intention of movement towards direction 6 using CAR+k-NN, CAR+FKNN and CAR+QDA combinations dwell within the ranges of 57.58%-66.22%, 57.58%-68.92% and 63.64%-74.32%, respectively. Apart from that, the classification results of LAP+k-NN, LAP+FKNN and LAP+QDA fall within the ranges of 48.48%-62.16%, 53.03%-64.86% and 60.61%-77.27%, respectively. In a comparison of the tetraplegic subjects that participated in the motor task experiment, ST11 had the highest accuracy classification results in most combinations of spatial filters with multiple classifiers.

The classification results for predicting intention of movement towards direction 9 using CAR+k-NN, CAR+FKNN and CAR+QDA dwell within the ranges of 58.88%-71.62%, 62.50%-75.68% and 55.88%-67.57%, respectively. On the other hand, results of LAP+k-NN, LAP+FKNN and LAP+QDA combinations lie within the ranges of 58.33%-68.92%, 57.81%-75.68% and 52.78%-67.19%, respectively. Among the four tetraplegic subjects that participated in the motor task experiment, only data from ST11 produced classification accuracy of more than 70.00% using both spatial filters combined with multiple classifiers.

172

Furthermore, the classification accuracy for predicting intention of movement towards direction 12 lie within 59.09%-67.74% using CAR+k-NN. CAR+FKNN produced classification results between 59.09%-69.44%, whereas 63.64%-72.58% was obtained from CAR+QDA. Besides that, the combinations of LAP+k-NN, LAP+FKNN and LAP+QDA achieved classification results within the ranges of 54.84%-61.29%, 51.61%-64.52% and 56.94%-77.27%, respectively. In comparison of the tetraplegic subjects, ST11 has the highest classification accuracy in most combinations of spatial filter and classifiers.
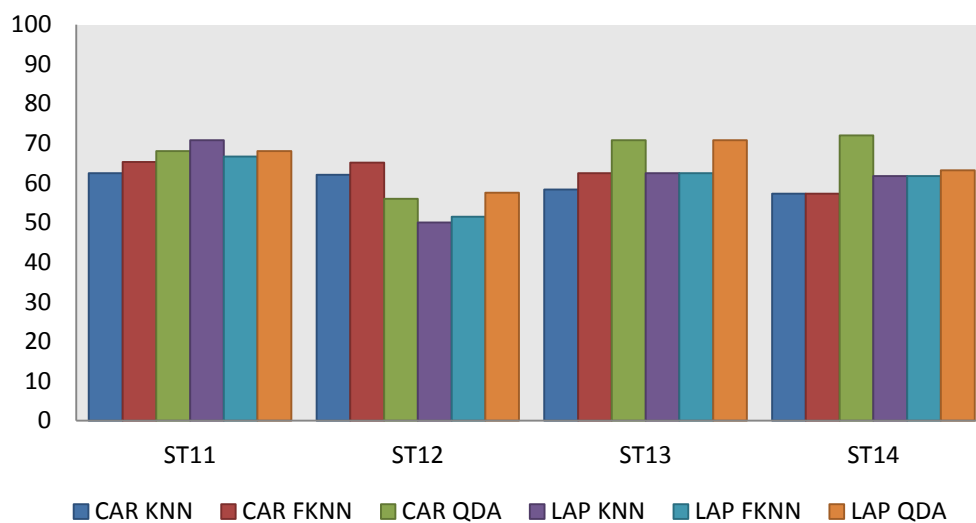
Figure 6.18: Classification results for tetraplegic subjects in predicting intention of movement towards direction 3. The classification results from each subject are presented based on the combinations of classifiers and spatial filters applied.

The frequency bands associated with the classification results depicted in Figure 6.18 were tabulated in Table 6.18. Data presented in this table illustrated that, majority of the classification results in Figure 6.18 were obtained either from alpha or gamma bands. This was supported by the finding that all (100.00%) of the classification results from CAR+FKNN were obtained from the alpha band. Similarly, 3 out of 4 (75.00%) of the classification results from CAR+k-NN classifier were also obtained from the alpha band. On the other hand, 2 out of 4 (50.00%) of the classification results from CAR+QDA were obtained either from gamma or beta band. As for the classification results from LAP+k-NN, 3 out of 4 (75.00%) of the classification results were obtained from the gamma band. Besides that, 2 out of 4 (50.00%) of the

classification results from LAP+QDA were also obtained from gamma band. On the other hand, 2 out of 4 (50.00%) of the classification results from LAP+FKNN were obtained either from the gamma or alpha band. The same analysis has been carried out for investigating the frequency band associated with classification results for predicting intention of movement towards direction 6, 9 and 12 (please refer to Appendix G for further detail).

In the meantime, majority of the classification results for predicting intention of movement towards direction 6 were obtained from the alpha band. This was shown by the observation that 3 out of 4 (75.00%) of the classification results from CAR+k-NN, CAR+QDA and LAP+FKNN were obtained from the alpha band. Besides that, all (100.00%) of the classification results from LAP+k-NN were also obtained from the alpha band. On the other hand, 2 out of 4 (50.00%) of the classification results from CAR+ FKNN and LAP+QDA classifier were obtained either from alpha or gamma bands.

Likewise, most of the classification results for predicting intention of movement towards direction 9 were also obtained from alpha and gamma bands. This is supported by the finding that 2 out of 4 (50.00%) of the classification results from CAR+k-NN, CAR+QDA and LAP+QDA were obtained either from alpha or gamma bands. Besides that, all (100.00%) of the classification results from LAP+FKNN were obtained from the alpha band. Furthermore, 2 out of 4 (50.00%) of the classification results from LAP+k-NN were also obtained from the alpha band. In addition, 3 out of 4 (75.00%) of the classification results from CAR+FKNN were obtained from alpha band signals.

Moreover, most of the classification results in predicting intention of movement towards direction 12 were also obtained from the alpha and gamma band. This was supported by 3 out of 4 (75.00%) of the classification results from CAR+FKNN and CAR+QDA were obtained from the gamma band. Besides that, 2 out of 4 (50.00%) of the classification results from CAR+k-NN were obtained either from alpha or gamma bands. Furthermore, 3 out of 4 (75.00%) of the classification results from LAP+k-NN were obtained from the alpha band. Apart from that, 2 out of 4 (50.00%) of the classification results from the LAP+QDA combination were also obtained

from the alpha band. On the other hand 2 out of 4 (50.00%) of the classification results from LAP+FKNN were obtained either from alpha or gamma bands.

Table 6.18: Frequency band associate with the classification results from tetraplegic subjects for predicting intention of movement towards direction 3.

Subject	Frequency band associated with the maximum classification accuracy					
	CAR			LAP		
	KNN	FKNN	QDA	KNN	FKNN	QDA
SP1	ALPHA	ALPHA	BETA	GAMMA	GAMMA	ALPHA
SP2	ALPHA	ALPHA	GAMMA	GAMMA	ALPHA	GAMMA
SP3	GAMMA	ALPHA	GAMMA	GAMMA	GAMMA	GAMMA
SP4	ALPHA	ALPHA	BETA	ALPHA	ALPHA	BETA

The list of recording electrodes associated with the classification results depicted in Figure 6.18 was tabulated in Table 6.19. Data from this table indicates that 2 out of 4 (50.00%) of the classification results from CAR+FKNN and CAR+k-NN were obtained either from contralateral or ipsilateral electrodes. Similarly, 2 out of 4 (50.00%) of the classification results from the combinations of LAP+FKNN and LAP+QDA were also obtained either from contralateral or ipsilateral electrodes. On the other hand, 3 out of 4 (75.00%) of the classification results from CAR+QDA were obtained from contralateral electrodes. Besides that, 3 out of 4 (75.00%) of the classification results from the combination of LAP+k-NN were obtained from contralateral electrodes.

Majority of the classification results in predicting intention of movement towards direction 6 were obtained from both contralateral and ipsilateral electrodes. All (100.00%) of the classification results from the combination of CAR+QDA were obtained from contralateral electrodes. On the other hand, 3 out of 4 (75.00%) of the classification results from CAR+k-NN were obtained from ipsilateral electrodes. Meanwhile, 2 out of 4 (50.00%) of the classification results from CAR+FKNN were obtained either from contralateral or ipsilateral electrodes. Besides that, 3 out of 4 (75.00%) of the classification results from the combinations of LAP+k-NN and LAP+QDA were obtained from contralateral electrodes. In contrast, 3 out of 4 (75.00%) of the classification results from LAP+FKNN were obtained from ipsilateral electrodes.

In the same way, majority of the classification results for predicting intention of movement towards direction 9 were recorded by both contralateral and ipsilateral electrodes. All (100.00%) of the classification results from CAR+FKNN were obtained from contralateral electrodes. Besides that, 3 out of 4 (75.00%) of the classification results from LAP+QDA and CAR+QDA were also obtained from contralateral electrodes. On the other hand, 2 out of 4 (50.00%) of the classification results from LAP+ k-NN and LAP+FKNN were obtained either from contralateral or ipsilateral electrodes. Similarly, 2 out of 4 (50.00%) of the classification results from CAR+k-NN were also obtained from either contralateral or ipsilateral electrodes.

Addition to that, majority of the classification results for predicting intention of movement towards direction 12 were also recorded from contralateral and ipsilateral electrodes. 2 out of 4 (50.00%) of the classification results from CAR+k-NN and CAR+QDA classifier were obtained either from contralateral or ipsilateral electrodes. Likewise, 2 out of 4 (50.00%) of the classifications from LAP+k-NN and LAP+FKNN were also obtained either from contralateral or ipsilateral electrodes. On the other hand, 3 out of 4 (75.00%) of the classification results from the combination of CAR+FKNN were obtained from contralateral electrodes. Besides that, 3 out of 4 (75.00%) of the classification results from the combination of LAP+QDA were obtained from contralateral electrodes.

Table 6.19: Recording electrode associated with the classification results from tetraplegic subjects for predicting intention of movement towards direction 3.

| Subject | Recording electrodes associated with the maximum classification accuracy | | | | | |
| | CAR | | | LAP | | |
	KNN	FKNN	QDA	KNN	FKNN	QDA
SP1	CCP5	C3	CP5	CP5	C5	CCP4
SP2	CFC4	CFC4	CP4	C5	FC5	FC4
SP3	CCP4	CCP5	CFC5	FC1	FC2	C5
SP4	CP5	CZ	CP1	CFC2	CZ	FC3

6.7.2.4 Predicting Intention of Movement towards Direction 3, 6, 9 and 12 from Paraplegic Subjects

The overall classification results obtained from the combinations of CAR or LAP spatial filters with *k*-NN, FKNN and QDA classifiers for predicting intention of movements towards direction 3 from paraplegic subjects was depicted in Figure 6.19. This figure demonstrates that, the classification results for the combination of CAR+*k*-NN lies within the range of 59.46%-65.52%. The combination of CAR+FKNN achieved classification results between 55.41%-68.97%, while 62.16%-75.86% was obtained from the combination of CAR+QDA. Meanwhile the classification results from LAP+*k*-NN, LAP+FKNN and LAP+QDA lie within the ranges of 71.62%-80.88%, 62.16%-85.29% and 73.40%-86.21%, respectively. In a comparison of these two types of spatial filter, the LAP approach offers higher classification accuracy than the CAR approach. The same procedure has been implemented for predicting intention of movement towards direction 6, 9 and 12 (please refer to Appendix G for further detail).

Maximum classification results for predicting intention of movement towards direction 6 from CAR+*k*-NN, CAR+FKNN and CAR+QDA fall within the ranges of 62.16%-80.88%, 59.46%-79.41% and 63.83%-66.18%, respectively. Besides that, classification results of LAP+*k*-NN, LAP+FKNN and LAP+QDA lie within the ranges of 68.92%-83.82%, 63.51%-85.29% and 63.51%-85.29%, respectively. Among all paraplegic subjects, subject SP4 has the highest classification results in all of these classification combinations.

Maximum classification results for predicting intention of movement towards direction 9 from CAR+*k*-NN, CAR+FKNN and CAR+QDA dwell within the ranges of 60.00%-72.22%, 61.43%-79.17% and 61.67%-89.39%, respectively. Furthermore, classification results of LAP+*k*-NN, LAP+FKNN and LAP+QDA lie within the ranges of 71.43%-80.30%, 72.22%-86.36% and 64.29%-90.91%, respectively. Between these two types of spatial filter, the LAP method offers higher classification accuracy compared to the CAR spatial filter.

Maximum classification results for predicting intention of movement towards direction 12 from CAR+k-NN, CAR+FKNN and CAR+QDA dwell within the ranges of 61.76%-87.50%, 63.24%-84.38% and 60.29%-78.13%, respectively. On the other hand, classification results of LAP+k-NN, LAP+FKNN and LAP+QDA lie within the ranges of 67.65%-84.38%, 70.59%-85.94% and 67.65%-90.62%, respectively. Among all of the paraplegic subjects that participated in motor task experiment, subject SP4 has a classification accuracy of more than 70% for both combinations of both spatial filters with multiple classifiers.
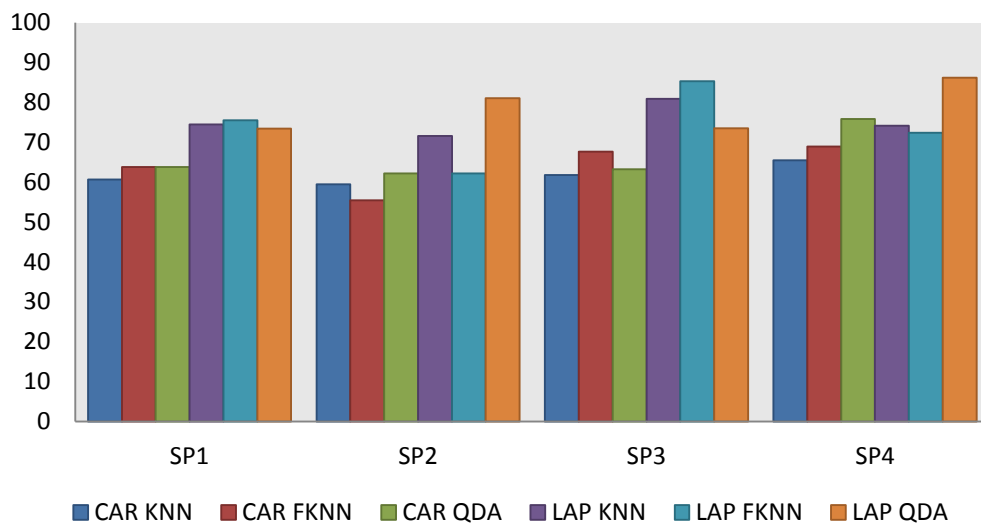
Figure 6.19: Classification results for paraplegic subjects in predicting intention of movement towards direction 3. The classification results from each subject are presented based on the combinations of classifiers and spatial filters used.

Tabulated data in Table 6.20 shows the frequency bands associated with the classification results depicted in Figure 6.19. In this figure, it demonstrated that 2 out of 4 (50.00%) of the classification results from CAR+k-NN and CAR+QDA were obtained either from alpha or gamma bands. Besides that, 3 out of 4 (75.00%) of the classification results from CAR+FKNN were obtained from the alpha band. On the other hand, 3 out of 4 (75.00%) of the classification results from LAP+ k-NN and LAP+FKNN were obtained from alpha band. Moreover, 2 out of 4 (50.00%) of the classification results from LAP+QDA were obtained from beta band. The same analytical process was carried out to investigate the frequency band associated with

highest classification accuracy results from predicting the intention of movement towards direction 6, 9 and 12 (please refer to Appendix G for further detail).

Majority of the highest classification results for predicting intention of movements towards direction 6 from paraplegic subjects were obtained from the alpha band. This was supported by the finding that all (100.00%) of the classification results from LAP+FKNN and CAR+FKNN were obtained from alpha band. Apart from that, 3 out of 4 (75.00%) of the classification results from LAP+k-NN, LAP+QDA, CAR+k-NN and CAR+QDA were also obtained from the alpha band.

Additionally, the alpha band was mostly associated with the highest classification results for predicting intention of movement towards direction 9. This was supported by the finding that all (100.00%) of the classification results from CAR+FKNN, and 3 out of 4 (75.00%) of the classification results from CAR+k-NN and CAR+QDA, were obtained from the alpha band. Meanwhile, 3 out of 4 (75.00%) of the classification results from LAP+k-NN were obtained from the gamma band. Moreover, 3 out of 4 (75.00%) of the classification results from LAP+QDA were obtained from the alpha band. Alpha band also contributed to 2 out of 4 (50.00%) of the classification results for LAP+FKNN.

Similarly, the majority of highest classification results for predicting intention of movement towards direction 12 were obtained from the alpha band. All (100.00%) of the classification results from CAR+FKNN, and 3 out of 4 (75.00%) of the classification results from CAR+k-NN and CAR+QDA, were obtained from alpha band. Besides that, 3 out of 4 (75.00%) of the classification results from LAP+k-NN, LAP+FKNN and LAP+QDA were also obtained from the alpha band.

Table 6.20: Frequency band associate with the classification results from paraplegic subjects for predicting intention of movement towards direction 3.

Subject	Frequency band associated with the maximum classification accuracy					
	CAR			LAP		
	KNN	FKNN	QDA	KNN	FKNN	QDA
SP1	ALPHA	ALPHA	GAMMA	ALPHA	ALPHA	GAMMA
SP2	ALPHA	ALPHA	ALPHA	GAMMA	ALPHA	BETA
ST3	GAMMA	ALPHA	ALPHA	ALPHA	ALPHA	ALPHA
SP4	GAMMA	GAMMA	GAMMA	ALPHA	ALPHA	BETA

The list of recording electrodes associated with the classification results displayed in Figure 6.19 was tabulated in Table 6.21. This table demonstrates that 3 out of 4 (75.00%) of the classification results from CAR+k-NN and LAP+FKNN were obtained from ipsilateral electrodes. Besides that, all (100.00%) of the classification results from CAR+FKNN were obtained from contralateral electrodes. Furthermore, 3 out of 4 (75.00%) results from CAR+QDA and LAP+QDA were obtained from contralateral electrodes. Meanwhile, 2 out of 4 (50.00%) of the classification results from LAP+k-NN were obtained either from ipsilateral or contralateral electrodes. The same process of analysis has been carried out for examining the recording electrodes associated with classification results used to predict intention of movement towards direction 6, 9 and 12 (please refer to Appendix G for further detail).

Correspondingly, majority of the highest classification results for predicting intention of movement towards direction 6 were obtained by both contralateral and ipsilateral electrodes. This is shown by, 2 out of 4 (50.00%) of the classification results from LAP+k-NN and CAR+k-NN were obtained either from ipsilateral or contralateral electrodes. Besides that, 3 out of 4 (75.00%) of the classification results from CAR+FKNN and CAR+QDA were obtained from contralateral electrodes. In contrast, 3 out of 4 (75.00%) of the classification results from LAP+FKNN and LAP+QDA combinations were obtained from ipsilateral electrodes.

On the other hand, majority of the classification results for predicting intention of movement towards direction 9 were obtained from contralateral electrodes. This was supported by all (100.00%) of the classification results from CAR+k-NN and CAR+QDA were obtained from contralateral electrodes. Similarly, all (100.00%) of the highest classification results from LAP+k-NN and LAP+FKNN were obtained from contralateral electrodes. Besides that, 3 out of 4 (75.00%) of the classification results from CAR+FKNN were obtained from contralateral electrodes. Apart from that, 2 out of 4 (50.00%) of the classification results from LAP+QDA were obtained either from ipsilateral or contralateral electrodes.

In addition, majority of the classification results for predicting intention of movement towards direction 12 were also recorded from both ipsilateral and contralateral electrodes. For instance, all (100.00%) of the classification results from the combinations of CAR+k-NN and CAR+FKNN were obtained from contralateral electrodes. Besides that, 3 out of 4 (75.00%) of the classification results from LAP+k-NN were obtained from contralateral electrodes. On the other hand, 2 out of 4 (50.00%) of the classification results from CAR+QDA, LAP+FKNN and LAP+QDA were obtained either from ipsilateral electrodes or contralateral electrodes.

Table 6.21: Recording electrode associated with the classification results from paraplegic subjects for predicting intention of movement towards direction 3.

Subject	Recording electrode associated with the maximum classification accuracy					
	CAR			LAP		
	KNN	FKNN	QDA	KNN	FKNN	QDA
SP1	CP1	CP1	C5	CP2	CP2	C5
SP2	C2	CP3	FC2	CCP5	CP5	CCP1
SP3	FC4	CFC3	CFC3	CPZ	CPZ	CCP2
SP4	FC4	CCP1	CCP1	CCP1	FC4	CCP1

6.7.3 Predicting Imagination/Intention and Direction of Movement

This section presented the directional information of the imagination/intention of movement. Results of predicting direction of imagination/intention of movement for paraplegic and tetraplegic subjects were presented in the following subsections.

6.7.3.1 Predicting Imagination and Direction of Movement from Tetraplegic Subjects

Figure 6.20 depicts the classification results for tetraplegic subjects in predicting imagination and direction of the movement. This figure indicates that the classification results from CAR+k-NN, CAR+FKNN and CAR+QDA dwell within the ranges of 34.17%-78.36%, 37.55%-75.31% and 27.94%-70.92%, respectively. On the other hand, the classification results from LAP+k-NN, LAP+FKNN and LAP+QDA lie within the ranges of 28.14%-79.57%, 25.22%-79.14% and 22.69%-

80.56%, respectively. In comparison to all tetraplegic subjects, only data from ST7 achieved classification accuracy of more than 70.00% for all combinations of spatial filters with multiple classifiers.

Figure 6.20: Classification results from tetraplegic subjects in predicting imagination and direction of the movement. The classification results for each subject were presented based on classifier and spatial filter.

The frequency bands associated with the classification results portrayed in Figure 6.20 were listed in Table 6.22. This table indicates that the classification results were obtained from delta, theta, alpha, beta and gamma bands. Although multiple frequency bands contributed to the classification results, 5 out of 12 (41.67%) of the classification results from CAR+k-NN and CAR+FKNN were obtained from the gamma band. Apart from that, 4 out of 12 (33.33%) of the classificationcresults from CAR+QDA were obtained from the beta band. On the other hand, 3 out of 12 (25.00%) of the classification results from LAP+k-NN and LAP+FKNN were obtained from delta, beta and gamma bands. Furthermore, 3 out of 12 (25.00%) of the classification results from LAP+QDA were obtained from theta, beta and gamma bands.

Table 6.22: Frequency band associate with the maximum the classification results from tetraplegic subjects for predicting imagination and direction of the movement.

Subject	Frequency band associated with the maximum classification accuracy					
	CAR			LAP		
	KNN	FKNN	QDA	KNN	FKNN	QDA
ST1	GAMMA	GAMMA	THETA	GAMMA	GAMMA	BETA
ST2	GAMMA	GAMMA	GAMMA	DELTA	GAMMA	ALPHA
ST3	ALPHA	DELTA	DELTA	THETA	DELTA	ALPHA
ST4	DELTA	THETA	THETA	GAMMA	ALPHA	THETA
ST5	GAMMA	GAMMA	BETA	GAMMA	GAMMA	ALPHA
ST6	BETA	GAMMA	BETA	BETA	DELTA	DELTA
ST7	GAMMA	DELTA	BETA	BETA	ALPHA	BETA
ST8	DELTA	THETA	GAMMA	DELTA	DELTA	GAMMA
ST9	THETA	BETA	ALPHA	ALPHA	BETA	BETA
ST10	GAMMA	GAMMA	BETA	DELTA	BETA	THETA
ST11	THETA	THETA	DELTA	BETA	BETA	THETA
ST12	BETA	THETA	DELTA	THETA	THETA	DELTA

The list of recording electrodes associated with the classification results illustrated in Figure 6.20 was tabulated in Table 6.23. This table shows that majority of the results were recorded from contralateral electrodes. This was evident shown by 10 out of 12 (83.33.00%) of the classification results from CAR+*k*-NN, CAR+FKNN and CAR+QDA were recorded from contralateral electrodes. Following this, 7 out of 12 (58.33%) of the classification results from LAP+*k*-NN and CAR+FKNN were obtained from contralateral electrodes. Meanwhile, 9 out of 12 (75.00%) of the classification results from LAP+QDA were recorded from contralateral electrodes.

Table 6.23: Recording electrode associate with the maximum classification results from tetraplegic subjects for predicting imagination and direction of the movement.

Subject	Frequency band associated with the maximum classification accuracy					
	CAR			LAP		
	KNN	FKNN	QDA	KNN	FKNN	QDA
ST1	FC3	FC3	FC3	FC2	CZ	CZ
ST2	FC1	FC1	CFC1	FC4	FC1	CFC1
ST3	CCP5	C5	CCP5	CCP5	CCP5	CCP5
ST4	FC4	FC4	FC4	FC4	FC4	CCP5
ST5	C5	C5	C1	FC4	FC4	FC4
ST6	FC3	FC3	FC3	C5	FC5	C5
ST7	FC1	FC3	FC1	CCP5	CCP5	CCP5
ST8	FC3	FC3	FC4	FC4	FC4	FC4

ST9	C5	C5	C5	C5	C5	C5
ST10	CP4	CP4	FC1	CCP5	CCP5	CCP5
ST11	C5	CFC5	CFC5	CCP5	CCP5	CCP5
ST12	FC5	FC1	FC1	C3	CCP4	C5

6.7.3.2 *Predicting Imagination and Direction of Movement from Paraplegic Subjects*

Summary of the classification results obtained from combinations of CAR and LAP spatial filters with *k*-NN, FKNN and QDA classifiers for predicting imagination and direction of movement from paraplegic subjects was depicted in Figure 6.21. This figure indicates that classification results from CAR+*k*-NN within the range of 50.90%-80.83%. The combination of CAR+FKNN produced classification results between 47.63%-80.00%, whereas results of 40.77%-75.83% were obtained from CAR+QDA. On the other hand, the classification results of LAP+*k*-NN, LAP+FKNN and LAP+QDA lie within the ranges of 49.40%-79.17%, 42.97%-80.83% and 30.76%-77.50%, respectively. In comparison to other paraplegic subjects, only SP4 data has classification results of more than 70.00% for all combinations of spatial filters and classifiers.

Figure 6.21: Classification results for paraplegic subjects in predicting imagination and direction of the movement. The classification results from each subject are presented based on the combinations of classifiers and spatial filters applied.

Table 6.24 details the frequency bands associated with the classification results depicted in Figure 6.21. This table shows that classification results were obtained from multiple frequency bands including delta, theta, alpha, beta, and gamma bands. Among these frequency bands, 2 out of 4 (50.00%) of the classification results from CAR+FKNN were obtained from the alpha band. Besides that, 2 out of 4 (50.00%) of the classification results from CAR+QDA were obtained from the theta band. On the other hand, 2 out of 4 (50.00%) of the classification results from LAP+k-NN were obtained from the alpha band. In addition, 2 out of 4 (50.00%) of the classification results from LAP+FKNN were obtained from the delta band.

Table 6.24: Frequency band associate with the maximum classification results from paraplegic subjects for predicting imagination and direction of the movement.

| Subject | Frequency band associated with the maximum classification accuracy | | | | | |
| | CAR | | | LAP | | |
	KNN	FKNN	QDA	KNN	FKNN	QDA
SP1	ALPHA	THETA	THETA	BETA	DELTA	GAMMA
SP2	DELTA	DELTA	ALPHA	THETA	ALPHA	THETA
SP3	BETA	ALPHA	THETA	ALPHA	DELTA	DELTA
SP4	GAMMA	ALPHA	BETA	ALPHA	GAMMA	BETA

Recording electrodes associated with the classification results depicted in Figure 6.21 were tabulated in Table 6.25. This table shows that majority of the classification results were recorded from contralateral electrodes. This is supported by the finding that all (100.00%) of the classification results from CAR+k-NN and CAR+FKNN were recorded from contralateral electrodes. Similarly, all (100.00%) of the results from LAP+k-NN were also recorded from contralateral electrodes. Apart from that, 3 out of 4 (75.00%) of the classification results from CAR+QDA and 3 out of 4 (75.00%) accuracy results from LAP+k-NN were also recorded from contralateral electrodes.

Table 6.25: Recording electrode associate with the maximum classification results from paraplegic subjects for predicting imagination and direction of the movement.

Subject	Recording electrode associated with the maximum classification accuracy					
	CAR			LAP		
	KNN	FKNN	QDA	KNN	FKNN	QDA
SP1	C5	C5	CP4	C5	C5	CCP4
SP2	CCP5	CCP5	CCP5	CCP5	CCP5	CCP5
SP3	CFC3	CFC3	CFC3	CFC3	CFC3	CFC3
SP4	CCP1	CCP1	CCP1	C1	CPZ	CZ

6.7.3.3 Predicting Intention and Direction of Movement from Tetraplegic Subjects

Classification results for predicting intention and direction of movement from tetraplegic subjects were displayed in Figure 6.22. In this figure, classification results from CAR+*k*-NN, CAR+FKNN and CAR+QDA lie within the ranges of 38.48%-55.00%, 37.88%-55.17% and 31.46%-46.00%, respectively. On the other hand, the classification results from combinations of LAP+*k*-NN, LAP+FKNN and LAP+QDA lie within the ranges of 35.64%-51.00%, 37.12%-65.00% and 26.09%-43.50%, respectively.
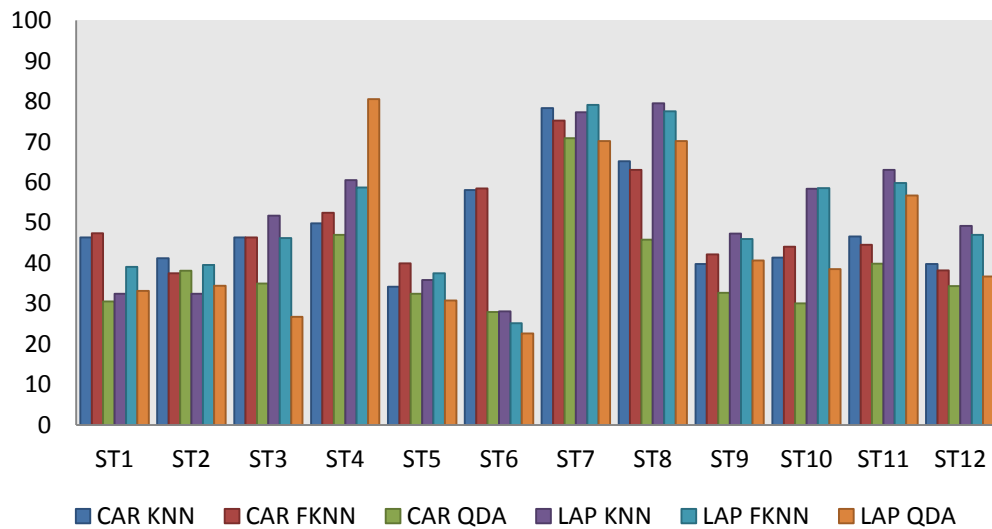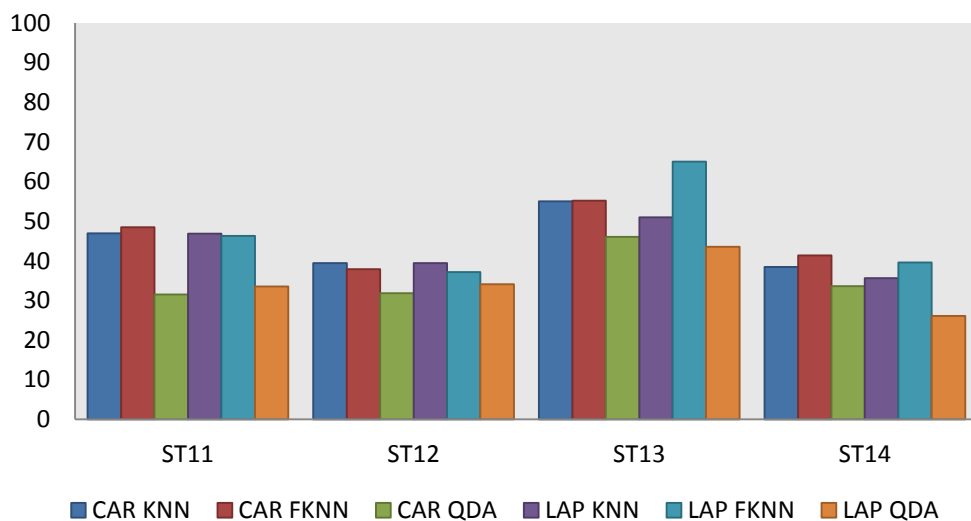

Figure 6.22: Classification results for tetraplegic subjects in predicting intention and direction of the movement. The classification results from each subject are presented based on the combinations of classifiers and spatial filters applied.

186

The frequency bands associated with classification results depicted in Figure 6.22 are listed in Table 6.26. Data from this table demonstrate that, most of the classification results were obtained from delta, theta, alpha, beta and gamma bands. Although multiple frequency bands contributed to the classification results, 3 out of 4 (75.00%) of the classification results from LAP+k-NN and LAP+FKNN were obtained from the gamma band. Besides that, 2 out of 4 (50.00%) of the classification results from CAR+k-NN and LAP+QDA were obtained from the beta band. On the other hand, 2 out of 4 (50.00%) classification results from CAR+QDA were obtained from the alpha band.

Table 6.26: Frequency band associate with the classification results from tetraplegic subjects for predicting intention and direction of the movement.

Subject	Frequency band associated with the maximum classification accuracy					
	CAR			LAP		
	KNN	FKNN	QDA	KNN	FKNN	QDA
ST11	BETA	BETA	DELTA	DELTA	THETA	BETA
ST12	GAMMA	ALPHA	BETA	GAMMA	GAMMA	DELTA
ST13	BETA	DELTA	ALPHA	GAMMA	GAMMA	GAMMA
ST14	ALPHA	GAMMA	ALPHA	GAMMA	GAMMA	BETA

List of recording electrodes associated with the classification results presented in Figure 6.22 was tabulated in Table 6.27. Data from this table indicate that, majority of the classification results were obtained from both contralateral and ipsilateral electrodes. This was supported by the finding that 3 out of 4 (75.00%) of the classification results from LAP+k-NN and LAP+QDA were obtained from contralateral electrodes. Similarly, 3 out of 4 (75.00%) of the classification results from CAR+QDA were also obtained from contralateral electrodes. On the other hand, 2 out of 4 (50.00%) of the classification results from LAP+FKNN, and 2 out of 4 (50.00%) of the classification results from CAR+k-NN and CAR+FKNN were obtained either from contralateral or ipsilateral electrodes.

Table 6.27: Recording electrode associate with the classification results from tetraplegic subjects for predicting intention and direction of the movement.

| Subject | Recording electrode associated with the maximum classification accuracy | | | | | |
| | CAR | | | LAP | | |
	KNN	FKNN	QDA	KNN	FKNN	QDA
ST11	CCP5	CP5	CCP5	CCP5	FC4	FC5
ST12	C5	CCP5	CCP5	C5	C5	CP3
ST13	FC4	FC4	C2	CCP1	CCP1	CP4
ST14	FC4	C4	FC3	C1	CP4	FC5

6.7.3.4 Predicting Intention and Direction of Movement from Paraplegic Subjects

The classification results for predicting intention and direction of movement from paraplegic subjects were illustrated in Figure 6.23. This figure indicates that, classification accuracies from CAR+k-NN, CAR+FKNN and CAR+QDA dwell within the ranges of 41.75%-52.47%, 41.49%-51.16% and 29.94%-42.67%, respectively. Apart from that, the classification results from LAP+k-NN, LAP+FKNN and LAP+QDA lie within the ranges of 51.59%-59.23%, 49.77%-59.72% and 31.72%-42.36%, respectively.
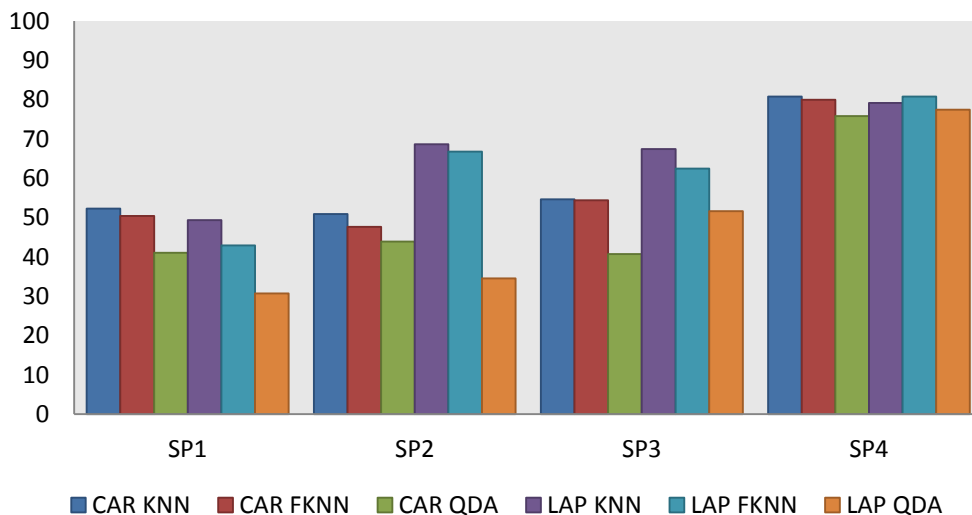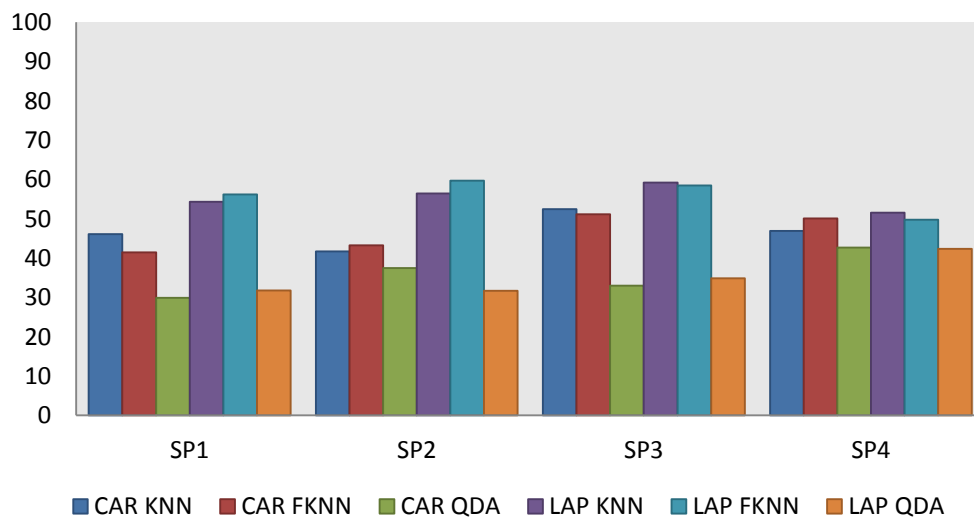

Figure 6.23: Classification results for paraplegic subjects in predicting intention and direction of the movement. The classification results from each subject are presented based on the combinations of classifiers and spatial filters applied.

The lists of frequency bands associated with the classification results depicted in Figure 6.23 was provided in Table 6.28. Data in this table indicates that, the classification results were obtained from multiple of EEG signal components namely delta, alpha, beta, and gamma bands. Although the classification results were obtained from different frequency bands for each subject, 2 out of 4 (50.00%) of the classification results from CAR+FKNN were obtained from the beta band and 3 out of 4 (75.00%) of the classification results from CAR+QDA were obtained from the delta band. On the other hand, 2 out of 4 (50.00%) of the classification results from the combinations of LAP+k-NN and LAP+FKNN were obtained from the delta band.

Table 6.28: Frequency band associate with the classification results from paraplegic subjects for predicting intention and direction of the movement..

Subject	Frequency band associated with the maximum classification accuracy					
	CAR			LAP		
	KNN	FKNN	QDA	KNN	FKNN	QDA
SP1	DELTA	BETA	DELTA	DELTA	DELTA	BETA
SP2	BETA	BETA	DELTA	ALPHA	ALPHA	DELTA
SP3	ALPHA	DELTA	ALPHA	DELTA	DELTA	DELTA
SP4	GAMMA	GAMMA	DELTA	GAMMA	GAMMA	DELTA

The list of recording electrodes associated with classification results portrayed in Figure 6.23 was tabulated in Table 6.29. This table indicates that all (100%) of the classification results from CAR+ FKNN were obtained from contralateral electrodes. Besides that, 3 out of 4 (75.00%) of the classification results from CAR+k-NN and CAR+QDA were also obtained from contralateral electrodes. Following this, all (100%) of the classification results from LAP+FKNN and LAP+k-NN were obtained from contralateral electrodes. On the other hand, 3 out of 4 (75.00%) of the classification results from LAP+QDA were obtained from ipsilateral electrodes.

Table 6.29: Recording electrode associate with the classification results from paraplegic subjects for predicting intention and direction of the movement..

Subject	Recording electrode associated with the maximum classification accuracy					
	CAR			LAP		
	KNN	FKNN	QDA	KNN	FKNN	QDA
SP1	C5	C5	C5	C5	C5	CP2
SP2	CP5	CP5	CP5	CCP5	CCP5	CCP5
SP3	C4	FC5	CFC2	CCP5	CFC5	CPZ
SP4	FC3	FC3	FC3	CFC3	CFC3	CPZ

6.8   Receiver Operating Characteristic Graph (ROC)

In this section the evaluation of the classification performance from SCI subjects were presented. The classification evaluations were presented separately according group of the subjects namely tetraplegic and paraplegic subjects. The details of the classification performance evaluation reported in the following subsections.

6.8.1 ROC for Predicting Imagination/Intention of Movement

The classification evaluation of predicting imagination of movement from tetraplegic and paraplegic subjects were presented in subsection of 6.8.1.1 and subsection of 6.8.1.2 respectively. On the other hand, the classification evaluation of predicting intention of movement from tetraplegic and paraplegic subjects were presented in subsection of 6.8.1.3 and subsection of 6.8.1.4 respectively.

ROC plots for combinations of CAR and LAP spatial filter with multiple classifiers for predicting imagination of movement from tetraplegic subjects were illustrated in Figure 6.24. Based on this figure, all of the points within the ROC space for both spatial filters belong to the upper triangle. Although all the points belong to the upper triangle, majority of the points within ROC space from the LAP spatial filter have higher TPR and lower FPR compared to points within ROC space from the CAR spatial filter. As for performance evaluation, LAP+k-NN had the best performance compared with the others based on average of highest TPR and low FPR.
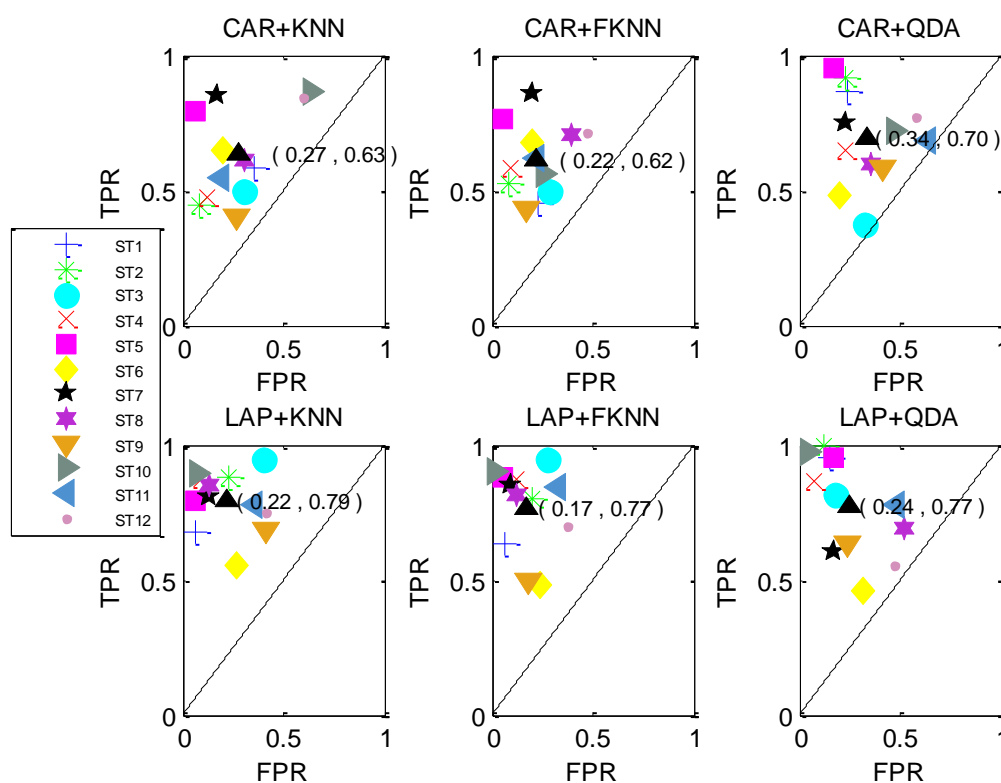
Figure 6.24: ROCs for predicting imagination of movement from tetraplegic subjects. The ROCs were presented based on different combination of spatial filter and classifier. Subjects were represented by different symbols and the average of the classification accuracy was represented by a black triangle.

191

ROC for combinations of CAR and LAP spatial filters with *k*-NN, FKNN and QDA classifiers in predicting imagination of movement from paraplegic subjects were depicted in Figure 6.25. This figure demonstrates that, majority of the points in the ROC space for both spatial filters belong to the upper triangle, except for CAR+QDA. In this combination subject SP2 belonged to the lower triangle (any point belonging to the lower triangle has high FPR compared to TPR). Besides that, the majority points within ROC space for the LAP spatial filter have higher TPR and lower FPR compared to points within ROC space for the CAR spatial filter. Among all combinations of spatial filters and classifiers, LAP+*k*-NN has the average of highest TPR and low FPR.
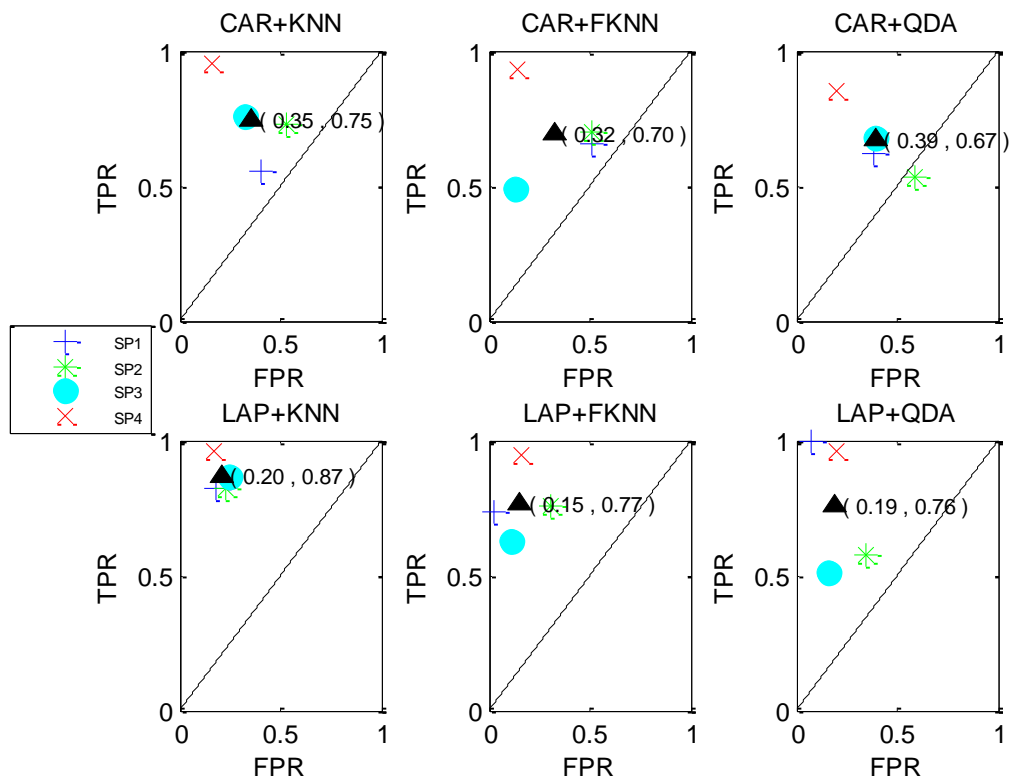
Figure 6.25: ROCs for predicting imagination of movement from paraplegic subjects. The ROCs were presented based on different combination of spatial filter and classifier. Subjects were represented by different symbols and the average of the classification accuracy was represented by a black triangle.

Evaluation of classification results for predicting intention of movement from tetraplegic subjects is presented in Figure 6.26. This figure shows that, all of the points within the ROC space for both spatial filters belong to the upper triangle. As for the performance evaluation, the combination of CAR+FKNN has average with moderate FPR and highest TPR, outperforming the other combinations.
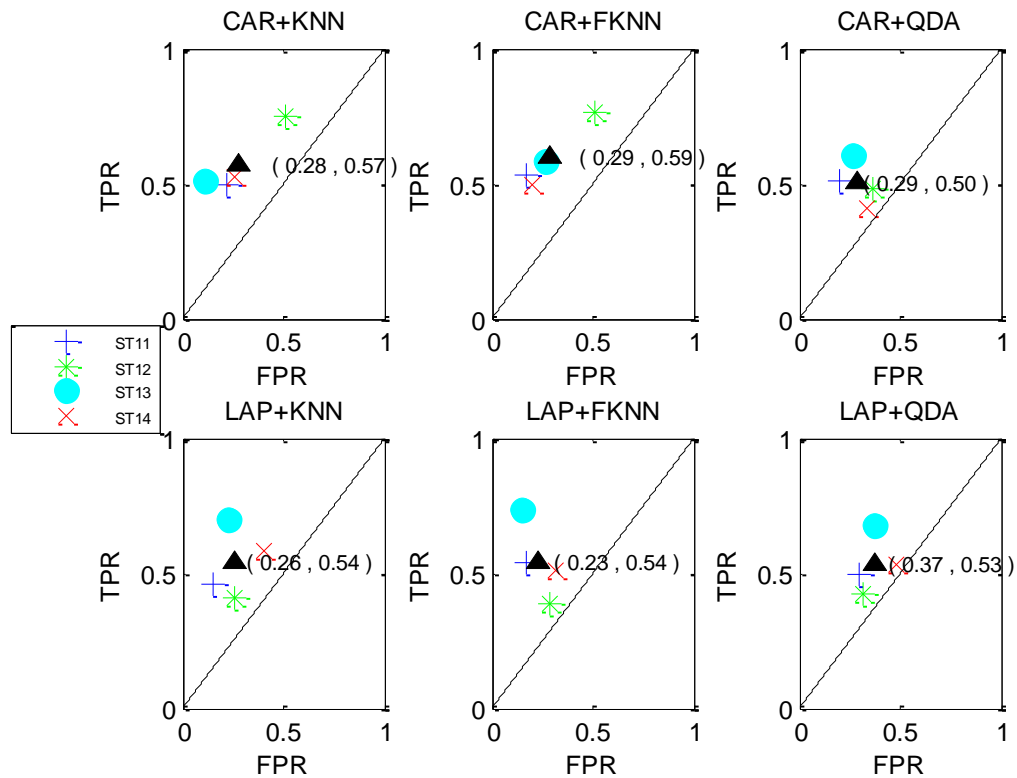
Figure 6.26: ROCs for predicting intention of movement from tetraplegic subjects. The ROCs were presented based on different combination of spatial filter and classifier. Subjects were represented by different symbols and the average of the classification accuracy was represented by a black triangle.

6.8.1.4   ROC for Predicting Intention of Movement from Paraplegic Subjects

Figure 6.27 depicts the ROC for predicting intention of movement from paraplegic subjects. This figure demonstrates that, all of the points within the ROC space for both spatial filters belong to the upper triangle (any point belonging to the lower triangle has high FPR compared to TPR). Majority of the points within the ROC space for the LAP spatial filter have higher TPR and lower FPR compared to the CAR spatial filter. As for the classifier performance, the combination of LAP+FKNN outperformed other combinations. This was because the combination of LAP+FKNN has the highest TPR and lowest FPR on average.
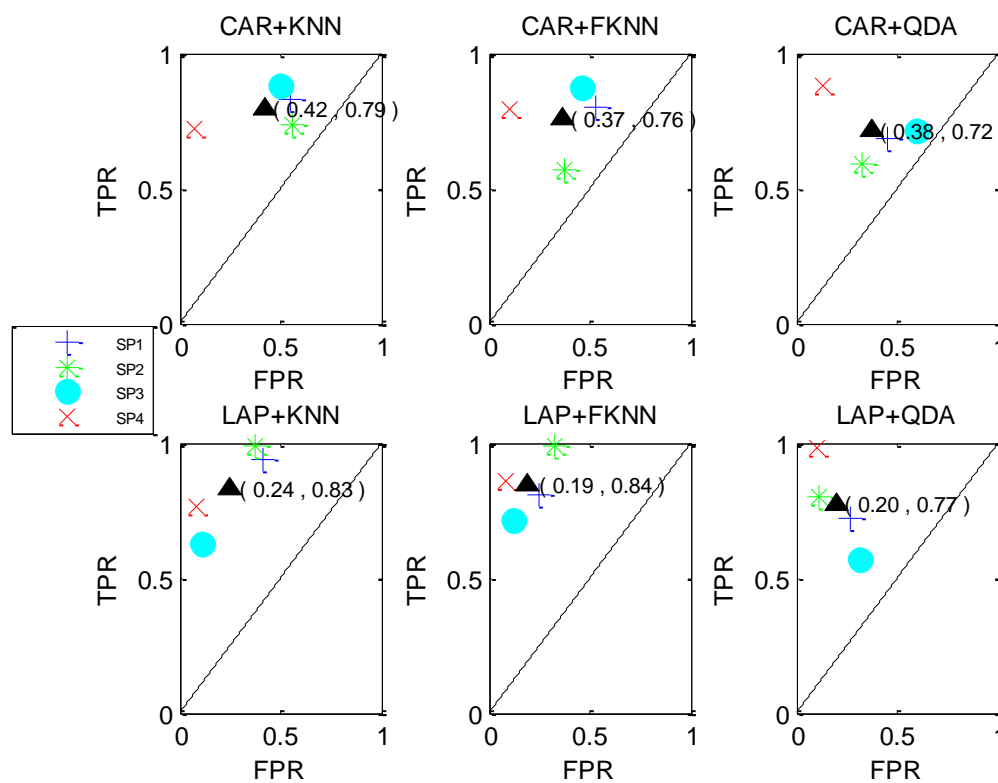
Figure 6.27: ROCs for predicting intention of movement from paraplegic subjects. The ROCs were presented based on different combination of spatial filter and classifier. Subjects were represented by different symbols and the average of the classification accuracy was represented by a black triangle.

6.8.2 ROC for Predicting Imagination/Intention of Movement towards Direction 3, 6, 9 and 12

In this section, the performance of classification based on different combinations of spatial filters and classifiers for predicting imagination/intention of movement towards direction 3, 6, 9 and 12 from paraplegic and tetraplegic subjects were presented. The performance of these classification methods were presented individually according to the direction of movement.

6.8.2.1 ROC for predicting Imagination of Movement towards Direction 3, 6, 9 and 12 from Tetraplegic Subjects

Classification evaluation for predicting imagination of movement towards direction 3 by tetraplegic subjects were implemented through ROC which presented by Figure 6.28. From this figure, it depicted that all of the point within ROC space for both of the spatial filter belongs to the upper triangle where majority of points within ROC space of LAP spatial filter have higher TPR and lower FPR compared to the points within ROC space of CAR spatial filter. Among all of the classification combination, combination of LAP+QDA has an average with highest TPR and lowest FPR which outperform other combinations. Same analysis procedures have been implemented for producing the ROC graphs for predicting imagination of movement towards direction 6, 9 and 12 (please refer Appendix H for further detail).

Apart from that, the ROC that evaluate classification results of predicting imagination of movement towards direction 6 indicate that all of the point within ROC space for both of the spatial filter belongs to the upper triangle where majority of the points within ROC space of LAP spatial filter have higher TPR and lower FPR compared to the points within ROC space of CAR spatial filter. As for the evaluation of the classification performance, combination LAP+QDA has an average of highest TPR and lowest FPR which outperformed others combination of classification.

Likewise, the ROC for predicting imagination of movement towards direction 9 shows that, all of the point within ROC space for both of the spatial filter belongs to the upper triangle where majority of the points within ROC space of LAP spatial

filter have higher TPR and lower FPR compared to the points within ROC space of CAR spatial filter. Besides that, combination of LAP+QDA which has average with highest TPR and low FPR outperform other classification combination.

Similarly, the ROC for predicting imagination of movement towards direction 12 portrayed that, all of the point within ROC space for both of the spatial filter belongs to the upper triangle where majority of the points within ROC space of LAP spatial filter have higher TPR and lower FPR compared to the points within ROC space of CAR spatial filter. As for the performance evaluation, combination of LAP+QDA outperformed others combination based on the average of highest TPR and low FPR.

Figure 6.28: ROCs for predicting imagination of movement towards direction 3 from tetraplegic subjects. The ROCs were presented based on combinations of spatial filters and classifiers. Subjects were represented by different symbols and the average of the classification accuracy was represented by a black triangle.

Performance evaluation of the classification results for predicting imagination of movement towards direction 3 by paraplegic subjects were depicted in Figure 6.29. The ROC demonstrates that all of the points within the ROC space for both of the spatial filter belong to the upper triangle. Majority of the points within ROC space of CAR spatial filter have lower FPR compared to the points within ROC space of LAP spatial filter. In term of performance evaluation, combination of LAP+QDA has average with highest TPR and low FPR which outperformed others combination. Same analysis procedures have been implemented for producing the ROC graphs for predicting imagination of movement towards direction 6, 9 and 12 (please refer Appendix H for further detail).

Addition to that, the ROC for predicting imagination of movement towards direction 6 shows that, all of the point within ROC space for both of the spatial filter belongs to the upper triangle where majority of the points within ROC space of LAP spatial filter have higher TPR and lower FPR compared to the points within ROC space of CAR spatial filter. Besides that, combination of LAP+FKNN which has average with high TPR and lower FPR outperform other classification combination.

Similarly, the ROC for predicting imagination of movement towards direction 9 depicted that, all of the point within ROC space for both of the spatial filter belongs to the upper triangle where majority of the points within ROC space of LAP spatial filter have higher TPR and lower FPR compared to the points within ROC space of CAR spatial filter. As for the evaluation of classification performance, combination of LAP+QDA has the average with high TPR and lower FPR which outperformed other combination.

Likewise, the ROC for predicting imagination of movement towards direction 12 portrayed that, all of the point within ROC space for both of the spatial filter belongs to the upper triangle where majority of points within ROC space of LAP spatial filter have higher TPR and lower FPR compared to the points within ROC space of CAR spatial filter. Combination of LAP+QDA has the average of high TPR and lower FPR which outperformed the classification combination.
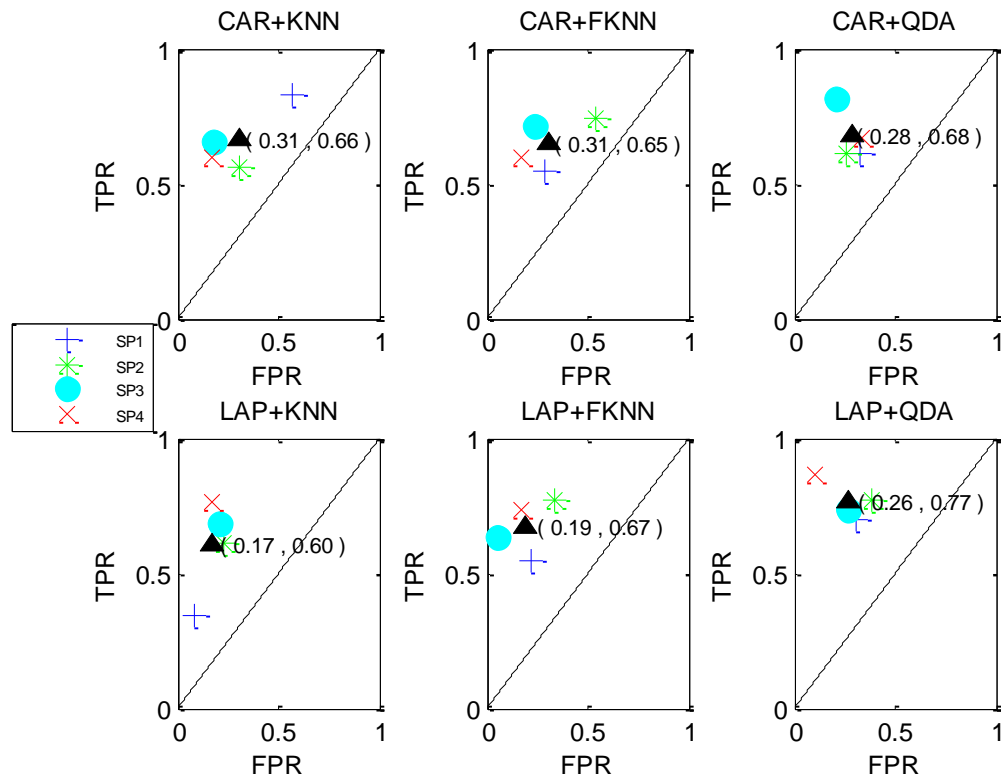
Figure 6.29: ROCs for predicting imagination of movement towards direction 3 from paraplegic subjects. The ROCs were presented based on combinations of spatial filters and classifiers. Subjects were represented by different symbols and the average of the classification accuracy was represented by a black triangle.

ROC for combinations of CAR and LAP spatial filters with k-NN, FKNN and QDA classifiers used to predict intention of movement towards direction 3 from tetraplegic subjects were presented in Figure 6.30. This figure illustrates that, all of the points within the ROC space for both spatial filters belong to the upper triangle. Majority of the points within ROC space from CAR spatial filter have higher TPR compared with points within ROC space from the LAP spatial filter. As for classification performance, the combination of CAR+QDA outperformed other combinations, having low FPR and high TPR on average. The same analysis has been implemented for producing ROC graphs for predicting intention of movement towards direction 6, 9 and 12 (please refer to Appendix H for further details).

Moreover, the ROC for predicting intention of movement towards direction 6 indicates that, majority of the points in the ROC space for both spatial filters belong to the upper triangle; except for one, which is the combination of LAP+k-NN. In this combination, subject ST14 belongs to the lower triangle (any point belong to the lower triangle has high FPR compared to TPR). Among all of the combinations, LAP+QDA has the best performance with the highest average of TPR and lowest average of FPR compared to the other combinations.

Besides that, the ROC for predicting intention of movement towards direction 9 indicates that all of the points within ROC space for both spatial filters belong to the upper triangle. In terms of classification performance, CAR+FKNN outperformed other combinations based on average of high TPR and low FPR.

Furthermore, the ROC for predicting intention of movement towards direction 12 indicates that all the points within ROC space for both spatial filters belong to the upper triangle. Additionally, majority of the points within ROC space for the CAR spatial filter have higher TPR and lower FPR compared to the points within ROC space for the LAP spatial filter. For evaluation of classification performance, combinations of CAR+QDA outperformed other combinations based having lowest FPR and highest TPR on average.
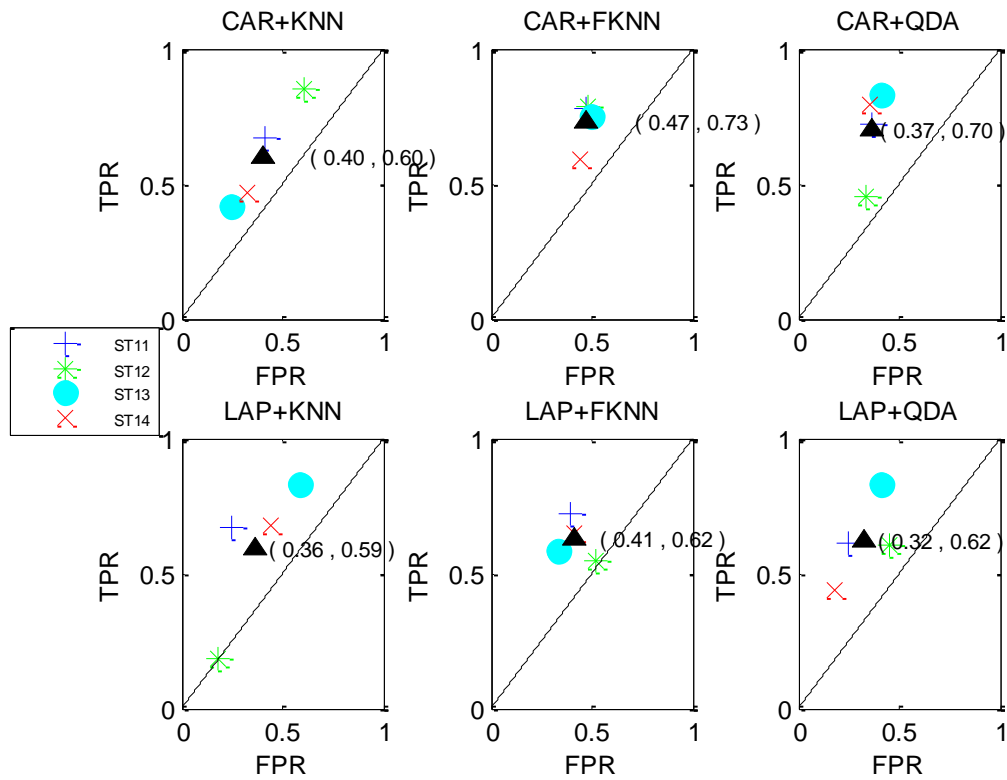
Figure 6.30: ROCs for predicting intention of movement towards direction 3 from tetraplegic subjects. The ROCs were presented based on combinations of spatial filters and classifiers. Subjects were represented by different symbols and the average of the classification accuracy was represented by a black triangle.

Figure 6.31 displays the ROC for combinations of CAR and LAP spatial filters with *k*-NN, FKNN and QDA classifiers in predicting intention of movement towards direction 3 from paraplegic subjects. This figure demonstrates that all of the points within the ROC space for both spatial filters belong to the upper triangle; whereas majority of the points within LAP ROC space have higher TPR and lower FPR compared to the points within the CAR ROC space. As for classifier evaluation, the combination of LAP+QDA outperformed other combinations based on average TPR and FPR. The same analysis has been implemented for producing ROC graphs for predicting intention of movement towards direction 6, 9 and 12 (please refer to Appendix H for further details).

Besides that, the ROC for predicting intention of movement towards direction 6 indicates that all the points within ROC space for both spatial filters belong to the upper triangle. Additionally, the majority of points within ROC space of the LAP spatial filter have higher TPR and lower FPR compared to the points within ROC space of the CAR spatial filter. Among all the combinations, LAP+QDA has the best performance with highest TPR and lowest FPR compared to other combinations.

Apart from that, the ROC for predicting intention of movement towards direction 9 shows that, all of the points within the ROC space for both of the spatial filters belong to the upper triangle. Majority of the points within ROC space of the LAP spatial filter have higher TPR and lower FPR compared to the points within ROC space of the CAR spatial filter. Combination of LAP spatial filter with FKNN classifier has the best performance because on average it produced highest TPR and lowest FPR compared to other combinations.

On the other hand, the ROC for predicting intention of movement towards direction 12 shows that, all of the points within the ROC space for both of the spatial filters belongs to the upper triangle. Majority of the points within ROC space from the LAP spatial filter have higher TPR compared to CAR spatial filter. As for the evaluation of classifiers, the combination of LAP+QDA outperforms other combinations based on having higher average TPR and lower average FPR.
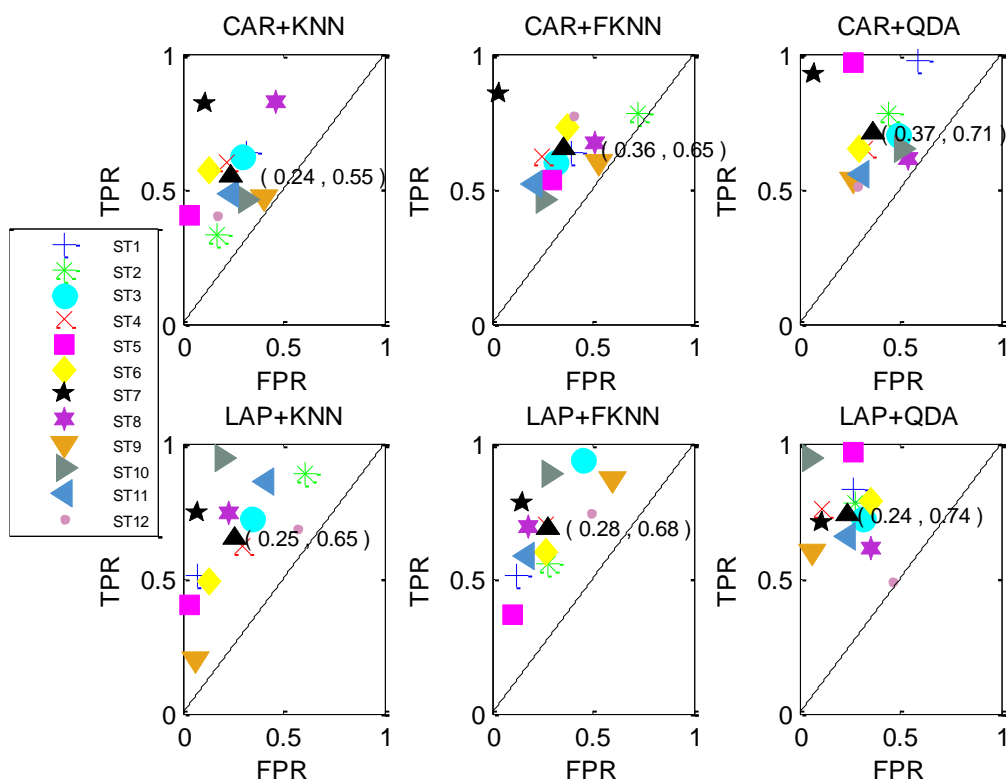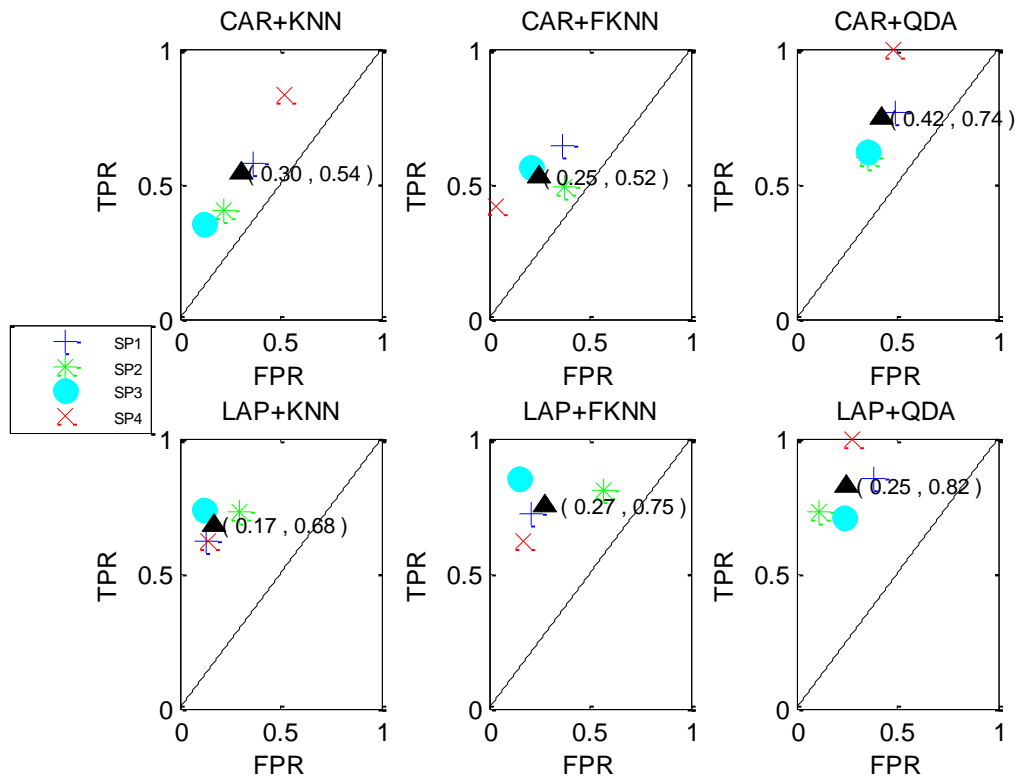
Figure 6.31: ROCs for predicting intention of movement towards direction 3 from paraplegic subjects. The ROCs were presented based on combinations of spatial filters and classifiers. Subjects were represented by different symbols and the average of the classification accuracy was represented by a black triangle.

6.8.3 ROC for Predicting Imagination/Intention and Direction of Movement

In this subsection, the classifier's performance for predicting imagination/intention and direction of the movement from tetraplegic and paraplegic subjects were presented.

6.8.3.1 ROC for Predicting Imagination and Direction of Movement from Tetraplegic Subjects

Classification performance from tetraplegic subjects for predicting imagination and direction of movement for subclass direction towards 3 was displayed by ROC in Figure 6.32. This figure demonstrates that, majority of the points within the ROC space for both spatial filters belong to the upper triangle; except for two combinations, CAR+k-NN and LAP+k-NN. Subject ST10 from CAR+k-NN and subject ST1 from LAP+k-NN belong to the lower triangle. As for classification evaluation, LAP+FKNN has the lowest FPR and highest TPR on average, which outperformed other classification combinations.

Figure 6.32: ROCs for predicting imagination and direction of movement from tetraplegic subjects (subclass for direction towards 3). The ROCs were presented based on combinations of spatial filters and classifiers. Subjects were represented by different symbols and the average of the classification accuracy was represented by a black triangle.

Additionally, Figure 6.33 displays the ROC that depicts classification performance evaluation from tetraplegic subjects for predicting imagination and direction of movement for subclass direction towards 6. This figure shows that only the combination of LAP+FKNN has all of the points within the ROC space in the upper triangle. Among all the combinations, LAP+FKNN outperformed the others, with average of highest TPR and lowest FPR.

Figure 6.33: ROCs for predicting imagination and direction of movement from tetraplegic subjects (subclass for direction towards 6). The ROCs were presented based on combinations of spatial filters and classifiers. Subjects were represented by different symbols and the average of the classification accuracy was represented by a black triangle.

Furthermore, Figure 6.34 depicts the ROC from tetraplegic subjects for predicting imagination and direction of movement for subclass direction towards 9. This figure demonstrates that only LAP+k-NN, CAR+k-NN and CAR+FKNN have all the points within the ROC space in the upper triangle. Subjects ST6 and ST10 from the combination of CAR+QDA, subjects ST2 and ST6 from LAP+FKNN, and subjects ST3, ST5 and ST6 from LAP+QDA belong to the lower triangle. As for classification performance, the combination of LAP+k-NN has the average highest TPR and lowest FPR, outperforming other classification combinations.

Figure 6.34: ROCs for predicting imagination and direction of movement from tetraplegic subjects (subclass for direction towards 9). The ROCs were presented based on combinations of spatial filters and classifiers. Subjects were represented by different symbols and the average of the classification accuracy was represented by a black triangle.

Figure 6.35 illustrates the ROC from tetraplegic subjects for predicting imagination and direction of movement for subclass direction towards 12. This figure indicates that, combinations of LAP+*k*-NN, CAR+*k*-NN and CAR+FKNN have all of the points within the ROC space in the upper triangle. Subjects ST2 and ST6 from CAR+QDA, subject ST1 from LAP+FKNN and subject ST6 from LAP+QDA belong to the lower triangle. In terms of classification performance, CAR+FKNN has the average of highest TPR and lowest FPR, showing better performance than other classification combinations.

Figure 6.35: ROCs for predicting imagination and direction of movement from tetraplegic subjects (subclass for direction towards 12). The ROCs were presented based on combinations of spatial filters and classifiers. Subjects were represented by different symbols and the average of the classification accuracy was represented by a black triangle.

The performance evaluation of predicting imagination and direction of movement for subclass direction towards 3 from paraplegic subjects was depicted in Figure 6.36. This figure demonstrates that, majority of the points within the ROC space for both spatial filters belong to the upper triangle; except for one, LAP+QDA, in which subjects SP1 and SP2 belong to the lower triangle. As for classification performance, the combination LAP+FKNN has an average with highest TPR and lowest FPR, which outperformed other classification combinations.

Figure 6.36: ROCs for predicting imagination and direction of movement from paraplegic subjects (subclass for direction towards 3). The ROCs were presented based on combinations of spatial filters and classifiers. Subjects were represented by different symbols and the average of the classification accuracy was represented by a black triangle.

Figure 6.37 illustrates the ROC from paraplegic subjects for predicting imagination and direction of movement for subclass direction towards 6. This figure demonstrates that all of the points within the ROC space for both spatial filters belong to the upper triangle. Among all classification combinations, CAR+k-NN has the best performance based on average of highest TPR and low FPR.

Figure 6.37: ROCs for predicting imagination and direction of movement from paraplegic subjects (subclass for direction towards 6). The ROCs were presented based on combinations of spatial filters and classifiers. Subjects were represented by different symbols and the average of the classification accuracy was represented by a black triangle.

Furthermore, the performance evaluation of classification results from paraplegic subjects for predicting imagination and direction of movement for subclass direction towards 9 were portrayed in Figure 6.38. This figure demonstrates that, majority of the points within the ROC space for both spatial filters belong to the upper triangle; except for one, LAP+QDA, where subject SP2 belonged to the lower triangle. This figure also shows that the combination of LAP+k-NN has lower average of FPR and highest TPR, outperforming other classification combinations.

Figure 6.38: ROCs for predicting imagination and direction of movement from paraplegic subjects (subclass for direction towards 9). The ROCs were presented based on combinations of spatial filters and classifiers. Subjects were represented by different symbols and the average of the classification accuracy was represented by a black triangle.

Figure 6.39 depicts the ROC from paraplegic subjects in predicting imagination and direction of movement for subclass direction towards 12. Based from this figure, all of the points within ROC space for both spatial filters belong to the upper triangle. As for classification performance, the combination of LAP+k-NN outperformed the others based on average of highest TPR and low FPR.

Figure 6.39: ROCs for predicting imagination and direction of movement from paraplegic subjects (subclass for direction towards 12). The ROCs were presented based on combinations of spatial filters and classifiers. Subjects were represented by different symbols and the average of the classification accuracy was represented by a black triangle.

The performance evaluation for predicting intention and direction of movement for subclass direction towards 3 from tetraplegic subjects was depicted by ROC in Figure 6.40. This figure exhibits that, majority of the points within ROC space for both spatial filters belong to the upper triangle; except for one, LAP+QDA, for which subject ST14 belongs to the lower triangle. Among all the classification combinations, LAP+FKNN has the best performance based on the average of low FPR and highest TPR.
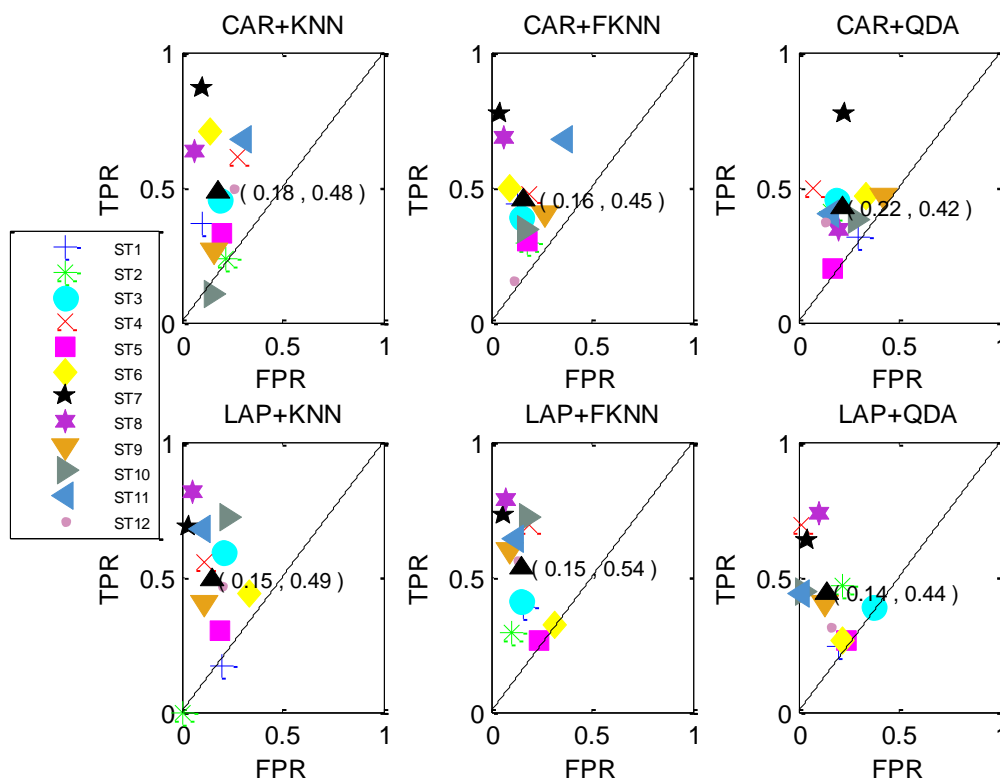

Figure 6.40: ROCs for predicting intention and direction of movement by tetraplegic subjects (subclass for direction towards 3). The ROCs were presented based on combinations of spatial filters and classifiers. Subjects were represented by different symbols and the average of the classification accuracy was represented by a black triangle.

Apart from that, Figure 6.41 illustrated the ROC of tetraplegic subjects in predicting intention and direction of movement for subclass direction towards 6. In this figure, it demonstrates that majority of the point within the ROC space for both of the spatial filters belong to the upper triangle except for two combinations, which are combination of CAR+QDA and combination of LAP+QDA. Subject ST14 from combination of CAR+QDA and subject ST13 from combination of LAP+QDA belong to the lower triangle (any point belong to the lower triangle has high FPR compared to TPR). As for the classification evaluation, combination of CAR+k-NN has an average with low FPR and highest TPR which outperformed other classification combination.
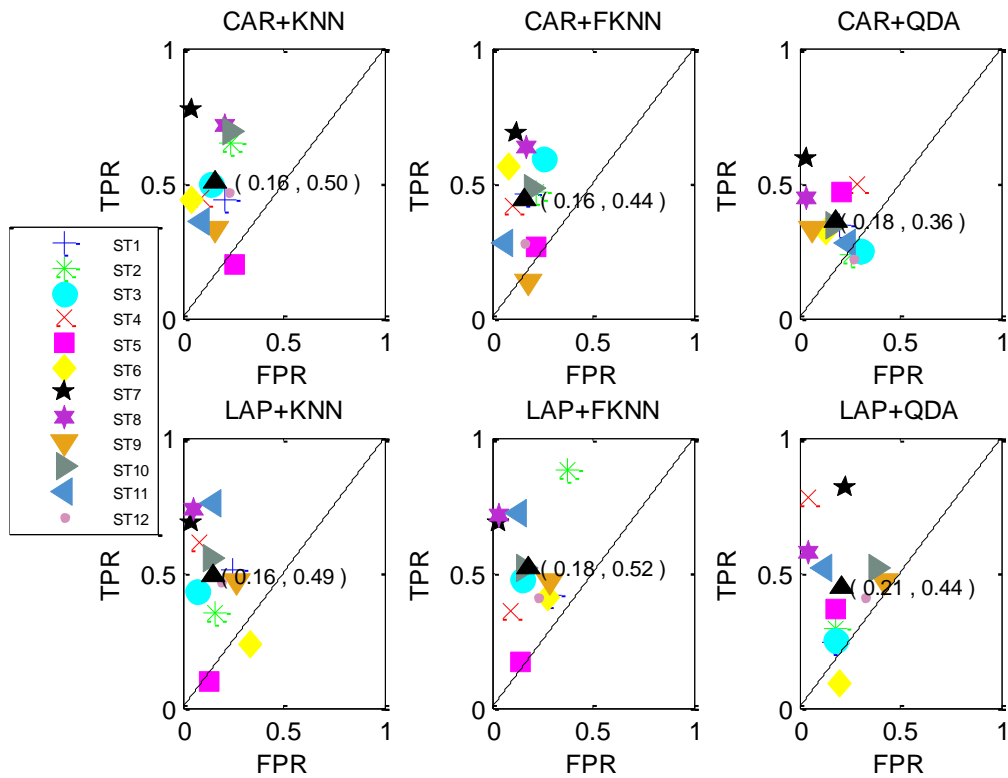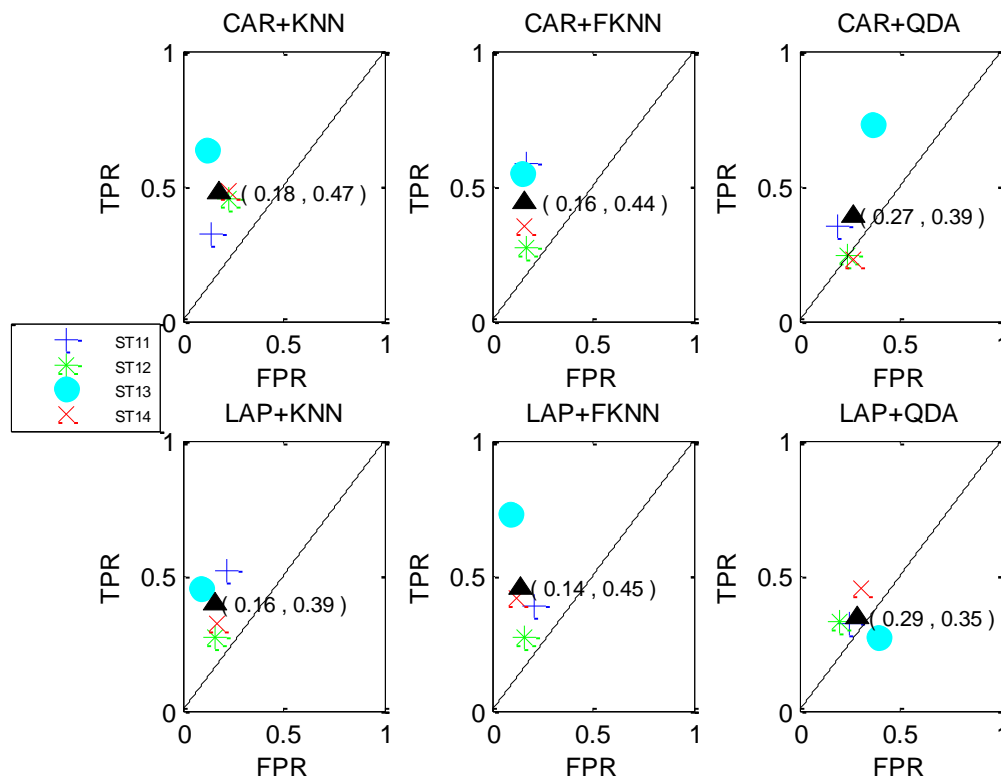

Figure 6.41: ROCs for predicting intention and direction of movement from tetraplegic subjects (subclass for direction towards 6). The ROCs were presented based on combinations of spatial filters and classifiers. Subjects were represented by different symbols and the average of the classification accuracy was represented by a black triangle.

Figure 6.42 demonstrates the ROC from tetraplegic subjects for predicting intention and direction of movement for subclass direction towards 9. This figure exhibits that, majority of the points within the ROC space for both spatial filters belong to the upper triangle except for three combinations; CAR+k-NN, CAR+QDA and LAP+QDA. Subject ST14 from CAR+k-NN, subject ST12 from CAR+QDA and subject ST14 from LAP+QDA were in the lower triangle. In terms of classification evaluation, the combination of CAR+k-NN has an average lowest FPR and highest TPR, which proved better than other combinations.
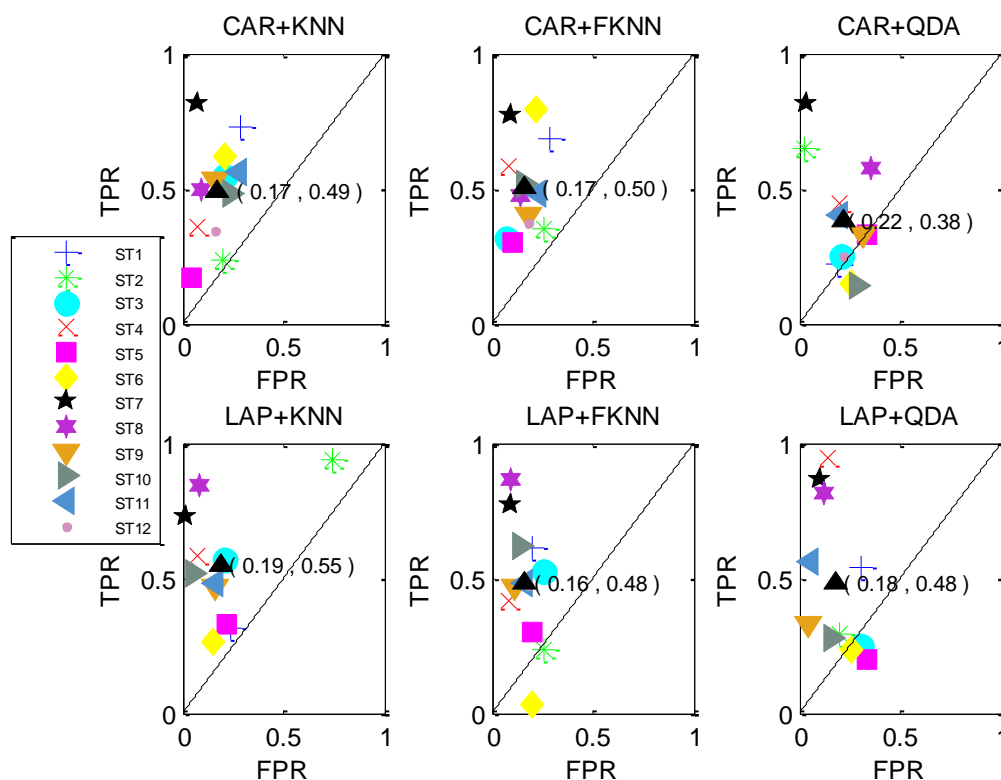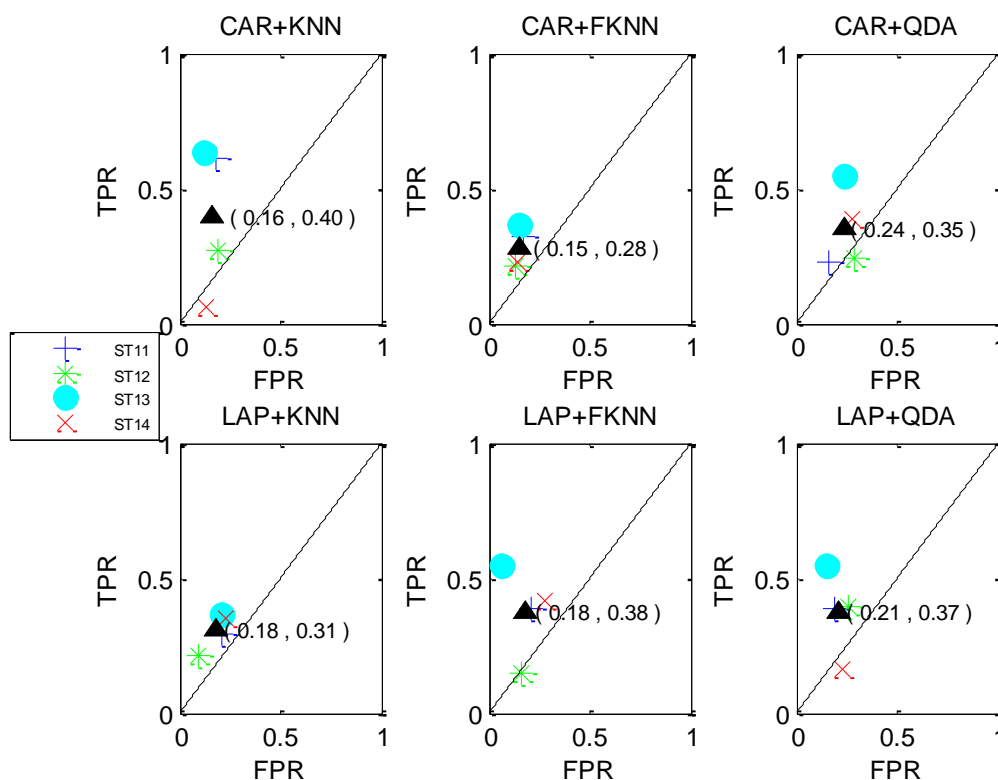

Figure 6.42: ROCs for predicting intention and direction of movement from tetraplegic subjects (subclass for direction towards 9). The ROCs were presented based on combinations of spatial filters and classifiers. Subjects were represented by different symbols and the average of the classification accuracy was represented by a black triangle.

Furthermore, Figure 6.43 presents the ROC from tetraplegic subjects for predicting intention and direction of movement for subclass direction towards 12. This figure shows that, majority of the points within ROC space for both spatial filters were in the upper triangle; except for one, CAR+QDA, in which subject ST11 belonged to the lower triangle. Among all the classification combinations, CAR+FKNN had the best performance based on the average of low FPR and highest TPR.
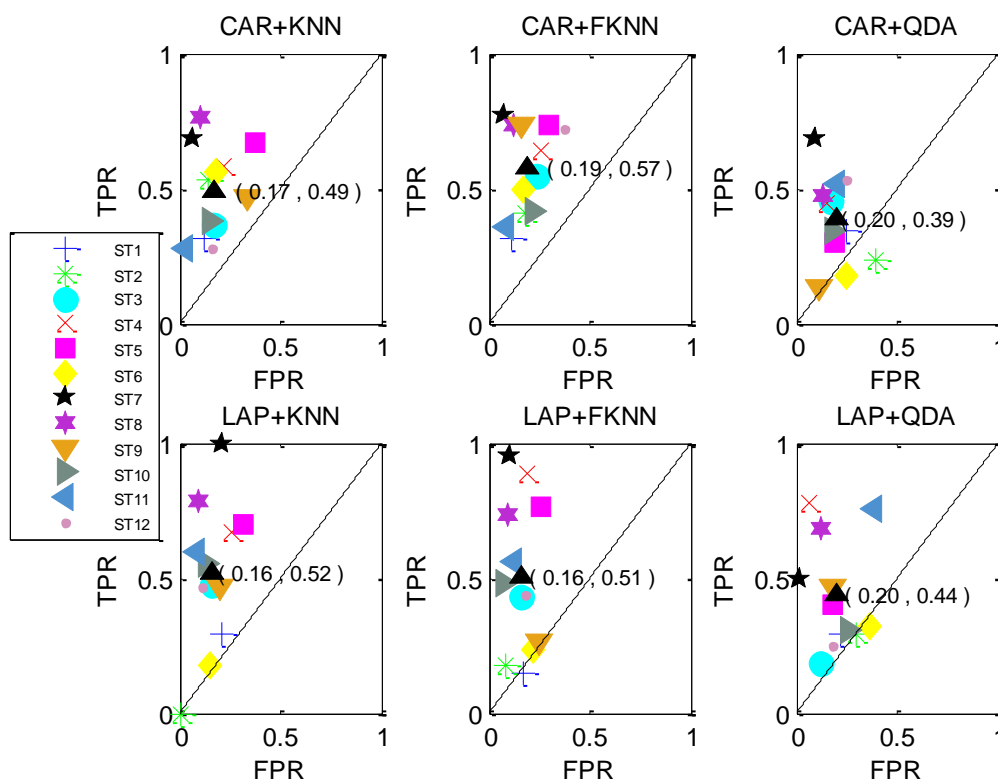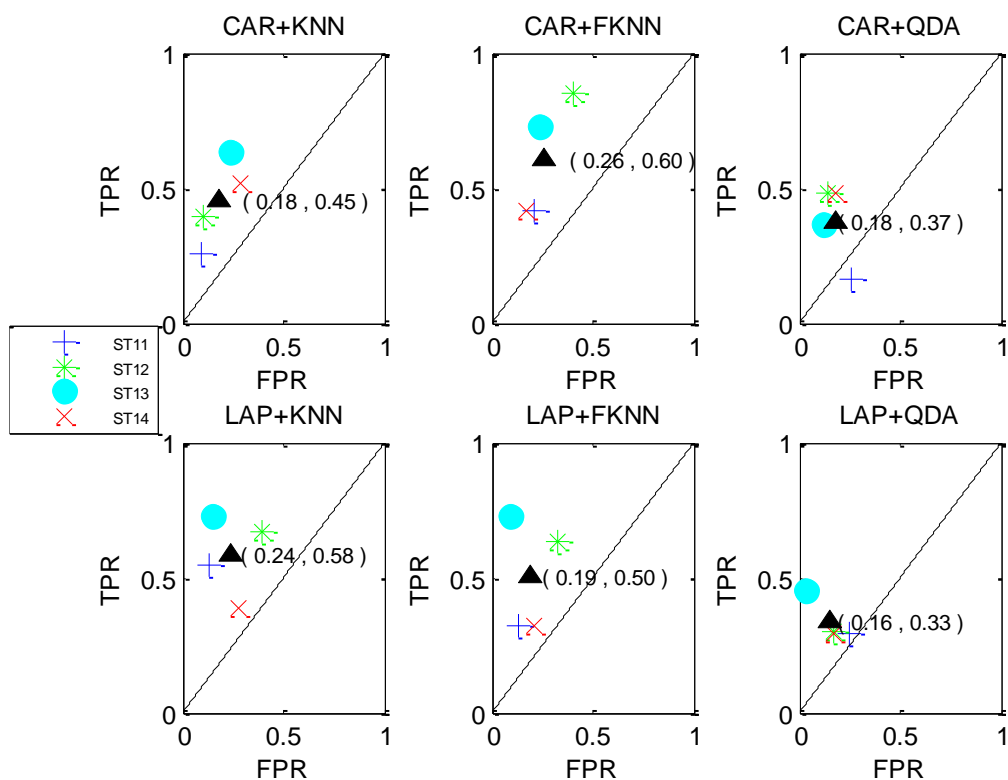

Figure 6.43: ROCs for predicting intention and direction of movement from tetraplegic subjects (subclass for direction towards 12). The ROCs were presented based on combinations of spatial filters and classifiers. Subjects were represented by different symbols and the average of the classification accuracy was represented by a black triangle.

6.8.3.4   ROC for Predicting Intention and Direction of Movement from Paraplegic Subjects

ROC that indicates the evaluation of classification performance for predicting intention and direction of movement for subclass direction towards 3 from paraplegic subjects was depicted by Figure 6.44. This figure demonstrates that, majority of the points within the ROC space for both spatial filters belong to the upper triangle; except for one, LAP+QDA, which belonged to the lower triangle. In this combination, subject SP1 belonged to the lower triangle. In terms of classification performance, the combination of LAP+k-NN has lowest FPR and highest TPR on average, outperforming the other combinations.
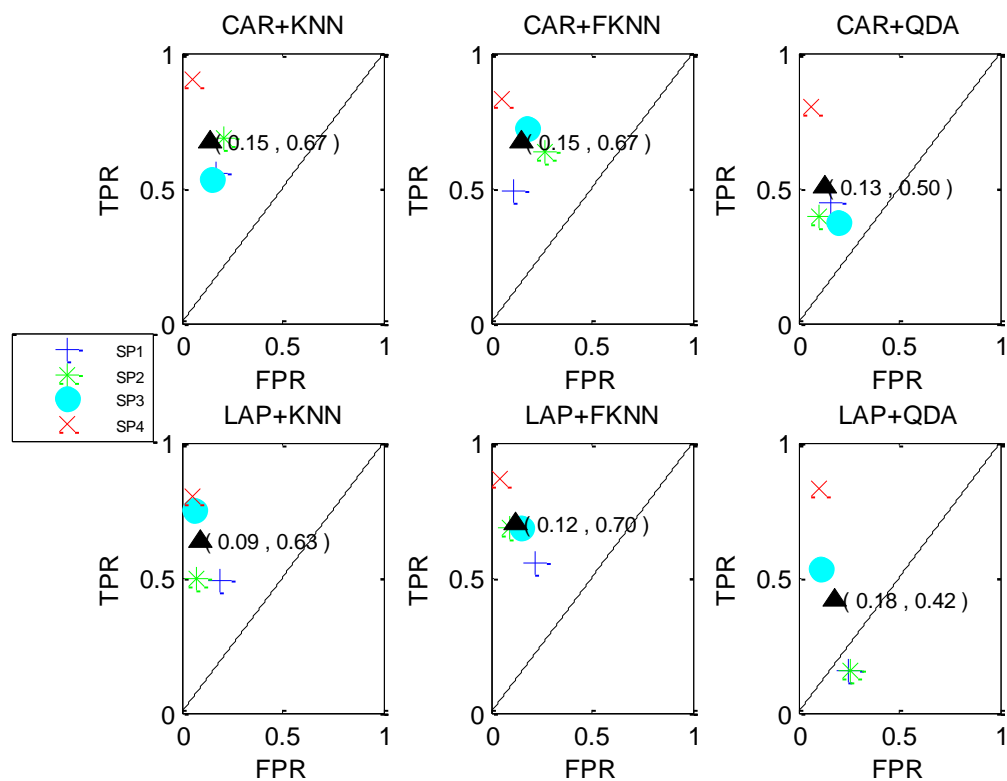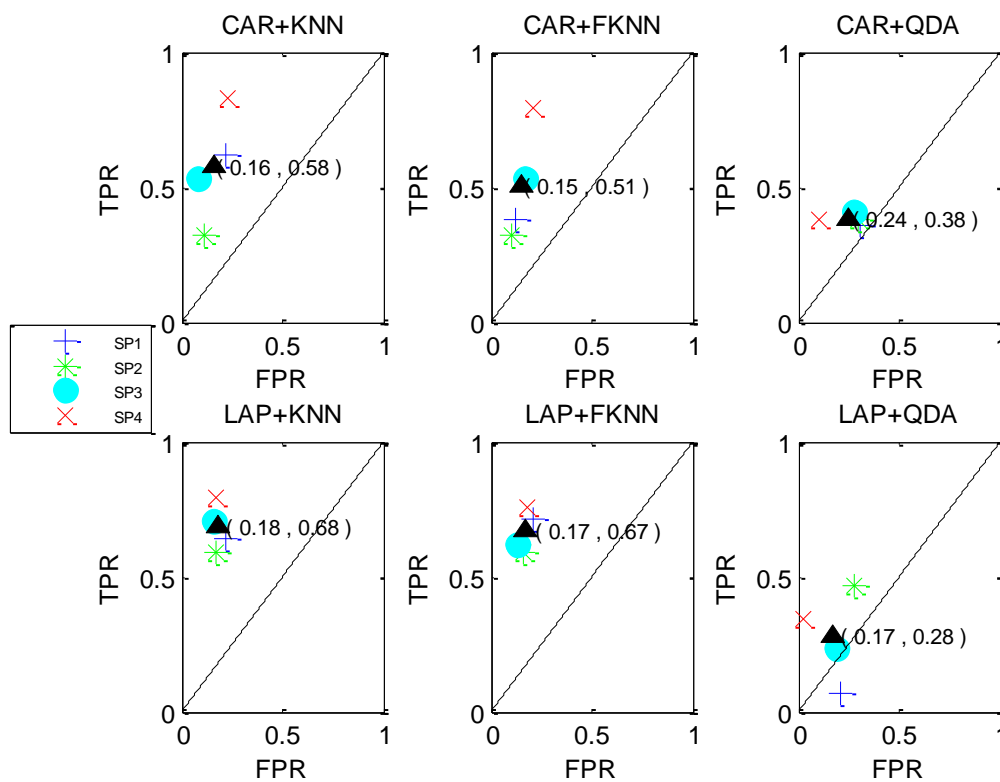

Figure 6.44: ROCs for predicting intention and direction of movement from paraplegic subjects (subclass for direction towards 3). The ROCs were presented based on combinations of spatial filters and classifiers. Subjects were represented by different symbols and the average of the classification accuracy was represented by a black triangle.

On the other hand, classification evaluation for predicting intention and direction of movement for subclass direction towards 6 from paraplegic subjects was portrayed in Figure 6.45. This figure demonstrates that, majority of the points within the ROC space for both spatial filters belong to the upper triangle; except for one, CAR+QDA, where subject SP1 belongs to the lower triangle. As for classification performance, the combination of LAP+FKNN outperformed the others based on the average of highest TPR and low FPR.
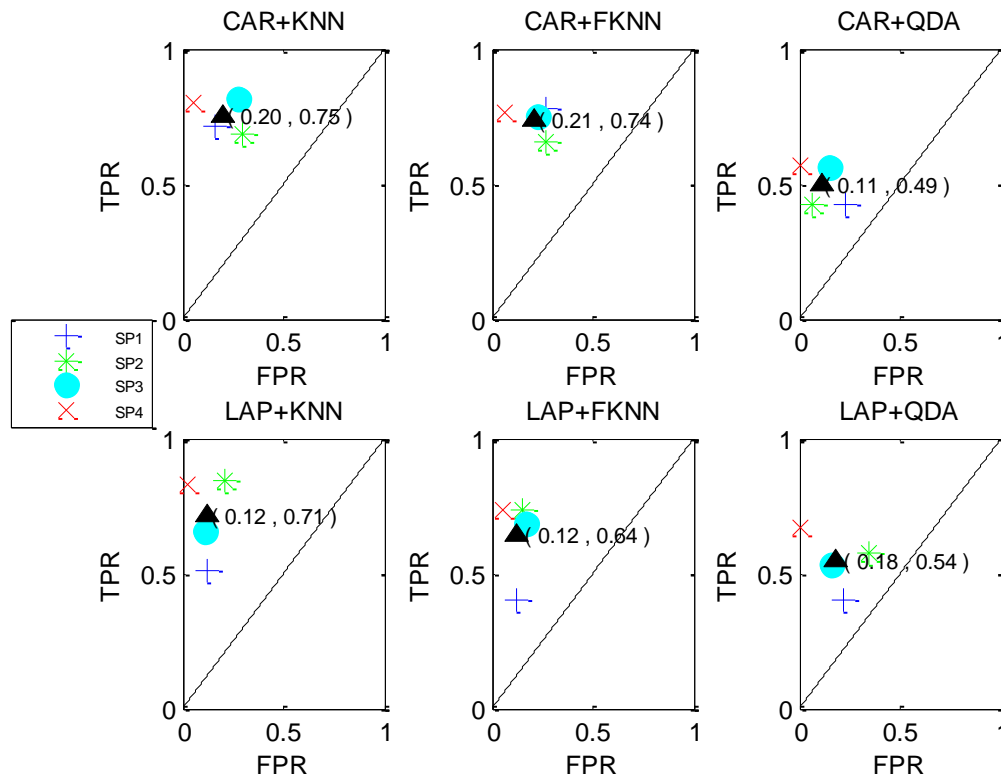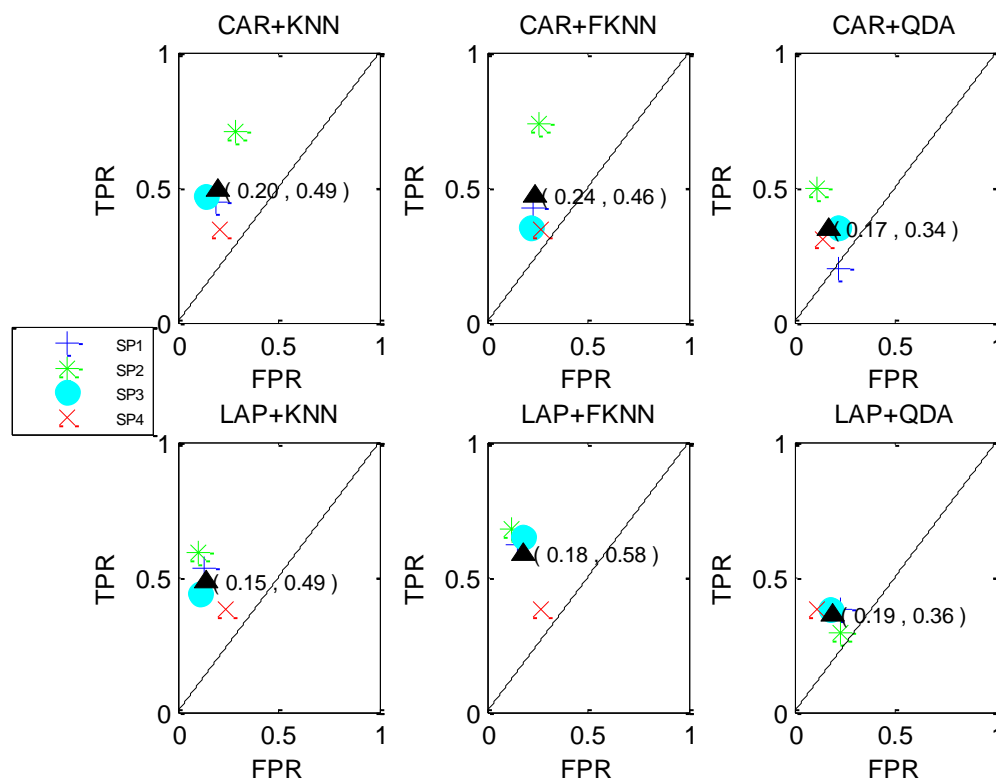

Figure 6.45: ROCs for predicting intention and direction of movement from paraplegic subjects (subclass for direction towards 6). The ROCs were presented based on combinations of spatial filters and classifiers. Subjects were represented by different symbols and the average of the classification accuracy was represented by a black triangle.

216

Furthermore, Figure 6.46 illustrates the ROC from paraplegic subjects for predicting intention and direction of movement for subclass direction towards 9. This figure demonstrates that, majority of the points within the ROC space for both spatial filters belong to the upper triangle; except for one, LAP+QDA, in which subject SP2 belonged to the lower triangle. Among all the classification combinations, LAP+*k*-NN has the best performance based on average of highest TPR and lowest FPR.
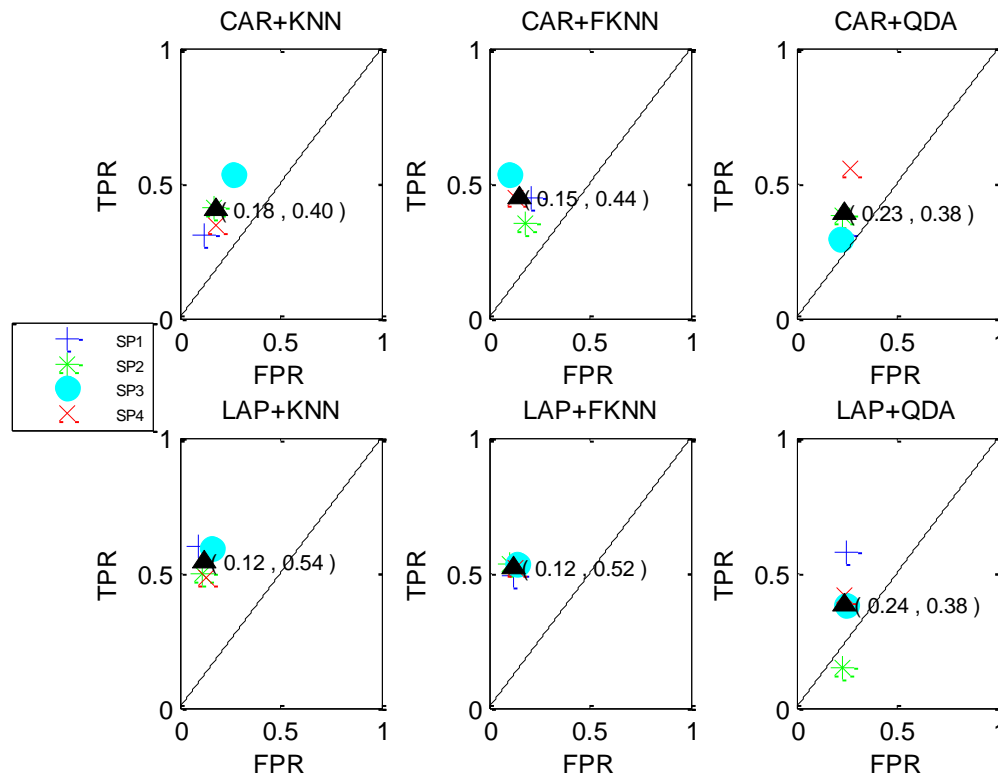
Figure 6.46: ROCs for predicting intention and direction of movement from paraplegic subjects (subclass for direction towards 9). The ROCs were presented based on combinations of spatial filters and classifiers. Subjects were represented by different symbols and the average of the classification accuracy was represented by a black triangle.

Moreover, Figure 6.47 portrays the ROC of paraplegic subjects in predicting intention and direction of movement for subclass direction towards 12. Based on this figure, all of the points within ROC space for both spatial filters belong to the upper triangle. As for classification performance, the combination of LAP+*k*-NN has the highest average TPR and lowest average FPR, outperforming other classification combinations.
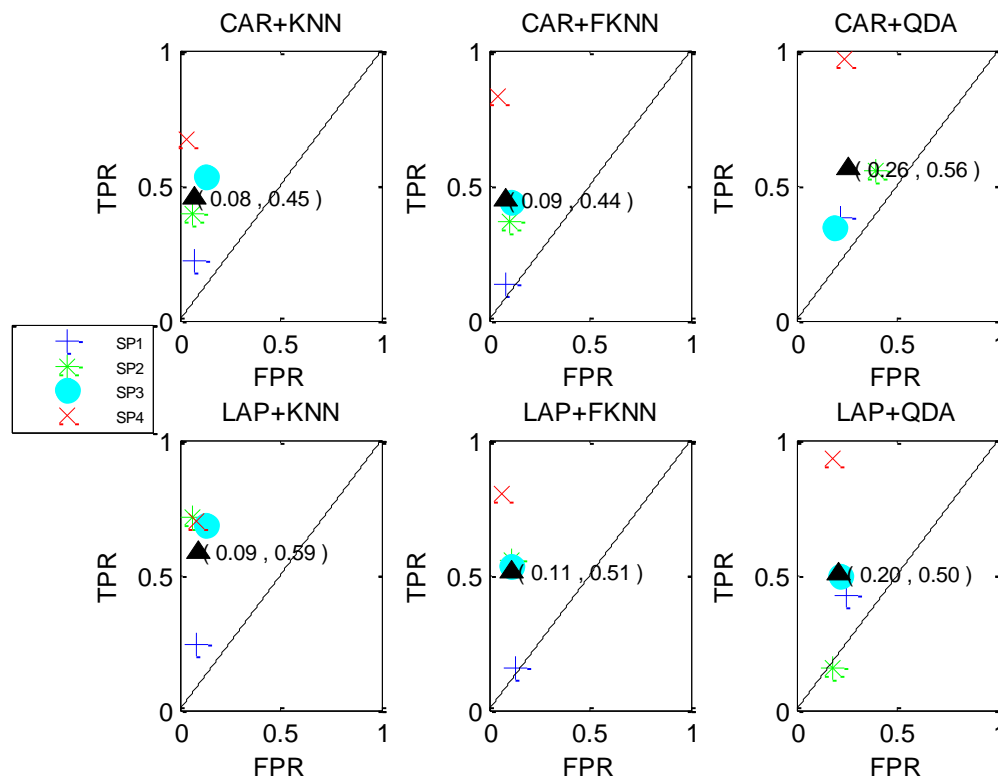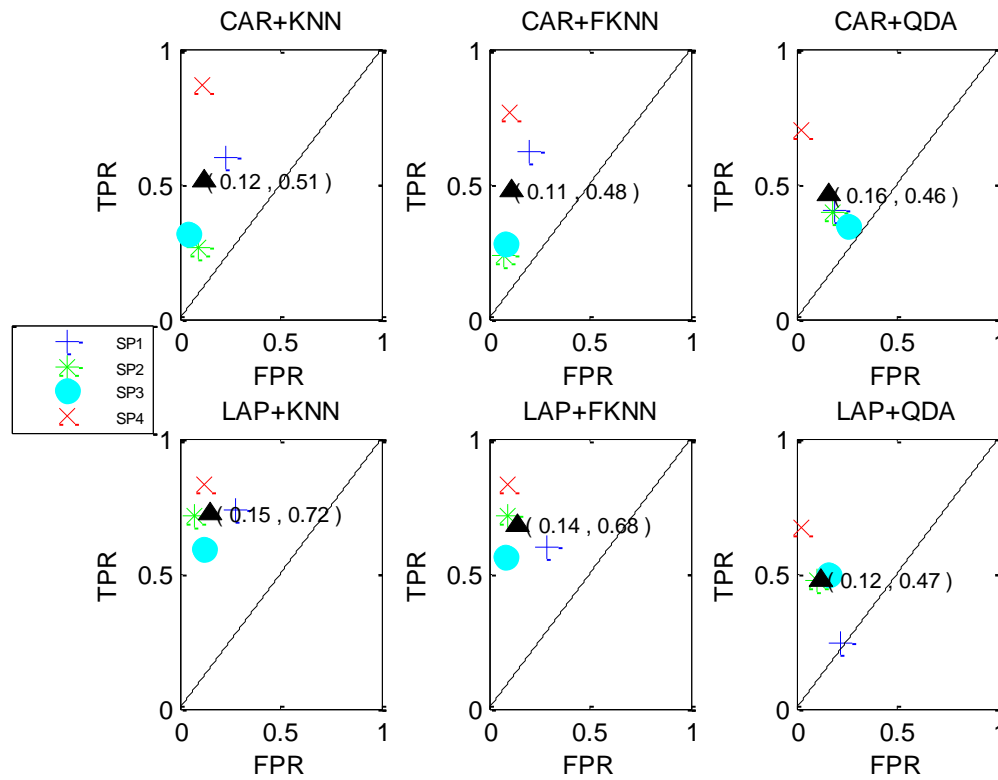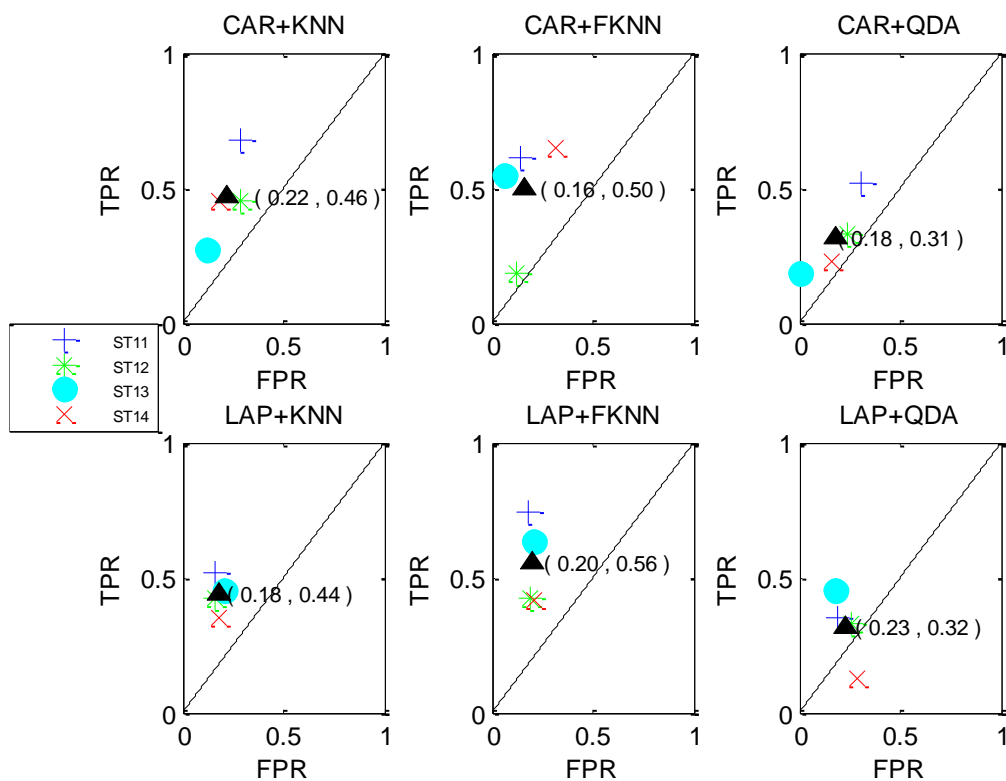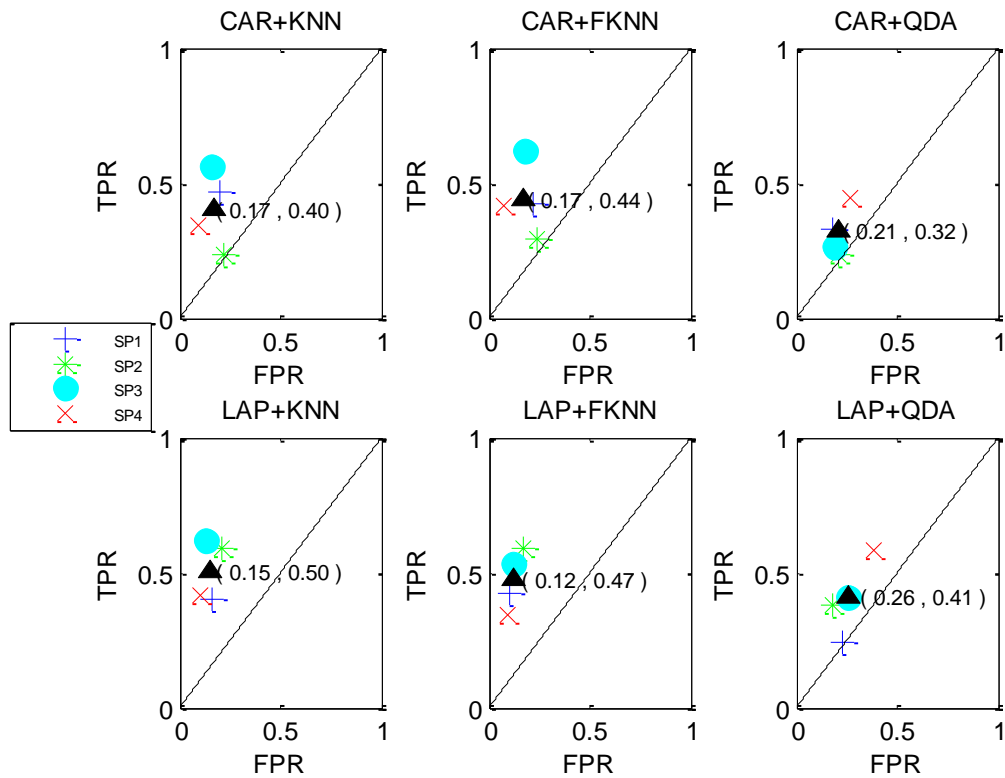

Figure 6.47: ROCs for predicting intention and direction of movement from paraplegic subjects (subclass for direction towards 12). The ROCs were presented based on combinations of spatial filters and classifiers. Subjects were represented by different symbols and the average of the classification accuracy was represented by a black triangle.

6.9   Summary

This chapter has presented the results of data analysis from SCI subjects who voluntarily participated in both motor task and motor imagery experiments. The findings presented have included various demographic characteristics, movement initiation time, normality test, movement-related cortical potential (MRCP), event-related spectral perturbation (ERSP), classification results and performance analysis.

Eighteen SCI subjects (14 tetraplegic and 4 paraplegic) participated in this study. Out of these 18 subjects, 8 of them were inpatients and 10 were outpatients. Demographic variability included level, cause and duration of injury, age, gender and lifestyle.

Movement initiation time from paraplegic and tetraplegic subjects in the motor task experiment show that only 3 (SP1, SP2 and SP3) out of 8 subjects demonstrate a significant difference in initiation time of movement towards 4 different directions. This suggests that for most of the participants of this study, there is no significant difference in movement initiation time towards 4 different directions. Also, the time of the visual cue and execution of the task from each subject are different.

In this study, a data normality test was implemented using the Kolmogorov-Smirnov test across 28 recording electrodes for both experiments. In the motor task experiment only data from one tetraplegic subject (ST13) and one paraplegic subject (SP1) contained channels that were not deemed to have a Gaussian distribution. As for the motor imagery experiment, this test result performed on data from paraplegic subjects showed that only one subject (SP4) did not have a Gaussian distribution. Similarly, only one tetraplegic subject (ST9) did not have a Gaussian distribution. In spite of a few subjects with non-Gaussian distribution in the recording electrodes, data distribution from the SCI subjects in this study are generally Gaussian in distribution.

In MRCP analysis, results of MTCAR, MTLAP, MICAR and MILAP demonstrate increasing amplitude negativity for all of 4 different directions. As for MTCAR and MTLAP, thin negative potential was observed from 500ms before movement onset, whereas for MICAR and MILAP the increase in negativity was detected 500ms after visual cue onset.

Furthermore, ERSP results of 4 different directions indicate detection of significant power changes in MTCAR, MTLAP, MICAR and MILAP. In MTCAR and MTLAP, power changes were detected before onset of the movement. Occurrence of prominent ERD within beta and gamma bands can be seen across ERSP of 4 different directions. On the other hand, detection of significant power changes in ERSP of 4 different directions in MICAR and MILAP are seen after visual cue onset. Corresponding ERD can be seen within beta and gamma bands. Moreover, statistical analyses with the ANOVA test were implemented across ERSP of MTCAR, MTLAP, MICAR and MILAP. Results (p values) of ANOVA tests showed that significant differences exist in time and frequency of the ERSP reflecting 4 different directions. This result provided features used to predict imagination/intention and direction of movement. The extracted features from MTCAR, MTLAP, MICAR and MILAP were classified using three classifiers; k-NN, FKNN and QDA approaches (described in METHODS CHAPTER).

In predicting imagination/intention of movement from paraplegic subjects, the highest classification accuracies were obtained from subject SP4 based on the features from alpha and gamma band signals recorded from electrode CCP1.On the other hand, when predicting imagination of movement from tetraplegic patients, data from ST5 and ST10 were classified with higher accuracy than the other subjects. These results were obtained from alpha and beta bands, recorded from both ipsilateral and contralateral electrodes. Apart from that, in predicting intention of movement the highest classification accuracy results were obtained from subject ST13; obtained from gamma and alpha bands using either contralateral or ipsilateral electrodes.

In predicting imagination/intention of movement towards direction 3, 6, 9 and 12 by paraplegic subjects, most of the highest accuracy classification results were produced by the subject SP4. Most of the results were obtained from alpha and gamma bands recorded from the CCP1 electrode. When predicting imagination of movement towards direction 3, 6, 9 and 12 by tetraplegic subjects, the highest accuracy classification results were generally produced by data from subjects ST5 and ST7. Subject ST5 results were obtained through the alpha band EEG recorded from

electrodes C2 and CFC4; ST7 results were obtained from the gamma band using electrodes FC3 and FC5. Meanwhile, when predicting intention of movement towards direction 3, 6, 9 and 12 from tetraplegic subjects, most of the highest accuracy classification results were obtained from subject ST11; from alpha and gamma bands using either contralateral or ipsilateral electrodes.

Furthermore, in predicting intention and direction of movement, the subjects SP3 and SP4 contributed to the majority of highest accuracy classification results. For subject SP3, most of the results were obtained from alpha and delta bands using electrodes FC5, CFC5 and CCP5. Subject SP4 produced the highest classification result through delta and gamma bands using electrodes FC3 and CFC3. In predicting imagination and direction of movement by paraplegic subjects, the highest accuracy classification results were produced by subject SP4. These results were obtained from alpha, beta and gamma bands using electrodes CCP1, C1, CPZ and CZ. On the other hand, in predicting imagination and direction of movement by tetraplegic subjects, most of the highest accuracy classification results were produced by subject ST7. These results were obtained from delta, alpha, beta and gamma bands using electrodes FC1, FC3 and CCP5. As for predicting intention and direction of movement by tetraplegic subjects, subject ST13 contributed most towards the highest accuracy classification result. Results were obtained from delta, alpha, beta and gamma bands using electrodes CCP1, FC4, CP4 and C2.

As for classifier performance, none of the classifiers stood-out constantly to outperform than the others. Nonetheless, the LAP spatial filter combined with various classifiers tended to produce higher classification accuracy results overall.

Chapter 7. Discussions

7.1   Introduction

This study focuses on exploring the feasibility of developing a BCI system which is well equipped with multi degree of freedom control based on a single limb movement for SCI patients. Results obtained in this study are interpreted, discussed and compared to other studies which involved SCI patients and to our control database.

7.2   Data Recording

This study implemented a motor imagery and motor task protocol which involved centre out, burst movement in multiple directions (direction towards 3, 6, 9, 12) using the right wrist. Healthy and paraplegic subjects participated in both of the experiments. On the other hand, due to the level of injury, the majority of the tetraplegic subjects were only capable of participating in the motor imagery experiment (except for subjects ST11, ST12, ST13 and ST14). Although, the tetraplegic subjects have no voluntary control over the right wrist, the implemented protocol of motor imagery is still suitable for them. This is because they still have an activated motor cortical area associated with body movement below the level of lesion (Mattia et al., 2009).

Even though the implemented protocols are suitable for both healthy and SCI subjects, there were a few issues raised by the participating subjects (healthy and SCI subjects) especially when they were attending the motor imagery experiment. During the data recording session of the motor imagery experiment, most of the healthy subjects complained that the experiment protocol was boring and sleep-inducing. On the other hand, the majority of the SCI subjects (tetraplegic and paraplegic) complain about feeling sleepy, tired, being unsure if they performed the right imagination, occurrences of spasm, inability to perform the imagery and possibly difficulty in maintaining concentration. These issues highlighted that; the healthy subjects cannot maintain their concentration whereas the SCI subjects suffer from the side effects of the prescribed medication that is being used to treat the secondary medical complications caused by SCI.

Side effects from the drug depend on the type and dosage of the prescribed medication. For instance, anti-spasmatic medication might cause the patients to feel sleepy and difficult to maintain concentration. Even though the anti-spasmatic medication can reduce the number of spasm occurrences, it also has a negative influence on vigilance and concentration, inducing drowsiness and weakness in patients (Thompson et al., 2005, Rupp, 2015). Besides that, some of the tetraplegic subjects were unable to perform and were not sure whether they performed the right imagination. These problems are most likely effect from the level of the injury because tetraplegic subjects that suffer a C5 and/or above injury, have limited control over shoulder and elbow function. Thus, the motor imagery experiment would be a challenging task for tetraplegic subjects due to the fact that the capability of performing the imagination is closely dependent on the current ability to perform the task physically (Olsson, 2012). In addition to that, the implemented protocol is also not a natural movement. Thus, this factor also might affect the imaginary capability in the tetraplegic subjects.

The above mentioned issues will have huge impact on the control and performance of the developed BCI system. Interference and disturbance before/during the motor imagery will effect the generation and detection of ERP and ERSP. Besides, it would be better to record EEG signal that reflect the mental task accurately so that it can be translated in command signal.

In order to overcome these problems a few approaches were adopted. For instance, we obtained verbal feedback from the subjects each time they completed the trial. By doing this, subjects not only had a longer time to relax but at the same time we could make sure that they were more alert and well prepared for the next trial. As for the occurrences of spasm, there was nothing that could be done apart from waiting for the spasms to lapse. After recovery, we asked SCI subjects if they were willing to continue with the experiment or repeat the trial. If the subject agreed to continue or repeat the trial, we proceeded. If they were not comfortable, we stopped the recording. We made sure that the subject's comfort was given priority throughout the experiment.

Furthermore, EMG and movement signals recorded from the tetraplegic subjects (especially those subjects who suffered a C5 and/or above injury) during the experiment could not be used for the pre-processing purpose. Due to the level of lesion, tetraplegic subjects were not able to hold the manipulandum and they also suffered from a secondary medical complication namely muscle atrophy on their arm. Due to the muscle atrophy, the arm becomes thinner and it was very challenging to locate the ECRL, ECRB, ECU and FCR muscles.

As mentioned in Chapter 4, the EMG and the movement signals were recorded so that we can confirm there were no movement attempts during motor imagery experiment and subjects performed the right movement according to the visual cue's direction in motor task experiment. Without these signals, the signal processing process for tetraplegic subjects (except for subject ST11, ST12, ST13 and ST14) was mainly depend on the EEG signal only. So there were possibilities that the recorded EEG signal was contaminated by motion artefact. Fortunately in this study, tetraplegic subjects (especially those subjects who suffered a C5 and/or above injury) have limited/no control over their wrist function so the possibilities can be ignored. Thus, EEG signal was enough for the pre-processing purpose.

To the best of our knowledge, before this research, there has not been any work conducted on multiclass BCI research (access brains signature through electrophysiological signal) involving SCI patients that employs motor imagery and motor task protocol based on a single limb. The majority of BCI research that involve SCI patients have more interest in motor imagery, motor attempt and motor task involves either single limb or combination of multiple limbs (López-Larraz et al., 2015, Müller-Putz et al., 2014, Lopez-Larraz et al., 2012).

7.3   Demographic Profiles and Prescribed Medications

Eighteen SCI subjects that participated in this study suffer from different level of injuries. Addition to that, SCI also inflicts secondary medical complications in all the subjects. Thus, in order to treat the complication, they were prescribed with certain doses of medication. The list of the prescribed medication of the subjects is listed below in Table 7.1.

Table 7.1: List of prescribed medication for all subjects.

Subjects	List of Medication	Function of Medication	Effect of the medication to the brain wave	References
ST1	Oxybutynin	Treat bladder problem	Lower the EEG spectral power	Rupp, 2015
	Bisacodyl and glycerine	Treat bowel problem	N/A	N/A
	Tizanidine	Treat spasticity	Increase slow brain wave and decrease alpha band	Mackel et al., 1984
ST2	Lactulose and laxido	Treat constipation problem	N/A	N/A
	Bisacodyl	Treat bowel problem	N/A	N/A
	Oxybutynin and tamsulosin	Treat bladder problem	Lower the EEG spectral power	Rupp, 2015
	Ephedrine	Treat hypotension problem and appetite suppressant	N/A	N/A
	Omeprazole	Treat gastroesophageal problem	N/A	N/A
	Piriton and flucloxacillin	Treat bacterial infection and allergies	N/A	N/A
	Benzoyl peroxide	Treat acne problem	N/A	N/A
	Gabapentin	Treat epilepsy problem	Decrease the peak frequency of alpha band (posterior region)	Salinsky et al., 2002
	Baclofen	Treat spasticity problem	Increase slow brain wave	Rupp, 2015

	Zopiclone	Treat insomnia problem	Increase delta band (anterior region)	Yamadera et al., 1996
ST3	Ciprofloxacin	Treat infection problem	N/A	N/A
	Calcichew	Supplement	N/A	N/A
ST4	Gabapentin	Treat epilepsy problem	Decrease the peak frequency of alpha band (posterior region)	Salinsky et al., 2002
	Paracetamol and ibuprofen	Pain reliever	Increase delta and theta bands Decrease alpha band of spontaneous EEG signal	Malver et al., 2014
ST5	Calsium supplement	Supplement	N/A	N/A
	Oxybutynin	Treat bladder problem	Lower the EEG spectral power	Rupp, 2015
	Rifampicin and ethambutol	Antibiotic	N/A	N/A
	Citalopram and diazepam	Treat depression and anxiety disorder	Increase delta band (posterior region)	Yamadera et al., 1996
	Pyridoxine	Treat nerve disorder	N/A	N/A
	Temazepam	Treat insomnia	N/A	N/A
	Baclofen	Treat spasticity problem	Increase slow brain wave	Rupp, 2015
ST6	Gabapentin	Treat epilepsy problem	Decrease the peak frequency of alpha band (posterior region)	Salinsky et al., 2002
	Paracetamol, ibuprofen and Oxynorm	Pain reliever	Increase delta and theta bands Decrease alpha band of spontaneous EEG signal	Malver et al., 2014
	Baclofen	Treat spasticity problem	Increase slow brain wave	Rupp, 2015
ST7	Bisacodyl	Treat bowel problem	N/A	N/A
	Movicol and senna	Treat constipation problem	N/A	N/A
	Gabapentin and	Treat epilepsy	Decrease the	Salinsky et

	clonazepam	problem and seizure attack	peak frequency of alpha band (posterior region)	al., 2002
	Baclofen	Treat spasticity problem	Increase slow brain wave	Rupp, 2015
ST8	Bisacodyl	Treat bowel problem	N/A	N/A
	Lactulose and senna	Treat constipation problem	N/A	N/A
	Paracetamol, Movelat gel and Diclofenac	Pain reliever	Increase delta and theta bands Decrease alpha band of spontaneous EEG signal	Malver et al., 2014
	Ascorbic acid	Supplement	N/A	N/A
	Distigmine and tamsulosin	Treat bladder problem	N/A	N/A
	Baclofen, Dantrolene and tizanidine	Treat spasticity problem	Increase slow brain wave Decrease alpha band	Rupp, 2015, Mackel et al., 1984
	Lignocaine patch	Local anaesthetic	N/A	N/A
	Rivaroxaban	Treat deep vein thrombosis problem	N/A	N/A
ST9	Temazepam	Treat insomnia	N/A	N/A
	Diazepam	Treat depression and anxiety disorder	Increase delta band (anterior region)	Yamadera et al., 1996
	Baclofen	Treat spasticity problem	Increase slow brain wave	Rupp, 2015
	Lactulose	Treat constipation problem	N/A	N/A
	Clonazepam	Treat epilepsy problem and seizure attack	N/A	N/A
	Pregabalin	Treat neuropathic pain	Increase theta band of spontaneous EEG signal	Malver et al., 2014
	Lignocaine patch	Local anaesthetic	N/A	N/A
	Glycerine	Treat bowel problem	N/A	N/A
	Senna and lactulose	Treat constipation problem	N/A	N/A
	Movelat gel	Pain reliever	N/A	N/A
	QVAR inhaler,	Treat asthma	N/A	N/A

ST10	salbutamol nebulisers, saline nebulisers and atropium nebulisers	problem		
	Tizanidine and baclofen	Treat spasticity problem	Increase slow brain wave Decrease alpha band	Mackel et al., 1984, Rupp, 2015
	Oxybutynin	Treat bladder problem	Lower the EEG spectral power	Rupp, 2015
	Ranitidine	Treat gastroesophageal problem	N/A	N/A
	Paracetamol and ibuprofen	Pain reliever	Increase delta and theta bands Decrease alpha band of spontaneous EEG signal	Malver et al., 2014
	Gabapentin	Treat epilepsy problem	Decrease the peak frequency of alpha band (posterior region)	Salinsky et al., 2002
	Fludrocortisone	Steroid that prevent released of substance that caused inflammation	N/A	N/A
ST11	Bisacodyl	Treat bowel problem	N/A	N/A
	Senna lactulose	Treat constipation problem	N/A	N/A
ST12	Tamsulosin	Treat bladder problem	N/A	N/A
ST13	Adcal D3	Supplement	N/A	N/A
	bisoprolol, candarsartan	Treat hypertension problem	N/A	N/A
	Bisacodyl	Treat bowel problem	N/A	N/A
	Amitriptyline	Treat depression and anxiety disorder	N/A	N/A
	Gliclazide and metformin	Treat diabetic problem	N/A	N/A
	Glycerine	Treat bowel problem	N/A	N/A
	Oxycodone and	Pain reliever	Increase delta	Malver et

	paracetamol		and theta bands Decrease alpha band of spontaneous EEG signal	al., 2014
	Laxido	Treat constipation problem	N/A	N/A
	Lansoprazole	Treat gastroesophageal problem	N/A	N/A
	Pregabalin	Treat neuropathic pain	Increase theta band of spontaneous EEG signal	Malver et al., 2014
	Warfarin	Anticoagulant drug	N/A	N/A
	Simvastatin	Statin drug	N/A	N/A
ST14	Ibuprofen, paracetamol, tramadol and trospium	Pain reliever	Increase delta and theta bands Decrease alpha band of spontaneous EEG signal	Malver et al., 2014
	Bisacodyl	Treat bowel problem	N/A	N/A
	Mirabegron	Treat bladder problem	N/A	N/A
	Senna	Treat constipation problem	N/A	N/A
SP1	Baclofen	Treat spasticity problem	Increase slow brain wave	Rupp, 2015
	Bisacodyl	Treat bowel problem	N/A	N/A
	Temazepam and zopiclone	Treat insomnia problem	Increase delta band (anterior region)	Yamadera et al., 1996
	Dihydrocodeine	Pain reliever	N/A	N/A
	Glycerol and lactulose	Treat constipation problem	N/A	N/A
	Mirtazapine	Treat depression and disorder	N/A	N/A
	Pregabalin	Treat neuropathic pain	Increase theta band of spontaneous EEG signal	Malver et al., 2014
	Tizanidine	Treat spasticity	Increase slow brain wave and decrease alpha	Mackel et al., 1984

			band	
SP2	Insulin	Treat diabetic problem	N/A	N/A
	Creon	Treat people who can't digest food normally	N/A	N/A
	Gabapentin	Treat epilepsy problem	Decrease the peak frequency of alpha band (posterior region)	Salinsky et al., 2002
	Tizanidine	Treat spasticity	Increase slow brain wave and decrease alpha band	Mackel et al., 1984
	Calcichew, vitamin C and forceval	Supplement	N/A	N/A
	Suppositories	Treat bowel problem	N/A	N/A
	Atorvastatin	Statin drug	N/A	N/A
	Aspirin and oxycodone	Pain reliever	N/A	N/A
	Cetirizine	Treat hay fever, allergies, angioedema and urticaria	N/A	N/A
	Nitrofurantoin	antibiotic	N/A	N/A
	Eye drops	Treat eye sores	N/A	N/A
	Senna	Treat constipation problem	N/A	N/A
	Amlodipine	Treat hypertension	N/A	N/A
	Omeprazole	Treat gastroesophageal problem	N/A	N/A
SP3	Metformin	Treat diabetic problem	N/A	N/A
	Nitrofurantoin	Treat bladder problem	N/A	N/A
	Senna and micralax	Treat constipation problem	N/A	N/A
	Baclofen	Treat spasticity problem	Increase slow brain wave	Rupp, 2015
	Anusol cream	Treat swelling, itching and discomfort of rectal condition	N/A	N/A
	Ascorbic acid	Supplement	N/A	N/A

SP4	Baclofen	Treat spasticity problem	Increase slow brain wave	Rupp, 2015
	Bumetanide	Treat swelling (edema caused by heart failure or kidney disease)	N/A	N/A
	Diazepam	Treat depression and anxiety disorder	Increase delta band (anterior region)	Yamadera et al., 1996
	Gabapentin	Treat epilepsy problem	Decrease the peak frequency of alpha band (posterior region)	Salinsky et al., 2002
	Glycerol, lactulose	Treat constipation problem	N/A	N/A
	Quinine	Treat malaria	N/A	N/A
	Sodium picosulphate, tolterodine	Treat bowel problem	N/A	N/A
	Warfarin	Anticoagulant drug	N/A	N/A

Referring to the Table 7.1, it can be seen that majority of the subjects suffer from bladder problem, bowel problem, spasticity, epilepsy, insomnia, depression and neuropathic pain. It is essential to emphasize that, the prescribed medication to treat these complications have negative effect towards EEG signal. For instance, oxybutynin can lead to significance lower spectral power within all relevance frequency bands of EEG component and baclofen can affect EEG spectral power distribution (increased slow brain waves) (Rupp, 2015).

Besides that, tizanidine can increase the slow wave of EEG activity and decrease the alpha activity (Mackel et al., 1984) whereas pregabalin increases the theta band of spontaneous EEG (Malver et al., 2014). Apart from that, administration of higher dose than 1.95g of paracetamol can generate a significant increase in delta and theta band whereas decrease in alpha band of spontaneous EEG (Malver et al., 2014). Furthermore, zopiclone can increase delta band of anterior region and diazepam can decrease delta band of posterior region (Yamadera et al., 1996). Addition to that, gabapentin can significantly decreased the peak frequency of the posterior alpha band (Salinsky et al., 2002).

Side effects of the medication on the EEG signal most probably have affected the results obtained from the SCI subjects. As mentioned in Chapter 4, this study extracted power spectrum features computed through ERSP. The power spectrum was calculated from the overlapping window, normalised with the baseline and average over all the trials (Grandchamp and Delorme, 2011). Thus, disturbances of the EEG signal component (delta, theta, alpha, beta and gamma bands) before, during and/or after the mental task (motor task/motor imagery experiment) will effected the ERSP.

For further clarification, the comparison of the frequency band that associated with the maximum classification results for the participated subjects were shown in Table 7.2.

Table 7.2: Comparison of the frequency band associated with the maximum classification result among the subjects group.

Subjects	Frequency band associated with the maximum classification result in predicting imagination and direction of the movement	Frequency band associated with the maximum classification result in predicting intention and direction of the movement
Healthy	Gamma band (refer to Table 5.13)	Gamma band (refer to Table 5.15)
Tetraplegic patients	Delta, theta, alpha, beta and gamma bands (refer to Table 6.22)	Alpha, beta and gamma bands (refer to Table 6.26)
Paraplegic patients	Delta, theta and alpha bands (refer to Table 6.24)	Delta and beta bands (refer to Table 6.28)

According to Table 7.2, it shows that majority of the maximum classification results in predicting imagination/intention and direction of the movement from the healthy subjects were obtained from the same frequency which was the gamma band. As for the paraplegic subjects, majority of the maximum classification results in predicting imagination/intention and direction of the movement were obtained from delta, theta, alpha and beta bands. On the other hand, the maximum classification results in predicting imagination/intention and direction of the movement from tetraplegic subjects were obtained from the entire EEG signal component namely delta, theta, alpha, beta and gamma bands.

Here we can see that, the directional information of the imagination /intention of the movement from SCI subjects were obtained from the lower frequency band (delta,

theta, alpha and beta bands) compared to the healthy subjects. These findings suggest that the side effect from the prescribed medication have huge impact on the control and performance of the developed BCI system. Therefore, it is important to highlight that for SCI patient, other than brain reorganisation and deafferentation, the type of medication is also one of the factor that affects the implementation and efficiency of BCI control.

7.4 Discussion of MRCP Results

MRCP is an event related potential locked to the onset of the movement (Spring et al., 2016) and related to the planning phase of a task force (Lattari et al., 2014). MRCP comprises of 2 pre-movement components namely early bereitschaft potential (BP) and late bereitschaft potential/negative slope (NS). BP refers to the readiness of the forthcoming action and reflects an early motor preparation in the supplementary motor area. BP occurs between 500ms and 1500ms before onset of the movement (Spring et al., 2016, Bozzacchi et al., 2012). On the other hand, NS refers to the urge to act, contralateral dominant and reflect activity in the pre-motor area. NS occurs between 500ms before onset of the movement (Spring et al., 2016, Bozzacchi et al., 2012).

Findings from the grand average of MRCP waveforms associated with motor imagery and motor task experiments among three different groups of subjects (healthy, tetraplegic and paraplegic subjects) indicate that, there were a lot of similarities especially when it comes to detection of MRCP component (late bereitschaft potential/negative slope (NS).

Grand average of the MRCP results (including healthy, tetraplegic and paraplegic subjects) associated with motor task (MT) and motor imagery experiments (MI) show the detection of MRCP components. In the grand average of the MRCPs associated with MT, NS was detected 500ms before onset of the movement whereas in the grand average of MRCP associated with MI NS was detected approximately 500ms after visual cue onset. Besides that, amplitudes of MRCP waveform in all 4 different directions of MT are greater than MI.

This result complements the finding by Miller et al., 2010. In their study, they recorded electrocorticographic cortical surface potential in eight subjects during overt action and kinaesthetic imagery of the same movement. They concluded that the magnitude of imagery induced cortical activity change comprised 25% of that with actual movement. In addition, Solodkin et al., 2004 claimed that although the active area of brain region between the motor execution and motor imagery are similar, volumes of activation tend to be larger during motor execution than during motor imagery. Besides that, the complexity of the movement also has a huge impact on the onset and the amplitude of both the MRCP components (Bozzacchi et al., 2012).

Detection of the MRCP activity from the normal and paraplegic subjects is expected because these two groups have full control over their wrist function. On the other hand, things are different when it comes to the tetraplegic subjects (especially those subjects who suffered a C5 and/or above injury). Tetraplegic subjects have limited access/control over their wrist function due to the reason that, there are no sensory/motor signals below level of lesion (especially with complete injury). Other than this, SCI also caused neuroplasticity/brain plasticity. Brain plasticity refer to the process of continuous alteration of the neural pathways and synapse of brains and nervous system in response to injury (Lynskey et al., 2008). Thus, brain plasticity makes it possible to detect the MRCP activity although tetraplegic subjects have no wrist control.

7.5 Discussion of ERSP Results

There are a lot of similarities in term of detection of power changes (occurrence of ERD and ERS) within the ERSP associated with MT and MI among the healthy, paraplegic and tetraplegic subjects (for further clarification please refer to Appendix F). For instance, in ERSP associated with the MT, ERD was detected within beta and gamma bands prior to onset of movement whereas in ERSP associated with the MI, ERD also detected approximately 300ms delay after onset of visual cue within the same frequency band (beta and gamma bands). Besides that, ERSP associated with

MT depicted more prominent detection of significant changes of power compared to the ERSP associated with MI.

Even though there are differences in time for detection of significant changes of power between ERSP associated MT and MI; ERSP associated with both of the experiments do have similarity in 2 aspects. First, ERSP using LAP spatial filter illustrated more prominent occurrence of ERD and ERS when compared to the ERSP using CAR spatial filter. Second, ANOVA test results (for further clarification please refer to Appendix F) indicate that there are significant differences in ERSP across the four different directions.

However, results in this study contradict the findings by Lopez-Larraz et al., 2012. In their study, they instruct subjects (three tetraplegic patients) to perform motor imagery and motor attempt of grasping with the right hand. Results from their study show detection of ERD in alpha and beta bands. The difference in detection of ERD between the current study (ERD detected in beta and gamma band) and theirs (ERD detected in alpha and beta band) might be caused of the type of task. Although both of the studies implemented imagination/movement of right hand, study by Lopez-Larraz et al., 2012 implementing the grasp movement whereas the present study implementing centre out, burst movement towards four different directions.

In general, ERD refers to the decreased power denoted by a negative value representing the activation of cortical area. On the other hand, ERS refers to the increased power usually reported by a positive value which demonstrates the idling condition of cortical area (Pfurtscheller, 2001, López-Larraz et al., 2015). Thus, occurrence of ERD in ERSP plot of four different directions before onset of the movement initiation in the motor task experiment indicates detection of the intention of movement towards four different directions. Besides that, the significant differences observed through ANOVA results in the ERSP plot of four different directions prior to onset of movement initiation also indicate that it is possible to recognise the intention and direction of the movement performed by subjects.

Similarly to the motor imagery experiment, occurrence of ERD with delay after onset of the visual cue in ERSP plot of four different directions shows a subject performing

motor imagery towards four different directions. The delay before occurrence of the ERD shows that subject needs time to perceive the visual cue and perform the imagination as per the visual cue directions. Significant differences found in the ANOVA results of the ERSP plot during the imagination of movement towards four different direction indicate that, it is possible to predict imagination and direction of the movement that are performed by subjects.

Furthermore, it is expected that ERSP of motor task will have more prominent detection of significant changes of power over the ERSP of motor imagery. This is because the ERD response of motor imagery only partially resembled the ERD response of motor task (Duann and Chiou, 2016). Addition to this, activation of brain region during the motor imagery is smaller compared to motor execution (Bozzacchi et al., 2012).

ERSP of LAP spatial filter demonstrated more prominent occurrence of ERD and ERS compared to the ERSP of CAR spatial filter which was caused by the characteristic of the of the spatial filter itself. Although both of the CAR and LAP spatial filter amalgamate channels linearly in order to produce a set of weight that is independent to the underlying data (Shakeel et al., 2015), LAP has an advantage over the CAR spatial filter. LAP derivation operate as high pass filter that enhance focal activity from local source and reduce wide distributed activity including that from distant source (Mouriño et al., 2001), reduce spatial noise and enhance identification of sources (McFarland, 2015).

7.6   Discussion of Classification Results and Performance Analysis

The classification results in this study indicate that the extracted features from EEG signal components 500ms before movement onset and 500ms after visual cue onset can be used to detect and predict imagination/intention and direction of movement for healthy and SCI patients. The comparison of classification results among three different subjects group were tabulated in Table 7.3 and Table 7.4.

Table 7.3: Comparison of the maximum classification result for predicting imagination and direction of movement among the subjects group.

| Subject | Classification results for predicting imagination and direction of movement | | | | | |
| | CAR | | | LAP | | |
	KNN	FKNN	QDA	KNN	FKNN	QDA
Healthy	35.00%-95.00%	35.00%-95.00%	29.00%-84.00%	37.00%-95.00%	37.50%-95.50%	32.00%-83.00%
	Six subjects manage to have classification results more than 70.00%					
Tetraplegic	34.17%-78.36%	37.55%-75.31%	27.94%-70.92%	28.14%-79.57%	25.22%-79.14%	22.69%-80.56%
	Three subjects manage to have classification results more than 70.00%					
Paraplegic	50.90%-80.83%	47.63%-80.00%	40.77%-75.83%	49.40%-79.17%	42.97%-80.83%	32.76%-77.50%
	One subjects manages to have classification results more than 70.00%					

Table 7.4: Comparison of the maximum classification result for predicting intention and direction of movement among the subjects group.

| Subject | Classification results for predicting intention and direction of movement | | | | | |
| | CAR | | | LAP | | |
	KNN	FKNN	QDA	KNN	FKNN	QDA
Healthy	29.00%-83.00%	28.00%-83.00%	29.00%-67.00%	47.00%-87.00%	47.50%-85.50%	34.00%-80.00%
	Two subjects manage to have classification results more than 70.00%					
Tetraplegic	38.48%-55.00%	37.88%-55.17%	31.46%-46.00%	35.64%-51.00%	37.12%-65.00%	26.09%-43.50%
	No subjects manage to have classification results more than 70.00%					
Paraplegic	47.75%-52.47%	41.49%-51.16%	29.94%-42.67%	51.59%-59.23%	49.77%-59.72%	31.72%-42.36%
	No subjects manage to have classification results more than 70.00%					

Table 7.3 and Table 7.4 compare the classification range of healthy, tetraplegic and paraplegic subjects in predicting imagination/intention and direction of the movement. Tabulated data from both of the tables show that healthy subjects have higher classification range compared to the SCI subjects. As for the comparison

238

between tetraplegic and paraplegic subjects, there are not much different for the maximum classification ranges.

Findings from this study highlighted that, there are few parameters that affecting the classification results such as numbers of accepted epochs for analysis and participation of the subjects during data recording session.

Numbers of epoch play a major role in classification process because these epochs were used to train the classifiers. If we have high number of epochs to trained the classifier, so it is highly possible to obtain good results. In comparison between healthy and SCI subjects, healthy subjects have more accepted epochs for the analysis process. Most of the epochs from the SCI subjects need to be discarded from the analysis due to the artefact contamination such as eye blinking, movement, spasm and falling asleep.

Besides that, participation of the subjects during the recording process also can contribute to a good and quality data. Majority of the healthy subjects have no problem to comply with the experiment protocol, whereas most of the SCI subjects find it difficult to stay focused and comply with the experiment protocol during the recording sessions (especially with reduced unnecessary movements). There are some possible factors that affect this parameter namely, age and side effect of the medication. The majority of the healthy subjects were young (mean age of 28.09) and free from any medication whereas most of the SCI subjects were old (mean age of 48.35) and prescribed with bunch of medications. There are highly possibilities that these two factor taking tolls on the SCI subjects which disturbing them to comply with the experiment protocol during the recording sessions.

It is important to mention that, the classification results across all subjects were contributed by three main parameters. These three main parameters include frequency band of the extracted features (explained in Section 7.3), the recording electrode and combination of spatial filter and classifier.

Majority of the maximum classification results in predicting imagination and direction of the movement from healthy (refer to Table 5.14), and SCI subjects

239

(tetraplegic (refer to Table 6.23) and paraplegic (refer to Table 6.25)) were obtained from contralateral electrodes. Similarly, the majority of the maximum classification results for predicting intention and direction of movement from healthy (refer to Table 5.16) and paraplegic (refer to Table 6.29) subjects were obtained from contralateral electrodes. In contrast, most of the maximum classification results for predicting intention and direction of movement from tetraplegic subjects were obtained from both of ipsilateral and contralateral electrodes (refer to Table 6.27).

It is undeniable that inter subject variability might be one of the factors that affects this, but the implication from the SCI have even a bigger impact on it. SCI caused deafferentation of cortical circuits which lead to the reorganisation of cortical topographic maps (Nardone et al., 2013, Bruehlmeier et al., 1998, Cramer et al., 2005, Shoham et al., 2001, Turner et al., 2003, Kokotilo et al., 2009, Aguilar et al., 2010). In other word, due to the brain reorganisation, the brain region that associated with below the level of lesion becomes shrunken. This is supported by finding from Levy Jr et al., 1990. Their finding discloses detection of enlarged cortical sensorimotor area for the preserved muscle above the lesion. Furthermore Green et al., 1998 also reported that, after SCI there is reorganisation of cortical motor activity to a more posterior location.

As for the combination of spatial filter and classifier, the maximum classification results in this study were provided by the implemented classifier namely *k*-NN, FKNN and QDA classifiers. Even though there is no specific classifier that contributed to the maximum result in all aspect, but there is one thing in common. Classification performance evaluation show that, combination of classifier with LAP spatial filter always outperformed combination of classifier with CAR spatial filter.

In comparison of the obtained results with the other studies (refer to Table 2.3) it indicates that, the present study manages to develop multi degree of freedom BCI system (four degree of freedom) based on imagination/intention of movement of single limb for SCI patients. Besides that, majority of the studies focused on producing BCI that capable of two-dimensional control whereas the current study is capable of producing BCI system with four-dimensional control. Moreover, most of the studies also include motor imagery/motor execution of combination of multiple

limbs (right hand, left hand, foot) and employ recording montage based on standard on 10-20 system. On the other hand, this study only includes single limb and uses a 10-10 (high density montage) recording system. This is because SCI patient especially tetraplegic subjects have crucial issues with assessing and voluntary control over four major limbs. Also, due to the deafferentation of the cortical circuits and reorganisation of the brain region, implementation of high density montage recording system might increase the chances of recording brain signature within the motor cortex region.

It is important to bear in mind that the implemented BCI system in this study is mainly based on endogenous synchronous BCI system. This type of BCI system is heavily dependent on how well the subjects regulate their brain rhythms (Roberto Hornero, 2012, Nicolas-Alonso and Gomez-Gil, 2012). In general, those who don't have good control over the modulation of sensorimotor rhythm are likely to be close to BCI illiteracy (Vidaurre and Blankertz, 2010). Despite of deafferentation of the cortical circuits, reorganisation of the brain region and side effect from the prescribed medication, BCI illiteracy is also one of the reasons to justify the poor classification results/performance by the SCI subjects in this study.

Chapter 8. Conclusions

8.1 Summary

The present study has investigated the feasibility of developing a BCI system that is capable to produce multi degree of freedom control based on imagination/intention of movement using single limb for SCI patients. In this endeavour, two main parameters that contributed to the effectiveness of BCI system were further explored. These two parameters include the frequency band and recording electrode that give highest results in predicting imagination/intention and direction of movement by SCI patients.

18 SCI patients (14 tetraplegics and 4 paraplegics) volunteered to take part in this study which was conducted at the QENSIU of Queen Elizabeth University Hospital. All the subjects were recruited by the consultants of QENSIU and this study was ethically approved from the NHS South Glasgow and Clyde Local Research Ethics Committee. Subjects managed to participate in two experiments namely motor task experiment (except for tetraplegic patients with injury level of C5 and above) and motor imagery experiment. The experimental protocol was designed in a manner so that the subject imagined (kinaesthetic imagery)/performed right wrist movement (burst, point to point centre out movement) towards multiple directions (direction towards 3, 6, 9 and 12) triggered by visual cue. EEG, EMG and movement signal were synchronised and simultaneously recorded using Curry Neuroimaging and CED 1401 software whilst subjects attending the experiments.

EMG and movement signal were used to validate and make sure that there are no overt movement during motor imagery experiment. Besides that, movement signal also was used to calculate movement initiation time and to make sure that subject performed the right movement according to the visual cue. The EEG signals were processed offline using signal processing methods which include pre-processing, statistical analysis, features extracting and classification. During pre-processing, EEG signal was segmented inti epoch and categorised according to the direction of movement. Noise and artefacts were removed from the epoch signal through visual inspection and filtering process that include notch filter, bandpass filter and spatial filters namely CAR and LAP spatial filter. Data distribution of the EEG signal was assessed using Kolmogorov-Smirnov test. Features (ERP and power spectrum) of

four different directions were extracted and visualised through MRCP and ERSP. In order to get the directional information from the extracted power spectrum features, ANOVA test was implemented. The extracted power spectrum features were also normalised using z score normalisation and size of the dimension were reduced using PCA. Later, the feature sets were cross validated using k fold cross validation and classified using three type of classifier namely, k-NN classifier, FKNN classifier and QDA classifier. Evaluation of the classification performance was implemented using ROC.

MRCP results shows that bereitschaft potential was detected 500ms prior to onset of the movement and 500ms after visual cue onset in MRCP waveform of four different directions. On the other hand, ERSP results indicate that detection of significant changes of power in ERSP of four different directions prior and during imagination/movement execution. Directional information also can be obtained from the ERSP due to the significant difference across ERSP of four different directions.

The majority maximum classification results in predicting imagination/intention of movement, predicting imagination/intention of movement towards direction 3, 6, 9, 12 and predicting imagination/intention and direction of movement were found to be more than 70.00%. Most of the results were obtained from the alpha band except for predicting imagination/intention and direction of movement where the maximum classification results were obtained from a wide range of EEG signal components that include delta, theta, alpha, beta and gamma band. The results also demonstrate that, most of the maximum classification results were recorded from the high density montage and contralateral electrode that were located more parietal of the motor cortex area. As for classification evaluation combination of classifier with LAP spatial filter always outperformed combination of classifier with CAR spatial filter.

Even though findings the from this study demonstrate the potential and capability of producing BCI system with multi degree of freedom control using motor task/motor imagery of single limb, we strongly believe that BCI system is not the best platform for the SCI community to communicate and control assistive and augmentative devices. From our point of view, instead of communicating/control assistive and augmentative devices we suggest that BCI is better used for neurorehabilitation

process. By implementing a BCI system which employs motor imagery/motor task paradigm for rehabilitation, it is believed that it might help with brain plasticity and slow down the brain reorganisation. These suggestions were made based on verbal feedback from the subjects. The majority of them claimed that motor imagery is a difficult task. Besides that, side-effect from the anti-spasmatic medication was also taxing for the patients due to whom they felt sleepy and hard to concentrate during the experiment.

Having said this, it doesn't rule out the possibility of the implemented BCI system is to be used for real time implementation. The suggestion which we believed can enhance the efficiency and performances of the BCI system are listed in the future work section.

8.2   Functional Significance

Findings from the present study demonstrate that it is possible to develop a BCI system equipped with 4 separate dimensional control using imagination/intention of right wrist movement towards 4 different directions. This BCI system also operates on single trial classification of a single channel. This claim was made based on detection of significant difference in ERSP of imagination/intention of movement towards four different directions. The detection of significant difference prior to movement and during imagination of movement provides directional information of the movement. Furthermore, imagination/intention and directional of the movement can be predicted based on single trial classification of single electrode.

8.3   Limitations

Finding from the present study reported the possibility and potential of developing BCI system for SCI community that is equipped with multi degree of freedom control using imagination/intention of right wrist movement. Although the results seem promising, there are a few limitations that are worth a review. These limitations include acquisition protocol, number of repetition and non-homogenous group.

The implemented experimental protocols for data recording in this study are based on motor execution and motor imagery of right wrist movement towards 4 different directions. In order to make sure that subjects performed the right movement according to the visual cue direction, movement signal was used to validate each of the trials of motor task experiment. Contrary with motor imagery experiment, there is no significant method that can be used to make sure that those subjects performed the right imagery (kinaesthetic imagery) according to the visual cue. Thus, in order to overcome this problem, we took the initiative to get verbal feedback from the subject each time after they completed the session. Surprisingly, all the subjects complained that it is difficult to perform the imagination of wrist movement. There was a subject who claimed that he couldn't perform the imagination of wrist movement but could imagine kicking a ball. Majority of the subjects claimed that, after attending two or three sessions of the experiment, they could imagine the wrist movement but were not sure whether it was the right imagination of movement or not. Although they couldn't confirm it, they did put all their effort to perform and complete the imagination experiment.

In each of the motor task and motor imagery experiment, subjects are required to participate in 10 sessions resulting 50 repetitions of imagination/movement for each of the 4 different directions. Although all the subjects managed to complete the experiment (except subject ST2), the issue here was that not all the 50 trials could be used for the analysis. This is because some of the trials needed to be discarded due to the artefacts caused by eye blinking, jaw clenching, swallowing, coughing, falling asleep and any inappropriate movement. The number of the trials that included in the analysis of data might have an effect on the classification results. On the other hand, the number of discarded trials totally depended on how well the subjects complied with the experiment procedure. This does not indicate that the subjects didn't cooperate purposely. It is the complication from the SCI that doesn't allow the patients to comply fully. For instance, subjects have no control over the spasm and side effect that caused by anti-spasmatic medication.

As mentioned earlier in this chapter, two main groups of SCI patients participated in this study namely tetraplegic and paraplegic patients. Although we have two

different groups, the challenge here was that neither tetraplegic nor paraplegic subjects were a homogeneous group. Despite this, we had to establish two heterogeneous groups instead of having two homogeneous groups. This is because, although the subjects were categorised within the same group due to the nature of injury, there were parameters that made them significantly different to one another. For instance level of injury, AIS scale, duration of injury before recording and type of medication. All of these parameters have high possibility of affecting the classification results. Due to this reason comparison can't be made within and between the two groups. Findings from the present study also can't be generalised to all SCI patients.

8.4 Future Work

Findings from this study reported the feasibility and potential of developing multi degree of freedom BCI system for SCI patients. The developed BCI system is capable of operating with 4 different control signals obtained from surface EEG signal that employed motor imagery and motor execution of single limb. Besides that, this system also required no training sessions from the subjects. On the other hand, we strongly believed there are still plenty of room for improvement in order to enhance the performance, efficiency and bring it to the other level in the future. Thus we would like to suggest approaches that possibly do that.

In present study, artefact detection depends on EMG and movement signal and as for artefact rejection it was done manually. The drawback of this method is that author needed to analyse EMG and movement signal separately. Results from these two signals were then used to remove artefact from EEG signal through visual inspection. This method consumes a lot of time, thus it is advisable in the future work the EMG, movement and EEG signal to be analysed simultaneously and artefact rejection was implemented automatically.

Besides that, in order to develop an efficient and practical BCI system it is important that the developed system is capable to detect and translate the imagination/intention of subject into control command that is capable to communicate/control assistive and

augmentative devices online. Thus, in future work it is advisable to develop BCI system that is capable to provide real time results to the subject regarding the classification result based on single trial.

Moreover, we would also like to recommend modification on the experimental protocol. According to the consultant in the QENSIU, the implemented experimental protocols which involved imagination of wrist movement towards four different directions were not natural movements. Imagination of non-natural movement is a challenging task for person who has no/limited voluntarily access towards their limbs. Thus, in future study it is recommended to employ a more naturalistic movement of single limb such as pronation, supination, flexion and extension using right arm. Execution of four different tasks by arm not only maintain the four degree of freedom, but at the same time it increase the participation of SCI patients to perform it physically. This is because, SCI patients that suffer injury at level of C5 and below still have some shoulder and elbow functions.

In order to develop functional and more generalised BCI systems it is essential to recruit more number of subjects and introduce multiple recording sessions. By having increased number of subject, the obtained results can be inferenced to represent population of SCI patients. Besides that, multiple recording sessions would enable subjects to have more 'training session' so that they could increase the capability in regulating their brain rhythm. Furthermore, multiple recording sessions can also reduce the effect of inter subject and intra subject variability.

References

ACKERMANN, H. & HERTRICH, I. 2000. The contribution of the cerebellum to speech processing. *Journal of Neurolinguistics,* 13**,** 95-116.

ACQUALAGNA, L., BOTREL, L., VIDAURRE, C., KUBLER, A. & BLANKERTZ, B. 2016. Large-Scale Assessment of a Fully Automatic Co-Adaptive Motor Imagery-Based Brain Computer Interface. *Plos One,* 11.

AGUILAR, J., HUMANES-VALERA, D., ALONSO-CALVINO, E., YAGUE, J. G., MOXON, K. A., OLIVIERO, A. & FOFFANI, G. 2010. Spinal Cord Injury Immediately Changes the State of the Brain. *Journal of Neuroscience,* 30**,** 7528-7537.

Ahmad Jamil, S.H.F.S, Lakany, H., Conway, B.A. (2016). Single Trial Classification of EEG in Predicting Intention and Direction of Wrist Movement: Translation Toward Development of Four-Class Brain Computer Interface System Based on a Single Limb. In Proc. COGNITIVE 2016, The Eight International Conference on Advanced Cognitive Technologies and Applications, pages 90-95.

AHMED, Z., PERVAIZ, Z., KHAN, M. S. & ASHRAF, M. W. 2014. Medical Diagnosis Using Brain-Computer Interface (BCI). *Journal of Biotechnology, Bioinformatics and Bioengineering,* 1(3)**,** 43-57.

AHN, M., CHO, H., AHN, S. & JUN, S. C. 2013. High Theta and Low Alpha Powers May Be Indicative of BCI-Illiteracy in Motor Imagery. *Plos One,* 8.

AL SHALABI, L., SHAABAN, Z. & KASASBEH, B. 2006. Data mining: A preprocessing engine. *Journal of Computer Science,* 2**,** 735-739.

AL-ANI, T. & TRAD, D. 2010. *Signal Processing and Classification Approaches for Brain-computer Interface*, INTECH Open Access Publisher.

AL-FAHOUM, A. S. & AL-FRAIHAT, A. A. 2014. Methods of EEG signal features extraction using linear analysis in frequency and time-frequency domains. *ISRN neuroscience,* 2014**,** 730218-730218.

ALDEA, R. & FIRA, M. 2014. Classifications of Motor Imagery Tasks in Brain Computer Interface Using Linear Discriminant Analysis. *International Journal of Advanced Research in Artificial Intelligence (ijarai),* 3.

ALKADHI, H., BRUGGER, P., BOENDERMAKER, S. H., CRELIER, G., CURT, A., HEPP-REYMOND, M. C. & KOLLIAS, S. S. 2005. What disconnection tells about motor imagery: Evidence from paraplegic patients. *Cerebral Cortex,* 15**,** 131-140.

ALLISON, B. Z., MCFARLAND, D. J., SCHALK, G., ZHENG, S. D., JACKSON, M. M. & WOLPAW, J. R. 2008. Towards an independent brain–computer interface using steady state visual evoked potentials. *Clinical neurophysiology,* 119**,** 399-408.

Apparelyzed 2015, Spinal cord injury, accesses 18 June 2015 <http://www.apparelyzed.com/statistics.html>

AYDEMIR, O. & KAYIKCIOGLU, T. 2013. Comparing common machine learning classifiers in low-dimensional feature vectors for brain computer interface applications. *International Journal of Innovative Computing, Information and Control,* 9**,** 1145-1157.

BAILLET, S., MOSHER, J. C. & LEAHY, R. M. 2001. Electromagnetic brain mapping. *Signal Processing Magazine, IEEE,* 18**,** 14-30.

BAILLIEUX, H., DE SMET, H. J., PAQUIER, P. F., DE DEYN, P. P. & MARIËN, P. 2008. Cerebellar neurocognition: insights into the bottom of the brain. *Clinical neurology and neurosurgery,* 110**,** 763-773.

BARBERO, A. & GROSSE-WENTRUP, M. 2010. Biased feedback in brain-computer interfaces. *Journal of Neuroengineering and Rehabilitation,* 7.

BARBOSA, A. O. G., DIAZ, D. R. A., VELLASCO, M. M. B. R., MEGGIOLARO, M. A. & TANSCHEIT, R. 2009. Mental Tasks Classification for a Noninvasive BCI Application. *Artificial Neural Networks - Icann 2009, Pt Ii,* 5769**,** 495-504.

BARRETO, G. A., FROTA, R. A. & DE MEDEIROS, F. N. S. 2004. On the classification of mental tasks: A performance comparison of neural and statistical approaches. *Machine Learning for Signal Processing Xiv***,** 529-538.

BASHASHATI, A., FATOURECHI, M. & WARD, R. K. 2007a. A survey of signal processing algorithms in brain–computer interfaces based on electrical brain signals. *Journal of Neural Engineering,* 4**,** 32-57.

BASHASHATI, A., FATOURECHI, M., WARD, R. K. & BIRCH, G. E. 2007b. A survey of signal processing algorithms in brain–computer interfaces based on electrical brain signals. *Journal of Neural engineering,* 4**,** R32.

BASHASHATI, H., WARD, R. K., BIRCH, G. E. & BASHASHATI, A. 2015. Comparing Different Classifiers in Sensory Motor Brain Computer Interfaces. *Plos One,* 10.

BAZIYAD, A. G. & DJEMAL, R. A Study and Performance Analysis of Three Paradigms of Wavelet Coefficients Combinations in Three-Class Motor Imagery Based BCI. 2014 5th International Conference on Intelligent Systems, Modelling and Simulation, 2014. IEEE, 201-205.

BENSCH, M., KARIM, A. A., MELLINGER, J., HINTERBERGER, T., TANGERMANN, M., BOGDAN, M., ROSENSTIEL, W. & BIRBAUMER, N. 2007. Nessi: an EEG-controlled web browser for severely paralyzed patients. *Computational intelligence and neuroscience,* 2007.

BERKOWITZ, A. 2012. Motor Output from the Brain and Spinal Cord. *eLS. John Wiley & Sons, Ltd: Chichester.*

BHATTACHARYYA, S., KHASNOBISH, A., CHATTERJEE, S., KONAR, A. & TIBAREWALA, D. Performance analysis of LDA, QDA and KNN algorithms in left-right limb movement classification from EEG data. Systems in Medicine and Biology (ICSMB), 2010 International Conference on, 2010. IEEE, 126-131.

BIRAN, R., MARTIN, D. C. & TRESCO, P. A. 2007. The brain tissue response to implanted silicon microelectrode arrays is increased when the device is tethered to the skull. *Journal of Biomedical Materials Research Part A,* 82**,** 169-178.

BIRBAUMER, N., ELBERT, T., CANAVAN, A. G. & ROCKSTROH, B. 1990. Slow Potentials of the Cerebral Cortex and Behavior. *Physiological Review,* 70**,** 1-41.

BIRBAUMER, N., GHANAYIM, N., HINTERBERGER, T., IVERSEN, I., KOTCHOUBEY, B., KÜBLER, A., PERELMOUTER, J., TAUB, E. & FLOR, H. 1999. A spelling device for the paralysed. *Nature,* 398**,** 297-298.

BIRBAUMER, N., HINTERBERGER, T., KÜBLER, A. & NEUMANN, N. 2003. The thought-translation device (TTD): neurobehavioral mechanisms and clinical outcome. *Neural Systems and Rehabilitation Engineering, IEEE Transactions on,* 11**,** 120-123.

BIRBAUMER, N., KÜBLER, A., GHANAYIM, N., HINTERBERGER, T., PERELMOUTER, J., KAISER, J., IVERSEN, I., KOTCHOUBEY, B., NEUMANN, N. & FLOR, H. 2000. The Thought Translation Device (TTD) for Completely Paralyzed Patients. *IEEE Transactions on rehabilitation Engineering,* 8**,** 190-193.

BLOKLAND, Y., VLEK, R., KARAMAN, B., OZIN, F., THIJSSEN, D., EIJSVOGELS, T., COLIER, W., FLOOR-WESTERDIJK, M., BRUHN, J., FARQUHAR, J. & IEEE. 2012. Detection of Event-related Desynchronization during Attempted and Imagined Movements in Tetraplegics for Brain Switch Control. 34th Annual International Conference of the IEEE Engineering-in-Medicine-and-Biology-Society (EMBS), 2012 Aug 28-Sep 01 2012 San Diego, CA. 3967-3969.

BOAS, G. 2004. Noninvasive imaging of the brain. *Optics and photonics news,* 15**,** 52-55.

BOGAARTS, J., HILKMAN, D., GOMMER, E., KRANEN-MASTENBROEK, V. & REULEN, J. 2016. Improved epileptic seizure detection combining dynamic feature normalization with EEG novelty detection. *Medical & biological engineering & computing*, 1-10.

BOSTANOV, V. 2004. BCI competition 2003 - Data sets Ib and IIb: Feature extraction from event-related brain potentials with the continuous wavelet transform and the t-value scalogram. *Ieee Transactions on Biomedical Engineering,* 51**,** 1057-1061.

BOZZACCHI, C., GIUSTI, M. A., PITZALIS, S., SPINELLI, D. & DI RUSSO, F. 2012. Similar cerebral motor plans for real and virtual actions. *PLoS One,* 7**,** e47783.

BRAINARD, D. H. 1997. The psychophysics toolbox. *Spatial vision,* 10**,** 433-436.

BRODU, N., LOTTE, F. & LÉCUYER, A. Comparative study of band-power extraction techniques for motor imagery classification. Computational Intelligence, Cognitive Algorithms, Mind, and Brain (CCMB), 2011 IEEE Symposium on, 2011. IEEE, 1-6.

BROMLEY, I. 2006. *Tetraplegia and paraplegia: a guide for physiotherapists*, Churchill Livingstone.

BROOKS, V. B. 1983. MOTOR CONTROL - HOW POSTURE AND MOVEMENTS ARE GOVERNED. *Physical Therapy,* 63**,** 664-673.

BRUEHLMEIER, M., DIETZ, V., LEENDERS, K., ROELCKE, U., MISSIMER, J. & CURT, A. 1998. How does the human brain deal with a spinal cord injury? *European Journal of Neuroscience,* 10**,** 3918-3922.

BRUMBERG, J. S. & GUENTHER, F. H. 2010. Development of speech prostheses: current status and recent advances. *Expert review of medical devices,* 7**,** 667-679.

BRUMBERG, J. S., NIETO-CASTANON, A., KENNEDY, P. R. & GUENTHER, F. H. 2010. Brain–computer interfaces for speech communication. *Speech communication,* 52**,** 367-379.

BRUNNER, P., JOSHI, S., BRISKIN, S., WOLPAW, J., BISCHOF, H. & SCHALK, G. 2010. Does the 'P300'speller depend on eye gaze? *Journal of neural engineering,* 7**,** 056013.

BUNKHUMPORNPAT, C., SINAPIROMSARAN, K. & LURSINSAP, C. 2009. Safe-Level-SMOTE: Safe-Level-Synthetic Minority Over-Sampling TEchnique for Handling the Class Imbalanced Problem. *Advances in Knowledge Discovery and Data Mining, Proceedings,* 5476**,** 475-482.

CASTERMANS, T., DUVINAGE, M., CHERON, G. & DUTOIT, T. 2013. Towards Effective Non-Invasive Brain-Computer Interfaces Dedicated to Gait Rehabilitation Systems. *Brain sciences,* 4**,** 1-48.

CASTRO, A., DIAZ, F. & VAN BOXTE, G. J. M. 2007. How does a short history of spinal cord injury affect movement-related brain potentials? *European Journal of Neuroscience,* 25**,** 2927-2934.

CHADWICK, N., MCMEEKIN, D. & TAN, T. Classifying eye and head movement artifacts in EEG Signals. Digital Ecosystems and Technologies Conference (DEST), 2011 Proceedings of the 5th IEEE International Conference on, 2011. IEEE, 285-291.

CHATTERJEE, S., BHATTACHARYYA, S., KONAR, A., TIBAREWALA, D., KHASNOBISH, A. & JANARTHANAN, R. Performance Analysis of Multiclass Common Spatial Patterns in Brain-Computer Interface. International Conference on Pattern Recognition and Machine Intelligence, 2013. Springer, 115-120.

CHEN, Y., TANG, Y., VOGEL, L. C. & DEVIVO, M. J. 2013. Causes of spinal cord injury. *Topics in spinal cord injury rehabilitation,* 19**,** 1-8.

CHENNU, S., ALSUFYANI, A., FILETTI, M., OWEN, A. M. & BOWMAN, H. 2013. The cost of space independence in P300-BCI spellers. *J. Neuroeng. Rehabil,* 10**,** 1-13.

CHEUNG, K. C. 2007. Implantable microscale neural interfaces. *Biomedical microdevices,* 9**,** 923-938.

CHU-ANDREWS, J. & JOHNSON, R. J. 1986. *Electrodiagnosis: an anatomical and clinical approach*, Lippincott.

CINCOTTI, F., KAUHANEN, L., ALOISE, F., PALOMÄKI, T., CAPORUSSO, N., JYLÄNKI, P., MATTIA, D., BABILONI, F., VANACKER, G. & NUTTIN, M. 2007. Vibrotactile feedback for brain-computer interface operation. *Computational intelligence and neuroscience,* 2007**,** 1-12.

COSTANZO, L. 2010. Brs Physiology (International Edition). *Brs Physiology (International Edition)-9781451103380-27, 00.*

COYLE, D., PRASAD, G. & MCGINNITY, T. M. Extracting features for a brain-computer interface by self-organising fuzzy neural network-based time series prediction. Engineering in Medicine and Biology Society, 2004. IEMBS'04. 26th Annual International Conference of the IEEE, 2004. IEEE, 4371-4374.

CRAIG, A. R., HANCOCK, K., CHANG, E. & DICKSON, H. 1998. Immunizing against depression and anxiety after spinal cord injury. *Archives of physical medicine and rehabilitation,* 79**,** 375-377.

CRAMER, S. C., LASTRA, L., LACOURSE, M. G. & COHEN, M. J. 2005. Brain motor system function after chronic, complete spinal cord injury. *Brain,* 128**,** 2941-2950.

CRAMER, S. C., ORR, E. L. R., COHEN, M. J. & LACOURSE, M. G. 2007. Effects of motor imagery training after chronic, complete spinal cord injury. *Experimental Brain Research,* 177**,** 233-242.

CUNNINGHAM, J. P. & GHAHRAMANI, Z. 2015. Linear dimensionality reduction: Survey, insights, and generalizations. *Journal of Machine Learning Research,* 16**,** 2859-2900.

CURT, A., BRUEHLMEIER, M., LEENDERS, K., ROELCKE, U. & DIETZ, V. 2002. Differential effect of spinal cord injury and functional impairment on human brain activation. *Journal of neurotrauma,* 19**,** 43-51.

CURT, A. & DIETZ, V. 1997. Ambulatory capacity in spinal cord injury: Significance of somatosensory evoked potentials and ASIA protocol in predicting outcome. *Archives of Physical Medicine and Rehabilitation,* 78**,** 39-43.

CURT, A. & DIETZ, V. 1999. Electrophysiological recordings in patients with spinal cord injury: significance for predicting outcome. *Spinal Cord,* 37**,** 157-165.

CURT, A., KECK, M. E. & DIETZ, V. 1998. Functional outcome following spinal cord injury: Significance of motor-evoked potentials and ASIA scores. *Archives of Physical Medicine and Rehabilitation,* 79**,** 81-86.

CVETKOVIC, D., ÜBEYLI, E. D. & COSIC, I. 2008. Wavelet transform feature extraction from human PPG, ECG, and EEG signal responses to ELF PEMF exposures: A pilot study. *Digital signal processing,* 18**,** 861-874.

DA SILVA, G. A., SCHOELLER, S. D., GELBCKE, F. L., FIGUEIREDO DE CARVALHO, Z. M. & DE JESUS PAULA DA SILVA, E. M. 2012. FUNCTIONAL ASSESSMENT OF PEOPLE WITH SPINAL CORD INJURY: USE OF THE FUNCTIONAL INDEPENDENCE MEASURE - FIM. *Texto & Contexto Enfermagem,* 21**,** 929-936.

DAVERAT, P., SIBRAC, M. C., DARTIGUES, J. F., MAZAUX, J. M., MARIT, E., DEBELLEIX, X. & BARAT, M. 1988. EARLY PROGNOSTIC FACTORS FOR WALKING IN SPINAL-CORD INJURIES. *Paraplegia,* 26**,** 255-261.

DE OLIVEIRA-SOUZA, R. 2012. The human extrapyramidal system. *Medical hypotheses,* 79**,** 843-852.

DE VOS, M., KROESEN, M., EMKES, R. & DEBENER, S. 2014. P300 speller BCI with a mobile EEG system: comparison to a traditional amplifier. *Journal of neural engineering,* 11**,** 1-8.

DELORME, A. & MAKEIG, S. 2004. EEGLAB: an open source toolbox for analysis of single-trial EEG dynamics including independent component analysis. *Journal of neuroscience methods,* 134**,** 9-21.

DIEN, J. 1998. Issues in the application of the average reference: Review, critiques, and recommendations. *Behavior Research Methods Instruments & Computers,* 30**,** 34-43.

DONCHIN, E., SPENCER, K. M. & WIJESINGHE, R. 2000. The mental prosthesis: assessing the speed of a P300-based brain-computer interface. *Rehabilitation Engineering, IEEE Transactions on,* 8**,** 174-179.

DONOGHUE, J. P. 2008. Bridging the brain to the world: a perspective on neural interface systems. *Neuron,* 60**,** 511-521.

DUANN, J.-R. & CHIOU, J.-C. 2016. A Comparison of Independent Event-Related Desynchronization Responses in Motor-Related Brain Areas to Movement Execution, Movement Imagery, and Movement Observation. *PLOS ONE,* 11**,** e0162546.

ELLIOTT, T. R. & RIVERA, P. 2003. Spinal cord injury. *Handbook of psychology.*

ENZINGER, C., ROPELE, S., FAZEKAS, F., LOITFELDER, M., GORANI, F., SEIFERT, T., REITER, G., NEUPER, C., PFURTSCHELLER, G. & MUELLER-PUTZ, G. 2008. Brain motor system function in a patient with complete spinal cord injury following extensive brain-computer interface training. *Experimental Brain Research,* 190**,** 215-223.

EVERETT, T. & KELL, C. 2010. *Human movement: an introductory text*, Churchill Livingstone.

FATOURECHI, M., BASHASHATI, A., WARD, R. K. & BIRCH, G. E. 2007. EMG and EOG artifacts in brain computer interface systems: A survey. *Clinical neurophysiology,* 118**,** 480-494.

FAWCETT, T. 2006. An introduction to ROC analysis. *Pattern Recognition Letters,* 27**,** 861-874.

FEHLINGS, M. G. & VAWDA, R. 2011. Cellular treatments for spinal cord injury: the time is right for clinical trials. *Neurotherapeutics,* 8**,** 704-720.

FERNANDEZ, E., GREGER, B., HOUSE, P. A., ARANDA, I., BOTELLA, C., ALBISUA, J., SOTO-SANCHEZ, C., ALFARO, A. & NORMANN, R. A. 2014. Acute human brain responses to intracortical microelectrode arrays: challenges and future prospects. *Frontiers in neuroengineering,* 7**,** 24-24.

FIELD-FOTE, E. C., FLUET, G. G., SCHAFER, S. D., SCHNEIDER, E. M., SMITH, R., DOWNEY, P. A. & RUHL, C. D. 2001. The Spinal Cord Injury Functional Ambulation Inventory (SCI-FAI). *Journal of Rehabilitation Medicine,* 33**,** 177-181.

FODOR, I. K. 2002. A survey of dimension reduction techniques. Technical Report UCRL-ID-148494, Lawrence Livermore National Laboratory.

FRANTZ, S. 2012. Embryonic stem cell pioneer Geron exits field, cuts losses. *Nature biotechnology,* 30**,** 12-13.

FURLAN, J. C., NOONAN, V., SINGH, A. & FEHLINGS, M. G. 2011. Assessment of Disability in Patients with Acute Traumatic Spinal Cord Injury: A Systematic Review of the Literature. *Journal of Neurotrauma,* 28**,** 1413-1430.

GALL, A., TURNER-STOKES, L. & GROUP, G. D. 2008. Chronic spinal cord injury: management of patients in acute hospital settings. *Clinical medicine,* 8**,** 70-74.

GAO, X., XU, D., CHENG, M. & GAO, S. 2003. A BCI-based environmental controller for the motion-disabled. *Neural Systems and Rehabilitation Engineering, IEEE Transactions on,* 11**,** 137-140.

GHASEMI, A. & ZAHEDIASL, S. 2012. Normality tests for statistical analysis: a guide for non-statisticians. *International journal of endocrinology and metabolism,* 10**,** 486-489.

GHEZ, C. & KRAKAUER, J. 1991. Voluntary movement. *Principles of neural science,* 3**,** 622-624.

GLASS, C. A., TESIO, L., ITZKOVICH, M., SONI, B. M., SILVA, P., MECCI, M., CHADWICK, R., EL MASRY, W., OSMAN, A., SAVIC, G., GARDNER, B., BERGSTROEM, E. & CATZ, A. 2009. SPINAL CORD INDEPENDENCE MEASURE, VERSION III: APPLICABILITY TO THE UK SPINAL CORD INJURED POPULATION. *Journal of Rehabilitation Medicine,* 41**,** 723-728.

GLICKSTEIN, M. 2007. What does the cerebellum really do? *Current Biology,* 17**,** R824-R827.

GONZÁLEZ-FRANCO, M., YUAN, P., ZHANG, D., HONG, B. & GAO, S. Motor imagery based brain-computer interface: a study of the effect of positive and negative feedback. Engineering in Medicine and Biology Society, EMBC, 2011 Annual International Conference of the IEEE, 2011. 6323-6326.

GRAIMANN, B. & PFURTSCHELLER, G. 2006. Quantification and visualization of event-related changes in oscillatory brain activity in the time–frequency domain. *Progress in brain research,* 159**,** 79-97.

GRANDCHAMP, R. & DELORME, A. 2011. Single-trial normalization for event-related spectral decomposition reduces sensitivity to noisy trials. *Frontiers in psychology,* 2**,** 236.

GREEN, J., SORA, E., BIALY, Y., RICAMATO, A. & THATCHER, R. 1998. Cortical sensorimotor reorganization after spinal cord injury an electroencephalographic study. *Neurology, 50***,** 1115-1121.

GREEN, J. B., ST ARNOLD, P. A., ROZHKOV, L., STROTHER, D. M. & GARROTT, N. 2003. Bereitschaft (readiness potential) and supplemental motor area interaction in movement generation: Spinal cord injury and normal subjects. *Journal of Rehabilitation Research and Development,* 40**,** 225-234.

GRESHAM, G. E., LABI, M. L. C., DITTMAR, S. S., HICKS, J. T., JOYCE, S. Z. & STEHLIK, M. A. P. 1986. THE QUADRIPLEGIA INDEX OF FUNCTION (QIF) - SENSITIVITY AND RELIABILITY DEMONSTRATED IN A STUDY OF 30 QUADRIPLEGIC PATIENTS. *Paraplegia,* 24**,** 38-44.

GROENEWEGEN, H. J. 2003. The basal ganglia and motor control. *Neural plasticity,* 10**,** 107-120.

HADLEY, M. N., WALTERS, B. C., AARABI, B., DHALL, S. S., GELB, D. E., HURLBERT, R. J., ROZZELLE, C. J., RYKEN, T. C. & THEODORE, N. 2013. Clinical Assessment Following Acute Cervical Spinal Cord Injury. *Neurosurgery,* 72**,** 40-53.

HALDER, P., CURT, A., BREM, S., LANG-DULLENKOPF, A., BUCHER, K., KOLLIAS, S. & BRANDEIS, D. 2006. Preserved aspects of cortical foot control in paraplegia. *Neuroimage,* 31**,** 692-698.

HARVEY, R. L., MACKO, R. F., STEIN, J., ZOROWITZ, R. D. & MACKO, R. 2008. *Stroke recovery and rehabilitation*, Demos Medical Publishing.

HASELSTEINER, E. & PFURTSCHELLER, G. 2000. Using time-dependent neural networks for EEG classification. *Ieee Transactions on Rehabilitation Engineering,* 8**,** 457-463.

HAW, C., LOWNE, D. & ROBERTS, S. 2006. *User specific template matching for event detection using single channel EEG*, na.

HAZRATI, M. K. & ERFANIAN, A. 2010. An online EEG-based brain–computer interface for controlling hand grasp using an adaptive probabilistic neural network. *Medical engineering & physics,* 32**,** 730-739.

HILLYARD, S. A. & KUTAS, M. 2002. Event-related potentials and magnetic fields in the human brain. *Neuropsychopharmacology: the Fifth Generation of Progress, Lippincott, Williams, and Wilkins, Baltimore*.

HINTERBERGER, T., SCHMIDT, S., NEUMANN, N., MELLINGER, J., BLANKERTZ, B., CURIO, G. & BIRBAUMER, N. 2004. Brain-computer communication and slow cortical potentials. *Biomedical Engineering, IEEE Transactions on,* 51**,** 1011-1018.

HOFFMAN, D. S. & STRICK, P. L. 1999. Step-tracking movements of the wrist. IV. Muscle activity associated with movements in different directions. *Journal of Neurophysiology,* 81**,** 319-333.

HOFFMANN, U., VESIN, J.-M., EBRAHIMI, T. & DISERENS, K. 2008. An efficient P300-based brain-computer interface for disabled subjects. *Journal of Neuroscience Methods,* 167**,** 115-125.

HOTZ-BOENDEN-NAKER, S., FUNK, M., SUMMERS, P., BRUGGER, P., HEPP-REYMOND, M.-C., CURT, A. & KOLLIAS, S. S. 2008. Preservation of motor programs in paraplegics as demonstrated by attempted and imagined foot movements. *Neuroimage,* 39**,** 383-394.

HSU, S. H., MULLEN, T., JUNG, T. P., CAUWENBERGHS, G. & IEEE. 2015. Validating Online Recursive Independent Component Analysis on EEG Data. 7th Annual International IEEE EMBS Conference on Neural Engineering (NER), Apr 22-24 2015 Montpellier, FRANCE. 918-921.

ITO, M. 2000. Mechanisms of motor learning in the cerebellum. *Brain research,* 886**,** 237-245.

ITO, M. 2012. *The cerebellum: brain for an implicit self*, FT press.

JAIN, A., NANDAKUMAR, K. & ROSS, A. 2005. Score normalization in multimodal biometric systems. *Pattern recognition,* 38**,** 2270-2285.

JENSEN, R. & CORNELIS, C. 2011. Fuzzy-rough nearest neighbour classification. *Transactions on rough sets XIII.* Springer.

JEROME BICKENBACH, INGA BOLDT, MARTIN BRINKHOF, JONVIEA CHAMBERLAIN, RAYMOND CRIPPS, MICHAEL FITZHARRIS, BONNE LEE, RUTH MARSHALL, SONJA MEIER, MICHAL NEUKAMP, PETER NEW, RICHARD NICOL, ALANA OFFICER, BRITTANY PEREZ, PER VON GROOTE & PETER WING 2013. *International perspectives on spinal cord injury*, World Health Organization.

JURCAK, V., TSUZUKI, D. & DAN, I. 2007. 10/20, 10/10, and 10/5 systems revisited: their validity as relative head-surface-based positioning systems. *Neuroimage,* 34**,** 1600-1611.

JURKIEWICZ, M. T., MIKULIS, D. J., MCILROY, W. E., FEHLINGS, M. G. & VERRIER, M. C. 2007. Sensorimotor cortical plasticity during recovery following spinal cord injury: a longitudinal fMRI study. *Neurorehabilitation and neural repair,* 21**,** 527-38.

KAPELLER, C., HINTERMULLER, C., ABU-ALQUMSAN, M., PRUCKL, R., PEER, A. & GUGER, C. A BCI using VEP for continuous control of a mobile robot. Engineering in Medicine and Biology Society (EMBC), 2013 35th Annual International Conference of the IEEE, 2013. 5254-5257.

KARIM, A. A., HINTERBERGER, T., RICHTER, J., MELLINGER, J., NEUMANN, N., FLOR, H., KÜBLER, A. & BIRBAUMER, N. 2006. Neural internet: Web surfing with brain potentials for the completely paralyzed. *Neurorehabilitation and Neural Repair,* 20**,** 508-515.

KAUHANEN, L., JYLANKI, P., LEHTONEN, J., RANTANEN, P., ALARANTA, H. & SAMS, M. 2007. EEG-based brain-computer interface for tetraplegics. *Computational intelligence and neuroscience***,** 23864-23864.

KAUR, M., AHMED, P. & RAFIQ, M. Q. 2012. Analyzing eeg based neurological phenomenon in bci systems. *International Journal of Computer Applications,* 57.

KELLER, J. M., GRAY, M. R. & GIVENS, J. A. 1985. A fuzzy k-nearest neighbor algorithm. *IEEE transactions on systems, man, and cybernetics***,** 580-585.

KIRSHBLUM, S. C., BURNS, S. P., BIERING-SORENSEN, F., DONOVAN, W., GRAVES, D. E., JHA, A., JOHANSEN, M., JONES, L., KRASSIOUKOV, A. & MULCAHEY, M. 2011. International standards for neurological classification of spinal cord injury (revised 2011). *The journal of spinal cord medicine,* 34**,** 535-546.

KLEBER, B. & BIRBAUMER, N. 2005. Direct brain communication: neuroelectric and metabolic approaches at Tübingen. *Cognitive Processing,* 6**,** 65-74.

KLOSE, K. J., GREEN, B. A., SMITH, R. S., ADKINS, R. H. & MACDONALD, A. M. 1980. University of Miami Neuro-Spinal Index (UMNI): a quantitative method for determining spinal cord function. *Spinal Cord,* 18**,** 331-336.

KOELSTRA, S., MÜHL, C. & PATRAS, I. EEG analysis for implicit tagging of video data. 2009 3rd International Conference on Affective Computing and Intelligent Interaction and Workshops, 2009. IEEE, 1-6.

KOKOTILO, K. J., ENG, J. J. & CURT, A. 2009. Reorganization and Preservation of Motor Control of the Brain in Spinal Cord Injury: A Systematic Review. *Journal of Neurotrauma,* 26**,** 2113-2126.

KRUSIENKI, D. J., MCFARLAND, D. J., PRINCIPE, J. C., WOLPAW, J. & WOLPAW, E. 2011. 7| BCI SIGNAL PROCESSING: FEATURE EXTRACTION. *Brain-Computer Interfaces: Principles and Practice***,** 123.

LAKANY, H. & CONWAY, B. 2005. Comparing EEG patterns of actual and imaginary wrist movements-a machine learning approach.

LAKANY, H. & CONWAY, B. Classification of wrist movements using EEG-based wavelets features. 2005 IEEE Engineering in Medicine and Biology 27th Annual Conference, 2006. IEEE, 5404-5407.

LAL, T. N., HINTERBERGER, T., WIDMAN, G., SCHRÖDER, M., HILL, N. J., ROSENSTIEL, W., ELGER, C. E., BIRBAUMER, N. & SCHÖLKOPF, B. Methods towards invasive human brain computer interfaces. Advances in neural information processing systems, 2004. 737-744.

LAMMERTSE, D., DUNGAN, D., DREISBACH, J., FALCI, S., FLANDERS, A., MARINO, R. & SCHWARTZ, E. 2007. From the 2006 NIDRR SCI measures FTI - Neuroimaging in traumatic spinal an evidence-based meeting cord injury: An evidence-based review for clinical practice and research. *Journal of Spinal Cord Medicine,* 30**,** 205-214.

LANDA, L., KRPOUN, Z., KOLAROVA, M. & KASPAREK, T. 2014. Event-related potentials and their applications. *Activitas Nervosa Superior,* 56**,** 17.

LATTARI, E., ARIAS-CARRIÓN, O., MONTEIRO-JUNIOR, R. S., PORTUGAL, E. M. M., PAES, F., MENÉNDEZ-GONZÁLEZ, M., SILVA, A. C., NARDI, A. E. & MACHADO, S. 2014. Implications of movement-related cortical potential for understanding neural adaptations in muscle strength tasks. *International archives of medicine,* 7**,** 1.

LAUREYS, S. & TONONI, G. 2011. *The neurology of consciousness: cognitive neuroscience and neuropathology*, Academic Press.

LEBEDEV, M. A. & NICOLELIS, M. A. L. 2006. Brain-machine interfaces: past, present and future. *Trends in Neurosciences,* 29**,** 536-546.

LEE, F., SCHERER, R., LEEB, R., NEUPER, C., BISCHOF, H. & PFURTSCHELLER, G. A comparative analysis of multi-class EEG classification for brain computer interface. Proceedings of the 10th Computer Vision Winter Workshop, 2005. 195-204.

LEE, W. L., LEUNG, Y. H. & TAN, T. P300 response classification in the presence of magnitude and latency fluctuations. Neural Information Processing, 2011. Springer, 352-359.

LEON, A. C., DAVIS, L. L. & KRAEMER, H. C. 2011. The role and interpretation of pilot studies in clinical research. *Journal of Psychiatric Research,* 45**,** 626-629.

LEVY JR, W. J., AMASSIAN, V. E., TRAAD, M. & CADWELL, J. 1990. Focal magnetic coil stimulation reveals motor cortical system reorganized in humans after traumatic quadriplegia. *Brain Research,* 510**,** 130-134.

LI, W., HUANG, Y., XU, J., CHEN, X. & WANG, X. 2009. The Assessment of EEG in Patients with Spinal Cord Injury to Movements. *Proceedings 2009 Third International Symposium on Intelligent Information Technology Applications Workshops***,** 74-77.

LIANG, N. & BOUGRAIN, L. 2012. Decoding Finger Flexion from Band-Specific ECoG Signals in Humans. *Frontiers in neuroscience,* 6**,** 1-6.

LIU, C., WANG, H., LU, Z. & IEEE. 2013. EEG Classification for Multiclass Motor Imagery BCI. 25th Chinese Control and Decision Conference (CCDC), 2013 May 25-27 2013 Guiyang, PEOPLES R CHINA. 4450-4453.

LOPEZ-LARRAZ, E., ANTELIS, J. M., MONTESANO, L., GIL-AGUDO, A., MINGUEZ, J. & IEEE. 2012. Continuous decoding of Motor Attempt and Motor Imagery from EEG Activity in Spinal Cord Injury Patients. 34th Annual International Conference of the IEEE Engineering-in-Medicine-and-Biology-Society (EMBS), 2012 Aug 28-Sep 01 2012 San Diego, CA. 1798-1801.

LOTTE, F., CONGEDO, M., LÉCUYER, A., LAMARCHE, F. & ARNALDI, B. 2007. A review of classification algorithms for EEG-based brain–computer interfaces. *Journal of neural engineering,* 4**,** R1.

LOTZE, M., LAUBIS-HERRMANN, U. & TOPKA, H. 2006. Combination of TMS and fMRI reveals a specific pattern of reorganization in M1 in patients after complete spinal cord injury. *Restorative neurology and neuroscience,* 24**,** 97-107.

LU, J., MCFARLAND, D. J. & WOLPAW, J. R. 2012. Adaptive Laplacian filtering for sensorimotor rhythm-based brain–computer interfaces. *Journal of neural engineering,* 10**,** 016002.

LÓPEZ-LARRAZ, E., MONTESANO, L., GIL-AGUDO, Á., MINGUEZ, J. & OLIVIERO, A. 2015. Evolution of EEG Motor Rhythms after Spinal Cord Injury: A Longitudinal Study. *PloS one,* 10**,** e0131759.

LYNSKEY, J. V., BELANGER, A. & JUNG, R. 2008. Activity-dependent plasticity in spinal cord injury. *Journal of Rehabilitation Research and Development,* 45**,** 229-240.

MA, C.-T., MAK, P.-I., VAI, M.-I., MAK, P.-U., PUN, S.-H., FENG, W. & MARTINS, R. 2009. Frequency-bandwidth-tunable powerline notch filter for biopotential acquisition systems. *Electronics letters,* 45**,** 197-199.

MACKEL, R., BRINK, E. & NAKAJIMA, Y. 1984. Action of tizanidine on responses of forearm flexors and extensors to torque disturbances. *Journal of Neurology, Neurosurgery & Psychiatry,* 47**,** 1109-1116.

MAK, J. N. & WOLPAW, J. R. 2009. Clinical applications of brain-computer interfaces: current state and future prospects. *Biomedical Engineering, IEEE Reviews in,* 2**,** 187-199.

MALVER, L. P., BROKJÆR, A., STAAHL, C., GRAVERSEN, C., ANDRESEN, T. & DREWES, A. M. 2014. Electroencephalography and analgesics. *British journal of clinical pharmacology,* 77**,** 72-95.

MANUEL, M. & ZYTNICKI, D. 2011. ALPHA, BETA AND GAMMA MOTONEURONS: FUNCTIONAL DIVERSITY IN THE MOTOR SYSTEM'S FINAL PATHWAY. *Journal of Integrative Neuroscience,* 10**,** 243-276.

MARINO, R. 2005. Neurological and functional outcomes in spinal cord injury: review and recommendations. *Topics in Spinal Cord Injury Rehabilitation,* 10**,** 51-64.

MARINO, R. J., JONES, L., KIRSHBLUM, S., TAL, J. & DASGUPTA, A. 2008. Reliability and repeatability of the motor and sensory examination of the International Standards for Neurological Classification of Spinal Cord Injury. *Journal of Spinal Cord Medicine,* 31**,** 166-170.

MARTIN, J. H. 2005. The corticospinal system: from development to motor control. *The Neuroscientist,* 11**,** 161-173.

MARTINI, F. 2005a. *Anatomy and Physiology'2007 Ed*, Rex Bookstore, Inc.

MARTINI, F. 2005b. *Human anatomy-/Frederic H. Martini, Michael J. Timmons, Robert B. Tallitsch; with William C. Ober...[etc.]*, San Francisco, PA [etc.]: Pearson/Benjamin Cummings.

MASON, S. G. & BIRCH, G. E. 2000. A brain-controlled switch for asynchronous control applications. *Ieee Transactions on Biomedical Engineering,* 47**,** 1297-1307.

MATTIA, D., CINCOTTI, F., ASTOLFI, L., DE VICO FALLANI, F., SCIVOLETTO, G., MARCIANI, M. G. & BABILONI, F. 2009. Motor cortical responsiveness to attempted movements in tetraplegia: evidence from neuroelectrical imaging. *Clinical Neurophysiology,* 120**,** 181-189.

MATTIA, D., CINCOTTI, F., MATTIOCCO, M., SCIVOLETTO, G., MARCIANI, M. G. & BABILONI, F. 2006. Motor-related cortical dynamics to intact movements in tetraplegics as revealed by high-resolution EEG. *Human Brain Mapping,* 27**,** 510-519.

MAYE, A., ZHANG, D., WANG, Y., GAO, S. & ENGEL, A. K. 2011. Multimodal brain-computer interfaces. *Tsinghua Science & Technology,* 16**,** 133-139.

MAYNARD, F. M., BRACKEN, M. B., CREASEY, G., DITUNNO, J. F., DONOVAN, W. H., DUCKER, T. B., GARBER, S. L., MARINO, R. J., STOVER, S. L., TATOR, C. H., WATERS, R. L., WILBERGER, J. E. & YOUNG, W. 1997. International standards for neurological and functional classification of spinal cord injury. *Spinal Cord,* 35**,** 266-274.

MCDONALD, J. W. & SADOWSKY, C. 2002a. Spinal cord injury - Reply. *Lancet,* 360**,** 1884-1884.

MCDONALD, J. W. & SADOWSKY, C. 2002b. Spinal-cord injury. *The Lancet,* 359**,** 417-425.

MCFADDEN, K. L. & ROJAS, D. C. 2013. *Electrophysiology of Autism*, INTECH Open Access Publisher.

MCFARLAND, D. J. 2015. The advantages of the surface Laplacian in brain–computer interface research. *International Journal of Psychophysiology,* 97**,** 271-276.

MCFARLAND, D. J., MCCANE, L. M., DAVID, S. V. & WOLPAW, J. R. 1997. Spatial filter selection for EEG-based communication. *Electroencephalography and clinical Neurophysiology,* 103**,** 386-394.

MCFARLAND, D. J. & WOLPAW, J. R. 2005. Sensorimotor rhythm-based brain-computer interface (BCI): Feature selection by regression improves performance. *Ieee Transactions on Neural Systems and Rehabilitation Engineering,* 13**,** 372-379.

MCKINLEY, W., SANTOS, K., MEADE, M. & BROOKE, K. 2007. Incidence and outcomes of spinal cord injury clinical syndromes. *Journal of Spinal Cord Medicine,* 30**,** 215-224.

MCKINLEY, W. O., JACKSON, A. B., CARDENAS, D. D. & MICHAEL, J. 1999. Long-term medical complications after traumatic spinal cord injury: a regional model systems analysis. *Archives of physical medicine and rehabilitation,* 80**,** 1402-1410.

MIKULIS, D. J., JURKIEWICZ, M. T., MCILROY, W. E., STAINES, W. R., RICKARDS, L., KALSI-RYAN, S., CRAWLEY, A. P., FEHLINGS, M. G. & VERRIER, M. C. 2002. Adaptation in the motor cortex following cervical spinal cord injury. *Neurology,* 58**,** 794-801.

MILLAN, J. D. R., GALÁN, F., VANHOOYDONCK, D., LEW, E., PHILIPS, J. & NUTTIN, M. Asynchronous non-invasive brain-actuated control of an intelligent wheelchair. Engineering in Medicine and Biology Society, 2009. EMBC 2009. Annual International Conference of the IEEE, 2009. IEEE, 3361-3364.

MILLER, K. J., SCHALK, G., FETZ, E. E., DEN NIJS, M., OJEMANN, J. G. & RAO, R. P. 2010. Cortical activity during motor execution, motor imagery, and imagery-based online feedback. *Proceedings of the National Academy of Sciences,* 107**,** 4430-4435.

MILLÁN, J. D. R. & CARMENA, J. 2010. Invasive or noninvasive: understanding brain-machine interface technology. *IEEE Engineering in Medicine and Biology Magazine,* 29**,** 16-22.

MILLÁN, J. D. R., RUPP, R., MÜLLER-PUTZ, G. R., MURRAY-SMITH, R., GIUGLIEMMA, C., TANGERMANN, M., VIDAURRE, C., CINCOTTI, F., KÜBLER, A. & LEEB, R. 2010. Combining brain–computer interfaces and assistive technologies: state-of-the-art and challenges. *Frontiers in Neuroscience,* Vol 4.

MINK, J. W. 1996. The basal ganglia: focused selection and inhibition of competing motor programs. *Progress in neurobiology,* 50**,** 381-425.

MIRVIS, S. E. & GEISLER, F. H. 1990. INTRAOPERATIVE SONOGRAPHY OF CERVICAL SPINAL-CORD INJURY - RESULTS IN 30 PATIENTS. *American Journal of Neuroradiology,* 11**,** 755-761.

MODEL, D. & ZIBULEVSKY, M. 2006. Learning subject-specific spatial and temporal filters for single-trial EEG classification. *NeuroImage,* 32**,** 1631-1641.

MOHAN KUMAR, C. E. & DHARANI KUMAR, S. V. 2014. Wavelet Based Feature Extraction Scheme of Electroencephalogram. *International Journal of Innovative Research in Science, Engineering and Technology,* 3**,** 908-913.

MONKHOUSE, S. 2005. *Cranial Nerves: Functional Anatomy*, Cambridge University Press.

MORSHED, B. I. & KHAN, A. 2014. A Brief Review of Brain Signal Monitoring Technologies for BCI Applications: Challenges and Prospects. *Journal of Bioengineering & Biomedical Science,* 4**,** 1-10.

MORTON, S. M. & BASTIAN, A. J. 2004. Cerebellar control of balance and locomotion. *The Neuroscientist,* 10**,** 247-259.

MOURIÑO, J., DEL R MILLAN, J., CINCOTTI, F., CHIAPPA, S., JANÉ, R. & BABILONI, F. Spatial filtering in the training process of a brain computer interface. Engineering in Medicine and Biology Society, 2001. Proceedings of the 23rd Annual International Conference of the IEEE, 2001. IEEE, 639-642.

MUELLER-PUTZ, G. R., RUPP, R., PFURTSCHELLER, G. & IEEE 2008. Graz Brain-Computer Interface: Control of Neuroprostheses for the upper extremity. *Isabel: 2008 First International Symposium on Applied Sciences in Biomedical and Commmunication Technologies***,** 39-40.

MUELLER-PUTZ, G. R., ZIMMERMANN, D., GRAIMANN, B., NESTINGER, K., KORISEK, G. & PFURTSCHELLER, G. 2007. Event-related beta EEG-changes during passive and attempted foot movements in paraplegic patients. *Brain Research,* 1137**,** 84-91.

MUGLERAB, E., BENSCHC, M., HALDERA, S., ROSENSTIELC, W., BOGDANCD, M., BIRBAUMERAE, N. & KÜBLERAF, A. 2008. Control of an internet browser using the P300 event-related potential. *IJBEM,* 10**,** 56-63.

MULLER-PUTZ, G. R., BREITWIESER, C., CINCOTTI, F., LEEB, R., SCHREUDER, M., LEOTTA, F., TAVELLA, M., BIANCHI, L., KREILINGER, A., RAMSAY, A., ROHM, M., SAGEBAUM, M., TONIN, L., NEUPER, C. & MILLAN, J. D. R. 2011. Tools for Brain-Computer Interaction: A General Concept for a Hybrid BCI. *Frontiers in neuroinformatics,* 5**,** 30-30.

MÜLLER-GERKING, J., PFURTSCHELLER, G. & FLYVBJERG, H. 1999. Designing optimal spatial filters for single-trial EEG classification in a movement task. *Clinical neurophysiology,* 110**,** 787-798.

MÜLLER-PUTZ, G., DALY, I. & KAISER, V. 2014. Motor imagery-induced EEG patterns in individuals with spinal cord injury and their impact on brain–computer interface accuracy. *Journal of neural engineering,* 11**,** 035011.

MÜLLER-PUTZ, G. R., SCHERER, R., PFURTSCHELLER, G. & RUPP, R. 2005. EEG-based neuroprosthesis control: a step towards clinical practice. *Neuroscience letters,* 382**,** 169-174.

NANAYAKKARA, A. & SAKKAFF, Z. 2012. Fixed distance neighbour classifiers in brain computer interface systems. *Journal of the National Science Foundation of Sri Lanka,* 40**,** 195-200.

NARDONE, R., HOELLER, Y., BRIGO, F., SEIDL, M., CHRISTOVA, M., BERGMANN, J., GOLASZEWSKI, S. & TRINKA, E. 2013. Functional brain reorganization after spinal cord injury: Systematic review of animal and human studies. *Brain Research,* 1504**,** 58-73.

NEUPER, C., SCHERER, R., REINER, M. & PFURTSCHELLER, G. 2005. Imagery of motor actions: Differential effects of kinesthetic and visual-motor mode of imagery in single-trial EEG. *Cognitive Brain Research,* 25**,** 668-677.

NICOLAS-ALONSO, L. F. & GOMEZ-GIL, J. 2012. Brain computer interfaces, a review. *Sensors,* 12**,** 1211-1279.

NIJBOER, F., FURDEA, A., GUNST, I., MELLINGER, J., MCFARLAND, D. J., BIRBAUMER, N. & KÜBLER, A. 2008. An auditory brain–computer interface (BCI). *Journal of neuroscience methods,* 167**,** 43-50.

NOOH, A. A., YUNUS, J. & DAUD, S. M. 2011. A review of asynchronous electroencephalogram-based brain computer interface systems. *International Conference on Biomedical Engineering and Technology IPCBEE,* 11**,** 55-59.

NORDHAUSEN, C. T., MAYNARD, E. M. & NORMANN, R. A. 1996. Single unit recording capabilities of a 100 microelectrode array. *Brain Research,* 726**,** 129-140.

OGAWA, S., LEE, T.-M., KAY, A. R. & TANK, D. W. 1990. Brain magnetic resonance imaging with contrast dependent on blood oxygenation. *Proceedings of the National Academy of Sciences,* 87**,** 9868-9872.

OLSSON, C.-J. 2012. Complex motor representations may not be preserved after complete spinal cord injury. *Experimental neurology,* 236**,** 46-49.

OMAR, T., WASSIM, Z., MOHAMED, B. & IEEE 2014. Brain-computer interface: frequency domain approach using the linear and the quadratic discriminant analysis. *2014 1st International Conference on Advanced Technologies for Signal and Image Processing (Atsip 2014)***,** 346-349.

ONISHI, A., NATSUME, K. & IEEE. 2013. Ensemble Regularized Linear Discriminant Analysis Classifier for P300-based Brain-Computer Interface. 35th Annual International Conference of the IEEE-Engineering-in-Medicine-and-Biology-Society (EMBC), 2013 Jul 03-07 2013 Osaka, JAPAN. 4231-4234.

ONOSE, G., GROZEA, C., ANGHELESCU, A., DAIA, C., SINESCU, C. J., CIUREA, A. V., SPIRCU, T., MIREA, A., ANDONE, I., SPANU, A., POPESCU, C., MIHAESCU, A. S., FAZLI, S., DANOCZY, M. & POPESCU, F. 2012. On the feasibility of using motor imagery EEG-based brain-computer interface in chronic tetraplegics for assistive robotic arm control: a clinical test and long-term post-trial follow-up. *Spinal Cord,* 50**,** 599-608.

ORTNER, R., BRUCKNER, M., PRÜCKL, R., GRÜNBACHER, E., COSTA, U., OPISSO, E., MEDINA, J. & GUGER, C. Accuracy of a P300 speller for people with motor impairments. Computational Intelligence, Cognitive Algorithms, Mind, and Brain (CCMB), 2011 IEEE Symposium on, 2011. IEEE, 1-6.

PALANIAPPAN, R. 2005. Brain computer interface design using band powers extracted during mental tasks. 2nd International IEEE/EMBS Conference on Neural Engineering, 2005 Mar 16-20 2005 Arlington, VA. 321-324.

PALANIAPPAN, R. 2011. *Biological signal analysis*, BookBoon.

PANG, H., TONG, T. J. & ZHAO, H. Y. 2009. Shrinkage-based Diagonal Discriminant Analysis and Its Applications in High-Dimensional Data. *Biometrics,* 65**,** 1021-1029.

PELLI, D. G. 1997. The VideoToolbox software for visual psychophysics: Transforming numbers into movies. *Spatial vision,* 10**,** 437-442.

PENNY, W. D., ROBERTS, S. J., CURRAN, E. A. & STOKES, M. J. 2000. EEG-Based communication: A pattern recognition approach. *Ieee Transactions on Rehabilitation Engineering,* 8**,** 214-215.

PFURTSCHELLER, G. 2001. Functional brain imaging based on ERD/ERS. *Vision Research,* 41**,** 1257-1260.

PFURTSCHELLER, G. 2004. Brain-Computer Interface-state of the art and future prospects. *Signal Processing Conference***,** 509-510.

PFURTSCHELLER, G. & DA SILVA, F. L. 1999. Event-related EEG/MEG synchronization and desynchronization: basic principles. *Clinical neurophysiology,* 110**,** 1842-1857.

PFURTSCHELLER, G., GUGER, C., MULLER, G., KRAUSZ, G. & NEUPER, C. 2000. Brain oscillations control hand orthosis in a tetraplegic. *Neuroscience Letters,* 292**,** 211-214.

PFURTSCHELLER, G., LINORTNER, P., WINKLER, R., KORISEK, G. & MULLER-PUTZ, G. 2009. Discrimination of motor imagery-induced EEG patterns in patients with complete spinal cord injury. *Computational intelligence and neuroscience***,** 104180-104180.

PFURTSCHELLER, G., MULLER, G. R., PFURTSCHELLER, J., GERNER, H. J. & RUPP, R. 2003. 'Thought' - control of functional electrical stimulation to restore hand grasp in a patient with tetraplegia. *Neuroscience Letters,* 351**,** 33-36.

PFURTSCHELLER, G., MULLER-PUTZ, G. R., PFURTSCHELLER, J. & RUPP, R. 2005. EEG-based asynchronous BCI controls functional electrical stimulation in a tetraplegic patient. *Eurasip Journal on Applied Signal Processing,* 2005**,** 3152-3155.

PFURTSCHELLER, G. & NEUPER, C. 2001. Motor imagery and direct brain-computer communication. *Proceedings of the IEEE,* 89**,** 1123-1134.

PIANGERELLI, M., CIAVARRO, M., PARIS, A., MARCHETTI, S., CRISTIANI, P., PUTTILLI, C., TORRES, N., BENABID, A. L. & ROMANELLI, P. 2014. A fully integrated wireless system for intracranial direct cortical stimulation, real-time electrocorticography data transmission, and smart cage for wireless battery recharge. *Frontiers in neurology,* 5**,** 1-5.

PLOW, E. B., ARORA, P., PLINE, M. A., BINENSTOCK, M. T. & CAREY, J. R. 2010. Within-limb somatotopy in primary motor cortex–revealed using fMRI. *Cortex,* 46**,** 310-321.

POLI, R., CINEL, C., CITI, L. & SALVARIS, M. A genetic programming approach to detecting artifact-generating eye movements from EEG in the absence of electro-oculogram. Neural Engineering (NER), 2011 5th International IEEE/EMBS Conference on, 2011. IEEE, 416-421.

POLICH, J., ELLERSON, P. C. & COHEN, J. 1996. P300, stimulus intensity, modality, and probability. *International Journal of Psychophysiology,* 23**,** 55-62.

PROCHAZKA, A., CLARAC, F., LOEB, G. E., ROTHWELL, J. C. & WOLPAW, J. R. 2000. What do reflex and voluntary mean? Modern views on an ancient debate. *Experimental Brain Research,* 130**,** 417-432.

PURKAYASTHA, S. S., JAIN, V. & SARDANA, H. 2014. Topical Review: A Review of Various Techniques Used for Measuring Brain Activity in Brain Computer Interfaces. *Advance in Electronic and Electric Engineering,* 4**,** 513-522.

PURVES, D., AUGUSTINE, G. J., FITZPATRICK, D., KATZ, L. C., LAMANTIA, A.-S., MCNAMARA, J. O. & WILLIAMS, S. M. 2001. *Neuroscience,* Sunderland, Mass. : Sinauer Associates.

QUIGLEY, H., COLLOBY, S. J. & O'BRIEN, J. T. 2011. PET imaging of brain amyloid in dementia: a review. *International Journal of Geriatric Psychiatry,* 26**,** 991-999.

RAJYALAKSHMI, M., RAO, T. K. & PRASAD, T. 2013. Exploration of Recent Advances in the Field of Brain Computer Interfaces. *International Organization of Scientific Research Journal of Computer Engineering.*

RAK, R. J., KOLODZIEJ, M. & MAJKOWSKI, A. 2012. BRAIN-COMPUTER INTERFACE AS MEASUREMENT AND CONTROL SYSTEM THE REVIEW PAPER. *Metrology and Measurement Systems,* 19**,** 427-444.

RAMOS-MURGUIALDAY, A., SCHÜRHOLZ, M., CAGGIANO, V., WILDGRUBER, M., CARIA, A., HAMMER, E. M., HALDER, S. & BIRBAUMER, N. 2012. Proprioceptive feedback and brain computer interface (BCI) based neuroprostheses. *PLoS ONE,* 7**,** 47048-47058.

REBY, D., LEK, S., DIMOPOULOS, I., JOACHIM, J., LAUGA, J. & AULAGNIER, S. 1997. Artificial neural networks as a classification method in the behavioural sciences. *Behavioural Processes,* 40**,** 35-43.

REFAEILZADEH, P., TANG, L. & LIU, H. 2009. Cross-validation. *Encyclopedia of database systems.* Springer.

RENU, B. & SWATI, G. 2013. A Study of The Effect of Sound on EEG. *International Journal of Electronics and Computer Science Engineering,* 2**,** 88-93.

REZAEI, S., TAVAKOLIAN, K., NASRABADI, A. M. & SETAREHDAN, S. K. 2006. Different classification techniques considering brain computer interface applications. *Journal of Neural Engineering,* 3**,** 139-144.

RIMKUS, C. M., MASCARENHAS, C., OTADUY, M. C. & LEITE, C. C. 2011. Imaging of the spinal cord injury: techniques for diagnosis, follow up and research. *16th Annual Conference of the International Functional Electrical Stimulation Society*, 037.

RIVET, B., CECOTTI, H., PHLYPO, R., BERTRAND, O., MABY, E. & MATTOUT, J. EEG sensor selection by sparse spatial filtering in P300 speller brain-computer interface. Engineering in Medicine and Biology Society (EMBC), 2010 Annual International Conference of the IEEE, 2010. IEEE, 5379-5382.

RIVET, B., SOULOUMIAC, A., GIBERT, G. & ATTINA, V. "P300 speller" Brain-Computer Interface: Enhancement of P300 evoked potential by spatial filters. Signal Processing Conference, 2008 16th European, 2008. IEEE, 1-5.

ROBERTO HORNERO, R. C., DANIEL ALVAREZ 2012. Brain Computer Interface (BCI) systems applied to cognitive training and home automation control to offset the effects of ageing. *Lychnos,* 8**,** 29-34.

ROBEVA, R., KIRKWOOD, J. R., DAVIES, R. L., FARHY, L., KOVATCHEV, B. P., STRAUME, M. & JOHNSON, M. L. 2007. *An invitation to biomathematics*, Academic Press.

ROBINSON, F. R. 1995. Role of the cerebellum in movement control and adaptation. *Current opinion in neurobiology,* 5**,** 755-762.

ROELCKE, U., CURT, A., OTTE, A., MISSIMER, J., MAGUIRE, R. P., DIETZ, V. & LEENDERS, K. L. 1997. Influence of spinal cord injury on cerebral sensorimotor systems: A PET study. *Journal of Neurology Neurosurgery and Psychiatry,* 62**,** 61-65.

ROH, S.-C., PARK, E.-J., PARK, Y.-C., YOON, S.-K., KANG, J.-G., KIM, D.-W. & LEE, S.-H. 2015. Quantitative Electroencephalography Reflects Inattention, Visual Error Responses, and Reaction Times in Male Patients with Attention Deficit Hyperactivity Disorder. *Clinical Psychopharmacology and Neuroscience,* 13**,** 180.

RUPP, R. 2015. Challenges in clinical applications of brain computer interfaces in individuals with spinal cord injury. *Front. Neuroeng,* 7.

SACH, M., WINKLER, G., GLAUCHE, V., LIEPERT, J., HEIMBACH, B., KOCH, M. A., BUCHEL, C. & WEILLER, C. 2004. Diffusion tensor MRI of early upper motor neuron involvement in amyotrophic lateral sclerosis. *Brain,* 127**,** 340-350.

SAFRI, N. M. & ADNAN, S. N. F. 2015. Eye Therapy Effects on Visual Stress based on Electroencephalogram Signals. *Jurnal Teknologi,* 74**,** 15-19.

269

SALINSKY, M. C., BINDER, L. M., OKEN, B. S., STORZBACH, D., ARON, C. R. & DODRILL, C. B. 2002. Effects of gabapentin and carbamazepine on the EEG and cognition in healthy volunteers. *Epilepsia,* 43**,** 482-490.

SCHMAHMANN, J. D. & CAPLAN, D. 2006. Cognition, emotion and the cerebellum. *Brain,* 129**,** 290-292.

SCHWARTZ, A. B., CUI, X. T., WEBER, D. J. & MORAN, D. W. 2006. Brain-controlled interfaces: movement restoration with neural prosthetics. *Neuron,* 52**,** 205-220.

SEMBULINGAM, K. & SEMBULINGAM, P. 2012. *Essentials of medical physiology*, JP Medical Ltd.

SEVERENS, M., FARQUHAR, J., DUYSENS, J. & DESAIN, P. 2013. A multi-signature brain–computer interface: use of transient and steady-state responses. *Journal of neural engineering,* 10**,** 026005.

SHAKEEL, A., NAVID, M. S., ANWAR, M. N., MAZHAR, S., JOCHUMSEN, M. & NIAZI, I. K. 2015. A review of techniques for detection of movement intention using movement-related cortical potentials. *Computational and mathematical methods in medicine,* 2015.

SHEN, H., TANG, Y., HUANG, L., YANG, R., WU, Y., WANG, P., SHI, Y., HE, X., LIU, H. & YE, J. 2007. Applications of diffusion-weighted MRI in thoracic spinal cord injury without radiographic abnormality. *International Orthopaedics,* 31**,** 375-383.

SHOHAM, S., HALGREN, E., MAYNARD, E. M. & NORMANN, R. A. 2001. Motor-cortical activity in tetraplegics. *Nature,* 413**,** 793-793.

SINCLAIR, C. M., GASPER, M. C. & BLUM, A. S. 2007. Basic electronics in clinical neurophysiology. *The Clinical Neurophysiology Primer.* Springer.

SNELL, R. S. 2010. *Clinical neuroanatomy*, Lippincott Williams & Wilkins.

SOLHJOO, S. & MORADI, M. Mental task recognition: A comparison between some of classification methods. BIOSIGNAL 2004 International EURASIP Conference, 2004. 24-26.

SOLODKIN, A., HLUSTIK, P., CHEN, E. E. & SMALL, S. L. 2004. Fine modulation in network activation during motor execution and motor imagery. *Cerebral cortex,* 14**,** 1246-1255.

SPRING, J., PLACE, N., BORRANI, F., KAYSER, B., BARRAL, J. & BERCHICCI, M. 2016. Movement-related cortical potential amplitude reduction after cycling exercise relates to the extent of neuromuscular fatigue. *Frontiers in Human Neuroscience,* 10**,** 257.

SRIDHAR, G. & RAO, D. P. M. 2012. A Neural Network Approach for EEG classification in BCI. *International Journal of Computer Science and Telecommunications,* 3**,** 44-48.

STEEVES, J. D., LAMMERTSE, D., CURT, A., FAWCETT, J. W., TUSZYNSKI, M. H., DITUNNO, J. F., ELLAWAY, P. H., FEHLINGS, M. G., GUEST, J. D., KLEITMAN, N., BARTLETT, P. F., BLIGHT, A. R., DIETZ, V., DOBKIN, B. H., GROSSMAN, R., SHORT, D., NAKAMURA, M., COLEMAN, W. P., GAVIRIA, M. & PRIVAT, A. 2007. Guidelines for the conduct of clinical trials for spinal cord injury (SCI) as developed by the ICCP panel: clinical trial outcome measures. *Spinal Cord,* 45**,** 206-221.

STIFANI, N. 2014. Motor neurons and the generation of spinal motor neuron diversity. *Frontiers in Cellular Neuroscience,* 8**,** 1-22.

STREHL, U., LEINS, U., GOTH, G., KLINGER, C., HINTERBERGER, T. & BIRBAUMER, N. 2006. Self-regulation of slow cortical potentials: a new treatment for children with attention-deficit/hyperactivity disorder. *Pediatrics,* 118**,** e1530-e1540.

STROMAN, P. W. 2005. Magnetic resonance imaging of neuronal function in the spinal cord: spinal FMRI. *Clinical medicine & research,* 3**,** 146-56.

SUNG, Y.-S., CHO, K.-G. & UM, K.-H. 2012. A Framework for processing brain waves used in a brain-computer interface. *Journal of Information Processing Systems,* 8**,** 315-330.

SUR, S. & SINHA, V. 2009. Event-related potential: An overview. *Industrial psychiatry journal,* 18**,** 70.

TALLON-BAUDRY, C. & BERTRAND, O. 1999. Oscillatory gamma activity in humans and its role in object representation. *Trends in cognitive sciences,* 3**,** 151-162.

TANAKA, K., KURITA, T., MEYER, F., BERTHOUZE, L. & KAWABE, T. Stepwise feature selection by cross validation for EEG-based Brain Computer Interface. The 2006 IEEE International Joint Conference on Neural Network Proceedings, 2006. IEEE, 4672-4677.

TAVELLA, M., LEEB, R., RUPP, R. & MILLÁN, J. D. R. 2010. Towards natural non-invasive hand neuroprostheses for daily living. *Engineering in Medicine and Biology Society (EMBC), Annual International Conference of the IEEE***,** 126-129.

TEPLAN, M. 2002. Fundamentals of EEG measurement. *Measurement science review,* 2**,** 1-11.

THOMAS, E., DYSON, M. & CLERC, M. 2013. An analysis of performance evaluation for motor-imagery based BCI. *Journal of Neural Engineering,* 10.

THOMAS, E., FRUITET, J. & CLERC, M. Investigating brief motor imagery for an ERD/ERS based BCI. Engineering in Medicine and Biology Society (EMBC), 2012 Annual International Conference of the IEEE, 2012. IEEE, 2929-2932.

THOMPSON, A., JARRETT, L., LOCKLEY, L., MARSDEN, J. & STEVENSON, V. 2005. Clinical management of spasticity. *Journal of Neurology, Neurosurgery & Psychiatry,* 76**,** 459-463.

TOLIC, M. & JOVIC, F. 2013. CLASSIFICATION OF WAVELET TRANSFORMED EEG SIGNALS WITH NEURAL NETWORK FOR IMAGINED MENTAL AND MOTOR TASKS. *Kinesiology,* 45**,** 130-138.

TOMASSEN, P. C. D., POST, M. W. M. & VAN ASBECK, F. W. A. 2000. Return to work after spinal cord injury. *Spinal Cord,* 38**,** 51-55.

TOPKA, H., COHEN, L. G., COLE, R. A. & HALLETT, M. 1991. Reorganization of corticospinal pathways following spinal cord injury. *Neurology,* 41**,** 1276-1276.

TOWNSEND, G., GRAIMANN, B. & PFURTSCHELLER, G. 2004. Continuous EEG classification during motor imagery-simulation of an asynchronous BCI. *Neural Systems and Rehabilitation Engineering, IEEE Transactions on,* 12**,** 258-265.

TOXOPEUS, C. M., DE JONG, B. M., VALSAN, G., CONWAY, B. A., LEENDERS, K. L. & MAURITS, N. M. 2011. Direction of movement is encoded in the human primary motor cortex. *PloS one,* 6**,** e27838.

TSUI, C. S. L. & GAN, J. Q. 2007. Asynchronous BCI control of a robot simulator with supervised online training. *Intelligent Data Engineering and Automated Learning-IDEAL 2007.* Springer.

TURNER, J. A., LEE, J. S., SCHANDLER, S. L. & COHEN, M. J. 2003. An fMRI investigation of hand representation in paraplegic humans. *Neurorehabilitation and Neural Repair,* 17**,** 37-47.

URBAN, P. P., VOGT, T. & HOPF, H. C. 1998. Corticobulbar tract involvement in amyotrophic lateral sclerosis - A transcranial magnetic stimulation study. *Brain,* 121**,** 1099-1108.

VALLABHANENI, A., WANG, T. & HE, B. 2005. Brain—computer interface. *Neural engineering.* Springer.

VALSAN, G., WORRAJIRAN, P., LAKANY, H. & CONWAY, B. Predicting intention and direction of wrist movement from EEG. Advances in Medical, Signal and Information Processing, 2006. MEDSIP 2006. IET 3rd International Conference On, 2006. IET, 1-4.

VAN GERVEN, M., FARQUHAR, J., SCHAEFER, R., VLEK, R., GEUZE, J., NIJHOLT, A., RAMSEY, N., HASELAGER, P., VUURPIJL, L. & GIELEN, S. 2009. The brain–computer interface cycle. *Journal of neural engineering,* 6**,** 041001.

VAN DER MAATEN, L., POSTMA, E. & VAN DEN HERIK, J. 2009. Dimensionality reduction: a comparative. *J Mach Learn Res,* 10**,** 66-71.

VAN MIDDENDORP, J. J., GOSS, B., URQUHART, S., ATRESH, S., WILLIAMS, R. P. & SCHUETZ, M. 2011. Diagnosis and prognosis of traumatic spinal cord injury. *Global spine journal,* 1**,** 1-7.

VIDAURRE, C. & BLANKERTZ, B. 2010. Towards a cure for BCI illiteracy. *Brain topography,* 23**,** 194-198.

WALDERT, S., PISTOHL, T., BRAUN, C., BALL, T., AERTSEN, A. & MEHRING, C. 2009. A review on directional information in neural signals for brain-machine interfaces. *Journal of Physiology-Paris,* 103**,** 244-254.

WALTERS-WILLIAMS, J. & LI, Y. 2010. Comparative Study of Distance Functions for Nearest Neighbors. *Advances Techniques in Computing Sciences and Software Engineering***,** 79-84.

WANG, D., MIAO, D. & BLOHM, G. 2012. Multi-class motor imagery EEG decoding for brain-computer interfaces. *Frontiers in neuroscience,* 6**,** 151.

WANG, S. & JAMES, C. J. 2005. Preprocessing the P300 word speller with ICA for Brain-Computer Interfacing.

WANG, S. & JAMES, C. J. 2007. Extracting rhythmic brain activity for brain-computer interfacing through constrained independent component analysis. *Computational intelligence and neuroscience,* 2007.

WANG, P., KING, C., SCHOMBS, A., LIN, J., SAZGAR, M., HSU, F., SHAW, S., MILLETT, D., LIU, C. & CHUI, L. 2013a. Electrocorticographic gamma band power encodes the velocity of upper extremity movements. *Proc 5th Int'l Brain-Computer Interface Meeting*.

WANG, W., COLLINGER, J. L., DEGENHART, A. D., TYLER-KABARA, E. C., SCHWARTZ, A. B., MORAN, D. W., WEBER, D. J., WODLINGER, B., VINJAMURI, R. K. & ASHMORE, R. C. 2013b. An electrocorticographic brain interface in an individual with tetraplegia. *PloS one,* 8**,** e55344.

WANG, Y., GAO, X., HONG, B., JIA, C. & GAO, S. 2008. Brain-computer interfaces based on visual evoked potentials. *Engineering in Medicine and Biology Magazine, IEEE,* 27**,** 64-71.

WARING, W. P., III, BIERING-SORENSEN, F., BURNS, S., DONOVAN, W., GRAVES, D., JHA, A., JONES, L., KIRSHBLUM, S., MARINO, R., MULCAHEY, M. J., REEVES, R., SCELZA, W. M., SCHMIDT-READ, M. & STEIN, A. 2010. 2009 Review and Revisions of the International Standards for the Neurological Classification of Spinal Cord Injury. *Journal of Spinal Cord Medicine,* 33**,** 346-352.

WATERS, R. L., ADKINS, R. H. & YAKURA, J. S. 1991. DEFINITION OF COMPLETE SPINAL-CORD INJURY. *Paraplegia,* 29**,** 573-581.

WIDERSTROM-NOGA, E. G., FELIPE-CUERVO, E. & YEZIERSKI, R. P. 2001. Relationships among clinical characteristics of chronic pain after spinal cord injury. *Archives of Physical Medicine and Rehabilitation,* 82**,** 1191-1197.

WOLF, U., RAPOPORT, M. J. & SCHWEIZER, T. A. 2009. Evaluating the affective component of the cerebellar cognitive affective syndrome. *The Journal of Neuropsychiatry,* 21**,** 245-256.

WOLPAW, J. R., BIRBAUMER, N., HEETDERKS, W. J., MCFARLAND, D. J., PECKHAM, P. H., SCHALK, G., DONCHIN, E., QUATRANO, L. A., ROBINSON, C. J. & VAUGHAN, T. M. 2000. Brain-computer interface technology: a review of the first international meeting. *IEEE transactions on rehabilitation engineering,* 8**,** 164-173.

WOLPAW, J. R., BIRBAUMER, N., MCFARLAND, D. J., PFURTSCHELLER, G. & VAUGHAN, T. M. 2002. Brain–computer interfaces for communication and control. *Clinical neurophysiology,* 113**,** 767-791.

XU, R., JIANG, N., VUCKOVIC, A., HASAN, M., MRACHACZ-KERSTING, N., ALLAN, D., FRASER, M., NASSEROLESLAMI, B., CONWAY, B. & DREMSTRUP, K. 2014. Movement-related cortical potentials in paraplegic patients: abnormal patterns and considerations for BCI-rehabilitation.

YAMADERA, H., KATO, M., TSUKAHARA, Y., BRANDEIS, D. & OKUMA, T. 1996. Zopiclone versus diazepam effects on EEG power maps in healthy volunteers. *Acta neurobiologiae experimentalis,* 57**,** 151-155.

YAZDANI, A., EBRAHIMI, T., HOFFMANN, U. & IEEE. 2009. Classification of EEG Signals Using Dempster Shafer Theory and a K-Nearest Neighbor Classifier. 4th International IEEE/EMBS Conference on Neural Engineering, 2009 Apr 29-May 02 2009 Antalya, TURKEY. 320-323.

YEOM, H.-G., SIM, K.-B. & IEEE 2008. ERS and ERD Analysis during The Imaginary Movement of Arms. *2008 International Conference on Control, Automation and Systems, Vols 1-4***,** 2131-2135.

YI, W., QIU, S., QI, H., ZHANG, L., WAN, B. & MING, D. 2013. EEG feature comparison and classification of simple and compound limb motor imagery. *J. Neuroeng. Rehabil,* 10**,** 1-12.

YONG, X. & MENON, C. 2015. EEG Classification of Different Imaginary Movements within the Same Limb. *PloS one,* 10**,** 1-24.

ÖZTUNA, D., ELHAN, A. H. & TÜCCAR, E. 2006. Investigation of four different normality tests in terms of type 1 error rate and power under different distributions. *Turkish Journal of Medical Sciences,* 36**,** 171-176.